

See discussions, stats, and author profiles for this publication at: <https://www.researchgate.net/publication/221721430>

Exploiting Transport Activity of P-Glycoprotein at the Blood-Brain Barrier for the Development of Peripheral Cannabinoid Type 1 Receptor Antagonists

ARTICLE *in* MOLECULAR PHARMACEUTICS · MARCH 2012

Impact Factor: 4.38 · DOI: 10.1021/mp200617z · Source: PubMed

CITATIONS

16

READS

23

7 AUTHORS, INCLUDING:



[Rick Greupink](#)

Radboud University Medical Centre (Radbo...

27 PUBLICATIONS 310 CITATIONS

[SEE PROFILE](#)



[Jeroen van den Heuvel](#)

Radboud University Nijmegen

33 PUBLICATIONS 958 CITATIONS

[SEE PROFILE](#)



[Petra van den Broek](#)

Radboud University Medical Centre (Radbo...

64 PUBLICATIONS 949 CITATIONS

[SEE PROFILE](#)



[Frans G M Russel](#)

Radboud University Medical Centre (Radbo...

269 PUBLICATIONS 6,116 CITATIONS

[SEE PROFILE](#)



PDF hosted at the Radboud Repository of the Radboud University Nijmegen

This full text is a publisher's version.

For additional information about this publication click this link.

[<http://hdl.handle.net/2066/95114>]

Please be advised that this information was generated on 2013-02-11 and may be subject to change.

The role of brain and intestinal efflux transporters in disposition of central nervous system drugs

Hanneke Wittgen

About the cover

Obesity is a serious disease that, unfortunately, is on the rise since the end of last century. The good news is: new treatments are on the way. Hanneke Wittgen studied rimonabant, a medicine that seems to prevent obesity, but has some severe side effects due to its effect on the brain. By preventing access of CB1 receptor antagonists, such as rimonabant, to the brain, this kind of medicine can no longer cause depression and fear but can still carry out its good work in preventing obesity. On the cover you see the journey of the medicine, flowing through the purple colored veins, characterized by a labyrinth. The medicine enters the blood via the intestine and leaves the body via the kidneys on the back of the cover. On its way, it spreads into the body in circles, but it cannot enter the brain because it is pumped out via drug efflux transporters. The journey of the medicine through the labyrinth parallels the journey of obtaining one's PhD degree: sometimes you take a wrong corner and have to back up, but you'll always find your way out. As long as you have a clear brain.

Marjolein Pijnappels (Studio Lakmoes)

The research presented in this thesis was performed at the department of Pharmacology and Toxicology, Radboud University Nijmegen Medical Centre, Nijmegen Centre for Molecular Life Sciences, Nijmegen, the Netherlands. The research project was funded by the Dutch Top Institute Pharma and was performed within the framework of project T5-105 *Nanoscience as a tool for improving bioavailability and blood-brain barrier penetration of CNS drugs*

Cover and page design: Studio Lakmoes and Hanneke Wittgen

Printed by Gildeprint Drukkerijen - Enschede

The role of brain and intestinal efflux transporters in disposition of central nervous system drugs

PROEFSCHRIFT

ter verkrijging van de graad van doctor

aan de Radboud Universiteit Nijmegen

op gezag van de rector magnificus prof. mr. S.C.J.J. Kortmann,

volgens het besluit van het college van decanen

in het openbaar te verdedigen op woensdag 29 augustus 2012

om 15.30 uur precies

door

Hanneke Geertje Maria Wittgen

geboren op 23 mei 1984

te Venray

Promotor

Prof. dr. F.G.M. Russel

Copromotor

Dr. J.B. Koenderink

Manuscriptcommissie

Prof. dr. R.J.M. Bindels (voorzitter)

Prof. dr. D.M. Burger

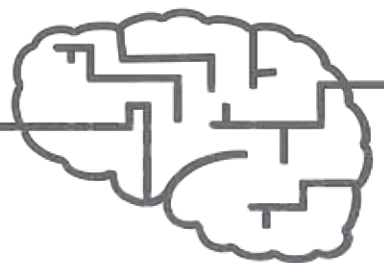
Dr. E.C.M. de Lange (LACDR, Leiden)

Table of contents

Chapter 1	7
General introduction	
Chapter 2	
Cannabinoid CB1 receptor antagonists modulate transport activity of multidrug resistance-associated proteins MRP1, MRP2, MRP3, and MRP4	25
Chapter 3	
Exploiting transport activity of P-glycoprotein at the blood-brain barrier for the development of peripheral cannabinoid type 1 receptor antagonists	45
Chapter 4	
Transport of the coumarin metabolite 7-hydroxycoumarin glucuronide is mediated via multidrug resistance-associated proteins 3 and 4	67
Chapter 5	
Synergistic interplay between efflux transporters and uridine 5'-diphospho glucuronosyltransferase (UGT) 2B15 in glucuronidation of 7-hydroxycoumarin	79
Chapter 6	
Phenylalanine 368 of multidrug resistance-associated protein 4 (MRP4/ABCC4) plays a crucial role in substrate-specific transport activity	97
Chapter 7	
General discussion	115
Chapter 8	137
Summary	139
Samenvatting	145
List of abbreviations and glossary	152
Curriculum vitae	156
List of publications	157
Dankwoord	159

Chapter 1

General introduction



Role of ABC transporters in pharmacokinetics

Absorption, distribution, metabolism, and excretion (ADME) are key determinants of drug efficacy and safety because these processes determine the availability of a drug at its target site. Before a drug reaches its site of action, it needs to cross several cellular barriers. Passage of a compound over these barriers is partly determined by its physicochemical characteristics, such as molecular size, lipophilicity, hydrogen bond donating or accepting capacity, or charge distribution.¹ However, predictions of cell permeability based on these characteristics did not always correlate to the actual permeability of compounds, and further studies revealed that transport via membrane transporters also plays a vital role in this process. The human genome encodes for more than 400 transporters, including uptake transporters of the solute-carrier (SLC) transporter family and efflux transporters of the ATP binding cassette (ABC) transporter family, many of which are known to influence the absorption, distribution, and excretion of drugs.²⁻⁴

In total, the ABC transporter family consists of 49 members.⁵ P-glycoprotein (P-gp/ABCB1), multidrug resistance-associated proteins (MRP/ABCC), and breast cancer resistance protein (BCRP/ABCG2) are efflux transporters of the ABC family that have been shown to transport clinically relevant drugs.^{2,6} In general, transporters of the ABC family comprise two nucleotide binding domains (NBD) and two transmembrane domains (TMD). However, some transporters have an extra transmembrane domain (MRP1, MRP2, MRP3), while BCRP is a half-transporter, consisting of only one NBD and one TMD, that needs to dimerize to form a fully functional ABC transporter (Fig. 1).^{6,7} The mechanism of substrate translocation across the membrane by these transporters has been investigated for more than 30 years. Functional and mutational analyses have mainly studied how ATP-hydrolytic activity is important for the activity of the transporter, and how these proteins can transport such a wide variety of substrates.⁸ These studies, first focusing on P-glycoprotein but later also on MRP1, 2, and 3, revealed that ATP binding and hydrolysis at the NBDs is necessary for transport function and that the TMDs form the main site for drug binding.^{7,9,10} Crystal structures of ABC transporters aid in visualizing the conformation of the transporter in different states of the transport cycle. Several bacterial ABC transporters have been successfully crystallized because of their relatively good water solubility, but to date this has only been achieved for one mammalian transporter, mouse P-glycoprotein.¹¹ This paper described two crystal structures with cyclic peptide inhibitors bound, providing a molecular basis for polyspecific drug binding sites in P-glycoprotein. Homology models for other mammalian ABC transporters based on this structure combined with mutational analysis studies are a good starting point for a better understanding of the binding pockets of these transporters.

MRP1-5, BCRP, and P-gp are expressed in many epithelia in the body, either at the apical or basolateral cell membrane depending on the cell type.^{6,12-16} Because efflux transporters are widely distributed in the body and they transport many different compounds, these proteins form a protective network against toxic compounds and drugs.^{5,6} This thesis



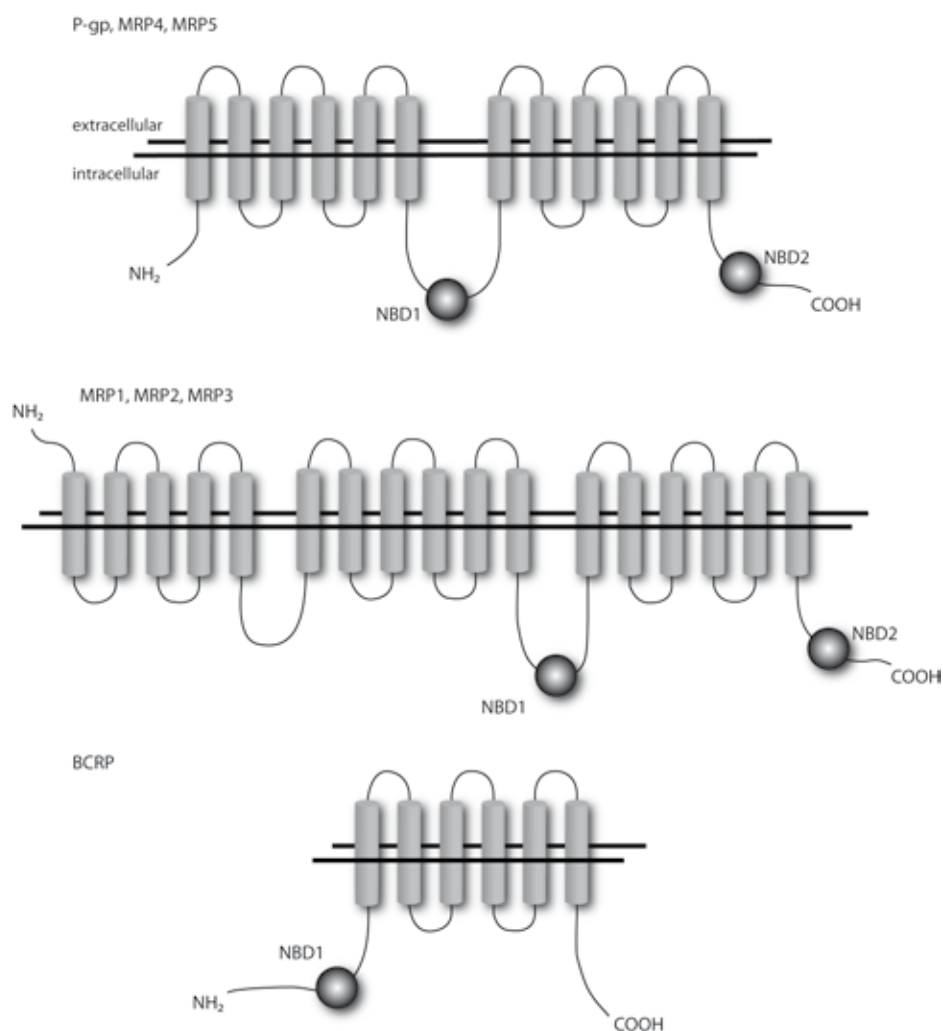


Figure 1 Molecular topology of the drug efflux transporters P-gp, MRP1-5, and BCRP

NBD, nucleotide binding domain; NH₂, aminotermius; COOH, carboxyterminus.

describes the role of intestinal and blood-brain barrier transporters in the disposition of a class of central nervous system (CNS) drugs, the cannabinoid type 1 receptor antagonists.

Expression and function of efflux transporters in the intestine

Oral administration is the most common route of administration for CNS drugs because it is non-invasive, convenient, and relatively cost-effective. However, with this type of administration, the systemic availability of a drug strongly depends on the passage through the intestinal wall and liver. If systemic availability is limited, the availability of a drug to the brain obviously will also be reduced.

There are two main routes through which compounds can enter the portal circulation: the paracellular and the transcellular route.¹⁷⁻¹⁹ Small hydrophilic, ionized drugs can be absorbed via the paracellular route, but their passage is limited by the presence of tight junctions between the epithelial cells. Therefore, the contribution of this route to absorption is considered to be small.¹⁸ This implies that most drugs enter the circulation via the transcellular route, where influx or efflux transporters at the apical and basolateral membranes of the cell, and metabolizing enzymes in the cytosol, could affect their bioavailability.^{20, 21} The lower intestinal tract consists of duodenum, jejunum, ileum, and colon, each of which segment expresses a range of influx and efflux transporters.

The main ABC transporters that are expressed in the intestine are MRP1-5, BCRP, and P-gp (Fig. 2). MRP1 is mainly expressed on the basolateral membranes of intestinal crypt cells.²² MRP3 is also localized to the basolateral membrane of intestinal cells, whereas P-glycoprotein, BCRP, and MRP2 are expressed apically.^{13, 16, 23-27} The cellular localization of MRP4 is still unclear, with either apical or basolateral localization in intestinal cell lines, and, to date, no immunohistochemical confirmation of the localization of MRP4 in human intestine.²⁸⁻³⁰ MRP5 has been detected at the mRNA level in the intestinal CaCo-2 cell line, but protein expression was not found, so its importance for intestinal drug transport remains to be investigated.³¹

Transporter expression in the epithelial cells lining the lower intestine is variable over the length of the tract (Table 1).^{17, 32-34} MRP2 is highly abundant in small intestine, whereas it is virtually absent towards the end of the intestinal tract.³³⁻³⁶ BCRP expression appears to be highest in the middle or lower part of the intestine and seems to decline along the length of the intestinal tract, whereas MRP3, MRP4, and P-gp expression seems to increase towards the distal part of the intestine.^{33, 34, 36-38} The varying expression of efflux transporters in the intestine is expected to influence the site of intestinal absorption of a drug that is substrate for one or more of these transporters.³⁹

Multiple studies have been performed to determine the involvement of efflux transporters in the oral availability of drugs, using *in vitro* models, such as CaCo-2 cells, or *in vivo* models, *e.g.* knockout animals, or inhibitors of efflux transporters in animals or humans.



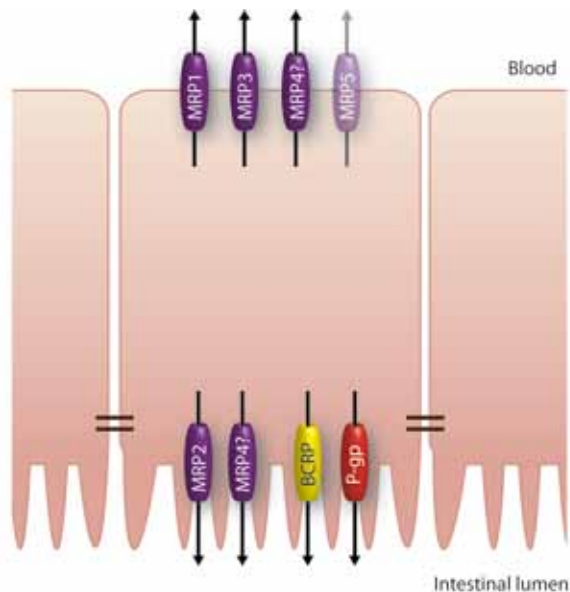


Figure 2 Localization of ATP-dependent drug efflux transporters in the intestinal wall

Transparency of MRP5 means that the relevance of this transporter for intestinal transport is unknown. Question mark behind MRP4 means that the exact location of this transporter has not been identified in intestinal tissue.

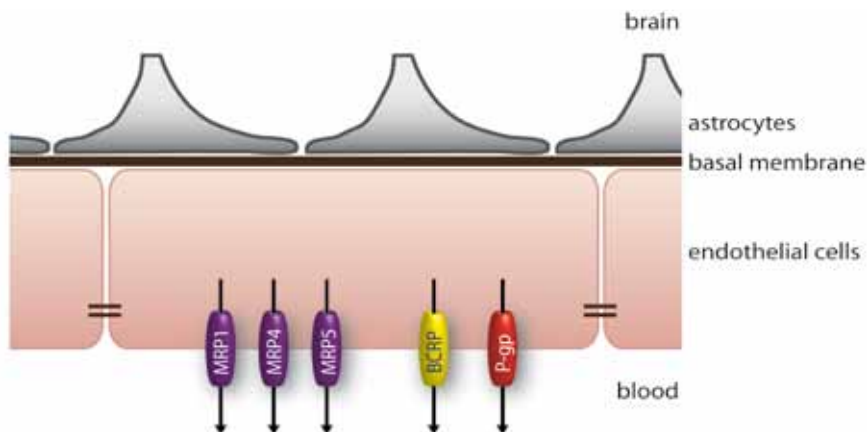


Figure 3 Localization of ATP-dependent drug efflux transporters in the human blood-brain barrier

Table 1 Rank order of mRNA expression of efflux transporters in different intestinal segments

Segment	Rank order
Duodenum	MRP3 >> P-gp > MRP2 > MRP5 > MRP4 > MRP1 ³³ BCRP >> P-gp ≈ MRP2 > MRP3 ³⁴
Jejunum	BCRP ≈ MRP2 > P-gp ≈ MRP3 > MRP5 ≈ MRP6 ≈ MRP1 ≈ MRP4 > MDR3 ³² MRP2 ≈ P-gp > BCRP > MRP3 ³⁶ BCRP >> MRP2 ≈ P-gp > MRP3 >> MRP6 ≈ MRP4 ≈ MRP1 ≈ MRP5 ⁴⁹ BCRP > P-gp >> MRP2 > MRP3 ³⁴
Ileum	P-gp > MRP3 >> MRP1 ≈ MRP4 ≈ MRP5 > MRP2 ³³ BCRP ≈ P-gp >> MRP2 > MRP3 ³⁴
Colon	MRP3 >> P-gp > MRP4 ≈ MRP5 > MRP1 >> MRP2 ³³ MRP3 > P-gp >> BCRP > MRP2 ³⁶ BCRP > P-gp > MRP3 >> MRP2 ³⁴

^{32, 33} mRNA expression levels determined by TaqMan quantitative real time PCR (Q-PCR) and normalized to enterocyte-specific villin expression.

³⁴ mRNA expression levels determined by TaqMan Q-PCR and normalized to 18S expression.

³⁶ mRNA expression levels determined by TaqMan Q-PCR and normalized to expression level of cytoplasmic protein cyclophilin A.

⁴⁹ mRNA expression levels determined by TaqMan Q-PCR and normalized to geometric mean of cyclophilin A and major vault protein LRP.

These studies have especially revealed a role for P-gp, BCRP, and MRP2 in decreasing the oral availability of drugs, whereas MRP3 could increase bioavailability.³⁹⁻⁴¹ For example, the oral availability of the anti-cancer drug paclitaxel is increased from 9% in wild type to 36% in P-gp knockout mice, and inhibition of P-gp in wild type mice with the mixed P-gp/BCRP inhibitor elacridar (GF120918) increased the oral availability to 40%.⁴² Also in humans, elacridar increased the oral availability of paclitaxel from 4 to 30%, indicating the importance of P-gp in limiting its oral availability.^{43,44} Inhibition of both BCRP and P-gp with elacridar increased the oral availability of the anti-cancer drug topotecan 9-fold in mice, and from 40% to 97% in humans.⁴⁵⁻⁴⁷ Although the role of MRP2 in decreasing the oral availability of drugs at the intestinal level appears to be less important than that of P-gp or BCRP, it appears to reduce the systemic exposure of the toxic food derived carcinogen 2-amino-1-methyl-6-phenylimidazo[4,5-*b*]pyridine (PhIP) in mice.⁴⁸ In contrast, using Mrp3 knockout mice, Kitamura and colleagues revealed a role for MRP3 in increasing the oral availability of methotrexate, because the systemic methotrexate exposure appeared to be lower in these animals.⁴¹ Studies regarding the role of efflux transporters on oral bioavailability of CNS drugs have mainly focused on P-gp. In humans, P-gp inhibition with itraconazole, verapamil, or quinidine increased the exposure of the orally administered anti-depressant paroxetine, anti-psychotic agent risperidone, and analgesic drug morphine



by 56%, 82%, and 60%, respectively.⁵⁰⁻⁵² These examples emphasize the role of intestinal efflux transporters in determining the oral availability of (CNS) drugs.

Interplay of metabolizing enzymes and transporters in the intestine

Another factor that can influence the oral availability of a drug is biotransformation via metabolizing enzymes, in both the intestine and the liver. Metabolism of drugs is important for their detoxication and elimination from the body. Although the liver has always been pointed out as the key player in first-pass metabolism, more recent studies have shown that metabolism in the intestine can also play a substantial role in this process.^{53, 54} The intestine expresses multiple metabolizing enzymes, including cytochrome P450 (CYP) metabolizing enzymes, uridine 5'-diphospho glucuronosyltransferases (UGT), glutathione S-transferases (GST), and sulfotransferases (SULT), which produce oxidized (Phase I), and glucuronide-, glutathione-, and sulfate-conjugated (Phase II) metabolites, respectively.⁵⁵ CYP3A4 is the most abundant CYP in the intestine, and it has overlapping substrate specificity with the efflux transporter P-gp. Multiple studies have shown that CYP3A4 and P-gp cooperate in limiting the absorption of shared substrates.⁵⁶ Many of the Phase II glucuronide-, sulfate-, and glutathione-conjugated products are substrates of MRPs and BCRP.⁵ One can imagine that these efflux transporters and Phase II metabolizing enzymes work in concert to rapidly eliminate harmful compounds from the body. Indeed, interplay between multiple enzyme-transporter combinations has been shown for metabolism and transport of different compounds, *e.g.* GST-MRP1 for 1-chloro-2,3-dinitrobenzene, SULT-BCRP for 4-methylumbelliferone, UGT-BCRP for apigenin and 4-methylumbelliferone, and UGT-MRP2/3 for raloxifene and morphine.⁵⁷⁻⁶² Some studies even suggest a synergistic interplay between these proteins, in which transport of metabolites increases the total metabolite formation.^{57, 63} The theory behind this synergism is based on the possibility that transport of metabolites from cells increases the metabolic rate through a reduction of product inhibition of the enzyme by intracellular metabolites. However, this hypothesis of synergistic interplay needs further experimental support by using *in vitro* model systems, in which an enzyme and a transporter can be introduced or knocked out individually or together, to study the effect of transport on total UGT-mediated metabolism.

Expression and function of efflux transporters at the blood-brain barrier

After passage of the intestine, the liver, and, subsequently, entering the general circulation, the final step for a CNS drug to reach the brain is passage through the blood-brain barrier (BBB). The BBB consists of endothelial cells that are tightly coupled to each other by tight junctions and which reside on a basal membrane that is surrounded by astrocytes. Together

with efflux transporters that are expressed at the luminal surface of the endothelial cells, a barrier arises that protects the brain from potentially harmful compounds, including drugs.⁶⁴⁻⁶⁷ The efflux transporters expressed at the luminal membrane of the human BBB are P-gp, BCRP, MRP1, MRP4, and MRP5, of which BCRP and P-gp have the highest abundance (Fig. 3).⁶⁸⁻⁷⁴

The importance of efflux transporters at the BBB in determining the brain concentration of drugs was discovered by a true case of serendipity. Schinkel *et al.* had developed *Mdr1a*^{-/-} knockout mice to evaluate the physiological role of Mdr1a, one of the orthologues of P-gp in mice.⁷⁵ In order to treat a mite infestation they sprayed the whole population of bred mice with ivermectin, which is normally a safe procedure. However, at this occasion it caused several deaths among the animals, which appeared to be due to neurotoxicity. Genotyping revealed that all deceased animals were *Mdr1a*^{-/-} knockout mice, indicating that Mdr1a plays an important role in protecting the CNS against this drug. Further analysis showed that this was due to efflux of ivermectin via Mdr1a at the BBB, thereby reducing the brain concentration of this compound. Additional studies using knockout animals for different efflux transporters showed the importance of P-gp, BCRP, and MRP4 in reducing the brain concentrations of various types of drug, of which P-gp is considered to be the most important gatekeeper of the brain.⁷⁶⁻⁸³ In humans, efflux transporters at the BBB are thought to limit the brain penetration of drugs that should enter the brain, such as anti-HIV medication, anti-epileptic and anti-cancer drugs, anti-depressants, and anti-psychotics.⁸⁴⁻⁸⁶ Therefore, transport of lead compounds via efflux transporters at the BBB is taken into consideration in the early development of CNS drugs, to prevent failure in later stages of drug development because of poor brain penetration.⁴

Difficulties in the development of CNS drugs

Although the demand for new CNS drugs is growing, the success rate of the clinical development of these drugs is lower than for drugs with other indications.⁸⁷ As explained above, the development of new CNS drugs is complicated because they need to be able to pass two barriers, the intestine and the BBB. A higher lipophilicity of compounds would favour the passage over membranes and diffusion into the brain tissue.⁸⁸ On the other hand, higher lipophilicity limits the solubility of compounds, thereby decreasing oral bioavailability.⁸⁸ Therefore, research has focused on other ways to get these compounds into the brain, for example through transport by uptake transporters in combination with limited transport by efflux transporters at the intestinal wall or BBB.^{88, 89} However, optimization of these compound characteristics to improve its membrane penetration might also adversely affect the target efficacy of the compound. Therefore, prodrugs are being developed that have improved oral availability or BBB penetration, *e.g.* due to increased water solubility, lipophilicity, or transport via uptake transporters, and that are



converted to the parent compound by local conditions or enzymes at their site of action.^{88, 89} In addition, there have also been efforts to develop nanotechnologies that can aid in the delivery of drugs at the intestine or the BBB.⁹⁰ The project described in this thesis is part of the Top Institute Pharma project T5-105, which used nanotechnologies to improve oral availability and brain penetration of CNS drugs, focusing on cannabinoid type 1 (CB1) receptor antagonists.⁹¹⁻⁹⁴

Development of CB1 receptor antagonists as an anti-obesity drug

Obesity is an illness defined by abnormal or excessive body fat accumulation that presents a risk to health. It is becoming an increasing burden to society and at least 2.8 million adults die each year as a result of overweight or obesity.⁹⁵ This is mainly due to co-morbidities that occur with increased intra-abdominal visceral body fat due to abnormal metabolic factors, leading to insulin resistance and type 2 diabetes, atherosclerosis, and cardiovascular disease.⁹⁶ During the past three decades, increasing evidence has pointed towards an important role for the endocannabinoid system, of which the CB1 receptor is one of the key players, in the development of obesity.

The CB1 receptor is expressed in central and peripheral tissues, such as brain, spinal cord, adipose tissue, skeletal muscle, liver, gut, and pancreas.⁹⁹ It belongs to the class A of G-protein coupled receptors and it has several natural agonists, of which the endocannabinoids anandamide and 2-arachidonoylglycerol and the cannabinoid derived from cannabis, Δ^9 -tetrahydrocannabinol, have been used frequently to study the physiological function

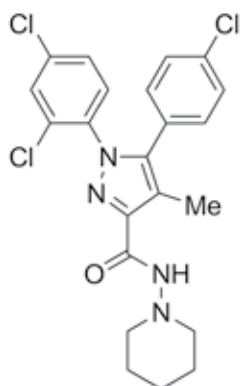


Figure 4 Chemical structure of rimonabant (Accomplia®)

Rimonabant was the first and only CB1 receptor antagonist that was released on the market to date.

of the receptor. Activation of the CB1 receptor reduces pain, anxiety, body temperature, blood pressure, gastrointestinal motility, hormone production, and smooth muscle tone, and induces neuroprotective effects.⁹⁸ Complementary to the known CB1 receptor agonists, Sanofi-Aventis developed a CB1 receptor antagonist, *N*-(piperidin-1-yl)-5-(4-chlorophenyl)-1-(2,4-dichlorophenyl)-4-methyl-1*H*-pyrazole-3-carboxamidehydrochloride (Fig. 4), that had a 1000-fold higher inhibitory affinity for the CB1 receptor than for the CB2 receptor.¹⁰⁰ This antagonist, which actually turned out to be an inverse agonist, was named SR141716A or rimonabant, and because of its high selectivity for the CB1 receptor it could be used as an additional tool to understand the physiological functions of the CB1 receptor.¹⁰⁰

One of these studies, by Arnone *et al.* (1997), showed that rimonabant reduces food and ethanol intake in mice.¹⁰¹ Further studies confirmed the involvement of the CB1 receptor in regulation of feeding behaviour, metabolism, and energy balance through central and peripheral mechanisms in several tissues (summarized in Table 2).^{97, 98} In obesity, the endocannabinoid system appears to be hyperactivated, contributing to dyslipidemia, insulin resistance, and overweight. For this reason, it was hypothesized that antagonism of the CB1 receptor would reduce food intake and improve cardiometabolic risk factors, and therefore could serve as an anti-obesity therapy.^{97, 99} Indeed, in rodents, antagonism of the receptor with rimonabant led to reduced food intake and weight reduction.¹⁰² Subsequently, one CB1 receptor antagonist was available for therapy and several CB1 receptor antagonists were

Table 2 Responses to modulation of the endocannabinoid system via the CB1 receptor (adapted from Andre *et al.*)⁹⁶⁻⁹⁸

Site of action	Stimulation	Overactivation	Inhibition
Brain	↑ food intake	↑ body weight / waist circumference	↓ food intake / waist circumference
Gastrointestinal tract	↓ satiety ↑ food assimilation	↑ body weight / waist circumference	
Liver	↑ lipogenesis	↑ dyslipidemia ↑ steatosis	↓ lipogenesis
Pancreas ^a	↑ insulin	↑ insulin resistance	↓ insulin hypersecretion
Muscle	↓ glucose uptake ↓ fatty acid oxidation	↑ insulin resistance ↓ energy expenditure	↓ insulin resistance ↑ glucose uptake ↑ energy expenditure
Adipose tissue	↓ adiponectin ↓ leptin ↑ lipogenesis	↑ visceral fat ↑ dyslipidemia ↑ insulin resistance	↑ adiponectin ↑ lipolysis ↓ fat energy storage ↑ thermogenesis

^a CB2 receptor is also expressed in pancreas and there is still controversy about the respective role of CB1 or CB2 activation in insulin secretion.



under development for the treatment of obesity at the start of this PhD project in January 2008.^{102, 103}

Rimonabant (Acomplia[®]) was the first and only selective CB1 receptor antagonist for therapeutic use in humans and was released on the European market in June 2006. Clinical studies in humans showed that rimonabant reduces body weight and waist circumference, and improves cardiometabolic risk factors, including triglycerides, low and high density lipoprotein-cholesterol, fasting glucose, and glycosylated hemoglobin A1c levels.^{104, 105} However, meta-analysis of the clinical studies performed with rimonabant, by Christensen and colleagues (2007) and the Food and Drug Administration (FDA), revealed that rimonabant treatment was also associated with more psychiatric adverse events, such as depressive mood disorders, anxiety, suicidal ideation, and sleeping disorders.^{106, 107} These findings prevented approval of rimonabant for the US market by the FDA in July 2007. In the same period, the European Medicines Agency (EMA) decided to add restrictions for prescription of the drug, and after additional clinical studies, it decided to suspend the drug from the European market in October 2008 due to the neuropsychiatric side effects.

Using efflux transporters in the development of peripheral CB1 receptor antagonists

Some of the metabolic effects of rimonabant were not entirely explained by weight loss, but appear to be due to an effect of rimonabant on CB1 receptors in peripheral tissues (Table 2).⁹⁶ On the other hand, the psychiatric side effects of rimonabant are caused by inhibition of the CB1 receptor in the brain. Therefore, it was hypothesized that peripheral CB1 receptor antagonists that do not enter the brain could still have beneficial effects on cardiometabolic risk factors without the psychiatric side effects.^{99, 103, 108}

This provided an interesting challenge: to develop CB1 receptor antagonists with limited brain penetration. As emphasized in the introduction, efflux transporters can be involved in limiting the access of drugs to the brain. Therefore, it would be interesting to use this brain-limiting mechanism in the development of peripheral CB1 receptor antagonists to reduce their brain penetration, and, consequently, their psychiatric side effects. Transport via efflux transporters at the BBB has already been proven to be a useful trait for some drugs, such as domperidone and loperamide, that exert beneficial effects in the periphery, but would have had unwanted side effects if distributed to the brain.^{64, 109, 110} If efflux transport proves to be useful to restrict CB1 receptor antagonists to the periphery, it might be used as a selection criterion in early drug development of these compounds.

Aim of this thesis

The research that resulted in this thesis was focused on the identification and characterization of efflux transporters that might play a role in the disposition of CB1 receptor antagonists at two important barriers in the body: the intestinal wall and the blood-brain barrier (BBB). To identify potential peripheral CB1 receptor antagonists, we investigated a series of 3,4-diarylpyrazoline CB1 receptor antagonists for their interaction with the efflux transporters MRP1-4, and P-gp. The results of these studies are described in Chapters 2 and 3.

To further investigate the interplay between drug metabolizing enzymes and transporters in the intestine, we used a model compound, 7-hydroxycoumarin (7-HC), and investigated which transporters are involved in the transport of the glucuronide metabolite of 7-HC. In collaboration with one of the TI Pharma project partners, the Department of Pharmacy of the University of Groningen (Prof. dr. Groothuis), we investigated the effect of metabolite transport via efflux transporters on the function of UGTs *in vitro* using HEK293 cells, and *ex vivo* using human intestinal tissue. The results of these studies are described in Chapters 4 and 5.

Finally, in Chapter 6 of this thesis we describe the molecular mechanisms of substrate transport by one of the major intestinal and BBB transporters, MRP4, in more detail. We aimed to elucidate the importance of the amino acids Phe³⁶⁸ in TM6, and Trp⁹⁹⁵ and Arg⁹⁹⁸ in TM12 of MRP4 for the transport of different substrates via this transporter.

The implications of the work presented in this thesis for the development of CB1 receptor antagonists as anti-obesity drugs and, in greater perspective, for CNS drug development are discussed in Chapter 7.

References

1. Lipinski, C. A.; Lombardo, F.; Dominy, B. W.; Feeney, P. J. Experimental and computational approaches to estimate solubility and permeability in drug discovery and development settings. *Adv. Drug Deliv. Rev.* **2001**, *46*, 3-26.
2. Szakács, G.; Váradi, A.; Özvegy-Laczka, C.; Sarkadi, B. The role of ABC transporters in drug absorption, distribution, metabolism, excretion and toxicity (ADME-Tox). *Drug Discov. Today* **2008**, *13*, 379-393.
3. Ayrton, A.; Morgan, P. Role of transport proteins in drug absorption, distribution and excretion. *Xenobiotica* **2001**, *31*, 469-497.
4. Giacomini, K. M.; Huang, S. M.; Tweedie, D. J.; Benet, L. Z.; Brouwer, K. L.; Chu, X. *et al.* Membrane transporters in drug development. *Nat. Rev. Drug Discov.* **2010**, *9*, 215-236.
5. Zhou, S. F.; Wang, L. L.; Di, Y. M.; Xue, C. C.; Duan, W.; Li, C. G. *et al.* Substrates and inhibitors of human multidrug resistance associated proteins and the implications in drug development. *Curr. Med. Chem.* **2008**, *15*, 1981-2039.
6. Schinkel, A. H.; Jonker, J. W. Mammalian drug efflux transporters of the ATP binding cassette (ABC) family: an overview. *Adv. Drug Deliv. Rev.* **2003**, *55*, 3-29.
7. Loo, T. W.; Clarke, D. M. Mutational analysis of ABC proteins. *Arch. Biochem. Biophys.* **2008**, *476*, 51-64.
8. Ambudkar, S. V.; Kim, I. W.; Sauna, Z. E. The power of the pump: mechanisms of action of P-glycoprotein (ABCB1). *Eur. J. Pharm. Sci.* **2006**, *27*, 392-400.
9. Deeley, R. G.; Cole, S. P. Substrate recognition and transport by multidrug resistance protein 1 (ABCC1). *FEBS Lett.* **2006**, *580*, 1103-1111.
10. Deeley, R. G.; Westlake, C.; Cole, S. P. Transmembrane transport of endo- and xenobiotics by mammalian



- ATP-binding cassette multidrug resistance proteins. *Physiol Rev.* **2006**, *86*, 849-899.
11. Aller, S. G.; Yu, J.; Ward, A.; Weng, Y.; Chittaboina, S.; Zhuo, R. *et al.* Structure of P-glycoprotein reveals a molecular basis for poly-specific drug binding. *Science* **2009**, *323*, 1718-1722.
 12. Flens, M. J.; Zaman, G. J.; van der Valk, P.; Izquierdo, M. A.; Schroeijers, A. B.; Scheffer, G. L. *et al.* Tissue distribution of the multidrug resistance protein. *Am. J. Pathol.* **1996**, *148*, 1237-1247.
 13. Maliepaard, M.; Scheffer, G. L.; Faneyte, I. F.; van Gastelen, M. A.; Pijnenborg, A. C.; Schinkel, A. H. *et al.* Subcellular localization and distribution of the breast cancer resistance protein transporter in normal human tissues. *Cancer Res.* **2001**, *61*, 3458-3464.
 14. Nies, A. T.; Keppler, D. The apical conjugate efflux pump ABC2 (MRP2). *Pflugers Arch.* **2007**, *453*, 643-659.
 15. Russel, F. G.; Koenderink, J. B.; Masereeuw, R. Multidrug resistance protein 4 (MRP4/ABCC4): a versatile efflux transporter for drugs and signalling molecules. *Trends Pharmacol. Sci.* **2008**, *29*, 200-207.
 16. Scheffer, G. L.; Kool, M.; de Haas, M.; de Vree, J. M.; Pijnenborg, A. C.; Bosman, D. K. *et al.* Tissue distribution and induction of human multidrug resistant protein 3. *Lab Invest* **2002**, *82*, 193-201.
 17. Chan, L. M.; Lowes, S.; Hirst, B. H. The ABCs of drug transport in intestine and liver: efflux proteins limiting drug absorption and bioavailability. *Eur. J. Pharm. Sci.* **2004**, *21*, 25-51.
 18. Lennernäs, H. Intestinal permeability and its relevance for absorption and elimination. *Xenobiotica* **2007**, *37*, 1015-1051.
 19. Murakami, T.; Takano, M. Intestinal efflux transporters and drug absorption. *Expert. Opin. Drug Metab Toxicol.* **2008**, *4*, 923-939.
 20. Dietrich, C. G.; Geier, A.; Oude Elferink, R. P. ABC of oral bioavailability: transporters as gatekeepers in the gut. *Gut* **2003**, *52*, 1788-1795.
 21. Varma, M. V.; Ambler, C. M.; Ullah, M.; Rotter, C. J.; Sun, H.; Litchfield, J. *et al.* Targeting intestinal transporters for optimizing oral drug absorption. *Curr. Drug Metab* **2010**, *11*, 730-742.
 22. Peng, K. C.; Cluzeaud, F.; Bens, M.; Duong Van Huyen, J. P.; Wioland, M. A.; Lacave, R. *et al.* Tissue and cell distribution of the multidrug resistance-associated protein (MRP) in mouse intestine and kidney. *J. Histochem. Cytochem.* **1999**, *47*, 757-768.
 23. Blokzijl, H.; Vander Borgh, S.; Bok, L. I.; Libbrecht, L.; Geuken, M.; van den Heuvel, F. A. *et al.* Decreased P-glycoprotein (P-gp/MDR1) expression in inflamed human intestinal epithelium is independent of PXR protein levels. *Inflamm. Bowel. Dis.* **2007**, *13*, 710-720.
 24. Thiebaut, F.; Tsuruo, T.; Hamada, H.; Gottesman, M. M.; Pastan, I.; Willingham, M. C. Cellular localization of the multidrug-resistance gene product P-glycoprotein in normal human tissues. *Proc. Natl. Acad. Sci. U. S. A* **1987**, *84*, 7735-7738.
 25. van Aubel, R. A.; Hartog, A.; Bindels, R. J.; Van Os, C. H.; Russel, F. G. Expression and immunolocalization of multidrug resistance protein 2 in rabbit small intestine. *Eur. J. Pharmacol.* **2000**, *400*, 195-198.
 26. Fromm, M. F.; Kauffmann, H. M.; Fritz, P.; Burk, O.; Kroemer, H. K.; Warzok, R. W. *et al.* The effect of rifampin treatment on intestinal expression of human MRP transporters. *Am. J. Pathol.* **2000**, *157*, 1575-1580.
 27. Rost, D.; Mahner, S.; Sugiyama, Y.; Stremmel, W. Expression and localization of the multidrug resistance-associated protein 3 in rat small and large intestine. *Am. J. Physiol Gastrointest. Liver Physiol* **2002**, *282*, G720-G726.
 28. Ming, X.; Thakker, D. R. Role of basolateral efflux transporter MRP4 in the intestinal absorption of the antiviral drug adefovir dipivoxil. *Biochem. Pharmacol.* **2010**, *79*, 455-462.
 29. Li, C.; Krishnamurthy, P. C.; Penmatsa, H.; Marrs, K. L.; Wang, X. Q.; Zaccolo, M. *et al.* Spatiotemporal coupling of cAMP transporter to CFTR chloride channel function in the gut epithelia. *Cell* **2007**, *131*, 940-951.
 30. Johnson, B. M.; Zhang, P.; Schuetz, J. D.; Brouwer, K. L. Characterization of transport protein expression in multidrug resistance-associated protein (Mrp) 2-deficient rats. *Drug Metab Dispos.* **2006**, *34*, 556-562.
 31. Prime-Chapman, H. M.; Fearn, R. A.; Cooper, A. E.; Moore, V.; Hirst, B. H. Differential multidrug resistance-associated protein 1 through 6 isoform expression and function in human intestinal epithelial Caco-2 cells. *J. Pharmacol. Exp. Ther.* **2004**, *311*, 476-484.
 32. Taipalensuu, J.; Törnblom, H.; Lindberg, G.; Einarsson, C.; Sjöqvist, F.; Melhus, H. *et al.* Correlation of gene expression of ten drug efflux proteins of the ATP-binding cassette transporter family in normal human jejunum and in human intestinal epithelial Caco-2 cell monolayers. *J. Pharmacol. Exp. Ther.* **2001**, *299*, 164-170.
 33. Zimmermann, C.; Gutmann, H.; Hruz, P.; Gutzwiller, J. P.; Beglinger, C.; Drewe, J. Mapping of multidrug resistance gene 1 and multidrug resistance-associated protein isoform 1 to 5 mRNA expression along the human intestinal tract. *Drug Metab Dispos.* **2005**, *33*, 219-224.
 34. Englund, G.; Rorsman, F.; Ronnblom, A.; Karlbom, U.; Lazorova, L.; Grasjo, J. *et al.* Regional levels of drug transporters along the human intestinal tract: co-expression of ABC and SLC transporters and comparison with Caco-2 cells. *Eur. J. Pharm. Sci.* **2006**, *29*, 269-277.
 35. Berggren, S.; Gall, C.; Wolfnitz, N.; Ekelund, M.; Karlbom, U.; Hoogstraate, J. *et al.* Gene and protein expression of P-glycoprotein, MRP1, MRP2, and CYP3A4 in the small and large human intestine. *Mol. Pharm.* **2007**, *4*,

- 252-257.
36. Seithel, A.; Karlsson, J.; Hilgendorf, C.; Björquist, A.; Ungell, A. L. Variability in mRNA expression of ABC- and SLC-transporters in human intestinal cells: comparison between human segments and Caco-2 cells. *Eur. J. Pharm. Sci.* **2006**, *28*, 291-299.
 37. Thorn, M.; Finnstrom, N.; Lundgren, S.; Rane, A.; Loof, L. Cytochromes P450 and MDR1 mRNA expression along the human gastrointestinal tract. *Br. J. Clin. Pharmacol.* **2005**, *60*, 54-60.
 38. Mouly, S.; Paine, M. F. P-glycoprotein increases from proximal to distal regions of human small intestine. *Pharm. Res.* **2003**, *20*, 1595-1599.
 39. Oostendorp, R. L.; Beijnen, J. H.; Schellens, J. H. The biological and clinical role of drug transporters at the intestinal barrier. *Cancer Treat. Rev.* **2009**, *35*, 137-147.
 40. Igel, S.; Drescher, S.; Mürdter, T.; Hofmann, U.; Heinkele, G.; Tegude, H. *et al.* Increased absorption of digoxin from the human jejunum due to inhibition of intestinal transporter-mediated efflux. *Clin. Pharmacokinet.* **2007**, *46*, 777-785.
 41. Kitamura, Y.; Hirouchi, M.; Kusuhara, H.; Schuetz, J. D.; Sugiyama, Y. Increasing systemic exposure of methotrexate by active efflux mediated by multidrug resistance-associated protein 3 (Mrp3/abcc3). *J. Pharmacol. Exp. Ther.* **2008**, *327*, 465-473.
 42. Bardelmeijer, H. A.; Beijnen, J. H.; Brouwer, K. R.; Rosing, H.; Nuijten, W. J.; Schellens, J. H. *et al.* Increased oral bioavailability of paclitaxel by GF120918 in mice through selective modulation of P-glycoprotein. *Clin. Cancer Res.* **2000**, *6*, 4416-4421.
 43. Malingre, M. M.; Beijnen, J. H.; Rosing, H.; Koopman, F. J.; Jewell, R. C.; Paul, E. M. *et al.* Co-administration of GF120918 significantly increases the systemic exposure to oral paclitaxel in cancer patients. *Br. J. Cancer* **2001**, *84*, 42-47.
 44. Meerum Terwogt, J. M.; Malingré, M. M.; Beijnen, J. H.; ten Bokkel Huinink, W. W.; Rosing, H.; Koopman, F. J. *et al.* Coadministration of oral cyclosporin A enables oral therapy with paclitaxel. *Clin. Cancer Res.* **1999**, *5*, 3379-3384.
 45. Jonker, J. W.; Smit, J. W.; Brinkhuis, R. F.; Maliapaard, M.; Beijnen, J. H.; Schellens, J. H. *et al.* Role of breast cancer resistance protein in the bioavailability and fetal penetration of topotecan. *J. Natl. Cancer Inst.* **2000**, *92*, 1651-1656.
 46. Poller, B.; Wagenaar, E.; Tang, S. C.; Schinkel, A. H. Double-transduced MDCKII cells to study human P-glycoprotein (ABCB1) and breast cancer resistance protein (ABCG2) interplay in drug transport across the blood-brain barrier. *Mol. Pharm.* **2011**, *8*, 571-582.
 47. Kruijtz, C. M.; Beijnen, J. H.; Rosing, H.; ten Bokkel Huinink, W. W.; Schot, M.; Jewell, R. C. *et al.* Increased oral bioavailability of topotecan in combination with the breast cancer resistance protein and P-glycoprotein inhibitor GF120918. *J. Clin. Oncol.* **2002**, *20*, 2943-2950.
 48. Dietrich, C. G.; de Waart, D. R.; Ottenhoff, R.; Schoots, I. G.; Elferink, R. P. Increased bioavailability of the food-derived carcinogen 2-amino-1-methyl-6-phenylimidazo[4,5-b]pyridine in MRP2-deficient rats. *Mol. Pharmacol.* **2001**, *59*, 974-980.
 49. Hilgendorf, C.; Ahlin, G.; Seithel, A.; Artursson, P.; Ungell, A. L.; Karlsson, J. Expression of thirty-six drug transporter genes in human intestine, liver, kidney, and organotypic cell lines. *Drug Metab Dispos.* **2007**, *35*, 1333-1340.
 50. Yasui-Furukori, N.; Saito, M.; Nioka, T.; Inoue, Y.; Sato, Y.; Kaneko, S. Effect of itraconazole on pharmacokinetics of paroxetine: the role of gut transporters. *Ther. Drug Monit.* **2007**, *29*, 45-48.
 51. Nakagami, T.; Yasui-Furukori, N.; Saito, M.; Tateishi, T.; Kaneo, S. Effect of verapamil on pharmacokinetics and pharmacodynamics of risperidone: in vivo evidence of involvement of P-glycoprotein in risperidone disposition. *Clin. Pharmacol. Ther.* **2005**, *78*, 43-51.
 52. Kharasch, E. D.; Hoffer, C.; Whittington, D.; Sheffels, P. Role of P-glycoprotein in the intestinal absorption and clinical effects of morphine. *Clin. Pharmacol. Ther.* **2003**, *74*, 543-554.
 53. Fisher, M. B.; Labissiere, G. The role of the intestine in drug metabolism and pharmacokinetics: an industry perspective. *Curr. Drug Metab* **2007**, *8*, 694-699.
 54. Glaeser, H.; Drescher, S.; Hofmann, U.; Heinkele, G.; Somogyi, A. A.; Eichelbaum, M. *et al.* Impact of concentration and rate of intraluminal drug delivery on absorption and gut wall metabolism of verapamil in humans. *Clin. Pharmacol. Ther.* **2004**, *76*, 230-238.
 55. Ritter, J. K. Intestinal UGTs as potential modifiers of pharmacokinetics and biological responses to drugs and xenobiotics. *Expert. Opin. Drug Metab Toxicol.* **2007**, *3*, 93-107.
 56. van Waterschoot, R. A.; Schinkel, A. H. A critical analysis of the interplay between cytochrome P450 3A and P-glycoprotein: recent insights from knockout and transgenic mice. *Pharmacol. Rev.* **2011**, *63*, 390-410.
 57. Adachi, Y.; Suzuki, H.; Schinkel, A. H.; Sugiyama, Y. Role of breast cancer resistance protein (Bcrp1/Abcg2) in the extrusion of glucuronide and sulfate conjugates from enterocytes to intestinal lumen. *Mol. Pharmacol.* **2005**, *67*, 923-928.
 58. Jiang, W.; Xu, B.; Wu, B.; Yu, R.; Hu, M. UGT1A9-overexpressing HeLa Cells Is a Appropriate Tool to Delineate



- the Kinetic Interplay between BCRP and UGT and to Rapidly Identify the Glucuronide Substrates of BCRP. *Drug Metab Dispos.* **2011**.
59. Kosaka, K.; Sakai, N.; Endo, Y.; Fukuhara, Y.; Tsuda-Tsukimoto, M.; Ohtsuka, T. *et al.* Impact of intestinal glucuronidation on the pharmacokinetics of raloxifene. *Drug Metab Dispos.* **2011**, *39*, 1495-1502.
 60. van de Wetering K.; Zelcer, N.; Kuil, A.; Feddema, W.; Hillebrand, M.; Vlaming, M. L. *et al.* Multidrug resistance proteins 2 and 3 provide alternative routes for hepatic excretion of morphine-glucuronides. *Mol. Pharmacol.* **2007**, *72*, 387-394.
 61. Zelcer, N.; Van de Wetering, K.; Hillebrand, M.; Sarton, E.; Kuil, A.; Wielinga, P. R. *et al.* Mice lacking multidrug resistance protein 3 show altered morphine pharmacokinetics and morphine-6-glucuronide antinociception. *Proc. Natl. Acad. Sci. U. S. A* **2005**, *102*, 7274-7279.
 62. Diah, S. K.; Smitherman, P. K.; Townsend, A. J.; Morrow, C. S. Detoxification of 1-chloro-2,4-dinitrobenzene in MCF7 breast cancer cells expressing glutathione S-transferase P1-1 and/or multidrug resistance protein 1. *Toxicol. Appl. Pharmacol.* **1999**, *157*, 85-93.
 63. Jiang, W.; Xu, B.; Wu, B.; Yu, R.; Hu, M. UGT1A9-overexpressing HeLa Cells Is a Appropriate Tool to Delineate the Kinetic Interplay between BCRP and UGT and to Rapidly Identify the Glucuronide Substrates of BCRP. *Drug Metab Dispos.* **2011**.
 64. Löscher, W.; Potschka, H. Drug resistance in brain diseases and the role of drug efflux transporters. *Nat. Rev. Neurosci.* **2005**, *6*, 591-602.
 65. Abbott, N. J.; Rönnbäck, L.; Hansson, E. Astrocyte-endothelial interactions at the blood-brain barrier. *Nat. Rev. Neurosci.* **2006**, *7*, 41-53.
 66. Shen, S.; Zhang, W. ABC transporters and drug efflux at the blood-brain barrier. *Rev. Neurosci.* **2010**, *21*, 29-53.
 67. Begley, D. J. ABC transporters and the blood-brain barrier. *Curr. Pharm. Des* **2004**, *10*, 1295-1312.
 68. Nies, A. T.; Jedlitschky, G.; König, J.; Herold-Mende, C.; Steiner, H. H.; Schmitt, H. P. *et al.* Expression and immunolocalization of the multidrug resistance proteins, MRP1-MRP6 (ABCC1-ABCC6), in human brain. *Neuroscience* **2004**, *129*, 349-360.
 69. Shawahna, R.; Uchida, Y.; Declèves, X.; Ohtsuki, S.; Yousif, S.; Dauchy, S. *et al.* Transcriptomic and quantitative proteomic analysis of transporters and drug metabolizing enzymes in freshly isolated human brain microvessels. *Mol. Pharm.* **2011**, *8*, 1332-1341.
 70. Dauchy, S.; Dutheil, F.; Weaver, R. J.; Chassoux, F.; Daumas-Duport, C.; Couraud, P. O. *et al.* ABC transporters, cytochromes P450 and their main transcription factors: expression at the human blood-brain barrier. *J. Neurochem.* **2008**, *107*, 1518-1528.
 71. Uchida, Y.; Ohtsuki, S.; Katsukura, Y.; Ikeda, C.; Suzuki, T.; Kamiie, J. *et al.* Quantitative targeted absolute proteomics of human blood-brain barrier transporters and receptors. *J. Neurochem.* **2011**, *117*, 333-345.
 72. Cordon-Cardo, C.; O'Brien, J. P.; Casals, D.; Rittman-Grauer, L.; Biedler, J. L.; Melamed, M. R. *et al.* Multidrug-resistance gene (P-glycoprotein) is expressed by endothelial cells at blood-brain barrier sites. *Proc. Natl. Acad. Sci. U. S. A* **1989**, *86*, 695-698.
 73. Cooray, H. C.; Blackmore, C. G.; Maskell, L.; Barrand, M. A. Localisation of breast cancer resistance protein in microvessel endothelium of human brain. *Neuroreport* **2002**, *13*, 2059-2063.
 74. Virgintino, D.; Robertson, D.; Errede, M.; Benagiano, V.; Girolamo, F.; Maiorano, E. *et al.* Expression of P-glycoprotein in human cerebral cortex microvessels. *J. Histochem. Cytochem.* **2002**, *50*, 1671-1676.
 75. Schinkel, A. H.; Smit, J. J.; van Tellingen, O.; Beijnen, J. H.; Wagenaar, E.; van Deemter, L. *et al.* Disruption of the mouse *mdr1a* P-glycoprotein gene leads to a deficiency in the blood-brain barrier and to increased sensitivity to drugs. *Cell* **1994**, *77*, 491-502.
 76. Dagenais, C.; Zong, J.; Ducharme, J.; Pollack, G. M. Effect of *mdr1a* P-glycoprotein gene disruption, gender, and substrate concentration on brain uptake of selected compounds. *Pharm. Res.* **2001**, *18*, 957-963.
 77. Doran, A.; Obach, R. S.; Smith, B. J.; Hosea, N. A.; Becker, S.; Callegari, E. *et al.* The impact of P-glycoprotein on the disposition of drugs targeted for indications of the central nervous system: evaluation using the MDR1A/1B knockout mouse model. *Drug Metab Dispos.* **2005**, *33*, 165-174.
 78. Linnet, K.; Ejlsing, T. B. A review on the impact of P-glycoprotein on the penetration of drugs into the brain. Focus on psychotropic drugs. *Eur. Neuropsychopharmacol.* **2008**, *18*, 157-169.
 79. Uhr, M.; Ebinger, M.; Rosenhagen, M. C.; Grauer, M. T. The anti-Parkinson drug budipine is exported actively out of the brain by P-glycoprotein in mice. *Neurosci. Lett.* **2005**, *383*, 73-76.
 80. Shaik, N.; Giri, N.; Pan, G.; Elmquist, W. F. P-glycoprotein-mediated active efflux of the anti-HIV1 nucleoside abacavir limits cellular accumulation and brain distribution. *Drug Metab Dispos.* **2007**, *35*, 2076-2085.
 81. Chen, C.; Hanson, E.; Watson, J. W.; Lee, J. S. P-glycoprotein limits the brain penetration of nonsedating but not sedating H1-antagonists. *Drug Metab Dispos.* **2003**, *31*, 312-318.
 82. Agarwal, S.; Sane, R.; Ohlfest, J. R.; Elmquist, W. F. The role of the breast cancer resistance protein (ABCG2) in the distribution of sorafenib to the brain. *J. Pharmacol. Exp. Ther.* **2011**, *336*, 223-233.
 83. Leggas, M.; Adachi, M.; Scheffer, G. L.; Sun, D.; Wielinga, P.; Du, G. *et al.* Mrp4 confers resistance to topotecan

- and protects the brain from chemotherapy. *Mol. Cell Biol.* **2004**, *24*, 7612-7621.
84. Potschka, H. Transporter hypothesis of drug-resistant epilepsy: challenges for pharmacogenetic approaches. *Pharmacogenomics*. **2010**, *11*, 1427-1438.
 85. Breedveld, P.; Beijnen, J. H.; Schellens, J. H. Use of P-glycoprotein and BCRP inhibitors to improve oral bioavailability and CNS penetration of anticancer drugs. *Trends Pharmacol. Sci.* **2006**, *27*, 17-24.
 86. Namanja, H. A.; Emmert, D.; Davis, D. A.; Campos, C.; Miller, D. S.; Hrycyna, C. A. *et al.* Toward Eradicating HIV Reservoirs in the Brain: Inhibiting P-Glycoprotein at the Blood-Brain Barrier with Prodrug Abacavir Dimers. *J. Am. Chem. Soc.* **2011**.
 87. Kola, I.; Landis, J. Can the pharmaceutical industry reduce attrition rates? *Nat. Rev. Drug Discov.* **2004**, *3*, 711-715.
 88. Müller, C. E. Prodrug approaches for enhancing the bioavailability of drugs with low solubility. *Chem. Biodivers.* **2009**, *6*, 2071-2083.
 89. Rautio, J.; Laine, K.; Gynther, M.; Savolainen, J. Prodrug approaches for CNS delivery. *AAPS. J.* **2008**, *10*, 92-102.
 90. Wong, H. L.; Wu, X. Y.; Bendayan, R. Nanotechnological advances for the delivery of CNS therapeutics. *Adv. Drug Deliv. Rev.* **2011**.
 91. van Rooy, I.; Mastrobattista, E.; Storm, G.; Hennink, W. E.; Schiffelers, R. M. Comparison of five different targeting ligands to enhance accumulation of liposomes into the brain. *J. Control Release* **2011**, *150*, 30-36.
 92. Georgieva, J. V.; Kalicharan, D.; Couraud, P. O.; Romero, I. A.; Weksler, B.; Hoekstra, D. *et al.* Surface characteristics of nanoparticles determine their intracellular fate in and processing by human blood-brain barrier endothelial cells in vitro. *Mol. Ther.* **2011**, *19*, 318-325.
 93. de Waard H.; Frijlink, H. W.; Hinrichs, W. L. Bottom-up preparation techniques for nanocrystals of lipophilic drugs. *Pharm. Res.* **2011**, *28*, 1220-1223.
 94. Brinkhuis, R. P.; Rutjes, F. P. J. T.; van Hest, J. C. M. Polymeric vesicles in biomedical applications. *Polymer Chemistry* **2011**, *2*, 1449-1462.
 95. World Health Organization. Obesity and overweight, Fact sheet No. 311. 2011. Ref Type: Internet Communication
 96. Di Marzo, V.; Després, J. P. CB1 antagonists for obesity - what lessons have we learned from rimonabant? *Nat. Rev. Endocrinol.* **2009**, *5*, 633-638.
 97. Silvestri, C.; Ligresti, A.; Di Marzo, V. Peripheral effects of the endocannabinoid system in energy homeostasis: Adipose tissue, liver and skeletal muscle. *Rev. Endocr. Metab. Disord.* **2011**, *12*, 153-162.
 98. André, A.; Gonthier, M. P. The endocannabinoid system: its roles in energy balance and potential as a target for obesity treatment. *Int. J. Biochem. Cell Biol.* **2010**, *42*, 1788-1801.
 99. Di Marzo, V. CB1 receptor antagonism: biological basis for metabolic effects. *Drug Discov. Today* **2008**, *13*, 1026-1041.
 100. Rinaldi-Carmona, M.; Barth, F.; Héaulme, M.; Shire, D.; Calandra, B.; Congy, C. *et al.* SR141716A, a potent and selective antagonist of the brain cannabinoid receptor. *FEBS Lett.* **1994**, *350*, 240-244.
 101. Arnone, M.; Maruani, J.; Chaperon, F.; Thiébot, M. H.; Poncelet, M.; Soubrié, P. *et al.* Selective inhibition of sucrose and ethanol intake by SR 141716, an antagonist of central cannabinoid (CB1) receptors. *Psychopharmacology (Berl)* **1997**, *132*, 104-106.
 102. Boyd, S. T.; Fremming, B. A. Rimonabant-a selective CB1 antagonist. *Ann. Pharmacother.* **2005**, *39*, 684-690.
 103. Bifulco, M.; Santoro, A.; Laezza, C.; Malfitano, A. M. Cannabinoid receptor CB1 antagonists: state of the art and challenges. *Vitam. Horm.* **2009**, *81*, 159-189.
 104. Van Gaal, L. F.; Rissanen, A. M.; Scheen, A. J.; Ziegler, O.; Rössner, S. Effects of the cannabinoid-1 receptor blocker rimonabant on weight reduction and cardiovascular risk factors in overweight patients: 1-year experience from the RIO-Europe study. *Lancet* **2005**, *365*, 1389-1397.
 105. Van Gaal, L. F.; Scheen, A. J.; Rissanen, A. M.; Rössner, S.; Hanotin, C.; Ziegler, O. Long-term effect of CB1 blockade with rimonabant on cardiometabolic risk factors: two year results from the RIO-Europe Study. *Eur. Heart J.* **2008**, *29*, 1761-1771.
 106. Christensen, R.; Kristensen, P. K.; Bartels, E. M.; Bliddal, H.; Astrup, A. Efficacy and safety of the weight-loss drug rimonabant: a meta-analysis of randomised trials. *Lancet* **2007**, *370*, 1706-1713.
 107. US Food and Drug Administration Advisory committee. FDA briefing document NDA 21-888: Zimulti (rimonabant) Tablets 20 mg. Sanofi-Aventis Advisory committee. 13-6-2007. Ref Type: Internet Communication
 108. Jones, D. End of the line for cannabinoid receptor 1 as an anti-obesity target? *Nat. Rev. Drug Discov.* **2008**, *7*, 961-962.
 109. Tsujikawa, K.; Dan, Y.; Nogawa, K.; Sato, H.; Yamada, Y.; Murakami, H. *et al.* Potentiation of domperidone-induced catalepsy by a P-glycoprotein inhibitor, cyclosporin A. *Biopharm. Drug Dispos.* **2003**, *24*, 105-114.
 110. Sadeque, A. J.; Wandel, C.; He, H.; Shah, S.; Wood, A. J. Increased drug delivery to the brain by P-glycoprotein inhibition. *Clin. Pharmacol. Ther.* **2000**, *68*, 231-237.



Chapter 2

Cannabinoid CB1 receptor antagonists modulate transport activity of multidrug resistance-associated proteins MRP1, MRP2, MRP3, and MRP4

Hanneke G.M. Wittgen¹, Jeroen J.M.W. van den Heuvel¹, Petra H.H. van den Broek¹, Heike Dinter-Heidorn², Jan B. Koenderink¹, Frans G.M. Russel¹

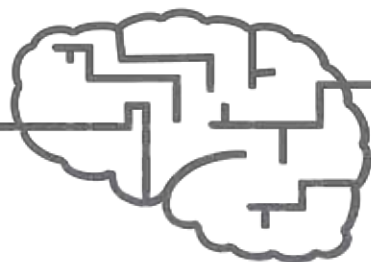
¹ Department of Pharmacology and Toxicology, Radboud University Nijmegen Medical Centre, Nijmegen Centre for Molecular Life Sciences, the Netherlands

² Abbott Products GmbH, Hannover, Germany

Published in *Drug Metabolism and Disposition*, July 2011 (39), p. 1294-1302

Reprinted with permission of the American Society for Pharmacology and Therapeutics. All rights reserved.

Copyright © 2011 by The American Society for Pharmacology and Experimental Therapeutics



Abstract

2 Cannabinoid type 1 (CB1) receptor antagonists have been developed for the treatment of obesity, but a major disadvantage is that they cause unwanted psychiatric effects. Selective targeting of peripheral CB1 receptors might be an option to circumvent these side effects. Multidrug resistance-associated proteins (MRPs) can influence the pharmacokinetics of drugs and thereby affect their disposition in the body. In this study, we investigated the interaction of the prototypic CB1 receptor antagonist rimonabant and a series of 3,4-diarylpyrazoline CB1 receptor antagonists with MRP1, MRP2, MRP3, and MRP4 *in vitro*. Their effect on ATP-dependent transport of estradiol 17- β -D-glucuronide was measured in inside-out membrane vesicles isolated from transporter-overexpressing HEK293 cells. Rimonabant inhibited MRP1 transport activity more potently than MRP4 (K_i of 1.4 μ M and 4 μ M, respectively), whereas the 3,4-diarylpyrazolines were stronger inhibitors of MRP4 than MRP1-mediated transport. A number of CB1 receptor antagonists, including rimonabant, stimulated MRP2 and MRP3 transport activity at low, but inhibited E₂17 β G transport at high substrate concentrations. The interaction of 3,4-diarylpyrazolines and rimonabant with MRP1-4 indicate their potential for drug-drug interactions. Preliminary *in vivo* data suggested that for some 3,4-diarylpyrazolines the relatively lower brain efficacy may be related to their inhibitory potency against MRP4 activity. Furthermore, this study shows that the modulatory effects of the 3,4-diarylpyrazolines were influenced by their chemical properties, and that small variations in structure can determine the affinity of these compounds for efflux transporters and thereby affect their pharmacokinetic behavior.

Introduction

The cannabinoid type 1 (CB1) receptor is involved in regulation of feeding behavior, metabolism, and energy balance.¹ Studies in rodents have shown that antagonism of this receptor leads to reduced food intake and weight reduction.² Several CB1 receptor antagonists were developed for the treatment of obesity, and clinical studies showed a reduction in appetite, weight loss, and improved metabolic risk factors.^{2,3} Rimonabant was the first and only selective CB1 receptor antagonist approved for therapeutic use. However, the drug was withdrawn from the market within two years of its introduction, because psychiatric adverse effects, in particular depression, were revealed in additional clinical studies.^{4,5}

The CB1 receptor is expressed in brain and peripheral tissues such as adipose, skeletal muscle, liver, gut, and pancreas.¹ In the brain, activation of the endocannabinoid system appears to be involved in coping with stress and anxiety. Therefore, the psychiatric side effects seen for CB1 receptor antagonists could be due to inhibition of the endocannabinoid system.³ It is believed that the positive effect of antagonists on metabolic factors could also be mediated via peripheral CB1 receptors.¹ Indeed, a recent study with a peripheral CB1 receptor antagonist in obese mice showed that this antagonist could improve the cardiometabolic risk in these mice without inhibition of the central CB1 receptor.⁶ Therefore, peripheral CB1 receptor antagonists might have therapeutic potential for improving metabolic risk in obese patients, without causing psychiatric side effects.

Multidrug resistance-associated proteins (MRPs) are efflux transporters that can influence drug disposition by transporting a wide variety of substrates out of the cell, preventing drugs from entering specific tissues or organs (*e.g.* intestine and brain), or increasing elimination of compounds, *e.g.* via liver and kidney.^{7,8} MRP1, MRP2, MRP3, and MRP4 belong to the ATP-binding cassette (ABC) transporter subfamily C, and have overlapping substrate specificities.⁹ MRP1 is present in many tissues, with highest protein expression in lung, adrenal gland, heart, and skeletal muscle, and lower amounts in brain, choroid plexus, spleen, kidney, intestine, testes, placenta, and liver.¹⁰⁻¹³ It is expressed basolaterally in most tissues, but it has an apical localization in brain capillary endothelial cells.^{12,13} MRP2 is highly expressed in liver, and lower expression levels can be found in the apical membranes of kidney tubules, gastrointestinal tract, gall bladder, placenta, and bronchi.^{14,15} MRP3 is expressed in kidney, colon, small intestine, liver, and gall bladder, where it is found mostly in basolateral membranes.¹⁶ MRP4 is widely distributed in tissues and blood cells and has a dual membrane localization, which is basolateral in prostate tubuloacinar cells, hepatocytes, and choroid plexus, and apical in kidney proximal tubule cells, and brain capillary endothelium.^{13,17} The expression of MRP1-4 at locations which are involved in drug disposition and penetration suggests that they influence drug concentrations in plasma and different organs, and, because of their presence in the blood-brain barrier (BBB) and choroid plexus, MRP4 and MRP1 might play a role in restricting CB1 receptor antagonists from the brain.



Interaction of a drug with efflux transporters could not only influence its own pharmacokinetics, but it can also change the disposition of other compounds that are substrates for the same transporter. Studies describing the interaction of CB1 receptor antagonists with MRP1-4 may not only give information on the pharmacokinetics of these antagonists, but also on possible drug-drug interactions. Here, we investigated the *in vitro* effect of a series of 3,4-diarylpyrazoline CB1 receptor antagonists (Fig. 1)¹⁸ and the prototypic CB1 receptor antagonist rimonabant on MRP1-4 transport activity. In addition, for some 3,4-diarylpyrazolines, we related their transporter interaction to preliminary *in vivo* pharmacodynamic effects measured in rats.

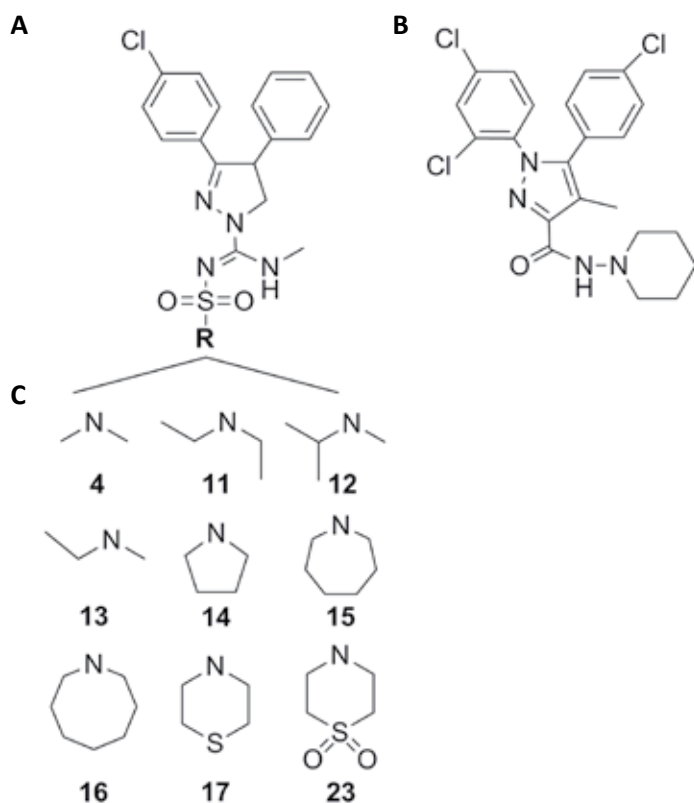


Figure 1 Chemical structure of CB1 receptor antagonists

Core structure of 3,4-diarylpyrazoline derivatives 4, 11-17, and 23 (A) with the chemical structures of R for the N-substituent of these compounds (B).¹⁸ Structure of rimonabant (C).

Materials and methods

Materials

[6,7-³H(N)]-estradiol 17-β-D-glucuronide (41.8 Ci/mmol) was purchased from Perkin Elmer (Groningen, the Netherlands). Bac-to-Bac and Gateway system, DMEM + Glutamax-I culture medium, and fetal calf serum were purchased from Invitrogen (Breda, the Netherlands). Triple flasks (500 cm²) were purchased from Sanbio BV Biological Products (Uden, the Netherlands). Estradiol 17-β-D-glucuronide (E₂17βG), adenosine 5'-triphosphate magnesium salt (from bacterial source) and adenosine 5'-monophosphate monohydrate (from yeast) were purchased from Sigma-Aldrich (Zwijndrecht, the Netherlands). Protein concentrations were determined with a Bio-Rad protein assay kit from Bio-Rad Laboratories (Veenendaal, the Netherlands). Monoclonal mouse-anti-human MRP3 antibody M3II-21 was purchased from Abcam (Cambridge, UK). Monoclonal mouse-anti-human MRP1 (QCRL-1) was kindly provided by dr. S.P.C. Cole (Queen's University Cancer Research Institute, Kingston, Canada). 3,4-Diarylpyrazoline CB1 receptor antagonists¹⁸ and rimonabant were kindly provided by Solvay Pharmaceuticals (Hannover, Germany - Solvay Pharmaceuticals is now Abbott).

Generation of baculovirus

Full-length human MRP1, MRP2, and MRP3 were cloned separately into the Gateway pDONR221vector. The sequence of MRP1 was equal to GenBank accession number NM_004996 except for three silent mutations at bp 1684, 1704, and 4002, which are known polymorphisms.¹⁹ The sequence of MRP2 was equal to NM_000392 except for three silent mutations at bp 264, 1167, and 3972, of which C3972T is a known polymorphism, and the sequence of MRP3 was equal to NM_003786.²⁰ Consequently, constructs were also cloned into a VSV-G improved pFastBacDual vector for mammalian cell transduction using the Gateway system.²¹ Full-length human MRP4 and enhanced yellow fluorescent protein (eYFP), which was used as a negative control, were already cloned before.²¹ Baculoviruses were produced as described in the Bac-to-Bac manual (Invitrogen).

Cell culture and transduction of HEK293 cells

HEK293 cells were grown in DMEM-Glutamax-I supplemented with 10% fetal calf serum at 37°C under 5% CO₂-humidified air. HEK293 cells were cultured in 500 cm² triple flasks until 40% confluent, after which culture medium was removed and 25 ml medium and 10 ml eYFP, MRP1, MRP2, MRP3, or MRP4 baculovirus was added. Cells were incubated for 15 min at 37°C, after which a further 40 ml medium was added. 5 mM sodium butyrate was added 24 hours after transduction. Three days after transduction, cells were harvested by centrifugation at 5000g for 5 minutes.



Isolation of membrane vesicles and protein analysis

Membranes were isolated according to a previously described method with slight modifications.²² In brief, harvested cell pellets were resuspended in ice-cold homogenization buffer (0.5 mM sodium phosphate and 0.1 mM EDTA) supplemented with protease inhibitors (100 μ M phenylmethylsulfonyl fluoride, 5 μ g/ml aprotinin, 5 μ g/ml leupeptin, 1 μ g/ml pepstatin, and 1 μ M E-64) and shaken at 4°C for 30 minutes. Lysed cells were centrifuged at 100,000g for 30 min at 4°C, and the pellets were homogenized in ice-cold TS buffer (10 mM Tris-HEPES, and 250 mM sucrose, pH 7.4) supplemented with protease inhibitors described above, using a tight-fitting Dounce homogenizer for 25 strokes. After centrifugation at 1000g for 20 minutes at 4°C, the supernatant was centrifuged at 100,000g for 60 min at 4°C. The resulting pellet was resuspended in TS buffer without protease inhibitors and passed through a 27-gauge needle 25 times. Protein concentration was determined by Bio-Rad protein assay kit. Crude membrane vesicles were dispensed in aliquots, frozen in liquid nitrogen, and stored at -80°C until further use.

Western blotting

Membrane vesicle preparations were solubilized in SDS-polyacrylamide gel electrophoresis sample buffer and separated on SDS gel, containing 7.5% acrylamide, according to Laemmli. Subsequently, they were blotted on nitrocellulose membrane using the iBlot dry blotting system (Invitrogen). Monoclonal mouse-anti-human MRP1 (QCRL-1, 1:700) and MRP3 (M3II-21, 1:200) antibodies and affinity-purified, polyclonal rabbit-anti-human MRP2 (pAb hM2-p2, 1:500) and MRP4 (pAb hM4-p4, 1:1000) were used to detect transporters.^{23, 24} The secondary antibodies used in 1:10000 dilution were fluorescent goat-anti-mouse IRdye800 (Rockland Immunochemicals, Gilbertsville, USA) and goat-anti-rabbit Alexa Fluor 680 (Invitrogen). Signals were visualized using the Odyssey imaging system (Li-Cor Biosciences, Lincoln, NE).

Vesicular transport assays

Uptake of [³H]E₂17 β G into membrane vesicles was performed using a rapid filtration technique.²⁵ 30 μ l reaction mix consisted of TS buffer, 4 mM ATP, 10 mM MgCl₂, E₂17 β G and 7.5 μ g of membrane vesicles. 0.1 (MRP1), 0.15 (MRP2, MRP4), and 0.2 μ Ci (MRP3) [³H]E₂17 β G was used, supplemented with unlabeled E₂17 β G to concentrations indicated in legends. The reaction was started when the mixture was incubated at 37°C and then stopped by placing samples on ice and adding 150 μ l of ice-cold TS buffer. A Multiscreen_{HTS} HV, 0.45 μ M, PVDF 96-well filter plate was pre-washed with TS buffer and diluted samples were filtered through this filter plate using a Multiscreen_{HTS}-Vacuum Manifold filtration device (Millipore, Etten-Leur, the Netherlands). The filters were washed twice with TS-buffer and were then separated from the plate. After addition of 2 ml of scintillation fluid to each filter and subsequent liquid scintillation counting, uptake of [³H]E₂17 β G into membrane vesicles was determined by measuring radioactivity associated with the filters. In control

experiments, ATP was substituted with AMP. Net ATP-dependent transport was calculated by subtracting values measured in the presence of AMP from those measured in the presence of ATP. Time-dependent transport was found to be linear up to 5 minutes for MRP1, MRP2, and MRP4, and up to 3 minutes for MRP3 (results not shown).

Vesicular interaction assays

To evaluate the inhibitory effects of 3,4-diarylpyrazolines and rimonabant on [^3H]E $_2$ 17 β G uptake in MRP1, 2, 3, and 4 inside-out membrane vesicles, the abovementioned transport assay was performed in the absence or presence of 10 and 100 μM of CB1 receptor antagonists. The concentration-dependent effect of 1-100 μM of compounds **13**, **15**, and rimonabant was measured at three different E $_2$ 17 β G concentrations: 0.16, 1, and 5 μM for MRP1; 2, 20, and 200 μM for MRP2; 0.08, 1, and 5 μM for MRP3; and 0.1, 0.3, and 1 μM for MRP4. ATP-dependent transport was calculated.

Determination of actual concentrations of 3,4-diarylpyrazolines and rimonabant with LC-MS/MS

The actual amount of CB1 receptor antagonists dissolved under vesicular transport assay conditions was measured. eYFP vesicles (7.5 μg) were added in each well to mimic the vesicle environment. The reaction mixture without [^3H]E $_2$ 17 β G was added on ice and only the AMP-condition was measured. The 96-wells plate was mixed and the total reaction mixture from one well was transferred to an eppendorf tube at room temperature. Sample was spun down at maximum speed (16,000-20,000g) for 5 minutes at room temperature and 10 μl of supernatant was reconstituted in 50% acetonitrile/water and 0.1% trifluoroacetic acid (TFA) prior to LC-MS/MS analysis. Determination of actual concentration was carried out using an Accela U-HPLC (Thermo Fisher Scientific) coupled to a TSQ Vantage (Thermo Fisher Scientific) triple quadrupole mass spectrometer. The CB1 receptor antagonists were separated on a Zorbax Eclipse Plus column (50 x 2.1 mm, 1.8 μm particle size; Agilent). The elution gradient was: 0 min 50% B, 5 min 90% B, 6 min 50% B. Solvent A consisted of 0.1% TFA in ultrapure water and solvent B consisted of 0.1% TFA in acetonitrile. The column temperature was set at 40°C and the flow rate was 200 $\mu\text{l}/\text{min}$. The effluent from the HPLC was passed directly into the electrospray ion source. Positive electrospray ionization was achieved using a nitrogen sheath gas with ionization voltage at 4 kV. The capillary temperature was set at 350°C. Detection of each analyte was based on isolation of the protonated molecular ion, $[\text{M}+\text{H}]^+$, and subsequent MS/MS fragmentations and a selected reaction monitoring (SRM) were carried out. The conditions per compound are summarized in Table 1. CB1 receptor antagonist 4 or 16 was used as internal standard and the response ratio of test compound to internal standard was used to determine the concentration. Actual assay concentration of compound was measured in duplicate in at least three independent experiments.



In vivo pharmacodynamic effect of 3,4-diarylpyrazolines on CP55,940 induced hypotension in rat

The ED_{50} of 3,4-diarylpyrazolines for attenuation of 5-(1,1-dimethylheptyl)-2-[5-hydroxy-2-(3-hydroxypropyl)cyclohexyl]phenol (CP55,940)-induced hypotension in male, normotensive, anaesthetized Wistar rats was determined according to a previously described method using different intravenous doses ($n = 2$ per dose) of CB1 receptor antagonists 10 minutes before CP55,940 (0.1 mg/kg i.v.) administration.²⁶ Hypotension was achieved within 1 minute after administration of the CB1 receptor agonist CP55,940, and the lowest blood pressure was the measure of the hypotensive effect. ED_{50} was calculated on the linear part of the percentage dose response curve and is the dose of antagonist that inhibited the hypotensive effect of CP55,940 by 50%. Experiments were approved by the local ethics committee on animal experimentation at Solvay Pharmaceuticals in Weesp.

Kinetic Analysis

All data were expressed as means \pm S.E.M.. Curve fitting of the resulting concentration-dependent transport curves and determination of IC_{50} values for the CB1 receptor antagonists was performed by non-linear regression analysis using GraphPad Prism software, version 5.02 (GraphPad Software Inc., San Diego, CA). The following equation was fitted to the data: $y = \text{bottom} + (\text{top} - \text{bottom}) / (1 + 10^{(\log IC_{50} - x) * \text{hill slope}})$, in which x is log inhibitor concentration and y is expressed as uptake versus control (%). Michaelis-Menten fit was used for MRP1, MRP3, and MRP4 E_2 17 β G curves, allosteric sigmoidal fit for MRP2. Log (inhibitor or stimulator) vs response with variable slope was used to plot the inhibition and stimulation curves with

Table 1 LC-MS/MS conditions for detection of CB1 receptor antagonists

Compound	Retention time (min)	Parent (m/z)	Product 1 (CE) (m/z) (eV)	Product 2 (CE) (m/z) (eV)	S-lens (V)
4	3.2	420.182	255.060 (27)	375.140 (13)	115
11	4.2	448.222	255.100 (26)	375.080 (16)	108
12	4.2	448.221	255.060 (30)	375.050 (14)	111
13	3.8	434.204	255.060 (26)	375.090 (14)	109
14	3.5	446.205	255.090 (28)	375.100 (16)	118
15	4.8	474.245	255.070 (29)	375.100 (28)	127
16	5.4	488.261	255.060 (31)	375.090 (19)	130
17	4.0	478.184	255.050 (28)	375.000 (15)	113
23	2.6	510.169	255.080 (29)	375.100 (15)	127
rimonabant	3.2	463.163	299.000 (46)	363.020 (29)	125

CE: collision energy

13, **15**, or rimonabant. Results of the inhibition assay for interaction of MRP1/4 with **13** and rimonabant were analyzed using Dixon's method combined with linear regression analysis to estimate the inhibitory constant (K_i). Statistical differences were determined using a one-way analysis of variance with Dunnett's multiple comparison test in GraphPad Prism. Differences were considered to be significant at $p < 0.05$.

Results

Expression of MRP1, MRP2, MRP3, and MRP4 in isolated membrane vesicles

Immunoblot analysis performed on membrane vesicles from HEK293 cells overexpressing MRP1, MRP2, MRP3, and MRP4 demonstrated that all four transporters were successfully expressed (data not shown). MRP1 seemed to be less glycosylated as indicated by a band at approximately 160 kD, but this had no influence on its transport activity (Fig. 2A). The negative control, consisting of membrane vesicles from eYFP-overexpressing HEK293 cells, showed no expression of MRP1-4.

Concentration-dependent transport of $E_217\beta G$ into MRP1, MRP2, MRP3, and MRP4 overexpressing membrane vesicles

Concentration-dependent uptake of $E_217\beta G$ into membrane vesicles was measured after 5 minutes for all transporters and typical curves are shown in Figure 2A-D. ATP-dependent $E_217\beta G$ transport reached maximum activities (V_{max}) of 31 ± 1 , 2220 ± 100 , and 94 ± 5 pmol $mg^{-1} min^{-1}$ for MRP1, MRP3, and MRP4, respectively. The affinity of $E_217\beta G$ (K_m) for MRP1, MRP3, and MRP4 was 7.5 ± 0.1 μM , 56 ± 6 μM , and 15 ± 3 μM , respectively. Repetition of the experiment for each transporter gave comparable kinetic parameters, only the V_{max} of MRP3 varied between different batches of membrane vesicles, due to different expression levels of the transporter. Transport activity of MRP2 followed a sigmoidal relationship with increased $E_217\beta G$ concentration (Fig. 2B). A Hill slope of 1.6 ± 0.03 was calculated for MRP2 activity, which is indicative of positive cooperativity.

Effects of 3,4-diarylpyrazolines and rimonabant on MRP1-, MRP2-, MRP3-, and MRP4-mediated $E_217\beta G$ transport

Based on the kinetics of $E_217\beta G$ uptake by MRP1-4, the following $E_217\beta G$ concentrations, well below the K_m , were chosen for interaction studies with 3,4-diarylpyrazolines and rimonabant (Fig. 1): 0.16 μM for MRP1, 20 μM for MRP2, 0.08 μM for MRP3, and 0.12 μM for MRP4. In the case of MRP2, 20 μM substrate was used to measure both stimulation and inhibition.

Figure 3 shows the effect of 10 and 100 μM of the CB1 receptor antagonists on $E_217\beta G$ transport by MRP1-4. Due to poor solubility, the actual concentrations of the 3,4-diarylpyrazolines and rimonabant were 3- to 100-fold lower than the predicted



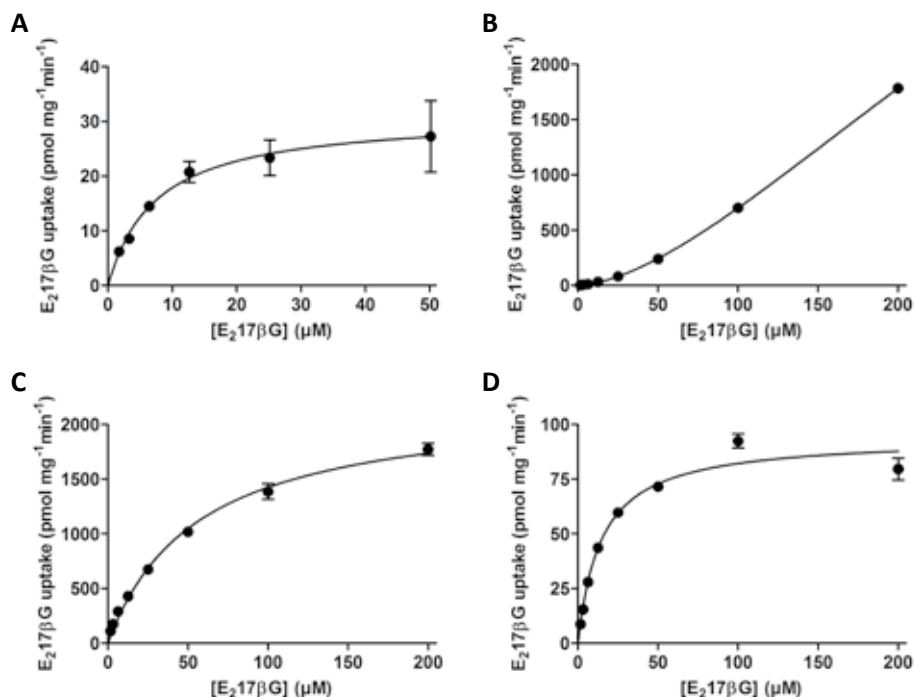


Figure 2 Kinetics of ATP-dependent $E_217\beta G$ transport into membrane vesicles of HEK293 cells overexpressing MRP1-4

Concentration-dependent $E_217\beta G$ transport was determined after 5 minutes for MRP1 (A), MRP2 (B), MRP3 (C), and MRP4 (D). ATP-dependent eYFP values were subtracted from corresponding ATP-dependent MRP values and K_m and V_{max} were determined by non-linear regression analysis. Data points represent the mean \pm S.E.M. of triplicate measurements in a representative experiment.

Figure 3 Effect of CB1 receptor antagonists on ATP-dependent transport of $E_217\beta G$ into MRP1-, MRP2-, MRP3-, or MRP4-overexpressing membrane vesicles

Transport was measured during five minutes at concentrations of 0.16, 20, 0.08, and 0.12 μM $E_217\beta G$, for MRP1 (A), MRP2 (B), MRP3 (C), and MRP4 (D), respectively, in the absence (white bars) or presence of CB1 receptor antagonists. Due to their poor solubility, concentrations in the low range varied between 0.4 and 2.2 μM (grey bars) and between 4 and 33 μM (black bars) for the 10-fold higher range. Actual concentrations of CB1 receptor antagonists corresponding to the grey bars were 2.2 μM for compound 4, 0.7-1.3 μM for **11-23**, and 0.4 μM for rimonabant. Actual concentrations corresponding to the black bars were 33 μM for CB1 receptor antagonist **4**, 7 μM for **11-12**, 12 μM for **13-14**, 1-3 μM for **15-23**, and 4 μM for rimonabant. ATP-dependent uptake in absence of CB1 receptor antagonists was set at 100% (white bar) and was also measured in presence of 100 μM $E_217\beta G$ (black bar). Mean \pm S.E.M. of three independent experiments is shown. Statistically significant differences from vehicle control: * $p < 0.05$, ** $p < 0.01$, and *** $p < 0.001$.

Figure 3 on next page

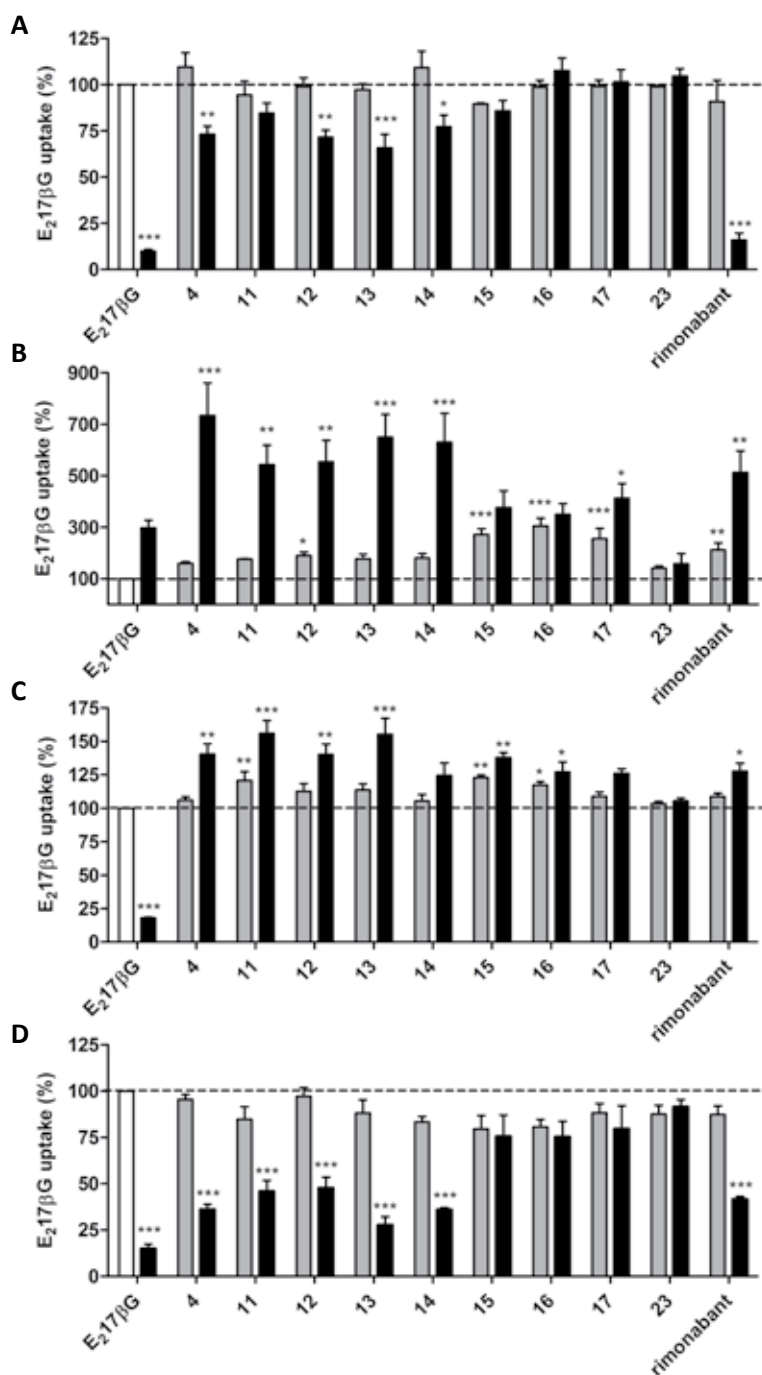


Figure 3 continued



concentrations (see legend of Fig. 3). The highest concentration of the series of 3,4-diarylpyrazolines inhibited MRP4 transport activity (Fig. 3D) more potently than MRP1 (Fig. 3A). Of the 3,4-diarylpyrazolines, compounds **4**, and **12-14** significantly inhibited MRP1- and MRP4-mediated E_2 17 β G transport. Compound **13** had the highest inhibitory effect on both transporters, with $-34 \pm 13\%$ and $-72 \pm 8\%$ for MRP1 and MRP4, respectively. Transport of E_2 17 β G by MRP1 and MRP4 was not inhibited by compounds **15-17**, and **23**, whereas compound **11** did inhibit MRP4, but not MRP1. Rimnabant inhibited MRP1 more potently than MRP4, *viz.* $-84 \pm 4\%$ versus $-58 \pm 3\%$ (Fig. 3A and 4D). In contrast to MRP1 and MRP4, MRP2 transport activity was stimulated by most compounds, at both concentrations tested (Fig. 3B). At the lower concentration, compounds **15-17** significantly increased uptake of E_2 17 β G into MRP2 vesicles (256-305%). Stimulation of MRP2 was strongest at the high concentration of compounds **4-14** (543-734%) and less by **15-17** (349-412%) and rimnabant (513%). Compound **23** did not significantly increase transport. Figure 3C shows that, although E_2 17 β G itself inhibited transport, MRP3-mediated E_2 17 β G transport was significantly stimulated by rimnabant and most 3,4-diarylpyrazolines, of which **11** and **13** had the highest stimulatory effect (approx. 155%).

Mechanism of modulation of MRP1-4 transport by compounds **13**, **15**, and rimnabant

To get a better understanding of the mechanism of interaction, we measured concentration-dependent effects of certain CB1 receptor antagonists on MRP1-4 transport at three different E_2 17 β G concentrations for each transporter (Fig. 4). 3,4-Diarylpyrazoline derivatives **13** and **15**, and rimnabant were selected for further investigation because the magnitude of their effects on the transport activity were different.

Increasing E_2 17 β G concentrations did not decrease the potency of 3,4-diarylpyrazolines **13** and **15**, and rimnabant for inhibiting MRP1 and MRP4 (Fig. 4A-C and 4J-L); the percentage of inhibition and the IC_{50} values of **13** and rimnabant for MRP4 and MRP1 were similar at different E_2 17 β G concentrations. Dixon plots for **13**- and rimnabant-mediated inhibition of MRP4 and MRP1 show that the lines intersected virtually at the x-axis for both compounds, which is indicative of non-competitive inhibition (Fig. 5A-C). The intersections corresponded to a K_i of approximately 1.4 μ M of rimnabant for MRP1, 4 μ M of rimnabant for MRP4, and 7 μ M of **13** for MRP4. 3,4-Diarylpyrazoline **15** did not inhibit MRP1 transport activity at any of the concentrations tested and only moderately inhibited MRP4 (Fig. 4A-C and 4J-L).

MRP2-mediated transport was stimulated by compounds **13**, **15**, and rimnabant at the lowest E_2 17 β G concentration of 2 μ M (Fig. 4D). Stimulation was decreased at 20 μ M E_2 17 β G, and transport was inhibited at 200 μ M of E_2 17 β G (Fig. 4D-F). Rimnabant and **15** appeared to have the same stimulatory and inhibitory potency on MRP2-mediated transport.

MRP3-mediated E_2 17 β G transport was stimulated at low substrate concentration, which gradually disappeared at higher substrate concentrations (Fig. 4G-I). At a concentration of 15 μ M E_2 17 β G, high concentrations of compounds **13**, **15**, and rimnabant inhibited E_2 17 β G transport via MRP3 (data not shown).

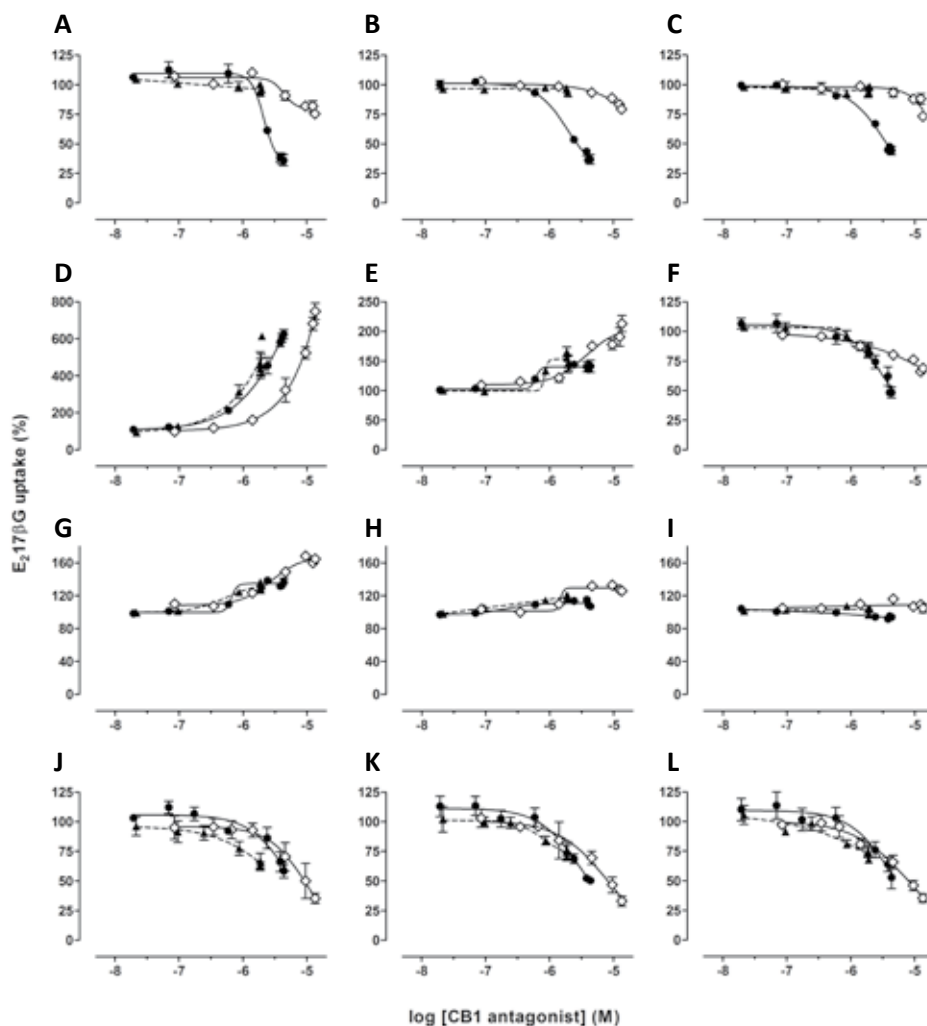


Figure 4 Effect of CB1 receptor antagonists **13** (\diamond), **15** (\blacktriangle , dotted line), and rimonabant (\bullet) on MRP-mediated $E_2 17\beta G$ transport at different substrate concentrations

$E_2 17\beta G$ concentrations were 0.16 (A), 1 (B), and 5 μM (C) for MRP1. For MRP2, these were 2 (D), 20 (E), and 200 μM (F), for MRP3 0.08 (G), 1 (H), and 5 μM (I), and for MRP4 0.1 (J), 0.3 (K), and 1 μM (L). ATP-dependent transport was determined after five minutes for MRP1, MRP2, and MRP4, and after 2 minutes for MRP3. Transport rates were expressed as a percentage of uptake measured in the absence of the CB1 receptor antagonist tested against the log drug concentration. Two to three independent experiments were performed in duplicate. Mean \pm S.E.M. of $n = 3-6$ is shown.



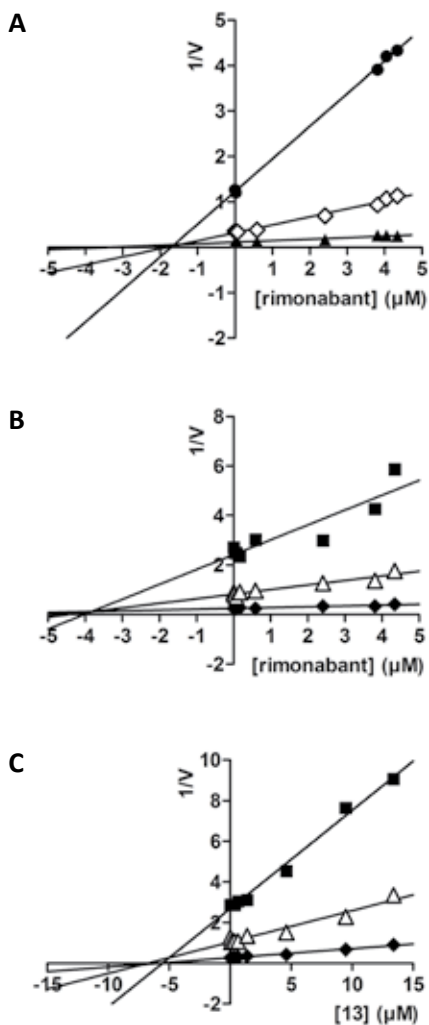


Figure 5 Dixon plots of inhibition of MRP1- and MRP4-mediated ATP-dependent $E_217\beta G$ transport by rimonabant and 3,4-diarylpyrazoline **13**

The reciprocal of transport velocity ($1/V$) of different substrate concentrations is plotted against the inhibitor concentration. Dixon plots of inhibition of MRP1 (A) and MRP4 (B) by rimonabant, and of MRP4 by **13** (C) at three different $E_217\beta G$ concentrations are shown (● 0.16 μM , ◇ 1 μM , and ▲ 5 μM for $E_217\beta G$ MRP1, and for MRP4, ■ 0.1 μM , △ 0.3 μM , and ◆ 1 μM $E_217\beta G$). Linear regression analysis was used for plotting lines and determination of K_i . Data represent the mean $1/V$ of duplicate measurements in a representative experiment.

In vivo pharmacodynamic effect of 3,4-diarylpyrazolines on CP55,940 induced hypotension in rat

To get an impression of the relative brain penetration of the 3,4-diarylpyrazolines, the CB1 receptor-mediated blood pressure effect of compounds **4**, **11**, **14**, and **15** was compared with their *in vitro* CB1 receptor binding affinity. For this purpose, in rats, the initial rapid effect was measured of CB1 receptor antagonists on CP55,940-induced hypotension, which is considered to originate primarily from a central sympathetic response.²⁷ Table 2 describes the effective intravenous dose (ED_{50}) that was needed for 50% inhibition of the hypotensive effect of CP55,940, and the binding affinity (expressed as K_i) of these compounds for the CB1 receptor, as determined previously.¹⁸ The *in vivo* data show that CB1 receptor antagonist **15**

Table 2 Pharmacodynamic characteristics of the CB1 receptor antagonists

Compound	CB1 _{rb} ^a K_i (nM)	ED ₅₀ (mg/kg, <i>i.v.</i>) ^b
4	223 ± 103	> 0.3
11	30 ± 14	0.2
14	231 ± 66	0.7
15	155 ± 69	0.1

^a CB1_{rb} displacement of specific CP55,940 binding in CHO cells stably transfected with human CB1 receptor, expressed as $K_i \pm$ S.E.M. (nM), adapted from Lange and colleagues.¹⁸

^b Dose of CB1 receptor antagonist that attenuates CP55,940 induced hypotension in rats (n = 2 per dose) with 50%.

had the lowest ED₅₀ value. If the ED₅₀ of **15** relative to its binding affinity is extrapolated to compounds **4**, **11**, and **14** on basis of their K_i values for the CB1 receptor, ED₅₀ values of 0.14, 0.02, and 0.15 mg/kg, respectively, would have been expected. However, the actual ED₅₀ values of compounds **4**, **11**, and **14** (Table 2) were >2, about 10, and 4.7 times higher than expected, indicating a lower brain permeability compared to **15**.

Discussion

This study shows that CB1 receptor antagonists interacted with the efflux transporters MRP1, MRP2, MRP3, and MRP4. E₂17βG was used as a model substrate to investigate the effect of CB1 receptor antagonists on transport activity of these transporters. The kinetic parameters for E₂17βG found in this study were comparable with literature.²⁸⁻³⁰ Unlike MRP1, MRP3, and MRP4, MRP2 transported E₂17βG in a positive cooperative manner, which was previously demonstrated by others.^{31, 32}

Actual tested concentrations of the very lipophilic CB1 receptor antagonists in the experimental assays were determined by LC-MS/MS and were 3- to 100-fold lower than expected. This may be due to incomplete dissolution or non-specific binding. In our study, compounds **15-17** stimulated MRP2 better than compounds **4-14** at low concentrations. In contrast, the opposite was found at higher concentrations, where the actual concentrations of compounds **15-17** were lower (1-3 μM) than those of **4-14** (7-33 μM) (Fig. 3). This indicates that compounds **15-17**, which contain N-substituents that make them more lipophilic, have a higher potency in affecting MRP2 but have a limited effect due to their low solubility. The same was found for MRP3, and the lack of effect of compounds **15-23** on MRP1 and MRP4 might also be explained by their low actual concentrations.

Although we used E₂17βG as a substrate for all transporters, the effect of the CB1



receptor antagonists on transport of this substrate via MRP1-4 was different. MRP1- and MRP4-mediated transport was inhibited by several CB1 receptor antagonists. The inhibitory affinity of rimonabant was somewhat higher for MRP1-mediated $E_217\beta G$ transport than for MRP4-mediated transport, with a K_i of approximately 1.4 μM versus 4 μM . The maximum plasma concentration found in male human subjects treated with a therapeutic dose of rimonabant is 0.4 μM .³³ Rimonabant and 3,4-diarylpyrazoline **13** appeared to inhibit MRP1 and MRP4 in a non-competitive manner (Fig. 5A-C). In addition, MRP1 and MRP4 were stimulated at low substrate and rimonabant concentrations, indicating that rimonabant probably does not compete for the $E_217\beta G$ binding site of both transporters (Fig. 4A and 4J). Whether rimonabant and the 3,4-diarylpyrazolines are only inhibitors or also substrates of MRP1 or MRP4 cannot be concluded from this study.

In contrast to MRP1 and MRP4, MRP2-mediated transport was stimulated by all CB1 receptor antagonists, except for compound **23**. The results presented in this study suggest that 3,4-diarylpyrazolines and rimonabant stimulate MRP2 allosterically at low $E_217\beta G$ concentrations and compete for the $E_217\beta G$ binding site at high concentrations. This type of interaction is supported by other studies.^{31, 34, 35} The study of Zelcer *et al.* (2003) showed that several aromatic compounds, most of them containing sulfoxide or tosyl groups, stimulate MRP2-mediated transport of $E_217\beta G$ into membrane vesicles. Compounds that normalized the stimulated transport rates at increasing concentrations, such as sulfinpyrazone and indomethacin, also appeared to be substrates for MRP2.^{31, 35} 3,4-Diarylpyrazolines chemically resemble sulfinpyrazone, which, together with the fact that compounds **13**, **15**, and rimonabant might compete with $E_217\beta G$ at higher substrate concentrations, could indicate that they are substrates for MRP2.

The CB1 receptor antagonists had comparable effects on MRP3 transport activity, but their effects were less pronounced than for MRP2 (Fig. 4G-I). Other studies reported that MRP3-mediated $E_217\beta G$ transport activity can be inhibited as well as stimulated by different compounds, *e.g.* E3040-sulfate, indomethacin, benzbromarone.^{32, 36, 37} This indicates that the 3,4-diarylpyrazolines and rimonabant would interact with a modulating site and the substrate site of MRP3, causing stimulation of $E_217\beta G$ transport at low substrate concentrations and inhibition at higher substrate concentrations due to competition for the substrate site.

Our results show that rimonabant and 3,4-diarylpyrazolines can modulate MRP1-4 transport activity, which implicates the possibility of drug-drug interactions. Because of the brief clinical use of rimonabant, few data are available on its *in vivo* interaction potential with drug transporters. Rimonabant was found to moderately affect the pharmacokinetics of the P-glycoprotein (P-gp/ABCB1) substrate cyclosporine A, but not of tacrolimus and digoxin.^{38, 39}

The pharmacokinetic data available for rimonabant do not suggest an important role for the MRPs in determining its disposition. Rimonabant is shown to accumulate in fat tissue, spleen, thyroid, thymus, liver, plasma, and brain and is reported to cross the placental barrier.^{40, 41} Although rimonabant showed a strong interaction with MRP1, its accumulation

in the brain and passage across the placental barrier indicates that it is either a poor substrate of this transporter, or MRP1 is not efficacious enough as a barrier for rimonabant.

MRP1 and MRP4 are expressed at the blood-brain barrier and the choroid plexus, where these transporters could be involved in limiting the brain penetration of the 3,4-diarylpyrazoline CB1 receptor antagonists. Because there are only minor differences in the structures of the 3,4-diarylpyrazolines, the rate and extent of passive diffusion of these compounds into the brain and other tissues is expected to be similar, which should reflect in a similar relationship between ED_{50} and CB1 receptor binding affinity (K_i). However, there was a difference in ED_{50} values for compounds **4**, **11**, **14**, and **15**, which could not solely be attributed to differences in CB1 receptor binding affinities. The ED_{50} of compounds **4**, **11**, and **14** relative to their K_i values were higher as compared to the ED_{50}/K_i ratio of compound **15** (Table 2). This suggests that an active mechanism is lowering the concentration of compounds **4**, **11** and **14** at the site of action, resulting in increased ED_{50} values. The rapid hypotensive action of CB1 receptor agonists was shown to be primarily dependent on centrally-mediated sympathetic tone, which could implicate that compounds **4**, **11** and **14**, but not **15**, have a higher ED_{50} because they are less brain permeable.²⁷ Our *in vitro* data suggest that MRP4 might be involved. To draw definite conclusions about the involvement of MRP1-4 in influencing tissue concentrations of 3,4-diarylpyrazolines, *in vivo* studies should be performed using specific transport inhibitors and/or *Mrp* knockout mice.

In addition, it will be important to measure direct transport of CB1 receptor antagonists by MRP1-4 *in vitro*. Isolated membrane vesicles are likely not useful for this purpose due to high nonspecific binding to lipid membranes and high passive diffusion of the lipophilic CB1 receptor antagonists (unpublished results). Cell-based accumulation or vectorial transport studies may be more suitable. Furthermore, the role of the blood-brain barrier and intestinal ABC transporters P-gp and breast cancer resistance protein (BCRP/ABCG2) as possible CB1 receptor antagonist efflux pumps should be investigated. The role of influx transporters should also be considered in the tissue distribution of the CB1 receptor antagonists, but it is to be expected that uptake of these lipophilic compounds will be governed largely by passive diffusion.

In conclusion, we have shown that 3,4-diarylpyrazolines and rimonabant inhibited MRP1- and MRP4-mediated $E_217\beta G$ transport and stimulated MRP2- and MRP3-mediated transport at low $E_217\beta G$ concentrations. Stimulation of MRP2 and MRP3 shifted to inhibition at increasing substrate concentrations. The effect of these compounds on the transport activity of MRP1-4 shows the potential for possible drug-drug interactions. Preliminary *in vivo* data suggested that MRP4 could be involved in the lower brain permeability of some of the 3,4-diarylpyrazolines. The actual role of MRPs in tissue distribution of 3,4-diarylpyrazolines and rimonabant remains to be investigated. In addition, this study shows that the modulatory effects of the 3,4-diarylpyrazolines were influenced by the properties of their N-substituent, which indicates that small variations in their chemical structure can determine the affinity for the efflux transporters and thereby possibly affect their pharmacokinetic behavior.



Acknowledgements

We thank Abbott Healthcare Products B.V. (formerly Solvay Pharmaceuticals) for providing the *in vivo* pharmacology data (Tiny J. P. Adolfs). We thank dr. Kevin Weigl (Abbott Products GmbH) for his critical reading of the manuscript. This work was funded by the Dutch Top Institute Pharma and was performed within the framework of project T5-105.

References

1. Di Marzo, V. CB1 receptor antagonism: biological basis for metabolic effects. *Drug Discov. Today* **2008**, *13*, 1026-1041.
2. Boyd, S. T.; Fremming, B. A. Rimonabant-a selective CB1 antagonist. *Ann. Pharmacother.* **2005**, *39*, 684-690.
3. Bifulco, M.; Santoro, A.; Laezza, C.; Malfitano, A. M. Cannabinoid receptor CB1 antagonists: state of the art and challenges. *Vitam. Horm.* **2009**, *81*, 159-189.
4. Jones, D. End of the line for cannabinoid receptor 1 as an anti-obesity target? *Nat. Rev. Drug Discov.* **2008**, *7*, 961-962.
5. Nissen, S. E.; Nicholls, S. J.; Wolski, K.; Rodés-Cabau, J.; Cannon, C. P.; Deanfield, J. E. *et al.* Effect of rimonabant on progression of atherosclerosis in patients with abdominal obesity and coronary artery disease: the STRADIVARIUS randomized controlled trial. *JAMA* **2008**, *299*, 1547-1560.
6. Tam, J.; Vemuri, V. K.; Liu, J.; Bátkai, S.; Mukhopadhyay, B.; Godlewski, G. *et al.* Peripheral CB1 cannabinoid receptor blockade improves cardiometabolic risk in mouse models of obesity. *J. Clin. Invest* **2010**, *120*, 2953-2966.
7. Zhou, S. F.; Wang, L. L.; Di, Y. M.; Xue, C. C.; Duan, W.; Li, C. G. *et al.* Substrates and inhibitors of human multidrug resistance associated proteins and the implications in drug development. *Curr. Med. Chem.* **2008**, *15*, 1981-2039.
8. Yu, X. Q.; Xue, C. C.; Wang, G.; Zhou, S. F. Multidrug resistance associated proteins as determining factors of pharmacokinetics and pharmacodynamics of drugs. *Curr. Drug Metab* **2007**, *8*, 787-802.
9. Kruh, G. D.; Belinsky, M. G. The MRP family of drug efflux pumps. *Oncogene* **2003**, *22*, 7537-7552.
10. Flens, M. J.; Zaman, G. J.; van der Valk, P.; Izquierdo, M. A.; Schroeijers, A. B.; Scheffer, G. L. *et al.* Tissue distribution of the multidrug resistance protein. *Am. J. Pathol.* **1996**, *148*, 1237-1247.
11. Rao, V. V.; Dahlheimer, J. L.; Bardgett, M. E.; Snyder, A. Z.; Finch, R. A.; Sartorelli, A. C. *et al.* Choroid plexus epithelial expression of MDR1 P glycoprotein and multidrug resistance-associated protein contribute to the blood-cerebrospinal-fluid drug-permeability barrier. *Proc. Natl. Acad. Sci. U. S. A* **1999**, *96*, 3900-3905.
12. Leslie, E. M.; Deeley, R. G.; Cole, S. P. Multidrug resistance proteins: role of P-glycoprotein, MRP1, MRP2, and BCRP (ABCG2) in tissue defense. *Toxicol. Appl. Pharmacol.* **2005**, *204*, 216-237.
13. Nies, A. T.; Jedlitschky, G.; König, J.; Herold-Mende, C.; Steiner, H. H.; Schmitt, H. P. *et al.* Expression and immunolocalization of the multidrug resistance proteins, MRP1-MRP6 (ABCC1-ABCC6), in human brain. *Neuroscience* **2004**, *129*, 349-360.
14. Nies, A. T.; Keppler, D. The apical conjugate efflux pump ABCC2 (MRP2). *Pflugers Arch.* **2007**, *453*, 643-659.
15. van Aabel, R. A.; Hartog, A.; Bindels, R. J.; Van Os, C. H.; Russel, F. G. Expression and immunolocalization of multidrug resistance protein 2 in rabbit small intestine. *Eur. J. Pharmacol.* **2000**, *400*, 195-198.
16. Scheffer, G. L.; Kool, M.; de Haas, M.; de Vree, J. M.; Pijnenborg, A. C.; Bosman, D. K. *et al.* Tissue distribution and induction of human multidrug resistant protein 3. *Lab Invest* **2002**, *82*, 193-201.
17. Russel, F. G.; Koenderink, J. B.; Masereeuw, R. Multidrug resistance protein 4 (MRP4/ABCC4): a versatile efflux transporter for drugs and signalling molecules. *Trends Pharmacol. Sci.* **2008**, *29*, 200-207.
18. Lange, J. H.; van Stuijvenberg, H. H.; Veerman, W.; Wals, H. C.; Stork, B.; Coolen, H. K. *et al.* Novel 3,4-diarylpyrazolines as potent cannabinoid CB1 receptor antagonists with lower lipophilicity. *Bioorg. Med. Chem. Lett.* **2005**, *15*, 4794-4798.
19. Conrad, S.; Kauffmann, H. M.; Ito, K.; Deeley, R. G.; Cole, S. P.; Schrenk, D. Identification of human multidrug resistance protein 1 (MRP1) mutations and characterization of a G671V substitution. *J. Hum. Genet.* **2001**, *46*, 656-663.
20. Ito, S.; Ieiri, I.; Tanabe, M.; Suzuki, A.; Higuchi, S.; Otsubo, K. Polymorphism of the ABC transporter genes, MDR1, MRP1 and MRP2/cMOAT, in healthy Japanese subjects. *Pharmacogenetics* **2001**, *11*, 175-184.
21. El-Sheikh, A. A.; van den Heuvel, J. J.; Koenderink, J. B.; Russel, F. G. Interaction of nonsteroidal anti-

- inflammatory drugs with multidrug resistance protein (MRP) 2/ABCC2- and MRP4/ABCC4-mediated methotrexate transport. *J. Pharmacol. Exp. Ther.* **2007**, *320*, 229-235.
22. El-Sheikh, A. A.; van den Heuvel, J. J.; Krieger, E.; Russel, F. G.; Koenderink, J. B. Functional role of arginine 375 in transmembrane helix 6 of multidrug resistance protein 4 (MRP4/ABCC4). *Mol. Pharmacol.* **2008**, *74*, 964-971.
 23. Smeets, P. H.; van Aubel, R. A.; Wouterse, A. C.; van den Heuvel, J. J.; Russel, F. G. Contribution of multidrug resistance protein 2 (MRP2/ABCC2) to the renal excretion of p-aminohippurate (PAH) and identification of MRP4 (ABCC4) as a novel PAH transporter. *J. Am. Soc. Nephrol.* **2004**, *15*, 2828-2835.
 24. van Aubel, R. A.; Smeets, P. H.; Peters, J. G.; Bindels, R. J.; Russel, F. G. The MRP4/ABCC4 gene encodes a novel apical organic anion transporter in human kidney proximal tubules: putative efflux pump for urinary cAMP and cGMP. *J. Am. Soc. Nephrol.* **2002**, *13*, 595-603.
 25. van Aubel, R. A.; Koenderink, J. B.; Peters, J. G.; Van Os, C. H.; Russel, F. G. Mechanisms and interaction of vinblastine and reduced glutathione transport in membrane vesicles by the rabbit multidrug resistance protein Mrp2 expressed in insect cells. *Mol. Pharmacol.* **1999**, *56*, 714-719.
 26. Lange, J. H.; Coolen, H. K.; van Stuivenberg, H. H.; Dijksman, J. A.; Herremans, A. H.; Ronken, E. *et al.* Synthesis, biological properties, and molecular modeling investigations of novel 3,4-diarylpyrazolines as potent and selective CB(1) cannabinoid receptor antagonists. *J. Med. Chem.* **2004**, *47*, 627-643.
 27. Vollmer, R. R.; Caverio, I.; Ertel, R. J.; Solomon, T. A.; Buckley, J. P. Role of the central autonomic nervous system in the hypotension and bradycardia induced by (-)-delta 9-trans-tetrahydrocannabinol. *J. Pharm. Pharmacol.* **1974**, *26*, 186-192.
 28. Loe, D. W.; Almquist, K. C.; Cole, S. P.; Deeley, R. G. ATP-dependent 17 β -estradiol 17-(β -D-glucuronide) transport by multidrug resistance protein (MRP). Inhibition by cholestatic steroids. *J. Biol. Chem.* **1996**, *271*, 9683-9689.
 29. Zeng, H.; Liu, G.; Rea, P. A.; Kruh, G. D. Transport of amphipathic anions by human multidrug resistance protein 3. *Cancer Res.* **2000**, *60*, 4779-4784.
 30. Chen, Z. S.; Lee, K.; Kruh, G. D. Transport of cyclic nucleotides and estradiol 17-beta-D-glucuronide by multidrug resistance protein 4. Resistance to 6-mercaptopurine and 6-thioguanine. *J. Biol. Chem.* **2001**, *276*, 33747-33754.
 31. Zelcer, N.; Huisman, M. T.; Reid, G.; Wielinga, P.; Breedveld, P.; Kuil, A. *et al.* Evidence for two interacting ligand binding sites in human multidrug resistance protein 2 (ATP binding cassette C2). *J. Biol. Chem.* **2003**, *278*, 23538-23544.
 32. Bodó, A.; Bakos, E.; Szeri, F.; Váradi, A.; Sarkadi, B. Differential modulation of the human liver conjugate transporters MRP2 and MRP3 by bile acids and organic anions. *J. Biol. Chem.* **2003**, *278*, 23529-23537.
 33. Turpault, S.; Kanamaluru, V.; Lockwood, G. F.; Bonnet, D.; Newton, J. Rimona-bant pharmacokinetics in healthy and obese subjects. *Clinical Pharmacology & Therapeutics* **2006**, *79*, 50.
 34. Bakos, E.; Evers, R.; Sinko, E.; Váradi, A.; Borst, P.; Sarkadi, B. Interactions of the human multidrug resistance proteins MRP1 and MRP2 with organic anions. *Mol. Pharmacol.* **2000**, *57*, 760-768.
 35. Evers, R.; de, H. M.; Sparidans, R.; Beijnen, J.; Wielinga, P. R.; Lankelma, J. *et al.* Vinblastine and sulfinpyrazone export by the multidrug resistance protein MRP2 is associated with glutathione export. *Br. J. Cancer* **2000**, *83*, 375-383.
 36. Akita, H.; Suzuki, H.; Hirohashi, T.; Takikawa, H.; Sugiyama, Y. Transport activity of human MRP3 expressed in Sf9 cells: comparative studies with rat MRP3. *Pharm. Res.* **2002**, *19*, 34-41.
 37. Bodó, A.; Bakos, E.; Szeri, F.; Váradi, A.; Sarkadi, B. The role of multidrug transporters in drug availability, metabolism and toxicity. *Toxicol. Lett.* **2003**, *140-141*, 133-143.
 38. Amundsen, R.; Asberg, A.; Robertsen, I.; Vethe, N. T.; Bergan, S.; Hartmann, A. *et al.* Rimona-bant affects cyclosporine A, but not tacrolimus pharmacokinetics in renal transplant recipients. *Transplantation* **2009**, *87*, 1221-1224.
 39. Kanamaluru, V.; Lockwood, G.; Bonnet, D.; Newton, J. Lack of effect of rimona-bant on the pharmacokinetics of digoxin. *Journal of Clinical Pharmacology* **2005**, *45*, 1081.
 40. Barna, I.; Till, I.; Haller, J. Blood, adipose tissue and brain levels of the cannabinoid ligands WIN-55,212 and SR-141716A after their intraperitoneal injection in mice: compound-specific and area-specific distribution within the brain. *Eur. Neuropsychopharmacol.* **2009**, *19*, 533-541.
 41. EMEA. Scientific discussion about Accomplia (rimonabant), **2006**.

Ref Type: Internet Communication



Chapter 3

Exploiting transport activity of P-glycoprotein at the blood-brain-barrier for the development of peripheral cannabinoid type 1 receptor antagonists

Hanneke G.M. Wittgen¹, Rick Greupink¹, Jeroen J.M.W. van den Heuvel¹, Petra H.H. van den Broek¹, Heike Dinter-Heidorn², Jan B. Koenderink¹, Frans G.M. Russel¹

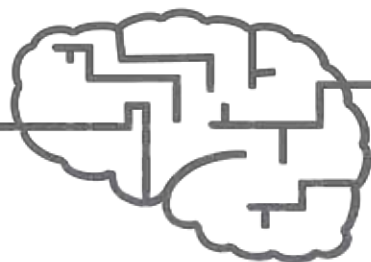
¹ Department of Pharmacology and Toxicology, Radboud University Nijmegen Medical Centre, Nijmegen Centre for Molecular Life Sciences, the Netherlands

² Abbott Products GmbH, Hannover, Germany

Published in *Molecular Pharmaceutics*, May 2012 (9), p. 1351-1360

Reproduced with permission from Molecular Pharmaceutics, March 2012, doi 10.1012/mp200617z.

Copyright © 2012 American Chemical Society.



Abstract

Although the CB1 receptor antagonist/inverse agonist rimonabant has positive effects on weight loss and cardiometabolic risk factors, neuropsychiatric side effects have prompted researchers to develop peripherally acting derivatives. Here, we investigated for a series of 3,4-diarylpyrazoline CB1 receptor antagonists if transport by the brain efflux transporter P-gp could be used as a selection criterion in the development of such drugs. All 3,4-diarylpyrazolines and rimonabant inhibited P-gp transport activity in membrane vesicles isolated from HEK293 cells overexpressing the transporter, but only the 1,1-dioxo-thiomorpholino analogue **23** exhibited a reduced accumulation ($-38 \pm 2\%$) in these cells, which could be completely reversed by the P-gp/BCRP inhibitor elacridar. In addition, **23** appeared to be a BCRP substrate, whereas rimonabant was not. In rats, the *in vivo* brain/plasma concentration ratio of **23** was significantly lower than for rimonabant (0.4 ± 0.1 vs. 6.2 ± 1.6 , $p < 0.001$). Co-administration of elacridar resulted in an 11-fold increase of the brain/plasma ratio for **23** ($p < 0.01$) and only 1.4-fold for rimonabant ($p < 0.05$), confirming the involvement of P-gp and possibly BCRP in limiting the brain entrance of **23** *in vivo*. In conclusion, these data support the conception that efflux via transporters such as P-gp and BCRP can limit the brain penetration of CB1 receptor antagonists, and that this property could be used in the development of peripheral antagonists.

Introduction

The cannabinoid type 1 (CB1) receptor is part of the endocannabinoid system, which is involved in regulation of feeding behavior, metabolism and energy balance.¹ Stimulation of the CB1 receptor in animals increases food intake and promotes weight gain, whereas inhibition of the receptor has opposite effects.² Therefore, several antagonists or inverse agonists of the CB1 receptor were developed for the treatment of obesity.² Rimonabant [*N*-piperidin-1-yl)-5-(4-chlorophenyl)-1-(2,4-dichlorophenyl)-4-methyl-1*H*-pyrazole-3-carboxamide] was the first and only selective CB1 receptor antagonist/inverse agonist approved for therapeutic use, after clinical studies had proved its positive effects on reduction of appetite, weight loss, and metabolic risk factors.^{2,3} However, additional clinical studies revealed neuropsychiatric adverse effects, in particular depression, which led to withdrawal of the drug from the market within two years after its introduction.^{4,5}

In the brain, activation of the endocannabinoid system appears to be involved in coping with stress and anxiety. Therefore, the psychiatric side effects of rimonabant are generally thought to be due to central CB1 receptor antagonism.³ Although it is well established that CB1 receptor inhibition in the brain reduces food intake, the presence of CB1 receptors in peripheral tissues, such as adipose tissue, skeletal muscle, liver, gut, and pancreas, has also been postulated to play a role in metabolism and energy expenditure.^{1,6} This implies that the positive effect on metabolic risk factors could also be mediated via peripheral CB1 receptors, which prompted the development of peripherally acting CB1 receptor antagonists.^{6,7} Recently, it was shown in obese mice that selective inhibition of peripheral CB1 receptors indeed enabled the reduction of cardiometabolic risk factors, without the disturbing central nervous system side effects.^{8,9}

P-glycoprotein (P-gp, also known as MDR1/ABCB1) is one of the most important drug efflux transporters expressed at the luminal side of brain capillary endothelial cells that form the blood-brain barrier.¹⁰ P-gp is a member of the ATP-binding cassette (ABC) family and it transports a wide variety of substrates in an ATP-dependent manner.¹¹ Studies with P-gp knockout mice showed that P-gp has an important role as gatekeeper of the brain.¹² This brain-penetration-limiting property of P-gp has been shown to be advantageous in the development of drugs such as domperidone and loperamide, that exert beneficial effects in the periphery, but would have unwanted side effects if also distributed to the brain.¹³⁻¹⁵ Consequently, transport of CB1 receptor antagonists via P-gp might also be used as an instrument to limit their brain penetration.

In this study, we investigated whether *in vitro* transport affinity for P-gp can be used to select CB1 receptor antagonists with limited *in vivo* brain penetration. For this purpose, we studied the interaction of a series of 3,4-diarylpyrazoline CB1 receptor antagonists (Fig. 1)¹⁶ and the prototypic CB1 receptor antagonist rimonabant with P-gp transport activity in membrane vesicles overexpressing the transporter. We then determined whether the compounds were substrates of P-gp, using a cellular accumulation assay, and for one



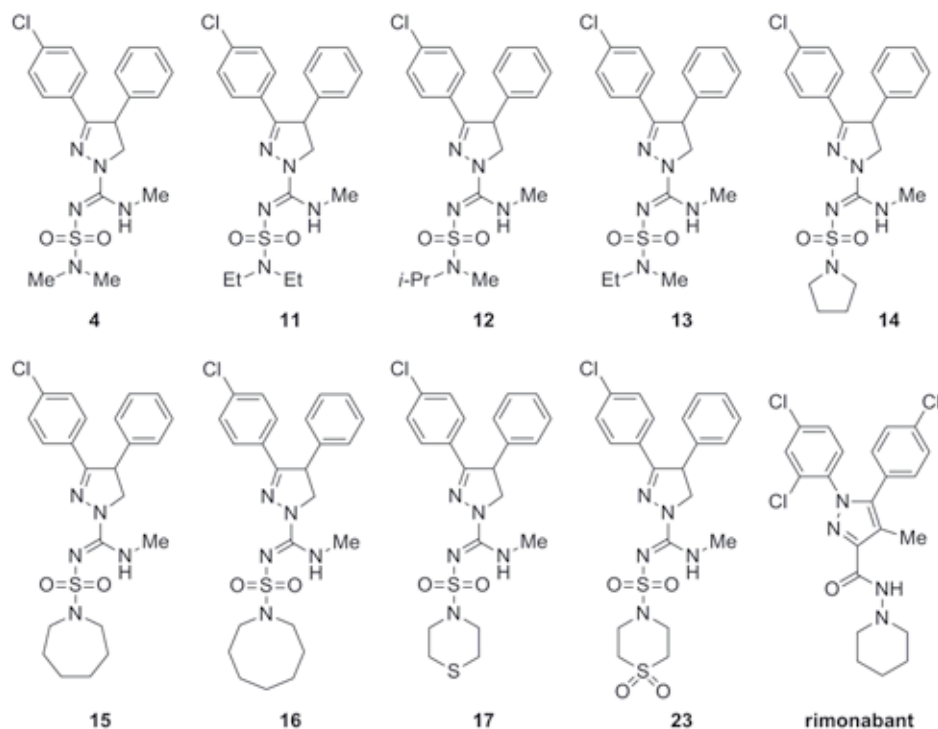


Figure 1 Chemical structure of 3,4-diarylpyrazoline CB1 receptor antagonists **4**, **11-17**, **23**, and rimonabant

CB1 receptor affinity (K_i) values of the compounds have been described previously.¹⁶

selected 3,4-diarylpyrazoline CB1 receptor antagonist we compared its brain penetration to rimonabant in rats, with and without coadministration of a potent P-gp inhibitor.

Materials and methods

Materials

[³H]*N*-methyl quinidinium chloride ([³H]NMQ) (85 Ci/mmol) and *N*-methyl quinidine (NMQ) were purchased from Solvo Biotechnology (Szeged, Hungary). Bac-to-Bac and Gateway system, and Dulbecco Eagle's modified medium (DMEM) + Glutamax-I culture medium were from Invitrogen (Breda, the Netherlands). Fetal calf serum was purchased from Greiner (Alphen a/d Rijn, the Netherlands), triple flasks (500 cm²) from Sanbio BV Biological Products (Uden, the Netherlands), and rat tail collagen (type I) from First Link Limited (United

Kingdom). Hank's Balanced Salt Solution (HBSS), optiMEM and 100x penicillin/streptomycin solution were purchased from Invitrogen (Breda, the Netherlands). Quinidine, adenosine 5'-triphosphate magnesium salt (from bacterial source), adenosine 5'-monophosphate monohydrate (from yeast), and sodium butyrate were purchased from Sigma-Aldrich (Zwijndrecht, the Netherlands), and elacridar (GF120918) from Sequoia Research Products Limited (Pangbourne, United Kingdom). Protein concentrations were determined with a Bio-Rad protein assay kit from Bio-Rad Laboratories (Veenendaal, the Netherlands). Monoclonal mouse-anti-human P-gp antibody C219 was purchased from Abcam (Cambridge, UK). Racemic mixtures of 3-(4-chlorophenyl)-4-phenyl-4,5-dihydro-1H-pyrazole-1-carboxamide derivatives **4**, **11-17**, and **23** (purity >95%, except for **15** and **17** it was 90%)¹⁶, in this paper referred to as 3,4-diarylpyrazoline CB1 receptor antagonists, and rimonabant (purity >95%), were kindly provided by Abbott Products GmbH (Hannover, Germany).

Generation of baculovirus

Full-length human P-glycoprotein (MDR1) was cloned from human kidney cDNA into the Gateway pDONR221 vector. The sequence of P-gp was equal to GenBank accession number NM_000927, except for one silent mutation at bp 1235. Subsequently, the P-gp construct was cloned into a VSV-G improved pFastBacDual vector for mammalian cell transduction using the Gateway system.¹⁷ Full-length human enhanced yellow fluorescent protein (eYFP) was cloned as described previously.¹⁷ Baculoviruses were produced using the Bac-to-Bac system, as described by the manufacturer (Invitrogen).

Cell culture

HEK293 cells were grown in DMEM-Glutamax-I supplemented with 10% fetal calf serum at 37°C under 5% CO₂-humidified air. MDCKII and MDCKII-BCRP cells¹⁸ were grown in DMEM-Glutamax-I supplemented with 10% fetal calf serum and 50 U/ml penicillin and 50 µg/ml streptomycin at 37°C under 5% CO₂-humidified air.

Transduction of HEK293 cells with P-gp

For the production of membrane vesicles, HEK293 cells were cultured in 500 cm² triple flasks until 40% confluent, after which culture medium was removed and 25 ml medium and 10 ml eYFP or P-gp baculovirus was added. Cells were incubated for 15 min at 37°C, after which a further 40 ml medium was added. 5 mM sodium butyrate was added 4-8 hours after transduction. Three days after transduction, cells were harvested by centrifugation at 3500g for 10 minutes. For the accumulation assay, 24-wells plates were coated with a 100 µg/ml rat tail collagen (type I) solution for at least two hours at 37°C. Coating was washed with phosphate-buffered saline once, and HEK293 cells were seeded 150,000 cells/well. Next day, cells were transduced with eYFP or P-gp virus, using 100 µl virus:medium mixture (2:3). After 15 minutes of incubation at room temperature, 400 µl medium and sodium butyrate was added up to 5 mM. Three days after transduction, the experiment was performed.



Isolation of membrane vesicles and protein analysis

Membranes were isolated according to a previously described method.¹⁹ In brief, harvested cell pellets were lysed in ice-cold homogenization buffer supplemented with protease inhibitors at 4°C for 30 minutes. Lysed cells were centrifuged at 100,000g for 30 min at 4°C, and the pellets were homogenized in ice-cold TS buffer (10 mM Tris-HEPES, and 250 mM sucrose, pH 7.4) supplemented with protease inhibitors, using a tight-fitting Dounce homogenizer for 25 strokes. After centrifugation at 1000g for 20 minutes at 4°C, the supernatant was centrifuged at 100,000g for 60 min at 4°C. The resulting pellet was resuspended in TS buffer without protease inhibitors and passed through a 27-gauge needle 25 times. Protein concentration was determined using the Bio-Rad protein assay kit. Crude membrane vesicles were dispensed in aliquots, frozen in liquid nitrogen, and stored at -80°C until further use.

Western blotting

HEK293-ctrl and -P-gp cell pellets were lysed in ultrapure water containing DNase I (20 U/μl) (Invitrogen) and Complete mini protease inhibitor cocktail (Roche Diagnostics, the Netherlands). A 40 μg protein sample of cell lysate and 15 μg of membrane vesicles were solubilized in SDS-polyacrylamide gel electrophoresis buffer and separated on SDS gel, containing 7.5% acrylamide, according to Laemmli. Subsequently, they were blotted on nitrocellulose membrane using the iBlot dry blotting system (Invitrogen). Monoclonal mouse-anti-human P-gp (C219, 1:250), followed by incubation with the secondary antibody fluorescent goat-anti-mouse IRdye800 (1:10000) (Rockland Immunochemicals, Gilbertsville, USA) was used for detection of P-gp. Signal was visualized using the Odyssey imaging system (Li-Cor Biosciences, Lincoln, NE).

Vesicular transport interaction assay

The effect of 3,4-diarylpyrazolines and rimonabant on P-gp-mediated [³H]NMQ uptake was measured in P-gp-overexpressing membrane vesicles. Uptake of [³H]NMQ into membrane vesicles was performed using a rapid filtration technique.²⁰ The 30 μl reaction mix consisted of TS buffer, 4 mM ATP, 10 mM MgCl₂, 7.5 μg of membrane vesicles, 0.015 μCi [³H]NMQ supplemented with unlabeled NMQ to 100 nM, and 0, 10, or 100 μM of CB1 receptor antagonist. The reaction was started when the mixture was incubated at 37°C, and stopped after two minutes by placing samples on ice and adding 150 μl of ice-cold TS buffer. A Multiscreen_{HTS} HV, 0.45 μm, glass fiber 96-well filter plate was prewashed with TS buffer and diluted samples were filtered through this filter plate using a Multiscreen_{HTS}-Vacuum Manifold filtration device (Millipore, Etten-Leur, the Netherlands). The filters were washed twice with TS-buffer and were then separated from the plate. After addition of 2 ml of scintillation fluid to each filter and subsequent liquid scintillation counting, uptake of [³H]NMQ into membrane vesicles was determined by measuring radioactivity associated with the filters, and uptake of total NMQ was calculated. In control experiments, ATP was

substituted with AMP. Net ATP-dependent transport was calculated by subtracting values measured in the presence of AMP from those measured in the presence of ATP.

Accumulation assay in HEK293-P-gp cells

To determine whether the 3,4-diarylpyrazolines or rimonabant were substrates of P-gp, we investigated the accumulation of these compounds in HEK293 cells overexpressing P-gp or, as negative control, eYFP, in a 24-wells plate. Cells were washed once with Tris-HEPES buffer (10 mM HEPES, 132 mM NaCl, 4.2 mM KCl, 1 mM CaCl_2 , 1 mM MgCl_2 , 5.5 mM D(+)-glucose, calibrated to pH 7.4 using 1M Tris solution), before incubation with Tris-HEPES buffer containing 1 μM CB1 receptor antagonists or quinidine, a well-known P-gp substrate, in absence or presence of 2 μM elacridar. After one hour at 37°C, cells were washed once with Tris-HEPES buffer containing 0.5% BSA, and washed twice with Tris-HEPES buffer. Cells were lysed using 1 ml 50% acetonitrile + internal standard (one of the CB1 receptor antagonists or NMQ) + 0.1% trifluoroacetic acid. Protein was precipitated for 30 minutes at -20°C, and samples were centrifuged for 5 minutes at 16,000g. Supernatant was analyzed using LC-MS/MS analysis.

Accumulation assay in MDCKII-BCRP cells

To determine whether **23** and rimonabant were substrates of BCRP, we investigated accumulation of these compounds into MDCKII (control) and MDCKII-BCRP cells. Cells were grown until 100% confluency in 24-wells plates and washed once with HBSS before 30 minute preincubation with optiMEM. After preincubation, cells were incubated with optiMEM containing 1 μM of **23** or rimonabant in absence or presence of 2 μM elacridar. After one hour at 37°C, cells were washed twice with HBSS + 0.5% BSA, and twice with HBSS. Cells were lysed using 1 ml 50% acetonitril + internal standard (**17** or rimonabant) + 0.1% trifluoroacetic acid. Protein was precipitated for 30 minutes at -20°C, and samples were centrifuged for 5 minutes at 16,000g. Supernatant was analyzed using LC-MS/MS analysis.

Experimental animals

Male Wistar rats (Charles River, Kisslegg, Germany) of 250–450 g were housed under a 12 h dark/light cycle at constant humidity and temperature. Animals were permitted free access to tap water and standard lab chow. All experiments were approved by the committee for care and use of laboratory animals of Abbott Products GmbH in Ludwigshafen and were performed according to strict governmental and international guidelines.

Effect of P-gp on disposition of **23**, rimonabant, and quinidine in rat brain

Elacridar and **23** were dissolved in ethanol/PEG400/5% glucose solution (20:60:20), rimonabant was dissolved in ethanol/PEG-25 hydrogenated castor oil/water (10:10:80), and quinidine was dissolved in 5% dextrose solution. Male Wistar rats ($n = 24$) were anaesthetized using isoflurane, and divided in two groups ($n = 12$), of which one group was injected



intravenously with the P-gp inhibitor elacridar (6 mg/kg). 30 minutes after treatment with elacridar or vehicle, each group was divided in three groups, and was injected intravenously with rimonabant (1 mg/kg), **23** (1 mg/kg), or quinidine (10 mg/kg) ($n = 4$ for each group). One hour after injection of the test compounds, animals were sacrificed and plasma and brain were collected. PBS was added to the brain (8v:w) and tissue was homogenized using the Geno/Grinder (Spex Sample Prep, USA). Proteins in samples were precipitated by addition of 400 μ l acetonitrile (with internal standard) to 100 μ l brain homogenate or 50 μ l plasma, and samples were centrifuged at 2000g for 10 minutes. Supernatant was 1:1 diluted with 10 mM ammonium acetate (pH 3) and the concentration of **23**, rimonabant, quinidine, and elacridar in brain and plasma was determined using LC-MS/MS. Subsequently, the brain/plasma concentration ratios were calculated for the different treatment groups.

3

LC-MS/MS quantification of CB1 receptor antagonists

Concentrations of the CB1 receptor antagonists and quinidine in the cell accumulation assays were measured using an Accela U-HPLC (Thermo Fisher Scientific) coupled to a TSQ Vantage (Thermo Fisher Scientific) triple quadrupole mass spectrometer. The compounds were separated on a Zorbax Eclipse Plus C18 column (50 x 2.1 mm, 1.8 μ m particle size; Agilent), preceded by a Zorbax Eclipse Plus C18 Guard column (12.5 x 1.2 mm, 5 μ m). The elution gradient was as follows: 0 min 50% B, 5 min 90% B, 6 min 50% B for the CB1 receptor antagonists, and 0 min 10% B, 3 min 40% B, 4 min 10% B, 9 min 10% B for quinidine and NMQ. Solvent A consisted of 0.1% trifluoroacetic acid (TFA) in ultrapure water and solvent B consisted of 0.1% TFA in acetonitrile. The column temperature was set at 40°C and the flow rate was 200 μ l/min. The effluent from the HPLC was passed directly into the electrospray ion source. The capillary temperature was set at 350°C. Positive electrospray ionization was achieved using a nitrogen sheath gas with ionization voltage at 4 kV. For the *in vivo* experiment, the concentrations of **23**, rimonabant, quinidine, and elacridar were measured using an Ab Sciex 5500 Qtrap and compounds were separated on a Phenomenex Kinetex C18 column (2.1 x 30 mm, 2.6 μ m particle size). The elution gradient was: 0 min 1% B, 0.4 min 99% B, 1.5 min 99% B, 1.51 min 1% B. Solvent A consisted of 10 mM ammonium acetate (pH 3) and solvent B of 100% acetonitrile. Flow rate was 900 μ l/min, and the capillary temperature was set at 950°C. Positive electrospray ionization was achieved using a nitrogen sheath gas with ionization voltage at 5.5 kV. Detection of each analyte was based on isolation of the protonated molecular ion, $[M+H]^+$, and subsequent MS/MS fragmentations and a selected reaction monitoring (SRM) were carried out (Table 1). Brain concentration (ng/g) was divided by the plasma concentration (ng/ml) to obtain the brain/plasma concentration ratio.

Calculation of physicochemical characteristics of test compounds

The physicochemical characteristics in Table 3 were calculated using add-ins in the program ChemBio3D Ultra version 12.0 (Cambridge Software). For the octanol:water participation

Table 1 LC-MS/MS conditions for detection of the compounds studied

Compound	Parent (<i>m/z</i>)	Product 1 (<i>m/z</i>)	Product 2 (<i>m/z</i>)	Product 3 (<i>m/z</i>)
4	420	255	375	
11	448	255	375	
12	448	255	375	
13	434	255	375	
14	446	255	375	
15	474	255	375	
16	488	255	375	
17	478	255	375	
23	510	255 ^a	375	
rimonabant	463	299	363 ^a	
quinidine	325	172	307	160 ^a
NMQ	339	58	160	
elacridar	564	167 ^a		

^a Product ion used for quantification of test compounds for *in vivo* experiment.

coefficient (cLogP) the add-in CambridgeSoft cLogP: partition coefficient was used. For the calculated polar surface area (cPSA) we used the add-in CambridgeSoft Molecular Topology: molecular polar surface area.

Kinetic analysis

All data were expressed as mean \pm S.E.M. Statistical difference for all experiments, except the vesicular transport assays, were determined using an unpaired Student's *t*-test in Graphpad Prism software (version 5.02; Graphpad Software Inc., San Diego, CA). For the vesicular transport data, a one-way analysis of variance with Dunnett's multiple comparison test was performed using GraphPad Prism. Differences were considered to be significant at $p < 0.05$.

Results

Expression of P-gp in HEK293 cells

Immunoblot analysis performed on lysate and membrane vesicles from HEK293 cells confirmed the successful overexpression of P-gp (Fig. 2). The prototypic P-gp substrate *N*-methyl quinidine (NMQ) was taken up into these vesicles in an ATP-dependent fashion,



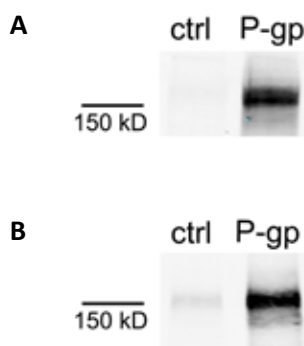


Figure 2 Western blot analysis of expression of P-gp in HEK293 cells

Cell lysate (A) or membrane vesicles (B) of HEK-ctrl (ctrl) and HEK-P-gp (P-gp) cells were used for blotting.

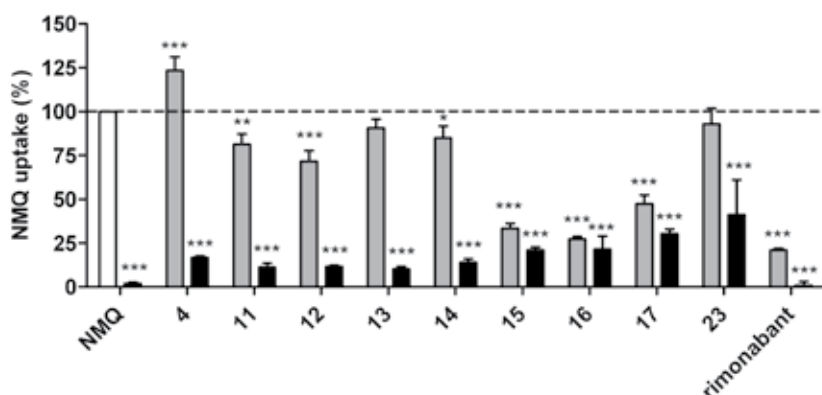


Figure 3 Effect of CB1 receptor antagonists on ATP-dependent transport of NMQ into P-gp-overexpressing membrane vesicles

Transport was measured after two minutes at a concentration of 100 nM NMQ in the absence (white bar) or presence of CB1 receptor antagonists (black and grey bars). Due to their poor solubility, concentrations in the low range varied between 0.4 and 2.2 μ M (grey bars) and for the 10-fold higher range between 4 and 33 μ M (black bars). Actual concentrations of CB1 receptor antagonists corresponding to the grey bars were 2.2 μ M for **4**, 0.7-1.3 μ M for **11-23**, and 0.4 μ M for rimonabant. Actual concentrations corresponding to the black bars were 33 μ M for **4**, 7 μ M for **11-12**, 12 μ M for **13-14**, 1-3 μ M for **15-23**, and 4 μ M for rimonabant. ATP-dependent uptake in absence of CB1 receptor antagonists was set at 100% (white bar) and was also measured in presence of 100 μ M NMQ (black bar). Mean \pm S.E.M. of three independent experiments is shown. Statistically significant differences from vehicle control were determined with one-way ANOVA, and a post-hoc Dunnett's test: * p < 0.05, ** p < 0.01, and *** p < 0.001.

and absolute transport values of NMQ without inhibitor varied between 8 and 28 pmol mg⁻¹ min⁻¹, dependent on the batch of vesicles used (Fig. 3).

Effects of 3,4-diarylpyrazoline CB1 receptor antagonists and rimonabant on P-gp-mediated NMQ transport into membrane vesicles

To investigate whether the CB1 receptor antagonists interact with P-gp, we studied their effects on P-gp-mediated transport. In Figure 3, the effect of 10 and 100 µM of the CB1 receptor antagonists on ATP-dependent NMQ transport by P-gp is shown. Previously, we have reported that the actual concentrations of these compounds in the assay are 3- to 100-fold lower because of their poor water solubility (see legend of Fig. 3).¹⁹ Nevertheless, even at these low concentrations, significant inhibition could be detected. At the lowest concentration tested, **15-17** and rimonabant inhibited P-gp transport by 67 ± 3%, 73 ± 1%, 53 ± 5%, and 79 ± 1%, respectively, whereas **4**, **11-14**, and **23** had no or only little inhibitory, or even stimulatory effects. At the highest concentration, all compounds inhibited NMQ transport almost completely, except for **23**, which only inhibited transport by 59 ± 20% (Fig. 3).

Identification of CB1 receptor antagonists that are substrates of P-gp in vitro

To identify whether the 3,4-diarylpyrazolines or rimonabant were transported via P-gp, the accumulation of 1 µM of these compounds in HEK293 cells overexpressing P-gp (HEK293-P-gp) or HEK293 control cells (HEK293-ctrl) was measured. Functional transport activity of P-gp in this assay was established by means of the control substrate quinidine, of which the accumulation was reduced to 34 ± 0.7% in HEK293-P-gp cells compared to HEK293-ctrl cells (Fig. 4K and Table 2). Next, we investigated the accumulation of the 3,4-diarylpyrazolines, and showed that accumulation of **23** in HEK293-P-gp cells was reduced significantly to 62 ± 2% compared to HEK293-ctrl cells (p<0.001), whereas the cellular accumulation of the other CB1 receptor antagonists, including rimonabant, was not significantly reduced (Fig. 4A-J, and a summary of normalized data in Table 2). The P-gp inhibitor elacridar, which had no effect on accumulation of quinidine and **23** in HEK293-ctrl cells, reversed the reduced accumulation of both quinidine and **23** in HEK293-P-gp cells to the levels found in HEK293-ctrl cells (Fig. 5).

Accumulation of **23** and rimonabant in MDCKII-BCRP cells

Since elacridar is an inhibitor of not only P-gp but also of the brain efflux transporter breast cancer resistance protein (BCRP)²¹, we studied whether **23** and rimonabant are BCRP substrates. We measured the accumulation of 1 µM of these compounds in MDCKII cells overexpressing BCRP (MDCKII-BCRP) or control MDCKII cells (Fig. 6). Overexpression of BCRP significantly reduced the accumulation of **23** to 63 ± 10% of control cells, which could be reversed by addition of elacridar (Fig. 6A). There was no effect of BCRP overexpression or inhibition on rimonabant accumulation (Fig. 6B).



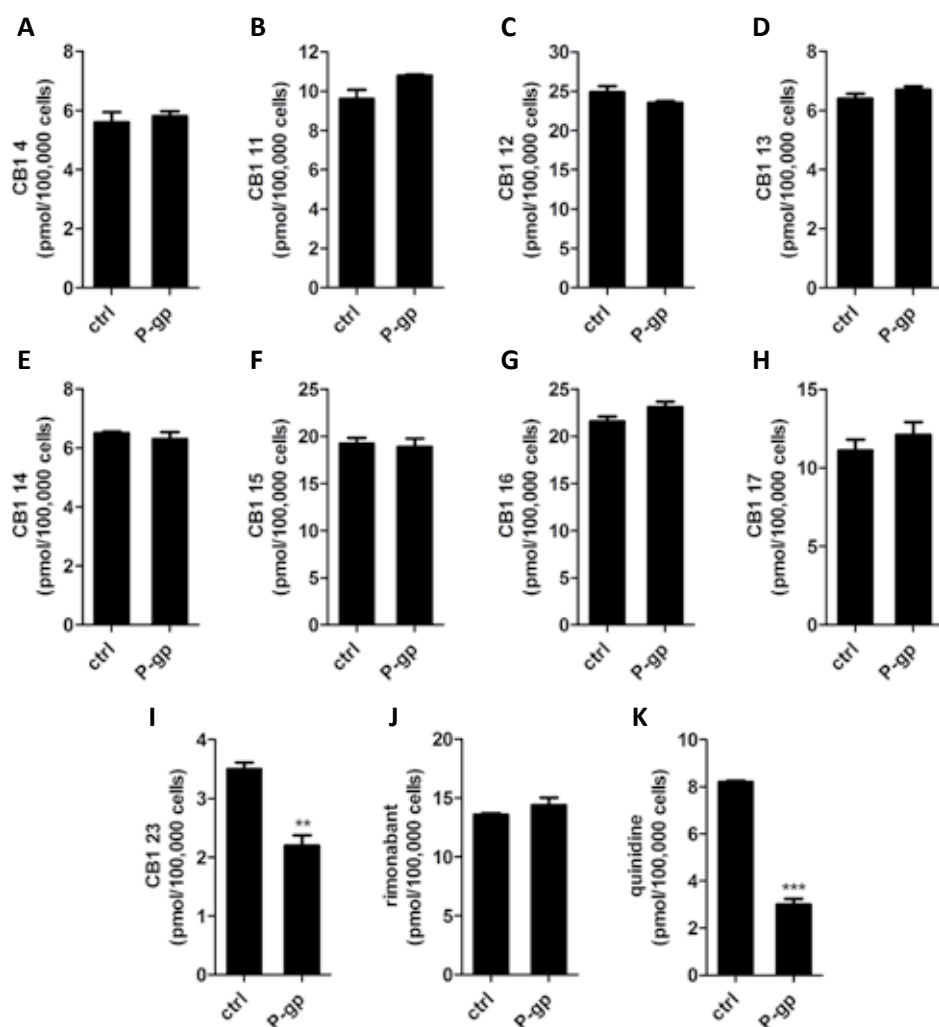


Figure 4 Accumulation of CB1 receptor antagonists in HEK293 cells overexpressing P-gp or a control protein

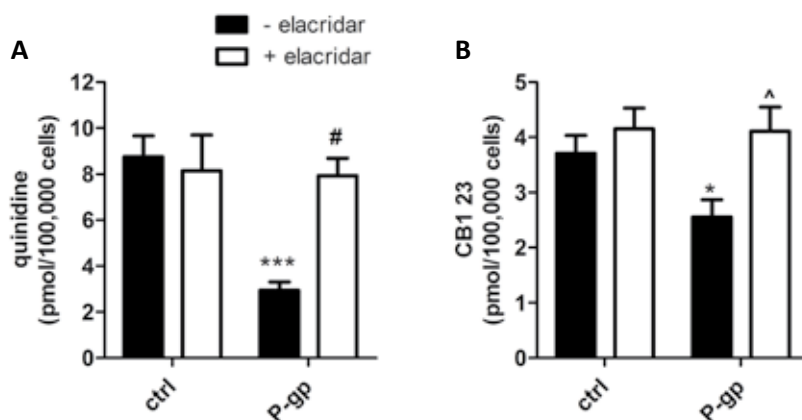
Accumulation was measured after one hour of exposure to the compounds at 37°C. 1 μ M of **4** (A), **11** (B), **12** (C), **13** (D), **14** (E), **15** (F), **16** (G), **17** (H), **23** (I), rimonabant (J) or quinidine (K), a known P-gp substrate, was used. Each experimental condition was performed in triplicate and mean \pm S.E.M. of a representative experiment from three independent experiments is shown. Statistical significance of accumulation in P-gp versus control condition was determined using an unpaired Student's *t*-test: ** $p = 0.0034$, and *** $p < 0.0001$.

Table 2 Accumulation of CB1 receptor antagonists in HEK293 cells overexpressing P-gp

Compound	Accumulation in P-gp cells vs. control (%) ^a	Ratio control:P-gp
quinidine	34 ± 0.8***	2.9
4	100 ± 5.5	1.0
11	103 ± 5.5	1.0
12	101 ± 3.5	1.0
13	100 ± 3.4	1.0
14	110 ± 7.3	1.0
15	100 ± 0.7	1.0
16	102 ± 2.4	1.0
17	102 ± 3.9	1.0
23	62 ± 2.2***	1.6
rimonabant	102 ± 3.6	1.0

^a Mean ± S.E.M. of normalized values of three independent experiments.

*** p < 0.001 compared to control (100 ± 0%) using one-way ANOVA test.

**Figure 5** Effect of elacridar on P-gp-mediated transport of quinidine and **23**

Accumulation of quinidine (A) and **23** (B) into HEK293 cells overexpressing P-gp or control protein was determined after one hour of exposure to 1 μ M of quinidine or **23** in absence (black bar) or presence (white bar) of 2 μ M elacridar. Mean \pm S.E.M. of seven (quinidine) or eight (**23**) independent experiments in triplicate are shown. Statistical significant differences were determined using an unpaired Student's *t*-test: * p = 0.022, and *** p < 0.0001 compared to control condition, # p < 0.0001, and ^ p = 0.012 compared to condition without elacridar.



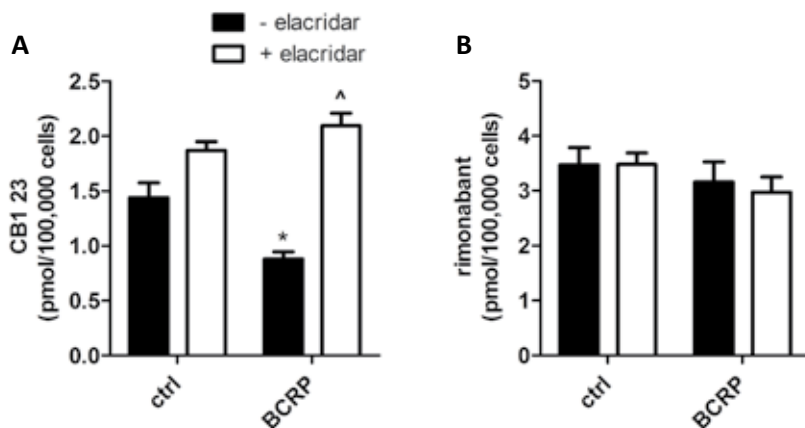


Figure 6 Effect of elacridar on accumulation of **23** and rimonabant in MDCKII and MDCKII-BCRP cells

Uptake was measured after one hour of exposure to 1 μ M of **23** (A) or rimonabant (B) in absence (black bar) or presence (white bar) of 2 μ M of the P-gp/BCRP inhibitor elacridar. Mean \pm S.E.M. of three independent experiments in triplicate are shown. Statistical significant differences were determined using an unpaired Student's *t*-test: * $p = 0.021$ compared to control condition, and [^] $p = 0.0008$ compared to condition without elacridar.

Effect of elacridar on brain penetration of **23** and rimonabant in rats

Blood-brain barrier penetration of **23** and rimonabant was determined by measuring their brain and plasma concentrations one hour after i.v. administration to rats in the absence or presence of elacridar. Quinidine was included in the experiment to verify the P-gp inhibitory action of elacridar. Plasma concentration of elacridar at the end of the experiment was 730 ± 60 nM, which is expected to have almost completely inhibited the *in vivo* P-gp transport during the experiment.²² In absence of elacridar, the concentration of **23** in the brain was significantly lower than that of rimonabant, 0.048 ± 0.007 nmol/g versus 0.33 ± 0.09 nmol/g ($p = 0.016$) (Fig. 7A), whereas the plasma concentration of **23** was higher, although not significantly, than that of rimonabant, 114 ± 22 nM and 60 ± 50 nM, respectively ($p = 0.17$) (Fig. 7B). Administration of elacridar did not affect the plasma concentrations of **23** and rimonabant (Fig. 7B), but it did induce an 11-fold increase in brain/plasma concentration ratio of **23**, from 0.4 ± 0.1 to 4.7 ± 0.9 ($p < 0.001$) (Fig. 7D), which was comparable to the 10-fold increase of quinidine brain/plasma ratio ($p = 0.009$) (Fig. 7C). The brain/plasma ratio of rimonabant was already 16-fold higher than that of **23** in absence of elacridar ($p < 0.001$), and was only 1.4-fold increased from 6.2 ± 1.6 to 8.7 ± 0.6 after administration of elacridar ($p = 0.026$) (Fig. 7D).

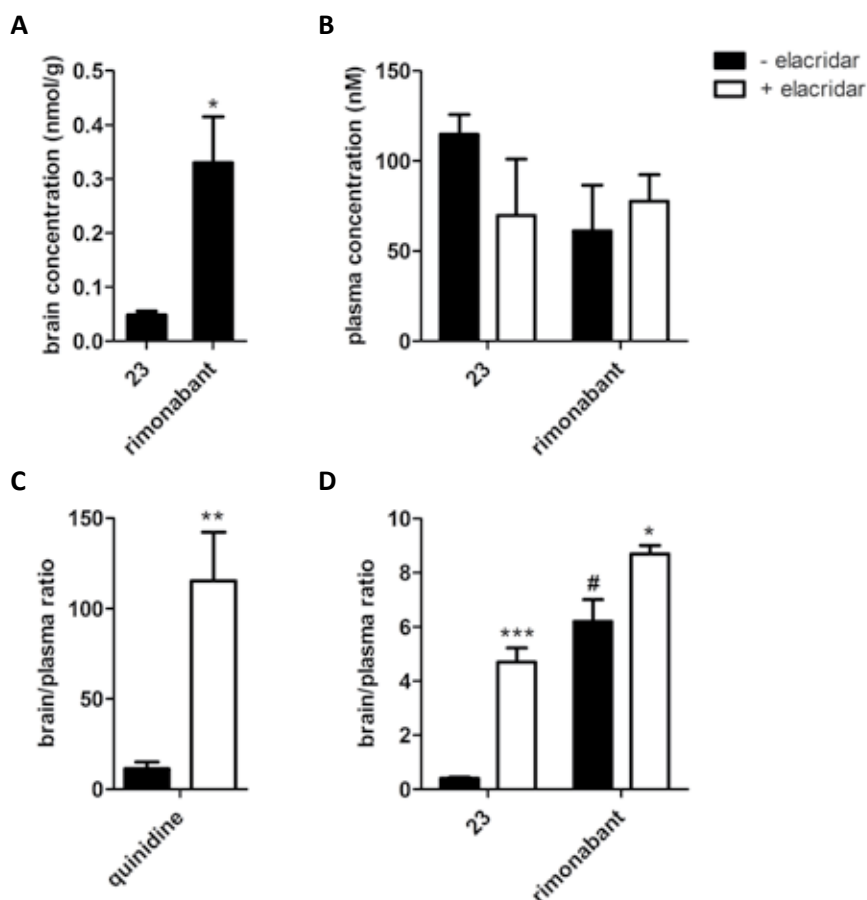


Figure 7 The effect of elacridar on the brain penetration of **23**, rimonabant and quinidine in rats

Half of the rats was injected intravenously with elacridar (6 mg/kg) 30 minutes prior to intravenous injection of quinidine (10 mg/kg), **23** (1 mg/kg) or rimonabant (1 mg/kg). Concentration of the compounds in plasma and brain was measured one hour after administration of the test compound. (A) Brain concentrations of **23** and rimonabant in absence of elacridar. Mean \pm S.E.M. of 4 rats is shown. Statistical analysis was performed using an unpaired Student's *t*-test: * $p = 0.0163$. (B) Plasma concentrations of **23** and rimonabant in absence (black bar) and presence (white bar) of elacridar. Mean \pm S.E.M. of 4 rats is shown, except for **23** with elacridar ($n = 3$). Statistical analysis using an unpaired Student's *t*-test showed no significant differences. (C and D) Brain/plasma concentration ratio of quinidine (C) and **23** and rimonabant (D) in absence (black bar) or presence (white bar) of elacridar. Mean \pm S.E.M. of 4 rats is shown, except for **23** with elacridar ($n = 3$). Statistical analysis was performed using an unpaired Student's *t*-test: * $p = 0.026$, ** $p = 0.0087$, and *** $p = 0.0002$ when compared to condition without elacridar, # $p = 0.0004$ when compared to brain/plasma ratio of **23** without elacridar.



Discussion

To circumvent the neuropsychiatric side effects of CB1 receptor antagonists, but maintain their beneficial cardiometabolic action, peripherally acting derivatives are being developed. In this study, we showed that the drug efflux transporter P-gp and, possibly, BCRP is involved in limiting the brain penetration of 3,4-diarylpyrazoline CB1 receptor antagonists, and that transport of a compound via P-gp can be used as a selection criterion in the development of peripheral CB1 receptor antagonists.

The inhibitory effect of the CB1 receptor antagonists on P-gp transport activity was measured to get an indication whether these compounds interact with the transporter and are possible substrates. We demonstrated that all 3,4-diarylpyrazolines and rimonabant inhibited P-gp-mediated transport in membrane vesicles (Fig. 3), indicating interaction of the compounds with P-gp. However, the accumulation assays in HEK293-ctrl and -P-gp cells revealed that only **23** was a substrate of P-gp, because the accumulation of this compound was significantly reduced in P-gp overexpressing cells (Fig. 4I), and could be reversed to control levels with the P-gp inhibitor elacridar²³ (Fig. 5B). Interestingly, rimonabant, which did not appear to be a substrate in the cell assay (Fig. 4J), was the most potent inhibitor of P-gp in the vesicular transport assay (Fig. 3), whereas **23** was a less potent inhibitor and a good substrate. This shows that inhibition of a compound in the vesicular interaction assay does not necessarily implicate its P-gp substrate activity. A better prediction could be achieved if the assay is also used to determine the mode of inhibition, differentiating between competitive (interaction with substrate binding pocket) and noncompetitive inhibitors (allosteric modulators that are less likely to be substrates).

Because the interaction with P-gp per se does not seem to be sufficient for the CB1 receptor antagonists to be transported, we further examined the structural features of the P-gp substrate **23**. This suggested that an electronegative group in addition to a heterocyclic ring structure, both present in the 1,1-dioxo-thiomorpholine group of this compound, are important for transport of these pyrazole CB1 receptor antagonists via P-gp. Other studies further support this theory, as the peripheral CB1 receptor antagonist AM6545 [5-(4-[4-cyanobut-1-ynyl]phenyl)-1-(2,4-dichlorophenyl)-4-methyl-*N*-(1,1-dioxo-thiomorpholino)-1*H*-pyrazole-3-carboxamide], which contains exactly the same substituent as **23**, is also a P-gp substrate.⁸ In addition, another study showed that adding an electronegative group, either methylsulfanyl, -sulfinyl, or -sulfonyl, to the imidazole core of similar CB1 receptor antagonists improved their transport via P-gp.²⁴ This knowledge could be used to optimize P-gp substrate affinity among this class of CB1 receptor antagonists.

As **23** appeared to be a substrate of P-gp, this compound was selected for a pharmacokinetic interaction study with elacridar in rats, to verify whether P-gp is also relevant in limiting its brain concentration *in vivo*. Because **23** also appeared to be a BCRP substrate, the effect of the mixed P-gp/BCRP inhibitor elacridar on brain penetration could have also been the result of BCRP inhibition (Fig. 6). Rimonabant, which was neither a P-gp nor a BCRP substrate, and

Table 3 Calculated physicochemical properties of the CB1 receptor antagonists

Compound	cLogP ^a	cPSA ^b (Å ²)
4	2.69	77
11	3.74	77
12	3.53	77
13	3.22	77
14	4.02	77
15	5.13	77
16	5.69	77
17	4.70	77
23	3.00	112
rimonabant	6.47	48

^a calculated octanol:water partition coefficient^b calculated polar surface area

which is known to distribute to the brain^{8,25}, served as a positive control for brain penetration. Indeed, the brain/plasma ratio of **23** was lower than that of rimonabant, and was largely increased by elacridar, whereas the inhibitor had only minor effects on the brain/plasma ratio of rimonabant (Fig. 7). Together with the data from the cellular accumulation assays, this suggests that P-gp, and possibly BCRP, are the limiting factors for brain penetration of **23** and not of rimonabant. Because P-gp is more abundant than BCRP at the blood-brain barrier of rats, and the potency of elacridar for BCRP inhibition is about 10- to 70-fold lower than for P-gp inhibition, the effect of BCRP on the brain penetration of **23** might have been less important, implicating a major role for P-gp in limiting the brain concentration of **23**.^{22, 26-28} However, because BCRP is more abundantly expressed in human than in rodent blood-brain barrier, it would be interesting to investigate the possibility to select for BCRP substrate activity in addition to P-gp activity to further reduce brain penetration of peripheral CB1 receptor antagonists.²⁹

The difference between **23** and the other CB1 receptor antagonists is not only the P-gp transport affinity but also the polar surface area of this compound. Compounds with a PSA over > 90 are considered to have a low probability to cross the blood-brain barrier.^{24, 30, 31} Addition of the electronegative group dramatically increases the polar surface area (PSA) of **23** (Table 3). Indeed, the brain/plasma ratio of **23** was much lower than that of rimonabant. However, the dramatic effect of elacridar on the brain/plasma ratio of **23**, increasing the ratio to the level of rimonabant, suggests that active transport plays a dominant role over PSA in determining the blood-brain barrier passage of **23**.



A general problem of using P-gp transport activity as a strategy to develop peripheral CB1 receptor antagonists could be a low oral absorption, because of the expression of P-gp in the intestine.³² However, the oral availability of the structurally related peripheral CB1 receptor antagonist and P-gp substrate AM6545 was not restricted by P-gp as its plasma concentration was similar after oral and peritoneal dosing.⁸ Furthermore, in the CaCo-2 cell model for oral availability, AM6545 had an efflux ratio of 1.1, which indicates that absorption is not limited by active transport.⁸ After oral administration, local drug concentrations in the intestine could reach high levels that saturate P-gp and limit its impact on absorption.³³ This contrasts to the situation at the blood-brain barrier where a much lower concentration of the compound will be presented to P-gp via the plasma.³³ Cellular assays to estimate the intestinal penetration have also been performed with the CB1 receptor antagonists from this study, and the efflux ratio for **23** in CaCo-2 cells was 1.5, and 28% of the dose passed a monolayer of LLC-PK1 cells overexpressing P-gp (data not shown). This suggests that intestinal P-gp activity is not expected to limit the oral availability of **23**.

Although inhibition of the central CB1 receptor plays an important role in the food intake lowering and weight reducing effects of rimonabant, studies with recently developed peripherally acting CB1 receptor antagonists have shown that these compounds decrease cardiometabolic risk factors, and even weight in obese mice.^{8, 9, 34, 35} To further evaluate the beneficial effects of inhibition of the peripheral CB1 receptor in obesity and its comorbidities, antagonists that target these receptors are needed that have a good pharmacokinetic and pharmacodynamic profile. The present study showed that P-gp and possibly BCRP transport could be used as a tool for selection of peripheral CB1 receptor antagonists, which could be a novel strategy for the development of this type of compound. The pharmacokinetic profile of **23** offers a good starting point, provided its affinity for the CB1 receptor (K_i of 830 ± 170 nM)¹⁶ is increased during lead optimization. It should be noted that our data represent brain penetration after single dose administration, whereas in clinical practice patients receive chronic treatment with CB1 receptor antagonists. Long-term studies are required to verify that, also upon repeated administration, brain concentrations remain below the level that could lead to central side effects.

In summary, by using an *in vitro* cellular accumulation assay we selected a 3,4-diarylpyrazoline CB1 receptor antagonist as a substrate of P-gp, and showed that P-gp and possibly BCRP limited the *in vivo* brain concentration of this compound in rats. Our results imply that it should be possible to further develop peripheral CB1 receptor antagonists based on their properties as substrates for brain efflux transporters.

Acknowledgements

We thank Abbott Products GmbH (Hannover, Germany) for providing the series of 3,4-diarylpyrazoline CB1 receptor antagonists and rimonabant, and for the pharmacokinetic

studies performed at Ludwigshafen (dr. R.A.B. van Waterschoot, dr. M. Schulz, dr. A. Netz, and their teams). We thank dr. A.H. Schinkel (The Netherlands Cancer Institute, Amsterdam, the Netherlands) for kindly providing the MDCKII and MDCKII-BCRP cell lines. We thank prof. dr. Floris Rutjes (Synthetic Organic Chemistry, Radboud University Nijmegen, the Netherlands) for critical reading of the manuscript. This work was supported by the Dutch Top Institute Pharma [Project T5-105].

References

1. Di Marzo, V. CB1 receptor antagonism: biological basis for metabolic effects. *Drug Discov. Today* **2008**, *13*, 1026-1041.
2. Boyd, S. T.; Fremming, B. A. Rimonabant-a selective CB1 antagonist. *Ann. Pharmacother.* **2005**, *39*, 684-690.
3. Bifulco, M.; Santoro, A.; Laezza, C.; Malfitano, A. M. Cannabinoid receptor CB1 antagonists: state of the art and challenges. *Vitam. Horm.* **2009**, *81*, 159-189.
4. Jones, D. End of the line for cannabinoid receptor 1 as an anti-obesity target? *Nat. Rev. Drug Discov.* **2008**, *7*, 961-962.
5. Nissen, S. E.; Nicholls, S. J.; Wolski, K.; Rodés-Cabau, J.; Cannon, C. P.; Deanfield, J. E.; Després, J. P.; Kastelein, J. J.; Steinhilb, S. R.; Kapadia, S.; Yasin, M.; Ruzyllo, W.; Gaudin, C.; Job, B.; Hu, B.; Bhatt, D. L.; Lincoff, A. M.; Tuzcu, E. M. Effect of rimonabant on progression of atherosclerosis in patients with abdominal obesity and coronary artery disease: the STRADIVARIUS randomized controlled trial. *JAMA* **2008**, *299*, 1547-1560.
6. Silvestri, C.; Ligresti, A.; Di Marzo, V. Peripheral effects of the endocannabinoid system in energy homeostasis: Adipose tissue, liver and skeletal muscle. *Rev. Endocr. Metab Disord.* **2011**, *12*, 153-162.
7. Ward, S. J.; Raffa, R. B. Rimonabant Redux and Strategies to Improve the Future Outlook of CB1 Receptor Neutral-Antagonist/Inverse-Agonist Therapies. *Obesity. (Silver. Spring)* **2011**, *19*, 1325-1334.
8. Tam, J.; Vemuri, V. K.; Liu, J.; Bátkai, S.; Mukhopadhyay, B.; Godlewski, G.; Osei-Hyiaman, D.; Ohnuma, S.; Ambudkar, S. V.; Pickel, J.; Makriyannis, A.; Kunos, G. Peripheral CB1 cannabinoid receptor blockade improves cardiometabolic risk in mouse models of obesity. *J. Clin. Invest* **2010**, *120*, 2953-2966.
9. Vijayakumar, R. S.; Lin, Y.; Shia, K. S.; Yeh, Y. N.; Hsieh, W. P.; Hsiao, W. C.; Chang, C. P.; Chao, Y. S.; Hung, M. S. Induction of fatty acid oxidation resists weight gain, ameliorates hepatic steatosis and reduces cardiometabolic risk factors. *Int. J. Obes.* **2011**, doi: 10.1038/ijo.2011.171.
10. Schinkel, A. H. P-Glycoprotein, a gatekeeper in the blood-brain barrier. *Adv. Drug Deliv. Rev.* **1999**, *36*, 179-194.
11. Begley, D. J. ABC transporters and the blood-brain barrier. *Curr. Pharm. Des* **2004**, *10*, 1295-1312.
12. Schinkel, A. H.; Wagenaar, E.; Mol, C. A.; van Deemter, L. P-glycoprotein in the blood-brain barrier of mice influences the brain penetration and pharmacological activity of many drugs. *J. Clin. Invest* **1996**, *97*, 2517-2524.
13. Loscher, W.; Potschka, H. Drug resistance in brain diseases and the role of drug efflux transporters. *Nat. Rev. Neurosci.* **2005**, *6*, 591-602.
14. Tsujikawa, K.; Dan, Y.; Nogawa, K.; Sato, H.; Yamada, Y.; Murakami, H.; Ohtani, H.; Sawada, Y.; Iga, T. Potentiation of domperidone-induced catalepsy by a P-glycoprotein inhibitor, cyclosporin A. *Biopharm. Drug Dispos.* **2003**, *24*, 105-114.
15. Sadeque, A. J.; Wandel, C.; He, H.; Shah, S.; Wood, A. J. Increased drug delivery to the brain by P-glycoprotein inhibition. *Clin. Pharmacol. Ther.* **2000**, *68*, 231-237.
16. Lange, J. H.; van Stuijvenberg, H. H.; Veerman, W.; Wals, H. C.; Stork, B.; Coolen, H. K.; McCreary, A. C.; Adolfs, T. J.; Kruse, C. G. Novel 3,4-diarylpyrazolines as potent cannabinoid CB1 receptor antagonists with lower lipophilicity. *Bioorg. Med. Chem. Lett.* **2005**, *15*, 4794-4798.
17. El-Sheikh, A. A.; van den Heuvel, J. J.; Koenderink, J. B.; Russel, F. G. Interaction of nonsteroidal anti-inflammatory drugs with multidrug resistance protein (MRP) 2/ABCC2- and MRP4/ABCC4-mediated methotrexate transport. *J. Pharmacol. Exp. Ther.* **2007**, *320*, 229-235.
18. Pavék, P.; Merino, G.; Wagenaar, E.; Bolscher, E.; Novotná, M.; Jonker, J. W.; Schinkel, A. H. Human breast cancer resistance protein: interactions with steroid drugs, hormones, the dietary carcinogen 2-amino-1-methyl-6-phenylimidazo(4,5-b)pyridine, and transport of cimetidine. *J. Pharmacol. Exp. Ther.* **2005**, *312*, 144-152.



19. Wittgen, H. G.; van den Heuvel, J. J.; van den Broek, P. H.; Dinter-Heidorn, H.; Koenderink, J. B.; Russel, F. G. Cannabinoid CB1 receptor antagonists modulate transport activity of multidrug resistance-associated proteins MRP1, MRP2, MRP3, and MRP4. *Drug Metab Dispos.* **2011**, *39*, 1294-1302.
20. van Aubel, R. A.; Koenderink, J. B.; Peters, J. G.; Van Os, C. H.; Russel, F. G. Mechanisms and interaction of vinblastine and reduced glutathione transport in membrane vesicles by the rabbit multidrug resistance protein Mrp2 expressed in insect cells. *Mol. Pharmacol.* **1999**, *56*, 714-719.
21. Cooray, H. C.; Blackmore, C. G.; Maskell, L.; Barrand, M. A. Localisation of breast cancer resistance protein in microvessel endothelium of human brain. *Neuroreport* **2002**, *13*, 2059-2063.
22. Sugimoto, H.; Hirabayashi, H.; Kimura, Y.; Furuta, A.; Amano, N.; Moriwaki, T. Quantitative investigation of the impact of P-glycoprotein inhibition on drug transport across blood-brain barrier in rats. *Drug Metab Dispos.* **2011**, *39*, 8-14.
23. Hyafil, F.; Vergely, C.; Du Vignaud, P.; Grand-Perret, T. In vitro and in vivo reversal of multidrug resistance by GF120918, an acridonecarboxamide derivative. *Cancer Res.* **1993**, *53*, 4595-4602.
24. Lange, J. H.; van der Neut, M. A.; Borst, A. J.; Yildirim, M.; van Stuijvenberg, H. H.; van Vliet, B. J.; Kruse, C. G. Probing the cannabinoid CB1/CB2 receptor subtype selectivity limits of 1,2-diarylimidazole-4-carboxamides by fine-tuning their 5-substitution pattern. *Bioorg. Med. Chem. Lett.* **2010**, *20*, 2770-2775.
25. Barna, I.; Till, I.; Haller, J. Blood, adipose tissue and brain levels of the cannabinoid ligands WIN-55,212 and SR-141716A after their intraperitoneal injection in mice: compound-specific and area-specific distribution within the brain. *Eur. Neuropsychopharmacol.* **2009**, *19*, 533-541.
26. Allen, J. D.; van, L. A.; Lakshai, J. M.; van, d., V.; van, T. O.; Reid, G.; Schellens, J. H.; Koomen, G. J.; Schinkel, A. H. Potent and specific inhibition of the breast cancer resistance protein multidrug transporter in vitro and in mouse intestine by a novel analogue of fumitremorgin C. *Mol. Cancer Ther.* **2002**, *1*, 417-425.
27. Matsson, P.; Pedersen, J. M.; Norinder, U.; Bergstrom, C. A.; Artursson, P. Identification of Novel Specific and General Inhibitors of the Three Major Human ATP-Binding Cassette Transporters P-gp, BCRP and MRP2 Among Registered Drugs. *Pharm. Res.* **2009**, *26*, 1816-1831.
28. Warren, M. S.; Zerangue, N.; Woodford, K.; Roberts, L. M.; Tate, E. H.; Feng, B.; Li, C.; Feuerstein, T. J.; Gibbs, J.; Smith, B.; de Morais, S. M.; Dower, W. J.; Koller, K. J. Comparative gene expression profiles of ABC transporters in brain microvessel endothelial cells and brain in five species including human. *Pharmacol. Res.* **2009**, *59*, 404-413.
29. Uchida, Y.; Ohtsuki, S.; Katsukura, Y.; Ikeda, C.; Suzuki, T.; Kamiie, J.; Terasaki, T. Quantitative targeted absolute proteomics of human blood-brain barrier transporters and receptors. *J. Neurochem.* **2011**, *117*, 333-345.
30. Kelder, J.; Grootenhuys, P. D.; Bayada, D. M.; Delbressine, L. P.; Ploemen, J. P. Polar molecular surface as a dominating determinant for oral absorption and brain penetration of drugs. *Pharm. Res.* **1999**, *16*, 1514-1519.
31. van de Waterbeemd, H.; Camenisch, G.; Folkers, G.; Chretien, J. R.; Raevsky, O. A. Estimation of blood-brain barrier crossing of drugs using molecular size and shape, and H-bonding descriptors. *J. Drug Target* **1998**, *6*, 151-165.
32. Oostendorp, R. L.; Beijnen, J. H.; Schellens, J. H. The biological and clinical role of drug transporters at the intestinal barrier. *Cancer Treat. Rev.* **2009**, *35*, 137-147.
33. Lin, J. H.; Yamazaki, M. Clinical relevance of P-glycoprotein in drug therapy. *Drug Metab Rev.* **2003**, *35*, 417-454.
34. Pang, Z.; Wu, N. N.; Zhao, W.; Chain, D. C.; Schaffer, E.; Zhang, X.; Yamdagni, P.; Palejwala, V. A.; Fan, C.; Favara, S. G.; Dressler, H. M.; Economides, K. D.; Weinstock, D.; Cavallo, J. S.; Naimi, S.; Galzin, A. M.; Guillot, E.; Pruniaux, M. P.; Tocci, M. J.; Polites, H. G. The central cannabinoid CB1 receptor is required for diet-induced obesity and rimonabant's antiobesity effects in mice. *Obesity (Silver Spring)* **2011**, *19*, 1923-1934.
35. Quarta, C.; Bellocchio, L.; Mancini, G.; Mazza, R.; Cervino, C.; Bräulke, L. J.; Fekete, C.; Latorre, R.; Nanni, C.; Bucci, M.; Clemens, L. E.; Heldmaier, G.; Watanabe, M.; Leste-Lassere, T.; Maitre, M.; Tedesco, L.; Fanelli, F.; Reuss, S.; Klaus, S.; Srivastava, R. K.; Monory, K.; Valerio, A.; Grandis, A.; De, G. R.; Pasquali, R.; Nisoli, E.; Cota, D.; Lutz, B.; Marsicano, G.; Pagotto, U. CB(1) signaling in forebrain and sympathetic neurons is a key determinant of endocannabinoid actions on energy balance. *Cell Metab* **2010**, *11*, 273-285.



Chapter 4

Transport of the coumarin metabolite 7-hydroxycoumarin glucuronide is mediated via multidrug resistance-associated proteins 3 and 4

Hanneke G.M. Wittgen¹, Jeroen J.M.W. van den Heuvel¹, Petra H.H. van den Broek¹, Sanna Siissalo², Geny M.M. Groothuis², Inge A.M. de Graaf², Jan B. Koenderink¹, Frans G.M. Russel¹

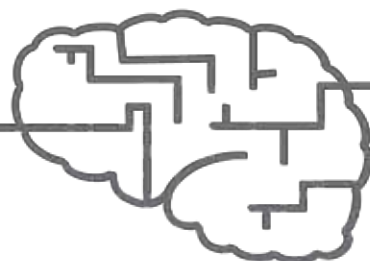
¹ Department of Pharmacology and Toxicology, Radboud University Nijmegen Medical Centre, Nijmegen Centre for Molecular Life Sciences, the Netherlands

² Division of Pharmacokinetics, Toxicology and Targeting, Department of Pharmacy, University of Groningen

Published in *Drug Metabolism and Disposition*, June 2012 (40), p. 1076-1079

Reprinted with permission of the American Society for Pharmacology and Therapeutics. All rights reserved.

Copyright © 2012 by The American Society for Pharmacology and Experimental Therapeutics.



Abstract

Coumarin (1, 2-benzopyrone) is a natural compound that has been used as a fragrance in food and perfume industry, and could have therapeutic usefulness in the treatment of lymphedema and different types of cancer. Previously, several pharmacokinetic studies of coumarin have been performed in humans, which revealed extensive first-pass metabolism of the compound. 7-Hydroxycoumarin (7-HC) and its glucuronide (7-HC-G) are the main metabolites formed in humans, and via this route, 80-90 percent of the absorbed coumarin is excreted into urine, mainly as 7-HC-G. Active transport processes play a role in the urinary excretion of 7-HC-G, however, until now, the transporters involved remained to be elucidated. In this study, we investigated whether the efflux transporters multidrug resistance-associated proteins (MRP) 1-4, breast cancer resistance protein (BCRP), or P-glycoprotein (P-gp), play a role in 7-HC and 7-HC-G transport. For this purpose, we measured uptake of the metabolites into membrane vesicles overexpressing these transporters. Our results showed that 7-HC is not transported by any of the efflux transporters tested, whereas 7-HC-G was a substrate of MRP3 and MRP4. These results are in line with the pharmacokinetic profile of coumarin, and suggest that MRP3 and MRP4 are the main transporters involved in the excretion of the coumarin metabolite 7-HC-G from liver and kidney.

Introduction

Coumarin (1, 2-benzopyrone) is a natural compound that is found in many plants, *e.g.* the tonka bean and cinnamon bark oil (Fig. 1A). It has been used as a fragrance in perfume and food, and coumarin and its metabolites have also been shown to be effective as a medicinal therapy, reducing lymphedema and having anti-tumor activity.^{1, 2} However, in rodents, coumarin causes hepatotoxicity, which led to restricted usage of this compound in the food and fragrance industry and in medicinal therapy.³

Because coumarin is naturally present in food and is suggested to have a potential therapeutic value, many studies have been performed to obtain insight into its pharmacokinetic characteristics in humans. Sampling human plasma after oral administration of coumarin showed that, although almost completely absorbed, only 2-6% reaches the systemic circulation.⁴ This is due to extensive first-pass metabolism of coumarin to 7-hydroxycoumarin (7-HC) by cytochrome P450 (CYP) 2A6, and, subsequently, to its glucuronide (7-HC-G) and sulfate (7-HC-S) conjugates by uridine 5'-diphospho glucuronosyltransferases (UGTs) and sulfotransferases, respectively.^{1, 4-6} Because coumarin 7-hydroxylation is mainly mediated via CYP2A6, it has been used as a model substrate for CYP2A6 activity in humans.¹ In addition, 7-HC is used as a model substrate for the investigation of glucuronidation activity of liver and intestinal models because many UGTs have the capability to glucuronidate this compound (Fig. 1).⁷⁻⁹

7-HC-G represents the main metabolite in plasma, indicating that it is formed in intestine or liver, and at a low dose of coumarin, approximately 80-90% of the absorbed dose of coumarin is excreted in urine, mainly as 7-HC-G, whereas less than one percent is excreted via the feces.¹⁰⁻¹² At higher doses of coumarin, the metabolism seems to become saturated, which is reflected in a lower percentage of 7-HC and 7-HC-G excretion in urine (55-63%).^{3, 13}

The clearance of 7-HC-G exceeds the glomerular filtration rate, therefore, it is considered to be actively secreted into the urine by the tubular segments in the kidney.¹² Efflux transporters belonging to the ATP-binding cassette (ABC) family, such as multidrug-resistance associated proteins (MRPs), breast cancer resistance protein (BCRP), and P-glycoprotein (P-gp) are known to play a role in the active tubular secretion of compounds from the kidney.^{14, 15} Until now, the ABC transporters involved in the disposition of the 7-hydroxycoumarin metabolites have not been identified. To study the role of the most important drug efflux transporters in the handling of 7-HC and 7-HC-G, we determined the ATP-dependent uptake of these metabolites in membrane vesicles overexpressing MRP1-4, P-gp, and BCRP.



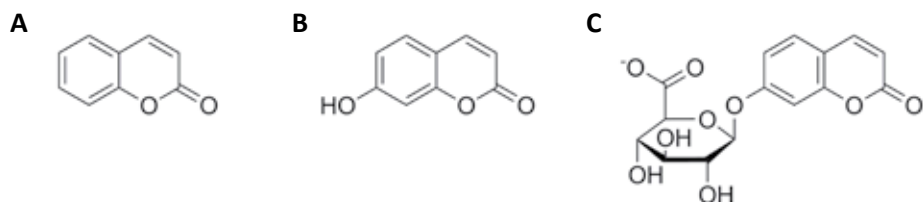


Figure 1 Chemical structures of coumarin (A), 7-hydroxycoumarin (B), and 7-hydroxycoumarin glucuronide (C)

Materials and methods

Materials

7-hydroxycoumarin (7-HC), 7-hydroxycoumarin glucuronide (7-HC-G), adenosine 5'-triphosphate magnesium salt (ATP) (from bacterial source), adenosine 5'-monophosphate monohydrate (from yeast), estrone sulfate (E_1S), estradiol 17- β -D-glucuronide ($E_217\beta G$), DL-dithiothreitol (DTT) and reduced glutathione (GSH) were purchased from Sigma-Aldrich (Zwijndrecht, the Netherlands). Multiscreen_{HTS} filter plates and Vacuum Manifold filtration device were from Millipore (Etten-Leur, the Netherlands). [6,7- $^3H(N)$]- $E_217\beta G$ (41.8 Ci/mmol) and [6,7- $^3H(N)$]- E_1S (54.3 Ci/mmol) were purchased from Perkin Elmer (Groningen, the Netherlands). ([3H])-*N*-methyl quinidine (NMQ) was from Solvo Biotechnology (Szeged, Hungary).

Production of membrane vesicles overexpressing the efflux transporters

HEK293 cells were transduced with baculovirus encoding MRP1-4, BCRP, P-gp, or enhanced yellow fluorescent protein (negative control protein), and three days after transduction, cells were harvested and membrane vesicles were made, following a previously described protocol, with the exception that during vesicle isolation, the homogenized cells were spun down at 4000g instead of 1000g for 20 minutes.¹⁶ Protein expression and the functionality of each batch of membrane vesicles were confirmed via immunoblot (data not shown) and in a radioactive vesicular transport assay using [3H]- $E_217\beta G$ for MRP1-4, and [6,7- $^3H(N)$]- E_1S for BCRP, according to the protocols described previously and using concentrations and time points as indicated in the legend of Figure 2.^{16, 17} Functionality of P-gp vesicles was tested following the protocol of the vesicular transport assay described below, with the exception that 0.015 μCi [3H]-NMQ in a total concentration of 100 nM NMQ was used instead of 7-HC or 7-HC-G. Furthermore, samples were separated using a pre-washed Multiscreen_{HTS} HV, 0.45 μM , glass fiber 96-well filter plate. NMQ was extracted from the filters using 2 ml of scintillation fluid, and by subsequent liquid scintillation counting of [3H]NMQ associated with the filters the uptake of total NMQ into the membrane vesicles was calculated.

Vesicular transport assay with 7-HC and 7-HC-G

Uptake of 7-HC and 7-HC-G into membrane vesicles was performed using a rapid filtration technique. 30 μ l reaction mix consisted of TS buffer (10 mM Tris-HEPES, and 250 mM sucrose, pH 7.4), 4 mM ATP, 10 mM MgCl_2 , 7-HC or 7-HC-G, and 7.5 μ g of membrane vesicles. Concentrations of 7-HC and 7-HC-G and time points taken for measurements are indicated in the figure legends. To test the effect of GSH on transport of 7-HC via MRP1-4 and transport of 7-HC-G via MRP1 and MRP2, the experiment was also performed in presence of 3 mM GSH and 10 mM DTT to prevent oxidation of GSH.^{18, 19} The reaction was started when the mixture was incubated at 37°C, and stopped by placing the samples on ice and adding 150 μ l of ice-cold TS buffer. A Multiscreen_{HTS} HV, 0.45 μ M, PVDF 96-well filter plate was pre-washed with TS buffer and diluted samples were filtered through this filter plate using a Multiscreen_{HTS}-Vacuum Manifold filtration device. The filters were washed twice with TS-buffer and were then separated from the plate. Compounds were extracted from filters by incubation with 20% acetonitrile for 1 hour at room temperature and vortexing thoroughly, and extracted samples were analyzed by HPLC. In control experiments, ATP was substituted with AMP. Net ATP-dependent transport was calculated by subtracting values measured in the presence of AMP from those measured in the presence of ATP.

HPLC analysis of 7-HC and 7-HC-G

The concentration of 7-HC and 7-HC-G in the samples was analyzed using reversed-phase high performance liquid chromatography (HPLC) and fluorescence detection with excitation and emission wavelength set at 316 nm and 382 nm. The HPLC consisted of a P2000 pump, an AS3000 autosampler and a FL3000 fluorescence detector (Thermo-Separation Products). Compounds were separated on a Grace-Smart RP-18 column (150x4.6 mm, 5 μ m, Grace Division Discovery Sciences). The temperature of the column was set at 40°C and the injection volume was 50 μ l. The mobile phase composition was 5% methanol and 0.2% acetic acid in water for solvent A, and 50% acetonitrile with 0.1% tetrahydrofuran for solvent B. Separation was achieved using a linear gradient from 20% B to 50% B in 8 minutes, with a flow rate of 1 ml/min. Standard curve calibrations were performed on a concentration range of 7-HC (0.3 – 5 μ M) and 7-HC-G (10 – 500 nM). Limit of quantification was 10 nM for 7-HC-G and 20 nM for 7-HC.

Data analysis

All data were expressed as mean \pm S.E.M.. Curve fitting of the concentration-dependent transport data was performed using Michaelis-Menten kinetic analysis in GraphPad Prism software, version 5.02 (GraphPad Software Inc., San Diego, CA).



Results

Identification of transporters involved in 7-HC and 7-HC-G transport

Transport of 7-HC and 7-HC-G via MRP1-4, BCRP, or P-gp, was investigated using membrane vesicles overexpressing these transporters. After incubation with 400 μM 7-HC, all values for 7-HC in the membrane vesicles were below the detection limit, and there was no ATP-dependent increase of 7-HC (data not shown). Addition of 3 mM reduced glutathione (GSH), a well-known co-factor for MRP-mediated transport, did not increase 7-HC uptake

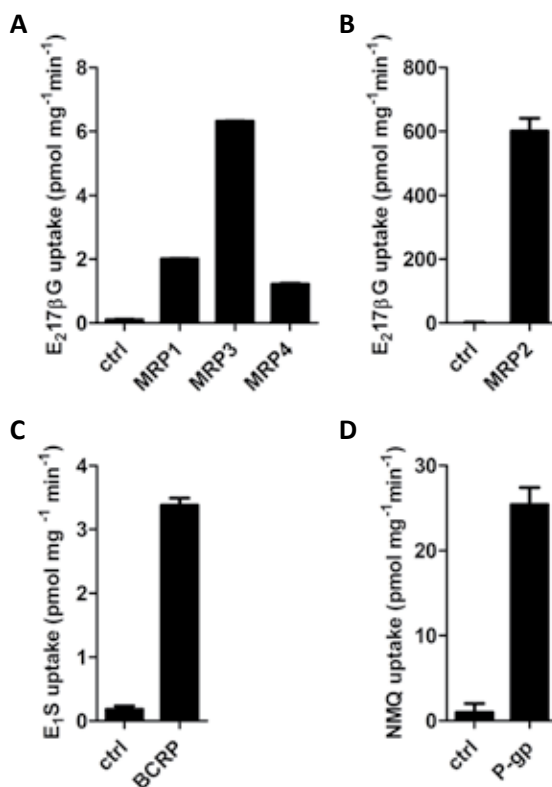


Figure 2 Transport of control substrates via MRP1-4, BCRP, and P-gp

Transport of these substrates into membrane vesicles containing these transporters or control protein (ctrl) was used as a measure of functionality of the transporters. (A) ATP-dependent transport of 100 nM estradiol-17 β -D-glucuronide ($E_217\beta G$) via MRP1, MRP3, and MRP4 during 5 minutes. (B) Transport of 50 μM of $E_217\beta G$ via MRP2 during 5 minutes. (C) BCRP-mediated transport of 300 nM estrone sulfate (E_1S) during 5 minutes. (D) ATP-dependent transport of 100 nM N-methyl quinidine (NMQ) via P-gp during 1 minute. Mean \pm S.E.M. of triplicate values of an experiment with one of the used batches of membrane vesicles is depicted for each transporter.

into MRP1-4 vesicles (data not shown). Transport of control substrates via MRP1-4, BCRP, and P-gp illustrated functionality of all transporters (Fig. 2). Therefore, the lack of ATP-dependent increase of 7-HC under the given circumstances, suggests that 7-HC is not a substrate for these transporters. Values for 7-HC-G in the presence of AMP were also below the detection limit for the glucuronide metabolite 7-HC-G after incubation with 400 μM 7-HC-G. However, there was a clear ATP-dependent increase of 7-HC-G into MRP3- and MRP4-overexpressing vesicles, which was highest for MRP4 (Fig. 3). No ATP-dependent uptake of 7-HC-G was observed in membrane vesicles overexpressing MRP1, MRP2, BCRP, or P-gp under the conditions used, and addition of 3 mM GSH did not increase transport via MRP1 and MRP2. This indicates that 7-HC-G is a substrate of MRP3 and MRP4, and not of the other transporters.

Kinetic characteristics of 7-HC-G transport via MRP3 and MRP4

Transport of 7-HC-G over time was linear up to 20 minutes for both MRP3 and MRP4 (Fig. 4A). Transport of different concentrations of 7-HC-G via MRP3 and MRP4 after 10 minutes showed normal Michaelis-Menten kinetics (Fig. 4B). K_m values for MRP3 and MRP4 were 187 ± 22 and 63 ± 11 μM , respectively. V_{\max} values for MRP3 and MRP4 were 460 ± 20 and 920 ± 50 $\text{pmol mg}^{-1} \text{min}^{-1}$, respectively.

4

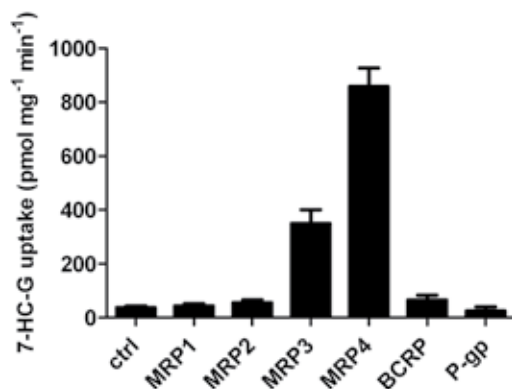


Figure 3 ATP-dependent transport of 7-HC-G by the efflux transporters MRP1-4, BCRP, and P-gp

Transport into membrane vesicles containing MRP1-4, BCRP, P-gp, or control protein (ctrl) was measured after 10 minutes of uptake in presence of 400 μM 7-HC-G at 37°C, and uptake per mg membrane vesicles per minute is plotted in the graph. Mean \pm S.E.M. of three independent experiments is shown.



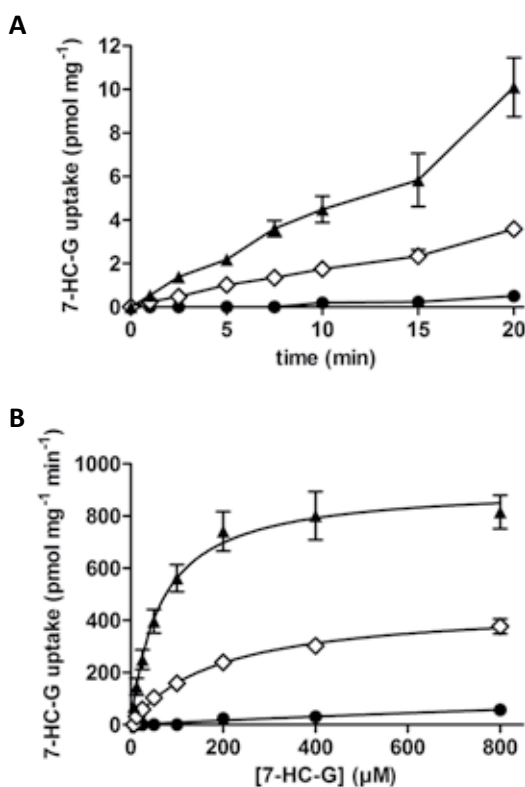


Figure 4 Time- and concentration-dependent uptake for 7-HC-G uptake into control (●), MRP3 (◇), and MRP4 (▲)containing membrane vesicles

(A) Uptake was measured in presence of 400 μM 7-HC-G at time points indicated on the x-axis, and uptake per mg membrane vesicles is plotted in the graph. (B) Uptake was measured after 10 minutes at concentrations of 7-HC-G indicated on the x-axis, and uptake per mg membrane vesicles per minute is plotted in the graph. A Michaelis-Menten curve was fitted through the data points. Mean ± S.E.M. of three independent experiments is shown for both graphs.

Discussion

In this study, we found that 7-HC-G is transported by the efflux transporters MRP3 and MRP4, whereas 7-HC is not transported by any of the efflux transporters studied. These results are in line with the distribution of these transporters in the human body, and the pharmacokinetic profile of coumarin and its metabolites.

The fact that 7-HC is not transported via efflux transporters is in accordance with a previous study, in which no transport of 7-HC via P-gp was found.²⁰ Furthermore, perfusion

studies in intestine from guinea pigs indicated that 7-HC is absorbed via passive transport processes in the intestine.²¹

The results from our transport studies with 7-HC-G point towards an important role for MRP3 in the efflux of this compound from the liver, and for MRP4 in the urinary excretion of 7-HC-G from the body. Although plasma concentrations in humans after clinical or food-derived doses of coumarin are low (1-4 μM) as compared to the K_m of 7-HC-G for MRP3 (187 μM) and MRP4 (63 μM), the rate of efflux will mainly depend on the intracellular concentration of 7-HC-G, which may very well be higher than the plasma 7-HC-G concentration.^{4, 22-24} MRP3 is mainly expressed at the basolateral surface of cells in the small intestine, colon, liver, and kidney (thick ascending loop and distal convoluted tubule cells), and MRP4 has a dual membrane localization, which is basolateral, but minimal, in hepatocytes, apical in kidney proximal tubule cells, and still unresolved in intestinal epithelium.^{25, 26} After oral administration, coumarin enters the enterocytes, most likely via a passive drug-transfer process.²¹ Because the intestine appears to lack CYP2A6, the 7-hydroxylating enzyme of coumarin, oxidative metabolism and subsequent glucuronidation of coumarin in enterocytes is limited.²⁷ After passage across the intestinal wall into the blood, coumarin will enter the liver, where 7-hydroxylation to 7-HC and glucuronidation to 7-HC-G will take place. Our results suggest that the glucuronide metabolite 7-HC-G is subsequently transported via the basolateral transporter MRP3 into the circulation, and not to the bile because it is not transported via the canalicular transporters MRP2, BCRP, or P-gp. After entering the general circulation, 7-HC-G will be taken up into the kidney proximal tubular cells, most likely via an organic anion transporter that remains to be identified (*e.g.* OAT1 or OAT3), and will be excreted via MRP4 at the apical side of these cells, which completes the urinary excretion of 7-HC-G.

Transporter-mediated efflux of glucuronide conjugates is an important step in the overall glucuronidation activity of a cell or tissue.²⁸ This implicates that not only UGT activity, but also MRP3 or MRP4 transport capacity of cells can influence the rate of glucuronidation, which should be kept in mind when using 7-HC as a model compound for determining UGT activity. Furthermore, deleterious polymorphisms of MRP3 and MRP4 might alter the metabolic route for coumarin from glucuronidation to sulfation, or possibly even towards more toxic pathways.^{1, 29-31}

In short, this study showed that MRP3 and MRP4 are the efflux transporters involved in disposition and excretion of the main metabolite of coumarin, 7-HC-G, in humans.

References

1. Lake, B. G. Coumarin metabolism, toxicity and carcinogenicity: relevance for human risk assessment. *Food Chem. Toxicol.* **1999**, *37*, 423-453.
2. Lacy, A.; O'Kennedy, R. Studies on coumarins and coumarin-related compounds to determine their therapeutic role in the treatment of cancer. *Curr. Pharm. Des* **2004**, *10*, 3797-3811.
3. Egan, D.; O'Kennedy, R.; Moran, E.; Cox, D.; Prosser, E.; Thornes, R. D. The pharmacology, metabolism, analysis,



- and applications of coumarin and coumarin-related compounds. *Drug Metab Rev.* **1990**, *22*, 503-529.
4. Ritschel, W. A.; Brady, M. E.; Tan, H. S. First-pass effect of coumarin in man. *Int. J. Clin. Pharmacol. Biopharm.* **1979**, *17*, 99-103.
 5. Wang, Q.; Ye, C.; Jia, R.; Owen, A. J.; Hidalgo, I. J.; Li, J. Inter-species comparison of 7-hydroxycoumarin glucuronidation and sulfation in liver S9 fractions. *In Vitro Cell Dev. Biol. Anim* **2006**, *42*, 8-12.
 6. Ford, R. A.; Hawkins, D. R.; Mayo, B. C.; Api, A. M. The in vivo dermal absorption and metabolism of [4-14C] coumarin by rats and by human volunteers under simulated conditions of use in fragrances. *Food Chem. Toxicol.* **2001**, *39*, 153-162.
 7. de Kanter R.; de Jager, M. H.; Draaisma, A. L.; Jurva, J. U.; Olinga, P.; Meijer, D. K. *et al.* Drug-metabolizing activity of human and rat liver, lung, kidney and intestine slices. *Xenobiotica* **2002**, *32*, 349-362.
 8. van de Kerkhof, E. G.; Ungell, A. L.; Sjöberg, A. K.; de Jager, M. H.; Hilgendorf, C.; de Graaf, I. A. *et al.* Innovative methods to study human intestinal drug metabolism in vitro: precision-cut slices compared with using chamber preparations. *Drug Metab Dispos.* **2006**, *34*, 1893-1902.
 9. Brown, L. A.; Arterburn, L. M.; Miller, A. P.; Cowger, N. L.; Hartley, S. M.; Andrews, A. *et al.* Maintenance of liver functions in rat hepatocytes cultured as spheroids in a rotating wall vessel. *In Vitro Cell Dev. Biol. Anim* **2003**, *39*, 13-20.
 10. Shilling, W. H.; Crampton, R. F.; Longland, R. C. Metabolism of coumarin in man. *Nature* **1969**, *221*, 664-665.
 11. Ford, R. A.; Hawkins, D. R.; Mayo, B. C.; Api, A. M. The in vivo dermal absorption and metabolism of [4-14C] coumarin by rats and by human volunteers under simulated conditions of use in fragrances. *Food Chem. Toxicol.* **2001**, *39*, 153-162.
 12. Ritschel, W. A.; Brady, M. E.; Tan, H. S.; Hoffmann, K. A.; Yiu, I. M.; Grummich, K. W. Pharmacokinetics of coumarin and its 7-hydroxy-metabolites upon intravenous and peroral administration of coumarin in man. *Eur. J. Clin. Pharmacol.* **1977**, *12*, 457-461.
 13. Asimus, S.; Hai, T.; Van Huong, N.; Ashton, M. Artemisinin and CYP2A6 activity in healthy subjects. *Eur. J. Clin. Pharmacol.* **2008**, *64*, 283-292.
 14. Schinkel, A. H.; Jonker, J. W. Mammalian drug efflux transporters of the ATP binding cassette (ABC) family: an overview. *Adv. Drug Deliv. Rev.* **2003**, *55*, 3-29.
 15. El-Sheikh, A. A.; Masereeuw, R.; Russel, F. G. Mechanisms of renal anionic drug transport. *Eur. J. Pharmacol.* **2008**, *585*, 245-255.
 16. Wittgen, H. G.; van den Heuvel, J. J.; van den Broek, P. H.; Dinter-Heidorn, H.; Koenderink, J. B.; Russel, F. G. Cannabinoid CB1 receptor antagonists modulate transport activity of multidrug resistance-associated proteins MRP1, MRP2, MRP3, and MRP4. *Drug Metab Dispos.* **2011**, *39*, 1294-1302.
 17. Mutsaers, H. A.; van den Heuvel, L. P.; Ringens, L. H.; Dankers, A. C.; Russel, F. G.; Wetzels, J. F. *et al.* Uremic toxins inhibit transport by breast cancer resistance protein and multidrug resistance protein 4 at clinically relevant concentrations. *PLoS. One.* **2011**, *6*, e18438.
 18. Leslie, E. M.; Ito, K.; Upadhyaya, P.; Hecht, S. S.; Deeley, R. G.; Cole, S. P. Transport of the beta -O-glucuronide conjugate of the tobacco-specific carcinogen 4-(methylnitrosamino)-1-(3-pyridyl)-1-butanol (NNAL) by the multidrug resistance protein 1 (MRP1). Requirement for glutathione or a non-sulfur-containing analog. *J. Biol. Chem.* **2001**, *276*, 27846-27854.
 19. Maeno, K.; Nakajima, A.; Conseil, G.; Rothnie, A.; Deeley, R. G.; Cole, S. P. Molecular basis for reduced estrone sulfate transport and altered modulator sensitivity of transmembrane helix (TM) 6 and TM17 mutants of multidrug resistance protein 1 (ABCC1). *Drug Metab Dispos.* **2009**, *37*, 1411-1420.
 20. Finn, G. J.; Creaven, B. S.; Egan, D. A. Investigation of intracellular signalling events mediating the mechanism of action of 7-hydroxycoumarin and 6-nitro-7-hydroxycoumarin in human renal cells. *Cancer Lett.* **2004**, *205*, 69-79.
 21. Kaul, S.; Ritschel, W. A. Studies of the intestinal transfer of coumarin and 7-hydroxycoumarin across guinea pig and rat small intestine. *Arzneimittelforschung.* **1981**, *31*, 790-795.
 22. Ritschel, W. A.; Hoffmann, K. A. Pilot study on bioavailability of coumarin and 7-hydroxycoumarin upon peroral administration of coumarin in a sustained-release dosage form. *J. Clin. Pharmacol.* **1981**, *21*, 294-300.
 23. Abraham, K.; Pfister, M.; Wöhrlin, F.; Lampen, A. Relative bioavailability of coumarin from cinnamon and cinnamon-containing foods compared to isolated coumarin: a four-way crossover study in human volunteers. *Mol. Nutr. Food Res.* **2011**, *55*, 644-653.
 24. Ford, R. A.; Hawkins, D. R.; Mayo, B. C.; Api, A. M. The in vivo dermal absorption and metabolism of [4-14C] coumarin by rats and by human volunteers under simulated conditions of use in fragrances. *Food Chem.*

- Toxicol.* **2001**, *39*, 153-162.
25. Scheffer, G. L.; Kool, M.; de Haas, M.; de Vree, J. M.; Pijnenborg, A. C.; Bosman, D. K. *et al.* Tissue distribution and induction of human multidrug resistant protein 3. *Lab Invest* **2002**, *82*, 193-201.
 26. Russel, F. G.; Koenderink, J. B.; Masereeuw, R. Multidrug resistance protein 4 (MRP4/ABCC4): a versatile efflux transporter for drugs and signalling molecules. *Trends Pharmacol. Sci.* **2008**, *29*, 200-207.
 27. Zhang, Q. Y.; Dunbar, D.; Ostrowska, A.; Zeisloft, S.; Yang, J.; Kaminsky, L. S. Characterization of human small intestinal cytochromes P-450. *Drug Metab Dispos.* **1999**, *27*, 804-809.
 28. Jeong, E. J.; Liu, X.; Jia, X.; Chen, J.; Hu, M. Coupling of conjugating enzymes and efflux transporters: impact on bioavailability and drug interactions. *Curr. Drug Metab* **2005**, *6*, 455-468.
 29. Abula, N.; Chinn, L. W.; Nakamura, T.; Liu, L.; Huang, C. C.; Johns, S. J. *et al.* The human multidrug resistance protein 4 (MRP4, ABCC4): functional analysis of a highly polymorphic gene. *J. Pharmacol. Exp. Ther.* **2008**, *325*, 859-868.
 30. Farinola, N.; Piller, N. B. CYP2A6 polymorphisms: is there a role for pharmacogenomics in preventing coumarin-induced hepatotoxicity in lymphedema patients? *Pharmacogenomics*. **2007**, *8*, 151-158.
 31. Kobayashi, K.; Ito, K.; Takada, T.; Sugiyama, Y.; Suzuki, H. Functional analysis of nonsynonymous single nucleotide polymorphism type ATP-binding cassette transmembrane transporter subfamily C member 3. *Pharmacogenet. Genomics* **2008**, *18*, 823-833.



Chapter 5

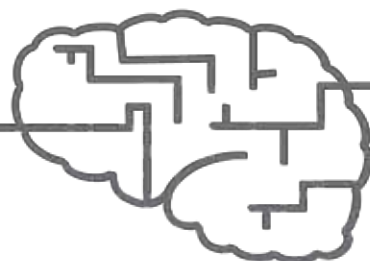
Synergistic interplay between efflux transporters and uridine 5'-diphospho glucuronosyltransferase (UGT) 2B15 in glucuronidation of 7-hydroxycoumarin

Hanneke G.M. Wittgen¹, Sanna Siissalo², Debbie G.M. Janssen¹, Jeroen J.M.W. van den Heuvel¹, Petra H.H. van den Broek¹, Marina H. de Jager², Jan B. Koenderink¹, Inge A.M. de Graaf², Geny M.M. Groothuis², Frans G.M. Russel¹

¹ Department of Pharmacology and Toxicology, Radboud University Nijmegen Medical Centre, Nijmegen Centre for Molecular Life Sciences, the Netherlands

² Division of Pharmacokinetics, Toxicology and Targeting, Department of Pharmacy, University of Groningen

Manuscript in preparation



Abstract

Glucuronidation of drugs by uridine 5'-diphospho glucuronosyltransferases (UGT) in enterocytes and hepatocytes plays an important role in first pass metabolism in intestine and liver. The hydrophilic glucuronide metabolites are excreted more effectively from the body via bile or urine than the unconjugated parent drug. Multidrug resistance-associated proteins (MRP) are necessary for the efflux of glucuronide conjugates from cells. As UGT activity can be decreased by product inhibition, it is hypothesized that UGTs and MRPs synergistically cooperate in the excretion of compounds from the body: MRPs remove the product and thereby prevent product inhibition of UGTs. In this study, we explored the possibility of synergistic interplay between MRP3/4 and UGT2B15 in HEK293 cells studying the glucuronidation of the model compound 7-hydroxycoumarin (7-HC) to 7-hydroxycoumarin glucuronide (7-HC-G). We identified sulindac as a potent inhibitor of MRP3 and MRP4, previously shown to be the transporters of 7-HC-G, at concentrations that do not inhibit UGT2B15. Inhibition of the efflux of 7-HC-G in HEK-UGT2B15 cells with sulindac increased its intracellular concentration and decreased its excretion. In addition, total metabolite formation was decreased, which suggests that efflux of 7-HC-G can influence the rate of metabolism of 7-HC. This indicates that UGTs and MRPs can cooperate in synergy, thereby providing an efficient route of elimination of drugs via glucuronidation.

Introduction

First pass metabolism plays a significant role in determining the systemic availability of orally administered drugs. Metabolism in the liver has always been pointed out as the key player in this process, but more recent studies have shown that metabolism in the intestine can also play a substantial role in first-pass metabolism.^{1,2} One type of first pass metabolism that can occur is glucuronidation, in which a glucuronic acid is conjugated to the drug by enzymes belonging to the superfamily of uridine 5'-diphospho (UDP) glucuronosyltransferases (UGTs). Glucuronidation is a Phase II type of metabolism, enhancing the urinary and biliary excretion of a drug by increasing its aqueous solubility.³ UGTs are membrane bound enzymes, and can be divided into two subfamilies, 1A and 2B, of which multiple members are expressed in the intestine.^{4,5} Glucuronidation is suggested to play a significant role in intestinal metabolism of drugs, *e.g.* of propofol and raloxifene.^{3,6}

Because glucuronidated metabolites are hydrophilic and ionized at physiological pH, they need transporters to be transferred across cell membranes.⁷ Indeed, many glucuronide conjugates are substrates of efflux transporters from the ATP-binding cassette (ABC) family including the multidrug resistance-associated proteins (MRP).⁸ Several MRPs are expressed on the plasma membrane of intestinal cells, either on the apical side (MRP2), or on the basolateral side (MRP1, MRP3), or possibly on both sides (MRP4).⁹⁻¹³ Thus, glucuronide conjugates can be transported out of enterocytes both to the intestinal lumen and to the blood perfusing the intestine.

Because MRPs mediate efflux of glucuronide metabolites that are produced intracellularly, MRPs and UGTs act in concert to excrete compounds from the body. For example, it has been shown that MRP transport increases the excretion of a glucuronide metabolite of morphine.¹⁴ Unfortunately, the authors did not describe whether this transport also increased the total metabolite formation. Therefore, this cooperation between UGTs and MRPs could simply be the result of an additive sequence of events, in which absence of the transporter limits the excretion but not the formation of the metabolite. The other possibility is that this interplay between MRPs and UGTs is synergistic, implicating that excretion of the glucuronide metabolite via MRPs prevents product inhibition by which the accumulated glucuronide conjugates inhibit the enzyme's metabolic activity.⁷ In this situation, the activity of UGTs is highly increased due to transport of the metabolite out of the cell (Fig. 1A). When efflux of the metabolite is reduced by inhibition of MRP activity, the intracellular glucuronide conjugate concentration increases, leading to inhibition of UGT metabolizing activity and a reduction of total metabolite formation by UGTs (Fig. 1B).

Here, we tested the hypothesis of synergistic interplay between MRPs and UGT2B15. For this purpose, we investigated the glucuronidation of the model compound 7-hydroxycoumarin (7-HC) to 7-hydroxycoumarin glucuronide (7-HC-G) by UGT2B15 overexpressed in HEK293 cells. UGT2B15 is one of the many UGTs that glucuronidates 7-HC to 7-HC-G, and that is also expressed in the intestine.¹⁵ In a previous study (Chapter 4) we showed that 7-HC-G is



transported via MRP3 and MRP4. To selectively inhibit efflux transport and not metabolism, we identified a MRP3 and MRP4 inhibitor with less inhibitory potency against UGT2B15 activity. We used this compound to investigate the effect of inhibiting 7-HC-G efflux on the rate of 7-HC glucuronidation by UGT2B15.

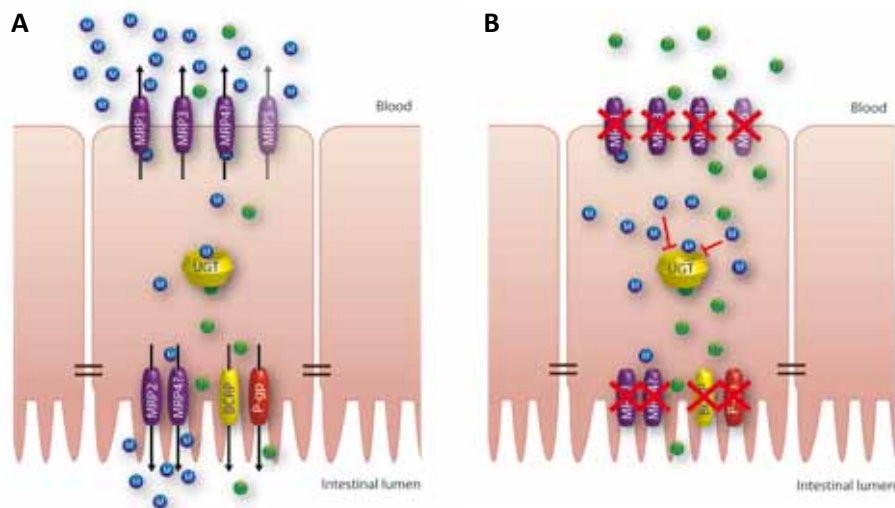


Figure 1 Model of interplay between UGTs and efflux transporters in the intestine

(A) Metabolism of drugs by UGTs in presence of active efflux transporters. (B) Metabolism of drugs by UGTs in absence of active efflux transporters. M, metabolite; D, drug.

Materials and methods

Materials

7-Hydroxycoumarin (7-HC), 7-hydroxycoumarin glucuronide (7-HC-G), adenosine 5'-triphosphate magnesium salt (ATP) (from bacterial source), adenosine 5'-monophosphate monohydrate (AMP) (from yeast), perchloric acid (PCA), sodium butyrate, sulindac, quercetin, benzbromarone, dipyrindamole, and uridine 5'-diphospho glucuronic acid (UDPGA) trisodium salt were purchased from Sigma-Aldrich (Zwijndrecht, the Netherlands). MK571 was from Biomol (Hamburg, Germany). Bac-to-Bac and Gateway system, and DMEM + GlutaMAX-I culture medium were purchased from Invitrogen (Breda, the Netherlands). Fetal calf serum, culture flasks (175 cm²), and CellStar 12- and 24-wells culture plates were purchased from Greiner (Alphen aan de Rijn, the Netherlands). Rat tail collagen (type I) was from First Link Limited (United Kingdom). Purified Max Pab mouse polyclonal human UGT2B15-antibody (B01P) was from Abnova (Tapei, Taiwan).

Generation of baculovirus coding for UGT2B15 and control protein

A Gateway pDONR223 vector containing the full-length human UGT2B15 sequence equal to NM_001076 (HsCD00080128) was purchased from Harvard PlasmID database (Boston, MA, USA). Subsequently, the UGT2B15 construct was cloned into a VSV-G improved pFastBacDual vector for mammalian cell transduction using the Gateway system (Invitrogen).¹⁷ Full-length human enhanced yellow fluorescent protein (eYFP) was cloned as described previously, and used as a negative control.¹⁷ Baculoviruses were produced using the Bac-to-Bac system, as described by the manufacturer (Invitrogen).

Cell culture and transduction of HEK293 cells

HEK293 cells were cultured in DMEM-GlutaMAX-I supplemented with 10% fetal calf serum at 37°C under 5% CO₂-humidified air. For the experiments, cells were transduced in different culture formats: 175 cm² flasks, 12- and 24-well culture plates. For transduction of cells in 175 cm² flasks, HEK293 cells were cultured 40% confluent, after which culture medium was removed and a concentrated virus/medium mixture (3:7) was added. Cells were incubated for 15 minutes at room temperature. After incubation, 20 ml medium and sodium butyrate (5 mM) was added to obtain a final virus:medium ratio of 1:17. For transduction of cells in 12- or 24-wells, respectively 350,000 and 150,000 cells were seeded in the wells. Before seeding the cells in 24-wells plates, the wells were coated with 500 µl of a 100 µg/ml rat tail collagen (type I) solution for at least two hours at 37°C. Coating was washed with phosphate-buffered saline once, and HEK293 cells were seeded. 24 hours after seeding, the cells were incubated for 15 minutes with a concentrated virus mixture, after which medium with a final concentration of 5 mM sodium butyrate was added reaching a final virus:medium ratio of 2:25 in a total of 1000 µl (12-well) and 500 µl (24-well). After transduction in both flasks and wells-plates, the cells were cultured for three more days under normal culture conditions before performing the experiment or harvesting the cells. Protein concentration of homogenates and western blot samples was determined with a Bio-Rad protein assay kit from Bio-Rad Laboratories (Veenendaal, the Netherlands).

Western blot

HEK293-ctrl and HEK293-UGT2B15 cell pellets were lysed in mQ containing DNase I (20 U/µl) (Invitrogen) and Complete mini protease inhibitor cocktail (Roche Diagnostics, the Netherlands). A 24 µg protein sample was solubilized in SDS-polyacrylamide gel electrophoresis buffer and separated on SDS gel containing 12% acrylamide. Subsequently, they were blotted on nitrocellulose membrane using the iBlot dry blotting system (Invitrogen). Overnight incubation with mouse-anti-human UGT2B15 (1:2000) followed by 1 hour incubation with the secondary antibody fluorescent goat-anti-mouse IRdye800 (1:10000) (Rockland Immunochemicals, Gilbertsville, USA) was used for detection of UGT2B15. Signal was visualized using the Odyssey imaging system (Li-Cor Biosciences, Lincoln, NE).



Glucuronidation of 7-HC by intact HEK-UGT2B15 cells

For the determination of the kinetic characteristics of 7-HC glucuronidation in HEK-UGT2B15 cells, we used HEK293 cells transduced with UGT2B15 in 12-wells culture plates. To determine the rate of glucuronidation, transduced cells were incubated at 37°C with 50 μ M 7-HC in Tris-HEPES buffer (10 mM HEPES, 132 mM NaCl, 4.2 mM KCl, 1 mM CaCl_2 , 1 mM MgCl_2 , 5.5 mM D(+)-glucose, calibrated to pH 7.4 using 1M Tris solution), and medium was sampled after 2.15, 3, 4, and 6 hours. To determine the concentration-dependency of glucuronidation, cells were incubated at 37°C with different concentrations of 7-HC (5-250 μ M) in Tris-HEPES buffer. Medium was sampled after 3 hours. 7-HC-G concentration in medium samples was determined by HPLC.

Homogenate production of HEK-UGT2B15 cells

For HEK-UGT2B15 cell homogenate production, HEK293 cells were cultured and transduced with UGT2B15 in 175 cm^2 flasks. Three days after transduction, cells were harvested by centrifugation at 2000g for 5 minutes. The cell pellet was resuspended in ice-cold homogenization buffer (50 mM HEPES, 150 mM KCl, 5mM MgCl_2 , pH was set at 7.4 with 1M Tris solution) and sonicated for 5 x 15 seconds, separated by 1 minute of cooling at 4°C, using the Bioruptor NextGen (Diagenode, Liège, Belgium). After centrifugation at 2500g for 10 minutes, the protein concentration of the supernatant was determined and aliquots were stored at -80°C.

7-HC glucuronidation by HEK-UGT2B15 homogenate and effect of MRP inhibitors

The kinetics of 7-HC glucuronidation by UGT2B15 were also determined in the HEK-UGT2B15 cell homogenate. For the time curve, the reaction mixture consisted of 10 mM UDPGA and 500 μ M of 7-HC filled up with homogenization buffer to a total of 200 μ l. After pre-incubation of this mixture, 0.25 mg/ml UGT2B15 homogenate was added in a total volume of 200 μ l and the mix was incubated for 0-4 hours at 37 °C. The reaction was stopped by adding 10 μ l 70% PCA and centrifugation at 16,000g for 10 minutes at 4°C. The concentration of 7-HC-G in the supernatant was measured by HPLC. For the concentration curve, 0-500 μ M of 7-HC was used and the mix was incubated for 1 hour at 37°C.

To test the effect of different MRP inhibitors on 7-HC glucuronidation by UGT2B15 alone, HEK-UGT2B15 homogenate was incubated with 100 μ M 7-HC and different concentrations (0-300 μ M) of benzbromarone, diprydamole, quercetin, MK571, and sulindac.

Effect of MRP inhibitors on 7-HC-G transport into MRP3 and MRP4 vesicles

Membrane vesicle expressing MRP3 or MRP4 protein were made following a protocol described previously, with the exception that during vesicle isolation, the homogenized cells were centrifuged at 4000g instead of 1000g for 20 minutes.¹⁶ Subsequently, the membrane vesicles were used to study the effect of different concentrations of sulindac, quercetin, benzbromarone, and diprydamol on the uptake of 7-HC-G into the membrane vesicles

using a rapid filtration technique. A sample of 30 μ l reaction mix consisted of TS buffer (10 mM Tris-HEPES, and 250 mM sucrose, pH 7.4), 4 mM ATP, 10 mM MgCl_2 , 100 μ M 7-HC-G, MRP inhibitors dipyridamole, benzbromarone, quercetin, or sulindac (0.1 – 100 μ M), and 7.5 μ g of membrane vesicles. The reaction was started when the mixture was incubated at 37°C, and stopped after 10 minutes by placing the samples on ice and adding 150 μ l of ice-cold TS buffer. A Multiscreen_{HTS} HV, 0.45 μ M, PVDF 96-well filter plate was pre-washed with TS buffer and diluted samples were filtered through this filter plate using a Multiscreen_{HTS}-Vacuum Manifold filtration device (Millipore, Etten-Leur, the Netherlands). The filters were washed twice with TS-buffer and were then separated from the plate. Compounds were extracted from filters by incubation with 20% acetonitrile for 1 hour at room temperature and vortexing thoroughly, and extracted samples were analyzed with HPLC. In control experiments, ATP was substituted with AMP. Net ATP-dependent transport was calculated by subtracting values measured in the presence of AMP from those measured in the presence of ATP.

Effect of sulindac on cellular glucuronidation in HEK-UGT2B15 cells

To investigate the effect of sulindac on glucuronidation in intact HEK-UGT2B15 cells, HEK293 cells were seeded and transduced in collagen-coated 24-wells plates. During the experiment, cells were incubated with 350 μ l of 100 μ M 7-HC and sulindac (0 - 50 μ M) in Tris-HEPES buffer at 37°C. After 2 hours of incubation, 200 μ l of medium was sampled, and 10 μ l of 100% PCA was added to the sampled medium to stop the reaction and precipitate detached cells. The rest of the incubation medium was aspirated, and cells were washed twice with warm Tris-HEPES buffer (37°C). Cells were lysed in 100 μ l mQ, and 5 μ l of 100% PCA was added to precipitate the protein. All samples were centrifuged at 16,000g for 5 minutes. Concentration of 7-HC-G in supernatant of these samples was analyzed by HPLC.

HPLC analysis of 7-HC-G

The concentration of 7-HC-G in the samples was analyzed using reversed-phase high performance liquid chromatography (HPLC) and fluorescence detection with excitation and emission wavelength set at 316 nm and 382 nm. The HPLC consisted of a P2000 pump, an AS3000 autosampler and a FL3000 fluorescence detector (Thermo-Separation Products). Compounds were separated on a Grace-Smart RP-18 column (150x4.6 mm, 5 μ m, Grace Division Discovery Sciences). The temperature of the column was set at 40°C and the injection volume was 50 μ l. The mobile phase composition was 5% methanol and 0.2% acetic acid in water for solvent A, and 50% acetonitril with 0.1% tetrahydrofuran for solvent B. Separation was achieved using a linear gradient from 20% B to 50% B in 8 minutes with a flow rate of 1 ml/min. The gradient was then immediately returned to 20% B and the initial conditions were restored in 5 minutes. Because sulindac disturbed the analysis of samples from the experiment with intact HEK-UGT2B15 cells and sulindac, a different gradient was used for these experiments: 20% B (0-1 min), gradient of 20 to 80% B (1-3 min), 80% B (3-



12 min), followed by re-equilibration of the column at 20% B until 18 min. Standard curve calibrations were performed on a concentration range of 7-HC (0.3 – 5 μM) and 7-HC-G (10 – 500 nM) with or without PCA, dependent on the method used for preparing the samples. The limit of quantification for 7-HC-G was 10 nM. This implicates that for the experiments measuring intracellular amounts of 7-HC-G, the limit of quantification was 1 pmol.

RNA isolation and quantitative PCR for MRP3 and MRP4 expression

HEK293 cells were seeded in duplicate and transduced with UGT2B15 in collagen-coated 24-wells plates. Three days after transduction, cells were harvested using trypsin and centrifugation at 2000g for 5 minutes. The cell pellets were resuspended in lysis buffer from the RNA isolation kit and, subsequently, RNA was isolated from the duplicate samples using the NucleoSpin® RNA II kit (Macherey-Nagel, Düren, Germany) according to the manufacturer's instructions. Subsequently, a reverse transcriptase reaction was performed with 1 μg RNA using random primers (Invitrogen, Breda, the Netherlands) and an Omniscript® RT kit (Qiagen, Hilden, Germany), following manufacturer's recommendations. Synthesized cDNA was used for quantitative PCR, performed in a C1000™ Thermal Cycler in combination with a CFX96™ Real-Time system (Bio-Rad Laboratories, Veenendaal, the Netherlands) by means of the TaqMan® protocol (Applied Biosystems, Warrington, UK). *ABCC3* (MRP3) and *ABCC4* (MRP4) mRNA expression (C_t) was normalized to the mRNA expression of the housekeeping gene β -actin (ΔC_t) ($n = 1$, in duplicate). The primer-probe sets were obtained from Applied Biosystems (β -actin, 4352933E; *ABCC3*, Hs00978473_m1; *ABCC4*, Hs00195260_m1).

5

Kinetic and statistical analysis

K_m and V_{max} values of UGT2B15-mediated 7-HC glucuronidation were determined according to Michaelis-Menten kinetics by using GraphPad Prism software, version 5.02 (GraphPad Software Inc., San Diego, CA). Inhibitory data of sulindac on MRP3- and MRP4-mediated transport of 7-HC-G and of 7-HC glucuronidation in HEK-UGT2B15 homogenate were analyzed according to a one-site binding model by non-linear regression analysis (GraphPad Prism 5.02) using the equation: $y = \text{bottom} + (\text{top} - \text{bottom}) / (1 + 10^{x - \log(IC_{50})})$. Statistical differences were determined using a one-way analysis of variance (ANOVA) followed by a Dunnett's multiple comparison test in GraphPad Prism. Differences were considered to be significant at $p < 0.05$.

Results

Metabolism of 7-HC to 7-HC-G in HEK293 cells overexpressing UGT2B15

Western blotting of UGT2B15-transduced HEK293 cells (HEK-UGT2B15) showed clear overexpression of this protein in comparison to HEK293 cells overexpressing a control protein (HEK-ctrl) (Fig. 2A). We determined kinetics of glucuronidation in intact cells by measuring

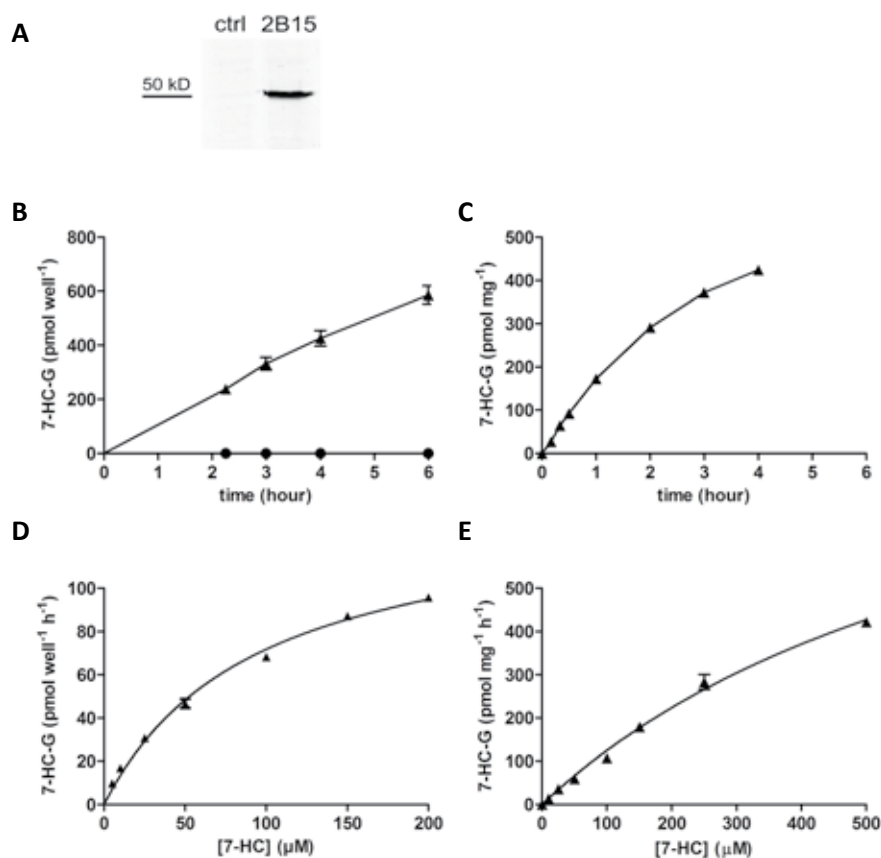


Figure 2 Metabolism of 7-HC to 7-HC-G in control (●) and UGT2B15 (▲) overexpressing HEK293 cells and HEK-UGT2B15 homogenate

(A) Immunoblot detection of UGT2B15 in HEK293 cells expressing control protein (ctrl) or UGT2B15 (2B15). (B) Time-dependent metabolism of 50 μM 7-HC to 7-HC-G in intact HEK293 cells overexpressing control or UGT2B15 protein. The graph shows the amount of 7-HC-G in the medium sampled per well at time points indicated on the x-axis. Mean \pm S.D. of duplicate determinations of a representative experiment is shown (two independent experiments have been performed, total $n = 2$). (C) Time-dependent metabolism of 500 μM 7-HC to 7-HC-G in HEK-UGT2B15 cell homogenate. Formation of 7-HC-G per mg of cell homogenate is plotted on the y-axis. Mean \pm S.D. of duplicate determinations of a representative experiment is shown (total $n = 3$). (D) Concentration-dependent metabolism of 7-HC to 7-HC-G in intact HEK-UGT2B15 cells. The graph depicts the amount of 7-HC-G excreted into the medium per well per hour during 3 hours at different concentrations of 7-HC. Mean \pm S.D. of duplicate determinations of a representative experiment is shown (total $n = 3$). (E) Concentration-dependent metabolism of 7-HC to 7-HC-G in HEK-UGT2B15 cell homogenate. The graph depicts the amount of 7-HC-G produced per mg cell homogenate per hour during 2 hours of incubation with different concentrations of 7-HC. Mean \pm S.D. of duplicate determinations of a representative experiment is shown (total $n = 3$).

the excreted metabolites, which represents approximately 98% of total metabolite formation at a concentration of 100 μM 7-HC (Fig. 4). Metabolism of 7-HC to 7-HC-G in HEK-UGT2B15 intact cells was time-dependent and linear up to 6 hours, at least, whereas there was no metabolism in HEK-ctrl cells (Fig. 2B). Metabolism to 7-HC-G by UGT2B15 in intact cells followed Michaelis-Menten kinetics, with a K_m of $61 \pm 19 \mu\text{M}$ and a V_{\max} of $119 \pm 23 \text{ pmol well}^{-1} \text{ h}^{-1}$ (Fig. 2D). In HEK-UGT2B15 cell homogenate, metabolism was linear up to 0.5 hours but K_m and V_{\max} could not be accurately determined in the concentration range used for this experiment. However, the K_m appeared to be much higher in cell homogenate than in intact HEK-UGT2B15 cells.

Expression of endogenous transporters

7-HC-G appeared to be excreted from HEK-UGT2B15 even though we did not overexpress transporters in these cells (Fig. 2B-C). This implicates that these cells express endogenous transporters, possibly the 7-HC-G transporters MRP3 and MRP4, that can efflux 7-HC-G into the medium. Quantitative PCR confirms the presence of MRP4 mRNA ($C_t = 26.6$, $\Delta C_t = 5.0$) in HEK-UGT2B15 cells, whereas there appears to be very little MRP3 mRNA present ($C_t = 35.0$, $\Delta C_t = 13.3$).

Table 1 Inhibitory effect of various MRP inhibitors on uptake of 7-HC-G via MRP3 and MRP4 into membrane vesicles and glucuronidation of 7-HC by HEK-UGT2B15 homogenate. Data are presented as mean (95% confidence interval) of non-linear regression analysis of data of two independent experiments in duplicate

Inhibitor	MRP3		MRP4		UGT2B15	
	$\text{IC}_{50} (\mu\text{M})$	$K_i (\mu\text{M})^a$	$\text{IC}_{50} (\mu\text{M})$	$K_i (\mu\text{M})^a$	$\text{IC}_{50} (\mu\text{M})$	$K_i (\mu\text{M})^a$
Dipyridamole	n.i.		26 (13-52)	10	38 (21-67)	33
Benzbromarone	55 (n.s.)	36	10 (7-13)	4	13 (11-17)	11
MK571	1 to >50 ^b		1-10 ^c		30 (22-41)	26
Quercetin	> 100	> 65	7 (n.s.)	3	39 (24-63)	34
Sulindac	39 (16-98)	25	2 (1.6-3.2)	0.8	300 (210-440)	265

n.i. not inhibited at concentrations tested (up to 100 μM).

n.s. 95% confidence interval could not be further specified due to too little data points at linear part of the inhibition curve.

^a K_i was calculated according to the formula: $K_i = \text{IC}_{50} / (1 + [S]/K_m)$, in which $[S]$ was 100 μM in all experiments and K_m values were 187 and 63 μM for 7-HC-G uptake into MRP3 and MRP4 vesicles and approximately 700 μM for 7-HC-G formation in UGT2B15 homogenate.

^b Literature IC_{50} values derived from inhibition of vesicular transport of estradiol-17 β -D-glucuronide and methotrexate with different concentrations of MK571.^{32, 33}

^c Literature IC_{50} values derived from inhibition of vesicular transport of fluorescent cyclic AMP and cellular efflux of 9-(2-phosphonylmethoxyethyl)adenine (PMEA).^{34, 35}

Identification of MRP3 and MRP4 inhibitors that do not inhibit UGT2B15

For the investigation of the influence of MRP3 and MRP4 on metabolism by UGTs in cells or tissues, an inhibitor should be used that only inhibits MRP-mediated transport of the glucuronide metabolite, and not the glucuronidation of the parent compound by the UGT itself. To identify such an inhibitor, we tested the potency of several known MRP4 inhibitors for inhibition of MRP3- and MRP4-mediated transport of 7-HC-G and of UGT2B15-mediated 7-HC glucuronidation in homogenate (Table 1). Sulindac appeared to be the most promising MRP3/4 inhibitor that inhibited UGT2B15 only at higher concentrations (Fig. 3). The concentration at which 50% of transport or metabolism was inhibited (IC_{50}) by sulindac was 39 μ M for transport of 7-HC-G via MRP3 (95% confidence interval (CI) of 17-98 μ M), 2 μ M for MRP4 transport (95% CI of 1.6-3.2 μ M), and 300 μ M for metabolism of 7-HC to 7-HC-G by UGT2B15 homogenate (95% CI of 210-440 μ M). This implicates that sulindac was approximately 150 and 10 times more potent in inhibiting MRP4 and MRP3, respectively, as compared to UGT2B15. The inhibitory potencies of the other compounds tested against MRP3, MRP4 and UGT2B15 activity were in a range similar to each other (Table 1). When calculated K_i values of sulindac are compared, sulindac is even 300 times more potent as an inhibitor of MRP4 than of UGT2B15 activity.

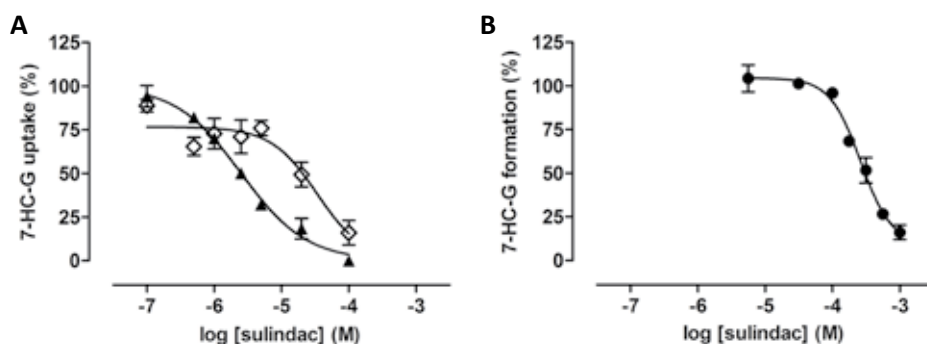


Figure 3 Effect of sulindac on MRP3- and MRP4-mediated 7-HC-G uptake into membrane vesicles and on 7-HC glucuronidation in HEK-UGT2B15 cell homogenate

(A) Effect of different concentrations of sulindac on transport of 100 μ M 7-HC-G via MRP3 (◇) and MRP4 (▲) at 10 minutes of incubation. Transport rates were expressed as a percentage of the uptake measured in the absence of sulindac. Data points represent mean percentage \pm S.D. of a representative experiment (total $n = 3$). (B) Effect of a range of concentrations of sulindac on metabolism of 100 μ M 7-HC to 7-HC-G after 3 hours of incubation with HEK-UGT2B15 homogenate. Glucuronidation rates were expressed as a percentage of the glucuronidation activity measured in the absence of sulindac. Data represent mean percentage \pm S.D. of a representative experiment (total $n = 2$).

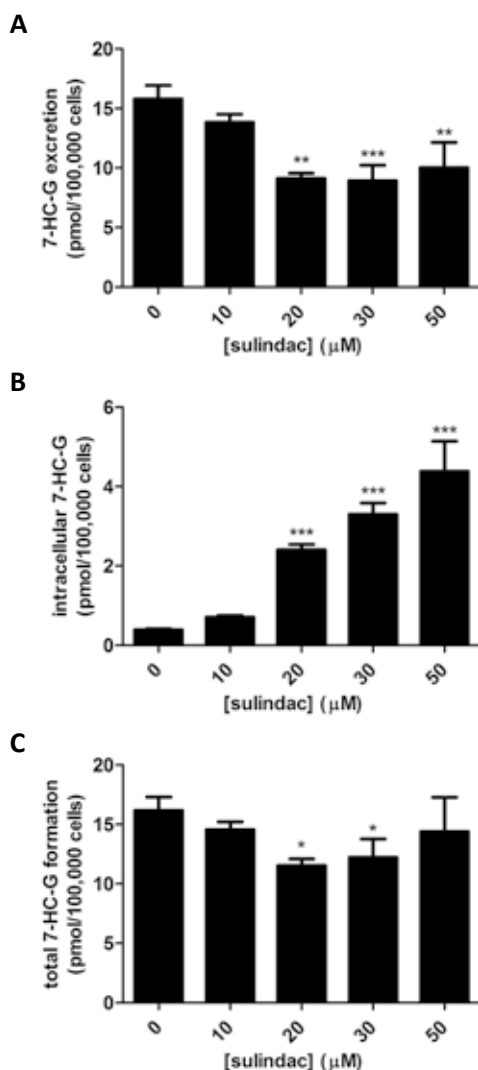


Figure 4 Effect of sulindac on 7-HC-G formation in intact HEK-UGT2B15 cells after two hours of incubation with 100 μM 7-HC

(A) Effect of different concentrations of sulindac on 7-HC-G excretion into the medium. (B) Effect of different concentrations of sulindac on the intracellular amount of 7-HC-G. (C) Effect of sulindac on total 7-HC-G produced per 100,000 cells (medium and intracellular compartment together). Mean \pm S.D. is shown of three independent experiments, except for data points at 20 and 50 μM sulindac ($n = 2$). Statistically significant differences were determined using a one-way ANOVA followed by a post-hoc Dunnett's multiple comparison test: * $p < 0.05$, ** $p < 0.01$, *** $p < 0.001$.

Effect of sulindac on glucuronidation and excretion of glucuronide metabolites from intact HEK-UGT2B15 cells

To test the effect of the MRP3/MRP4 inhibitor sulindac on 7-HC-G formation and excretion in intact cells, we measured the intracellular and extracellular amounts of 7-HC-G produced by HEK-UGT2B15 cells in presence of different concentrations of sulindac (Fig. 4). The amount of glucuronide excreted in the medium was approximately 50% reduced at a concentration of 20 μ M sulindac (Fig. 4A). The amount of intracellular 7-HC-G accumulated with increasing concentration of sulindac (Fig. 4B). Adding up the intracellular and extracellular amounts of 7-HC-G produced per 100,000 cells showed that the total amount of glucuronides that was produced decreased by 30% in presence of 20 μ M sulindac (Fig. 4C).

Discussion

In this study we investigated the cooperation between MRPs and UGTs. For this purpose, we developed assays to measure the amount of glucuronidation by UGT2B15 in intact HEK-UGT2B15 cells and in homogenates of these cells. After testing the selectivity of multiple MRP inhibitors for inhibition of MRP3, MRP4, and UGT2B15, we selected sulindac as the most selective inhibitor of transport via MRP3/MRP4. Using sulindac, we investigated the effect of inhibition of efflux of 7-HC-G from HEK-UGT2B15 cells on total metabolite formation.

During the development of the metabolic assays, we discovered a difference in the K_m of 7-HC-G formation in intact HEK-UGT2B15 cells and in homogenate of these cells, the K_m in homogenate being much higher than in intact HEK-UGT2B15 cells. This phenomenon also occurs for other glucuronidation models, *e.g.* human liver microsomes and hepatocytes, in which the K_m appears to be higher in the microsomes than in the intact hepatocytes.¹⁷ The K_m can be decreased by different incubation conditions, such as type of buffer, pH, and ionic strength, and the presence of pore-forming activators, which decrease the latency of the reaction.¹⁷⁻²⁰ Furthermore, these differences in kinetic characteristics could have effect on the inhibitory potency of compounds against UGT activity.^{17, 20} Therefore, for future studies, it would be good to test different incubation conditions to lower the K_m of UGT2B15 7-HC glucuronidation in the homogenates towards the K_m of intact HEK-UGT2B15 cells, to improve comparison between these *in vitro* systems.

Due to their hydrophilic nature, glucuronide metabolites require transport via influx or efflux transporters to pass cellular membranes. Since 7-HC-G is excreted into the medium by HEK-UGT2B15 cells (Fig. 2) and the intracellular level of 7-HC-G is low under normal conditions (Fig. 4B), HEK293 cells likely express endogenous transporters on their plasma membrane that are able to efflux 7-HC-G into the medium. From a previous study we know that MRP3 and MRP4 mediate transport of 7-HC-G (Chapter 4), and therefore these transporters might be involved in the endogenous efflux of this metabolite. By means of quantitative PCR, we showed that MRP4 is endogenously expressed in HEK293-UGT2B15 cells,



whereas there is very little to no MRP3 expression, which is comparable to other studies investigating transporter expression in HEK293 cells.^{21, 22} Although we cannot exclude the possibility that other endogenously expressed transporters are involved in the transport of 7-HC-G out of HEK-UGT2B15 cells, MRP4 is a good candidate for this process because it transports 7-HC-G and is expressed in HEK293 cells.

To investigate the MRP4-UGT2B15 interplay in HEK-UGT2B15 cells endogenously expressing MRP4 we needed an MRP4 inhibitor that did not inhibit UGT2B15. Testing several MRP inhibitors, we showed that some caution has to be taken with the use of alleged specific MRP inhibitors in the investigation of enzyme-transporter interplay. We showed that several of these inhibitors also inhibited UGT2B15 (Table 1), rendering them unsuitable for separation of the UGT- from the MRP-component in metabolism of 7-HC. Because sulindac had the most favourable UGT2B15 and MRP4 inhibition profile, we selected this inhibitor for further investigation of transporter-enzyme interplay.

Our results suggest that MRP4 and UGT2B15 act synergistically in the removal of 7-HC. Using the selected MRP4 inhibitor sulindac, we showed that the intracellular 7-HC-G amount is increased in HEK-UGT2B15 cells upon sulindac treatment, most likely due to inhibition of transport via MRP4 (Fig. 4). Furthermore, the excretion of 7-HC-G is reduced by 50% in presence of 20 μ M sulindac, a concentration at which UGT2B15 activity in homogenate was not inhibited, whereas MRP4 vesicular transport activity was inhibited by 85% (Fig. 3). This suggests that the decreased excretion is due to decreased efflux of the metabolite and not to inhibition of UGT2B15. At the same concentration of sulindac, total metabolite formation was reduced, implicating that this was a result of the impaired efflux of the glucuronide metabolites. Thus, transport of 7-HC-G out of the cell appears to increase the rate of metabolism of 7-HC to 7-HC-G by UGT2B15, suggesting a synergistic interplay between MRP4 and UGT2B15. Previous studies have also suggested that efflux transport is a rate limiting step in glucuronide excretion, for example for naringenin glucuronide.²³ In addition, critical review of studies employing similar techniques as ours suggests a synergistic interplay between UGTs and transporters *in vitro*, for example between UGT2B7 and MRP1, MRP2, and MRP3 in morphine glucuronidation, and between UGT1A1 and breast cancer resistance protein in genistein glucuronidation.²⁴⁻²⁶ Therefore, these studies appear to support our hypothesis of a synergistic interplay, at least *in vitro*, between UGT enzymes and efflux transporters.

The mechanistic basis of the synergistic cooperation of transporters and UGT enzymes remains to be revealed. Although there is evidence that glucuronide metabolites can inhibit UGT enzymes, there is no proof of an inhibitory capacity of 7-HC-G towards UGT2B15 yet.²⁷ The decreased amount of 7-HC-G conjugation due to inhibition of efflux of 7-HC-G could also be explained by an increased deconjugation of the metabolite, for which β -glucuronidase that is located in the endoplasmic reticulum (ER) is thought to be responsible.^{7, 28} After glucuronidation by UGTs in the ER, glucuronide metabolites are transported to the cytosol before excretion via efflux transporters.²⁸⁻³⁰ If the cytosolic concentration of 7-HC-G is

increased due to lowered efflux, this might also increase the concentration of 7-HC-G in the ER and thereby its deconjugation by β -glucuronidase, resulting in a lower total 7-HC-G formation. However, in HEK293 cells, the β -glucuronidase activity appears to be low, and therefore it is questionable if deconjugation can be the explanation of the lowered metabolism.³¹ Further studies should be performed to unravel the mechanism responsible for the lower metabolism in absence of a functional efflux transporter.

In summary, this study showed that efflux of 7-HC-G from HEK-UGT2B15 cells is important for the glucuronidation of 7-HC and the excretion of 7-HC-G, and endogenously expressed MRP4 is hypothesized to be responsible for this transport. Our results suggest that the cooperation between UGT2B15 and the transporter is synergistic. Because glucuronide metabolites are often transported by multiple transporters, this could mean that in the *in vivo* situation, where multiple transporters are present in enterocytes or hepatocytes, transport will not be a limiting factor of the rate of metabolism.²³ Networks of UGTs and transporters in intestine and liver will therefore provide an efficient route of elimination of drugs.

References

1. Fisher, M. B.; Labissiere, G. The role of the intestine in drug metabolism and pharmacokinetics: an industry perspective. *Curr. Drug Metab* **2007**, *8*, 694-699.
2. Glaeser, H.; Drescher, S.; Hofmann, U.; Heinkele, G.; Somogyi, A. A.; Eichelbaum, M.; Fromm, M. F. Impact of concentration and rate of intraluminal drug delivery on absorption and gut wall metabolism of verapamil in humans. *Clin. Pharmacol. Ther.* **2004**, *76*, 230-238.
3. Fisher, M. B.; Paine, M. F.; Strelevitz, T. J.; Wrighton, S. A. The role of hepatic and extrahepatic UDP-glucuronosyltransferases in human drug metabolism. *Drug Metab Rev.* **2001**, *33*, 273-297.
4. Nakamura, A.; Nakajima, M.; Yamanaka, H.; Fujiwara, R.; Yokoi, T. Expression of UGT1A and UGT2B mRNA in human normal tissues and various cell lines. *Drug Metab Dispos.* **2008**.
5. Ohno, S.; Nakajin, S. Determination of mRNA expression of human UDP-glucuronosyltransferases and application for localization in various human tissues by real-time reverse transcriptase-polymerase chain reaction. *Drug Metab Dispos.* **2009**, *37*, 32-40.
6. Kosaka, K.; Sakai, N.; Endo, Y.; Fukuhara, Y.; Tsuda-Tsukimoto, M.; Ohtsuka, T.; Kino, I.; Tanimoto, T.; Takeba, N.; Takahashi, M.; Kume, T. Impact of intestinal glucuronidation on the pharmacokinetics of raloxifene. *Drug Metab Dispos.* **2011**, *39*, 1495-1502.
7. Jeong, E. J.; Liu, X.; Jia, X.; Chen, J.; Hu, M. Coupling of conjugating enzymes and efflux transporters: impact on bioavailability and drug interactions. *Curr. Drug Metab* **2005**, *6*, 455-468.
8. Zhou, S. F.; Wang, L. L.; Di, Y. M.; Xue, C. C.; Duan, W.; Li, C. G.; Li, Y. Substrates and inhibitors of human multidrug resistance associated proteins and the implications in drug development. *Curr. Med. Chem.* **2008**, *15*, 1981-2039.
9. Li, C.; Krishnamurthy, P. C.; Penmatsa, H.; Marrs, K. L.; Wang, X. Q.; Zaccolo, M.; Jalink, K.; Li, M.; Nelson, D. J.; Schuetz, J. D.; Naren, A. P. Spatiotemporal coupling of cAMP transporter to CFTR chloride channel function in the gut epithelia. *Cell* **2007**, *131*, 940-951.
10. Ming, X.; Thakker, D. R. Role of basolateral efflux transporter MRP4 in the intestinal absorption of the antiviral drug adefovir dipivoxil. *Biochem. Pharmacol.* **2010**, *79*, 455-462.
11. Peng, K. C.; Cluzeaud, F.; Bens, M.; Duong Van Huyen, J. P.; Wioland, M. A.; Lacave, R.; Vandewalle, A. Tissue and cell distribution of the multidrug resistance-associated protein (MRP) in mouse intestine and kidney. *J. Histochem. Cytochem.* **1999**, *47*, 757-768.
12. Scheffer, G. L.; Kool, M.; de Haas, M.; de Vree, J. M.; Pijnenborg, A. C.; Bosman, D. K.; Oude Elferink, R. P.; van der Valk, P.; Borst, P.; Schepers, R. J. Tissue distribution and induction of human multidrug resistant protein 3. *Lab Invest* **2002**, *82*, 193-201.



13. van Aubel, R. A.; Hartog, A.; Bindels, R. J.; Van Os, C. H.; Russel, F. G. Expression and immunolocalization of multidrug resistance protein 2 in rabbit small intestine. *Eur. J. Pharmacol.* **2000**, *400*, 195-198.
14. van de Wetering K.; Zelcer, N.; Kuil, A.; Feddema, W.; Hillebrand, M.; Vlaming, M. L.; Schinkel, A. H.; Beijnen, J. H.; Borst, P. Multidrug resistance proteins 2 and 3 provide alternative routes for hepatic excretion of morphine-glucuronides. *Mol. Pharmacol.* **2007**, *72*, 387-394.
15. Hakala, K. S.; Suchanova, B.; Luukkanen, L.; Ketola, R. A.; Finel, M.; Kostianen, R. Rapid simultaneous determination of metabolic clearance of multiple compounds catalyzed in vitro by recombinant human UDP-glucuronosyltransferases. *Anal. Biochem.* **2005**, *341*, 105-112.
16. Wittgen, H. G.; van den Heuvel, J. J.; van den Broek, P. H.; Dinter-Heidorn, H.; Koenderink, J. B.; Russel, F. G. Cannabinoid CB1 receptor antagonists modulate transport activity of multidrug resistance-associated proteins MRP1, MRP2, MRP3, and MRP4. *Drug Metab Dispos.* **2011**, *39*, 1294-1302.
17. Engtrakul, J. J.; Foti, R. S.; Strelevitz, T. J.; Fisher, M. B. Altered AZT (3'-azido-3'-deoxythymidine) glucuronidation kinetics in liver microsomes as an explanation for underprediction of in vivo clearance: comparison to hepatocytes and effect of incubation environment. *Drug Metab Dispos.* **2005**, *33*, 1621-1627.
18. Soars, M. G.; Ring, B. J.; Wrighton, S. A. The effect of incubation conditions on the enzyme kinetics of udp-glucuronosyltransferases. *Drug Metab Dispos.* **2003**, *31*, 762-767.
19. Boase, S.; Miners, J. O. In vitro-in vivo correlations for drugs eliminated by glucuronidation: investigations with the model substrate zidovudine. *Br. J. Clin. Pharmacol.* **2002**, *54*, 493-503.
20. Miners, J. O.; Mackenzie, P. I.; Knights, K. M. The prediction of drug-glucuronidation parameters in humans: UDP-glucuronosyltransferase enzyme-selective substrate and inhibitor probes for reaction phenotyping and in vitro-in vivo extrapolation of drug clearance and drug-drug interaction potential. *Drug Metab Rev.* **2010**, *42*, 196-208.
21. Taub, M. E.; Mease, K.; Sane, R. S.; Watson, C. A.; Chen, L.; Ellens, H.; Hirakawa, B.; Reyner, E. L.; Jani, M.; Lee, C. A. Digoxin is not a substrate for organic anion-transporting polypeptide transporters OATP1A2, OATP1B1, OATP1B3, and OATP2B1 but is a substrate for a sodium-dependent transporter expressed in HEK293 cells. *Drug Metab Dispos.* **2011**, *39*, 2093-2102.
22. Wielinga, P. R.; Reid, G.; Challa, E. E.; van der Heijden, I.; van Deemter, L.; de Haas, M.; Mol, C.; Kuil, A. J.; Groeneveld, E.; Schuetz, J. D.; Brouwer, C.; De Abreu, R. A.; Wijnholds, J.; Beijnen, J. H.; Borst, P. Thiopurine metabolism and identification of the thiopurine metabolites transported by MRP4 and MRP5 overexpressed in human embryonic kidney cells. *Mol. Pharmacol.* **2002**, *62*, 1321-1331.
23. Xu, H.; Kulkarni, K. H.; Singh, R.; Yang, Z.; Wang, S. W.; Tam, V. H.; Hu, M. Disposition of naringenin via glucuronidation pathway is affected by compensating efflux transporters of hydrophilic glucuronides. *Mol. Pharm.* **2009**, *6*, 1703-1715.
24. Jiang, W.; Xu, B.; Wu, B.; Yu, R.; Hu, M. UGT1A9-overexpressing HeLa Cells Is a Appropriate Tool to Delineate the Kinetic Interplay between BCRP and UGT and to Rapidly Identify the Glucuronide Substrates of BCRP. *Drug Metab Dispos.* **2011**.
25. van de Wetering K.; Zelcer, N.; Kuil, A.; Feddema, W.; Hillebrand, M.; Vlaming, M. L.; Schinkel, A. H.; Beijnen, J. H.; Borst, P. Multidrug resistance proteins 2 and 3 provide alternative routes for hepatic excretion of morphine-glucuronides. *Mol. Pharmacol.* **2007**, *72*, 387-394.
26. Zelcer, N.; Van de Wetering, K.; Hillebrand, M.; Sarton, E.; Kuil, A.; Wielinga, P. R.; Tephly, T.; Dahan, A.; Beijnen, J. H.; Borst, P. Mice lacking multidrug resistance protein 3 show altered morphine pharmacokinetics and morphine-6-glucuronide antinociception. *Proc. Natl. Acad. Sci. U. S. A* **2005**, *102*, 7274-7279.
27. Luukkanen, L.; Taskinen, J.; Kurkela, M.; Kostianen, R.; Hirvonen, J.; Finel, M. Kinetic characterization of the 1A subfamily of recombinant human UDP-glucuronosyltransferases. *Drug Metab Dispos.* **2005**, *33*, 1017-1026.
28. Csala, M.; Bánhegyi, G.; Benedetti, A. Endoplasmic reticulum: a metabolic compartment. *FEBS Lett.* **2006**, *580*, 2160-2165.
29. Battaglia, E.; Gollan, J. A unique multifunctional transporter translocates estradiol-17beta-glucuronide in rat liver microsomal vesicles. *J. Biol. Chem.* **2001**, *276*, 23492-23498.
30. Csala, M.; Marcolongo, P.; Lizák, B.; Senesi, S.; Margittai, E.; Fulceri, R.; Magyar, J. E.; Benedetti, A.; Bánhegyi, G. Transport and transporters in the endoplasmic reticulum. *Biochim. Biophys. Acta* **2007**, *1768*, 1325-1341.
31. Oleson, L.; Court M.H. Effect of the beta-glucuronidase inhibitor saccharolactone on glucuronidation by human tissue microsomes and recombinant UDP-glucuronosyltransferases. *J. Pharm. Pharmacol.* **2008**, *60*, 1175-1182.
32. Bodó, A.; Bakos, E.; Szeri, F.; Váradi, A.; Sarkadi, B. The role of multidrug transporters in drug availability, metabolism and toxicity. *Toxicol. Lett.* **2003**, *140-141*, 133-143.
33. Letourneau, I. J.; Bowers, R. J.; Deeley, R. G.; Cole, S. P. Limited modulation of the transport activity of the human multidrug resistance proteins MRP1, MRP2 and MRP3 by nicotine glucuronide metabolites. *Toxicol. Lett.* **2005**, *157*, 9-19.

34. Reichel, V.; Kläs, J.; Fricker, G.; Masereeuw, R. Fluo-cAMP is transported by multidrug resistance-associated protein isoform 4 in rat choroid plexus. *J. Neurochem.* **2010**, *115*, 200-208.
35. Reid, G.; Wielinga, P.; Zelcer, N.; de Haas, M.; van Deemter, L.; Wijnholds, J.; Balzarini, J.; Borst, P. Characterization of the transport of nucleoside analog drugs by the human multidrug resistance proteins MRP4 and MRP5. *Mol. Pharmacol.* **2003**, *63*, 1094-1103.



Chapter 6

Phenylalanine 368 of multidrug resistance-associated protein 4 (MRP4/ABCC4) plays a crucial role in substrate-specific transport activity

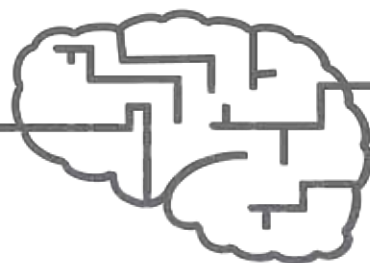
Hanneke G.M. Wittgen^a*, Jeroen J.M.W. van den Heuvel^a*, Elmar Krieger^b, Gijs Schaftenaar^b, Frans G.M. Russel^a, and Jan B. Koenderink^a

^a Department of Pharmacology and Toxicology, Radboud University Nijmegen Medical Centre, Nijmegen Centre for Molecular Life Sciences, the Netherlands

^b Centre for Molecular and Biomolecular Informatics, Radboud University Nijmegen, Nijmegen Centre for Molecular Life Sciences, the Netherlands

* both authors contributed equally to this work

Published in *Biochemical Pharmacology*, August 2012 (84), p. 366-373



Abstract

Multidrug resistance-associated protein 4 (MRP4) is a membrane transporter that mediates the cellular efflux of a wide range of anionic drugs and endogenous molecules. MRP4 transport can influence the pharmacokinetics of drugs and their metabolites, therefore more knowledge about the molecular determinants important for its transport function would be of relevance. Here, we substituted amino acids Phe³⁶⁸, Trp⁹⁹⁵, and Arg⁹⁹⁸ with conservative or non-conservative residues, and determined the effect on transport of the model substrates estradiol 17- β -D-glucuronide (E₂17 β G), cyclic guanosine monophosphate (cGMP), methotrexate (MTX), and folic acid into membrane vesicles isolated from baculovirus transduced HEK293 cells overexpressing the mutant MRP4 proteins. This revealed that all Arg⁹⁹⁸ mutations appeared to be deleterious, whereas the effect of a Phe³⁶⁸ or Trp⁹⁹⁵ replacement was dependent on the amino acid introduced and the substrate studied. Substitution of Phe³⁶⁸ with Trp (F368W) induced a gain-of-function of E₂17 β G transport and a loss-of-function of MTX transport, which could not be attributed to an altered substrate binding. Moreover, we did not observe any modification in ATP or ADP handling for F368W. These results, in combination with docking of substrates in a homology model of MRP4 in the inward- and outward-facing conformation, suggest that Phe³⁶⁸ and Trp⁹⁹⁵ do not play an important role in the initial binding of substrates. They, however, might interact with the substrates during rearrangement of helices for substrate translocation, funneling the substrates to the exit site in the outward-facing conformation.

Introduction

Multidrug resistance-associated protein 4 (MRP4/ABCC4) is a member of the C subfamily of ATP-binding cassette (ABC) transporters. This drug efflux transporter translocates substrates across the plasma membrane of the cell in an ATP-dependent manner.¹ MRP4 is known to transport a wide variety of drugs, including antiviral, antibiotic, cardiovascular, and cytotoxic agents, and endogenous molecules that are involved in cellular signaling and communication, such as cyclic nucleotides, ADP, eicosanoids, uric acid, conjugated steroid hormones, folic acid, bile acids, and glutathione.¹ MRP4 is widely expressed in various blood cells, neurons, cardiovascular tissue, and epithelia of organs that are involved in determining the disposition of drugs, including kidney, liver, blood-brain barrier and intestine, where it can be located either apically or basolaterally depending on the cell type.¹⁻⁴ Because of its localization and its broad substrate specificity, MRP4 plays a role in the disposition of various drugs and their metabolites, and could have a key function in cellular protection and extracellular signaling pathways.¹ MRP4 is encoded by the *ABCC4* gene, comprising a protein of 1325 amino acids with a typical ABC transporter core structure. It is composed of two membrane spanning domains (TMDs), each consisting of six transmembrane helices (TM) important for drug binding, and two nucleotide binding domains (NBDs), which bind and hydrolyze ATP to drive transport. *ABCC4* is a highly polymorphic gene, and several non-synonymous polymorphisms have been found in different human populations. Previous studies showed that some of the polymorphisms in *ABCC4* affect transport of substrates (*e.g.* antiviral agents and chemotherapeutic drugs), mainly by affecting the MRP4 protein expression and localization, and might thereby affect the pharmacokinetics of these drugs.⁵⁻⁷

Because MRP4 plays an important role in the distribution and excretion of drugs and their metabolites, it would be interesting to gain more knowledge about the molecular determinants important for its transport function. To understand the molecular basis of transport, mutational studies of functionally important amino acids are indispensable. In contrast to MRP1, 2, and 3, for MRP4 only one study has been performed that focused on identification of amino acids important for substrate recognition and binding. In that study, we revealed that Phe³⁶⁸, Phe³⁶⁹, Glu³⁷⁴, Arg³⁷⁵, and Glu³⁷⁸ in TM6, and Arg⁹⁹⁸ in TM12 of MRP4 are important for its transport function.⁸ In addition, we demonstrated that Arg³⁷⁵ is involved in MTX transport, but not in cGMP transport.

To further explore which amino acids are important for the transport functionality of MRP4, we investigated the effect of Phe³⁶⁸ (TM6), Trp⁹⁹⁵ and Arg⁹⁹⁸ (TM12) amino acid substitutions on the substrate-dependent transport activity of MRP4. We selected Trp⁹⁹⁵ and Arg⁹⁹⁸ because these amino acids are highly conserved within the MRP family (Fig. 1). Moreover, our previously described homology model showed that Phe³⁶⁸ was located opposite to Trp⁹⁹⁵ in the substrate binding cavity of MRP4.⁸ Hence, Phe³⁶⁸, Trp⁹⁹⁵, and Arg⁹⁹⁸ mutants were expressed in human embryonic kidney 293 (HEK293) cells. Several functional characteristics of the transporters were investigated using membrane vesicles isolated from



```

MRP1  586  LALFNILRFPLN-ILPMVISSIVQ . . . . SYSLQVTTYLNWLVRMSSEMETNIVAV 1261
MRP2  583  ITLFNILRFPLS-MLPMMISSMLQ . . . . SNALNITQTLNWLVRMTSEIETNIVAV 1269
MRP3  572  VSLFNILRLPLN-MLPQLISNLTQ . . . . SYSLQVTFALNWMIRMSDLESNIVAV 1257
MRP4  355  VTLYGAVRLTVTIFPSAIERVSE . . . . SYALTLMGMFQCCVQSAEVENMMISV 1010
MRP5  437  VTVFNSMTFALK-VTPFSVKSLSE . . . . SYAVQLTGLFQFTVRLASETEARFTSV 1160
MRP6  571  LTVLNILNKAQA-FLPFSIHSLVQ . . . . SAALQVTQTLQWVVRNWTDLNSIVSV 1233

```

Figure 1 Alignment (ClustalW2) of amino acid sequences of human MRP1-MRP6

The marked amino acids, F368 in TM6, and W995 and R998 in TM12 of MRP4 have been substituted in this study.

these cells. The results from this study suggest that sequential to initial substrate binding, the aromatic amino acids in TM6 and TM12 can induce substrate-dependent conformational changes, which funnel the substrates to their exit sites.

Materials and Methods

Materials

[6,7-³H(N)]-estradiol 17-β-D-glucuronide (E₂17βG) (41.8 Ci/mmol) was purchased from Perkin Elmer (Groningen, the Netherlands). [3,5,7-³H(N)]-methotrexate disodium salt (MTX) (23 Ci/mmol), [8-³H]-guanosine 3',5'-cyclic monophosphate ammonium salt (cGMP) (13.5 Ci/mmol), and [3,5,7,9-³H(N)]-folic acid diammonium salt (48.6 Ci/mmol) were purchased from Moravek, Inc. (Brea, USA). Bac-to-Bac and Gateway system, DMEM + Glutamax-I culture medium, Tris and fetal calf serum were purchased from Life Technologies (Bleiswijk, the Netherlands). Triple flasks (500 cm²) were purchased from Sanbio BV Biological Products (Uden, the Netherlands). Unlabeled E₂17βG, cGMP, folic acid, and MTX, sodium butyrate, HEPES, DL-dithiothreitol (DTT), and adenosine 5'-triphosphate magnesium salt (ATP) (from bacterial source), and adenosine 5'-monophosphate monohydrate (AMP) (from yeast) were purchased from Sigma-Aldrich (Zwijndrecht, the Netherlands). Sodium monovanadate (anhydrous) was from E. Merck (Darmstadt, Germany) and MgCl₂ was from BOOM (Meppel, the Netherlands). D(+)-saccharose was purchased from VWR (Leuven, Belgium). Protein concentrations were determined with a Bio-Rad protein assay kit from Bio-Rad Laboratories (Veenendaal, the Netherlands).

Site-directed mutagenesis of MRP4 and generation of expression vectors and baculovirus

The previously described Gateway entry vector containing the human MRP4 coding sequence⁸ was used as a template for site-directed mutagenesis of the following amino acids: F368W, F368Y, F368A, W995F, W995Y, W995A, R998S, R998K, R998Y, and R998L. The mutagenesis was performed as described previously.⁸ Briefly, forward and reverse primers

(Biolegio, Nijmegen, the Netherlands) were designed for the specific amino acid substitutions and were used to perform a site-directed mutagenesis PCR on the MRP4 entry vector. After confirmation of the mutations by sequence analysis, the MRP4 mutant entry vectors were cloned into a VSV-G improved pFastBacDual vector for mammalian cell transduction using the Gateway system.⁸ Baculoviruses were produced as described in the Bac-to-Bac manual (Life Technologies, Bleiswijk, the Netherlands).

Cell culture and transduction of HEK293 cells with baculovirus of MRP4 and mutants

HEK293 cells were grown in DMEM-Glutamax-I supplemented with 10% fetal calf serum at 37°C under 5% CO₂-humidified air. For transduction, HEK293 cells were seeded in 500 cm² triple flasks at a confluence of 20%. After 24 hours, the culture medium was removed and a mixture of 25 ml medium and 10 ml of the negative control (enhanced yellow fluorescent protein/eYFP), wild type MRP4, or MRP4 mutant baculovirus was added. After an incubation of 15 min at 37°C, another 40 ml medium was added. Sodium butyrate (5 mM) was added 6 hours after transduction and the cells were further incubated at 37°C under 5% CO₂-humidified air. Three days after transduction, the cells were harvested by spinning them down at 3500g for 10 minutes. Pellets were stored at -80°C until further use.

Isolation of membrane vesicles

Isolation was performed according to a previously described method, with slight modifications.⁹ Briefly, cells were lysed in ice-cold hypotonic buffer supplemented with protease inhibitors and centrifuged at 100,000g. The pellet was homogenized in ice-cold TS buffer (10 mM Tris-HEPES, and 250 mM sucrose, pH 7.4) with protease inhibitors using a Dounce homogenizer and the suspension was centrifuged at 2000g. Membranes (in supernatant) were spun down by a 100,000g centrifugation step and vesicles were produced using passage through a 27-gauge needle. Protein concentrations were determined by Bio-Rad protein assay kit, and crude membrane vesicles were dispensed in aliquots, frozen in liquid nitrogen, and stored at -80°C until further use.

Western blotting

15 µg of membrane vesicle preparation was solubilized in Laemmli loading buffer with 0.1 M DTT, and loaded onto a 7.5% SDS-polyacrylamide gel, after which gel electrophoresis was performed to separate proteins. Subsequently, they were blotted on nitrocellulose membrane using the iBlot dry blotting system (Life Technologies, Bleiswijk, the Netherlands). MRP4 and its mutant proteins were detected using the polyclonal rabbit-anti-human MRP4 antibody (pAb hM4, 1:5000)¹⁰ and the secondary goat-anti-rabbit antibody Alexa Fluor 680 (Life Technologies, Bleiswijk, the Netherlands, 1:10000). Signals were visualized using the Odyssey imaging system (Li-Cor Biosciences, Lincoln, NE) and the expression ratio between wild type MRP4 and mutant protein per membrane vesicle preparation was determined using Odyssey software version 2.1. We used this ratio to correct transport activity for



protein expression of each mutant protein in separate batches of membrane vesicles.

Vesicular transport assay to screen transport activity of mutant MRP4 proteins for different substrates

Transport activity of control (eYFP), MRP4, and all MRP4 mutant proteins was tested using different substrates. Uptake of [^3H]-E₂17βG, [^3H]-cGMP, [^3H]-MTX or [^3H]-folic acid into membrane vesicles was performed using a rapid filtration technique as described previously.⁹ Briefly, 7.5 μg of membrane vesicles was incubated in TS buffer with 4 mM AMP or ATP, 10 mM MgCl₂ and one of the radioactive substrates at the concentration indicated in the legend, at 37°C for 5 ([^3H]-E₂17βG), 7.5 ([^3H]-folic acid), or 10 minutes ([^3H]-cGMP and [^3H]-MTX), time points for which time-dependent transport was found to be linear (data not shown). The concentrations of radiolabeled substrates used in the screen were 0.12 μM radiolabeled E₂17βG, 10.8 μM cGMP (0.8 μM radiolabeled and 10 μM unlabeled), 0.5 μM MTX (0.22 μM radiolabeled and 0.28 μM unlabeled), and 0.1 μM radiolabeled folic acid. After stopping the reaction with ice-cold TS buffer, the samples were filtered by a Multiscreen HTS-Vacuum Manifold filtration device (Millipore, Etten-Leur, the Netherlands) through a 0.45 μm pore, PVDF 96-well filter plate (Millipore) and washed twice with TS buffer. After separation from the plate, 2 ml of scintillation fluid was added to each filter and radioactivity was measured using a liquid scintillation counter. Net ATP-dependent transport was calculated by subtracting values measured in the presence of AMP from those measured in the presence of ATP. The transport data were corrected for expression of mutant compared to wild type MRP4 of each different batch, and experiments were performed in three different batches of membrane vesicles. In this setup (ATP present in the incubation media and not inside the vesicles) only the transport into inside-out vesicles is measured.

Kinetic analysis of MRP4 mutant proteins

To determine the apparent K_m and V_{max} values of wild type and mutant MRP4 proteins F368W, F368Y, W995F, and W995Y, concentration curves were made for the different substrates. Transport was performed as described in the previous section, and the same concentrations of radiolabeled substrates were supplemented with unlabeled substrate to obtain different concentrations. Each experiment was performed with three different batches of vesicles. The concentration-dependent transport was corrected for expression levels compared to control of each batch. For mutant F368W the K_m value of ATP was determined by measuring the uptake rate of 200 μM E₂17βG in presence of different concentrations of ATP (up to 4 mM). K_m and V_{max} values were determined by non-linear regression analysis of the data according to the Michaelis-Menten equation using GraphPad Prism, version 5.02 (GraphPad Software Inc., San Diego, CA).

Trapping of ADP during E₂17βG transport using vanadate

To test the effect of ADP trapping on E₂17βG transport via MRP4 and mutant F368W, the

vesicular transport assay was performed for E₂17βG transport according to description in the section for the vesicular transport assay, using 100 μM E₂17βG in presence of different concentrations of vanadate. Inhibitory data of vanadate were fitted to a one-site binding model by non-linear regression analysis (GraphPad Prism 5.02) using the equation: $y = \text{bottom} + (\text{top} - \text{bottom}) / (1 + 10^{x - \log(\text{IC}_{50})})$.

Molecular modeling and docking

The homology model of MRP4 was built with the YASARA molecular modeling program.¹¹ The outward-facing model has been described previously.⁸ For the inward-facing model the X-ray structure of P-glycoprotein (P-gp) from *Mus musculus* solved at 3.8-Å resolution¹² was used as a template (PDB ID: 3G5U). The alignment of the MRP4 sequence against this template was created with the T-Coffee multiple alignment algorithm¹³, using additional sequences to guide the alignment. The resulting alignment was manually tuned to account for single residue insertions and deletions. Loops were modeled by scanning a non-redundant subset of the PDB (>8000 structures) for fragments with matching anchor points, a minimal number of bumps, and maximal sequence similarity. Side chains were added with YASARA's implementation of SCWRL¹⁴, and then the model was subjected to an energy minimization with the YAMBER force field as described previously.¹¹ Since membrane was absent during this minimization, the backbone of residues copied from the template was kept fixed. Validation of the model with WHAT_CHECK¹⁵ yielded an average quality Z-score of -1.47, which is better than the template (-4.72). A PDB file of the model and the alignment is available upon request.

Docking was performed with AutoDock 4.2¹⁶ using the default docking parameters supplied in the AutoDock 'examples' subdirectory and point charges assigned according to the AMBER03 force field.¹⁷ The MRP4 homology models were used as receptors, and E₂17βG, MTX, cGMP, and folic acid structures, retrieved from PubChem (CID 66424, 126941, 24316, 6037, respectively), were used as ligand. The simulation cell was defined by selection of 5 Å box around the amino acids involved in binding.¹² The setup was done with the YASARA molecular modeling program.¹¹





Figure 2 Western blot analysis of wild type MRP4 and MRP4 mutant protein expression

Membrane vesicles from HEK293 cells overexpressing wild type MRP4 and Phe³⁶⁸, Trp⁹⁹⁵, and Arg⁹⁹⁸ mutants were loaded on SDS-PAGE and blotted. eYFP expressing membrane vesicles were loaded as a negative control (ctrl). Polyclonal rabbit-anti-human MRP4 antibody was used for detection.

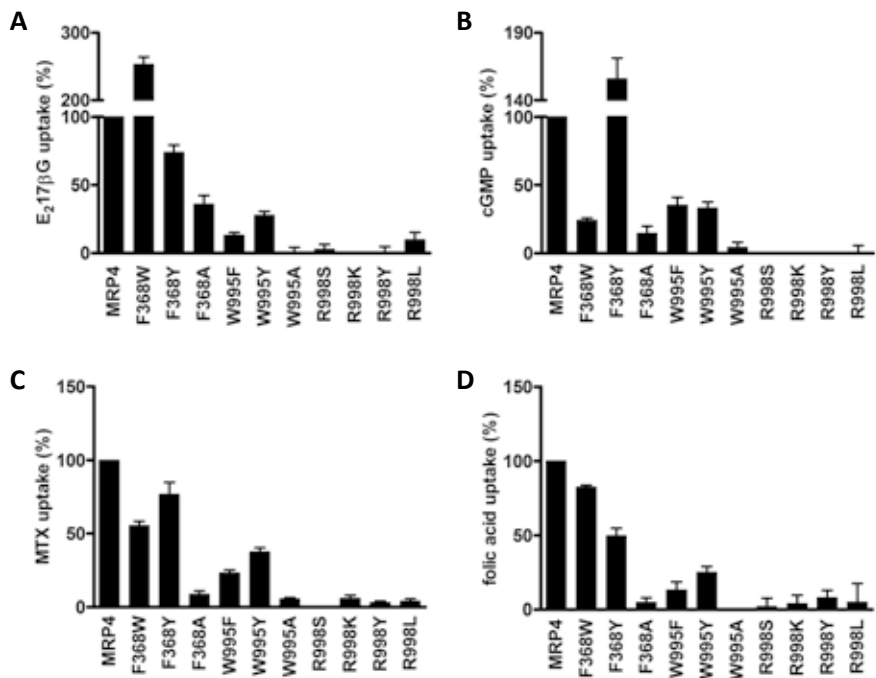


Figure 3 Effect of MRP4 amino acid substitutions of Phe³⁶⁸, Trp⁹⁹⁵, and Arg⁹⁹⁸ on transport of different substrates

Uptake was measured in presence of 4 mM AMP or ATP into membrane vesicles from HEK293 cells containing wild type and MRP4 mutants. Radiolabeled substrates were used in the following concentrations: 0.12 μM E₂17βG (A), 10.8 μM cGMP (B), 0.5 μM MTX, or 0.1 μM folic acid (D). All transport values were corrected for endogenous transport in control membrane vesicles. ATP-dependent transport activity of wild type MRP4 was set at 100% for each experiment and transport activity was corrected for protein expression of the mutants in each batch. Mean percentage ± S.E.M. of transport activity in three independent experiments, using different batches of membrane vesicles, is shown.

Results

Expression of MRP4 wild type and Phe³⁶⁸, Trp⁹⁹⁵, and Arg⁹⁹⁸ mutants in isolated membrane vesicles

Using site directed mutagenesis, the aromatic amino acids phenylalanine at position 368 in TM6 (Phe³⁶⁸/F368) and tryptophan at position 995 (Trp⁹⁹⁵/W995) in TM12 of MRP4 were exchanged with alanine (Ala/A) or the aromatic amino acids Phe, Trp, or tyrosine (Tyr/Y). The positively charged amino acid arginine at position 998 (Arg⁹⁹⁸/R998) was substituted with the positively charged lysine (Lys/K), the polar uncharged serine (Ser/S), the aromatic Tyr, or the hydrophobic leucine (Leu/L). Sequence analysis confirmed the construction of the correct mutants (data not shown). Next, immunoblot analysis performed on membrane vesicles from HEK293 cells overexpressing MRP4 wild type and mutant transporters showed a clear expression of all MRP4 proteins compared to the negative control (Fig. 2). Overall, the expression levels of the mutants and wild type MRP4 were similar.

cGMP, E₂17βG, MTX, and folic acid transport by MRP4 wild type and mutants

The effect of MRP4 amino acid substitutions was investigated with a vesicular transport assay using the [³H]-labeled substrates E₂17βG, cGMP, MTX, and folic acid (Fig. 3A-D). Transport values of these substrates for wild type MRP4 were 0.58 ± 0.03 , 3.5 ± 0.3 , 0.65 ± 0.14 , 0.27 ± 0.04 pmol mg⁻¹ min⁻¹ for E₂17βG, cGMP, MTX, and folic acid, respectively. Substitution of Phe³⁶⁸ and Trp⁹⁹⁵ with Ala, and all amino acid substitutions of Arg⁹⁹⁸ almost completely disrupted transport activity for all substrates tested. Transport via W995F and W995Y was not completely abolished, but the aromatic substitutions significantly decreased transport of all substrates compared to wild type MRP4. Whereas amino acid substitutions of Trp⁹⁹⁵ and Arg⁹⁹⁸ diminished or completely abolished transport of all substrates, substitutions F368W and F368Y had dual effects on the transport function, which appeared to be substrate- and mutation-dependent. F368Y-mediated cGMP transport was increased to $160 \pm 15\%$ (Fig. 3B), while transport of the other substrates was decreased by 20-50% compared to wild type MRP4 activity (Fig. 3A,C-D). Moreover, F368W-mediated E₂17βG transport was increased to $250 \pm 11\%$ of wild type MRP4 (Fig. 3A), whereas cGMP transport was drastically decreased to $24 \pm 2\%$ (Fig. 3B), and MTX and folic acid transport was also reduced to 55-80% of wild type transport activity (Fig. 3C-D).

Kinetic properties of MRP4 wild type and F368W, F368Y, W995F, and W995Y mutants

To further explore the mechanism by which the amino acid substitutions affected MRP4 transport activity, we determined the apparent affinity (K_m) and maximum transport capacity (V_{max}) of wild type MRP4 and mutants F368W, F368Y, W995F and W995Y for E₂17βG, cGMP, MTX, and folic acid. As F368A, W995A, and all mutations of Arg⁹⁹⁸ completely disrupted the transport activity of MRP4, it was not possible to include these mutant proteins into the kinetic analysis. Figure 4 shows the concentration-dependency of E₂17βG, cGMP, MTX,



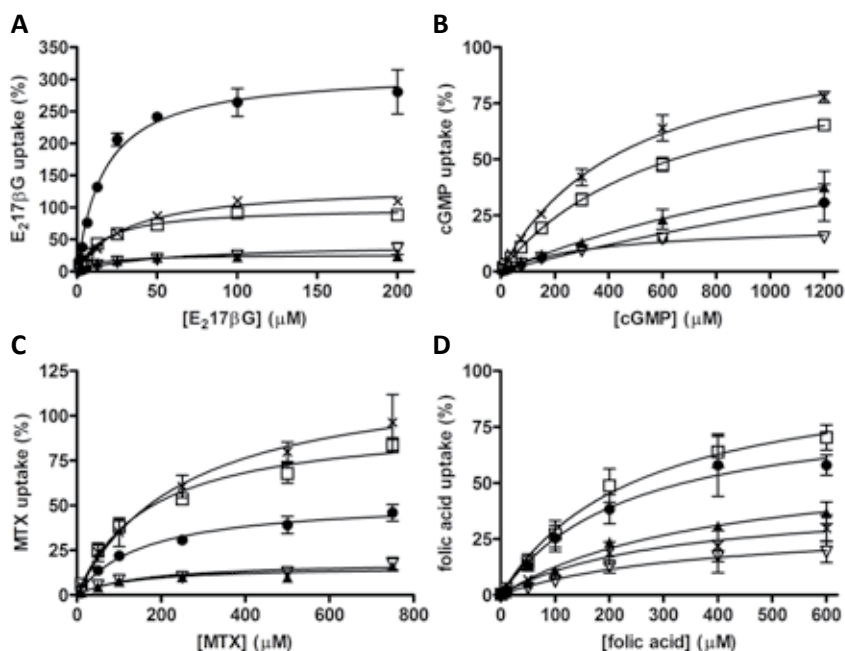


Figure 4 Kinetics of ATP-dependent transport of different substrates into membrane vesicles from HEK293 cells containing wild type MRP4 (□) or MRP4 mutants F368W (●), F368Y (×), W995F (▽), and W995Y (▲)

Concentration-dependent transport of $E_217\beta G$ (A), cGMP (B), MTX (C), and folic acid (D) was determined in presence of 4 mM AMP or ATP. ATP-dependent uptake is expressed as percentage compared to control (%), with V_{max} of wild type MRP4 set at 100% per batch of membrane vesicles. Data points represent mean \pm S.E.M. of three different batches of membrane vesicles, corrected for protein expression. Curves were plotted and K_m and V_{max} were determined by non-linear regression analysis based on one-site Michaelis-Menten kinetics.

6

and folic acid transport of the wild type and mutant transporters tested. K_m and V_{max} values derived from these plots are presented in Table 1.

Most of the effects on transport activity by the aromatic amino acid substituted Phe³⁶⁸ and Trp⁹⁹⁵ mutants in Figure 3 appeared to be due to changes in the V_{max} , only sporadically accompanied by a change in apparent K_m (Table 1). Surprisingly, the significant gain of $E_217\beta G$ transport function by mutant F368W appeared to be completely due to a 3-fold increase in V_{max} , whereas the K_m was exactly the same as for wild type MRP4. For MTX transport by this mutant, the K_m was also unaffected, but in contrast to $E_217\beta G$, the V_{max} was significantly reduced.

Table 1 Kinetic characteristics of transport via MRP4 mutants F368W, F368Y, W995F, and W995Y in comparison to wild type MRP4

	E₂17βG		cGMP		MTX		folic acid	
	K_m (μM)	V_{max} (%)	K_m (μM)	V_{max} (%)	K_m (μM)	V_{max} (%)	K_m (μM)	V_{max} (%)
MRP4	17 ± 2	99 ± 3	630 ± 67	99 ± 5	170 ± 30	97 ± 6	250 ± 73	100 ± 13
F368W	17 ± 3	310 ± 14***	> 2000	n.d.	160 ± 36	53 ± 4*	240 ± 100	85 ± 15
F368Y	31 ± 3	130 ± 5***	480 ± 63	110 ± 7	260 ± 89	130 ± 17	300 ± 182	42 ± 12***
W995F	54 ± 24**	42 ± 7 ***	360 ± 46	21 ± 1**	150 ± 81	19 ± 3***	350 ± 275	31 ± 12***
W995Y	13 ± 4	26 ± 2 ***	1800 ± 1020	94 ± 36	130 ± 48	16 ± 2***	390 ± 116	61 ± 9**

n.d. not determined; concentration of cGMP in the experiment was not high enough to accurately determine V_{max}.

K_m and V_{max} values (mean ± S.D.) were tested for significant differences compared to control MRP4 kinetic characteristics using one-way ANOVA, followed by a post-hoc Dunnett's multiple comparison test, * p < 0.05, ** p < 0.01, *** p < 0.001.



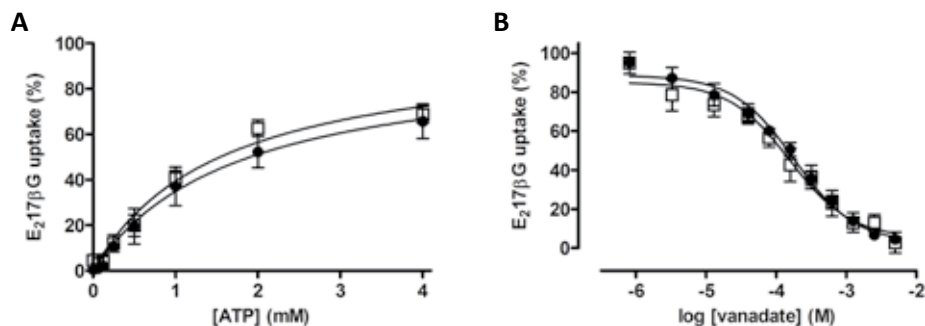


Figure 5 Effect of different concentrations of ATP (A) and vanadate (B) on ATP-dependent $E_217\beta G$ uptake into membrane vesicles containing wild type (□) and mutant F368W (●) MRP4

(A) Uptake of 200 μM $E_217\beta G$ was measured after 10 minutes in presence of different ATP concentrations. Data were normalized to V_{max} , which was set at 100%, and subsequently pooled. Mean \pm S.E.M. of four independent experiments is shown. (B) ATP-dependent transport of 100 μM $E_217\beta G$ was measured after 10 minutes in presence of different concentrations of vanadate. V_{max} was set at 100%, and mean \pm S.E.M. of four to five independent experiments are shown.

ATP and ADP handling of MRP4 wild type and F368W mutant

We explored the possibility of a changed handling of ATP or ADP by F368W during $E_217\beta G$ transport. For this purpose, we investigated $E_217\beta G$ transport by mutant F368W and wild type MRP4 in presence of different concentrations of ATP, and the inhibitory effect of vanadate, which traps ADP to the NBDs. Figure 5A shows the ATP-dependency of $E_217\beta G$ transport via MRP4 and F368W at a fixed $E_217\beta G$ concentration (200 μM). The K_m values of the wild type and F368W mutant were similar (1.5 ± 0.4 mM and 1.7 ± 0.7 mM, respectively). In addition, Figure 5B shows that vanadate inhibited $E_217\beta G$ transport by MRP4 and F368W with comparable IC_{50} values (160 ± 40 μM and 180 ± 30 μM , respectively).

Docking of substrates in MRP4

The homology model of the MRP4 outward-facing state was based on the Sav1866 structure (Fig. 6B).^{8, 18} In addition, we constructed a new inward-facing model of MRP4 based on the mouse P-gp structure (Fig. 6A).¹² These MRP4 models were used as receptor for docking of $E_217\beta G$, MTX, cGMP, and folic acid structures. The maximum binding energies were 11.0, 6.8, 7.7, and 7.7 kcal/mol in the inward-facing model, and 10.6, 6.2, 7.2, and 7.9 kcal/mol in the outward-facing model, for binding of $E_217\beta G$, MTX, cGMP, and folic acid, respectively. The highest binding energy of $E_217\beta G$ was in good agreement with the highest binding affinity (17 μM) we determined. It is difficult to predict which binding site within the pocket is used by the substrates. We therefore depicted the molecular surface of all 100 $E_217\beta G$ docking results, which provides a good indication of the substrate-binding pocket (Fig. 6).

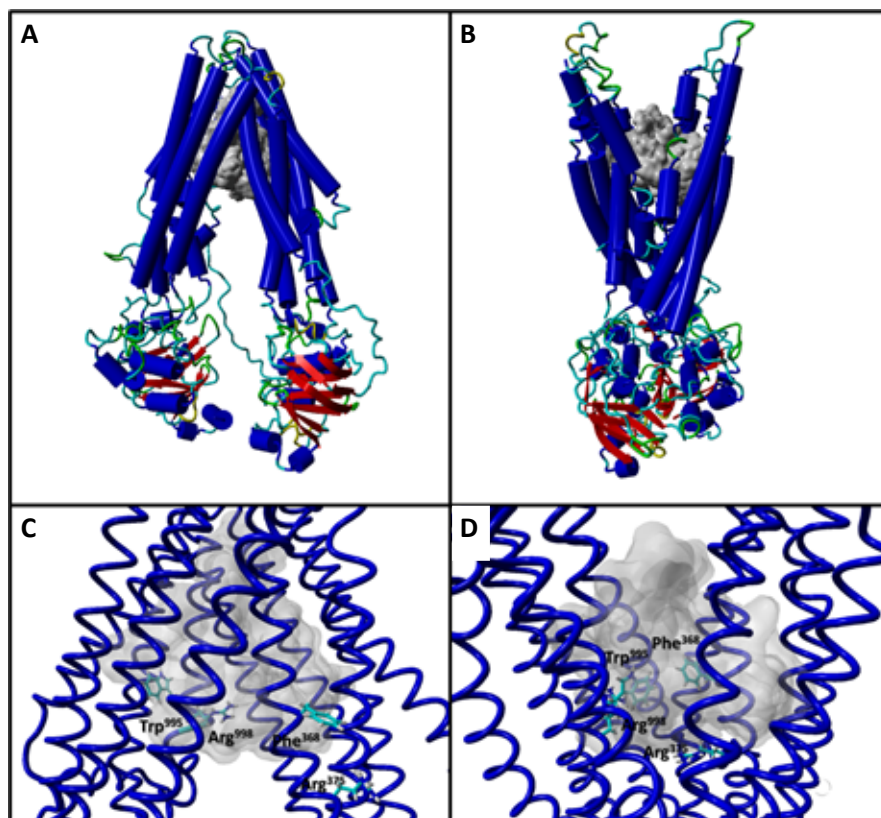


Figure 6 Homology models of MRP4

MRP4 in the inward- (A) and outward-facing (B) conformation. The molecular surface of all 100 E₂ 17bG docking results is shown in grey in each panel. In addition, the side chains of Phe³⁶⁸, Arg³⁷⁵, Trp⁹⁹⁵ and Arg⁹⁹⁸ are shown in a close-up of the substrate-binding pocket in the inward- (C) and outward-facing (D) state.

6

Discussion

In the present study, we used mutational analysis to explore the role of amino acids Phe³⁶⁸ in TM6, and Trp⁹⁹⁵ and Arg⁹⁹⁸ in TM12 in transport activity of MRP4. All amino acid substitutions of Arg⁹⁹⁸ appeared to be deleterious, whereas the effect of Phe³⁶⁸ or Trp⁹⁹⁵ substitutions was dependent on the amino acid introduced and the substrate studied. We found substrate-dependent effects for the transport activity of mutant F368W that were not related to a change in apparent K_m but due to an altered V_{max} . We hypothesize that in this mutant, not the binding of the substrate is altered, but that the subsequent conformational changes,



ultimately leading to substrate release, are affected in a substrate-dependent manner.

The substitutions of Arg⁹⁹⁸ appeared to be deleterious for transport of all substrates tested (Fig. 3). In a previous study we already showed that R998A disrupted transport of MTX and cGMP.⁸ Here, we showed that replacing Arg⁹⁹⁸ with another positively charged amino acid (Lys) is not sufficient to maintain transport activity. Similar results were obtained with the MRP1 homolog of Arg⁹⁹⁸, Arg¹²⁴⁹, for which mutation to Ala, Asp or Lys, completely disrupted transport of different substrates and binding of leukotriene C₄ (LTC₄), indicating its importance for substrate binding.^{19,20} According to the homology model of the inward-facing pump, Arg⁹⁹⁸ is located at the cytosolic interface of TM12, at the bottom of the substrate binding pocket, pointing into the pore (Fig. 6). This localization, in combination with the mutagenesis results, suggests that Arg⁹⁹⁸ plays a prominent role in gating the substrates into their binding site.

Trp⁹⁹⁵ is a highly conserved amino acid in the ABCC family (Fig. 1). In this study, we showed that substitution of Trp⁹⁹⁵ in MRP4 with Ala completely disrupted transport activity, whereas the substitution with more conservative amino acids (Phe and Tyr) led to a decreased transport activity for all substrates tested. To obtain more information on the role of the amino acids of interest in substrate handling, we determined K_m and V_{max} values of the mutant transporters for different substrates; K_m representing the apparent affinity for substrate binding of the transporter, and V_{max} being the maximum transport rate of the transporter. The decreased transport of W995F and W995Y appeared to be mainly caused by a decreased V_{max} , indicating a decreased catalytic turnover number of these MRP4 mutants. In addition, the increased apparent K_m for cGMP (W995Y) indicates that binding of this substrate might have been affected (Fig. 4 and Table 1). The conserved amino acid homologues of this amino acid have also been studied in MRP1, MRP2, and MRP3 (Trp¹²⁴⁶, Trp¹²⁵⁴, and Trp¹²⁴², respectively). Conservative substitutions of these Trp residues with Phe and Tyr revealed substrate-selective effects, supposedly due to decreased binding of the substrate to the mutant transporters.²¹⁻²³ However, the apparent affinities of these mutants for different substrates were not reported. Trp⁹⁹⁵ is predicted to be located in TM12 at the bottom of the binding pocket just above Arg⁹⁹⁸ (Fig. 6). Our results indicate that Trp⁹⁹⁵ might only play a minor role in binding of some substrates (*e.g.* cGMP), which is also suggested by its position in the inward-facing conformation (at the edge of the binding pocket).

Mutation of Phe³⁶⁸ to Ala decreased transport of all substrates tested, whereas conservative substitutions with the aromatic Trp and Tyr residues caused substrate-dependent effects. Similar effects have also been shown for Phe⁵⁹⁴ substitutions in MRP1 (equal to Leu³⁶³ in MRP4) (Fig. 1). Phe⁵⁹⁴ was hypothesized to be implicated in substrate binding, because mutation of this amino acid to Ala abrogated binding and transport of LTC₄ by MRP1.²⁴ In the present study, we observed that the F368W mutation induced an increased transport rate of E₂17βG, whereas transport rates of cGMP and MTX were reduced. The decreased transport of cGMP could be explained by an increased K_m value, which implicates a reduced substrate binding. However, F368W did not affect the K_m values for MTX and E₂17βG

transport, implicating it is not involved in initial binding of these substrates. Although we cannot exclude a possible effect of this mutation on the number of substrate binding sites for E₂17βG and MTX, this does not seem a very plausible explanation because this would most likely have affected the K_m values. Therefore, the effects of F368W on E₂17βG and MTX transport appeared to be caused by an oppositely directed change in V_{max} , indicating that the transport rate of F368W is influenced in a substrate-dependent fashion.

Mutations in a TM domain could affect ATP binding and hydrolysis, or ADP release at the NBDs.¹⁹ E₂17βG transport activity of F368W and wild type MRP4 (Fig. 5A) revealed no effect of F368W substitution on the apparent affinity for ATP, indicating that it does not affect the rate of ATP binding and release. In addition, inhibition of E₂17βG transport with increasing concentrations of vanadate, a phosphate analog that traps ADP to the NBDs²⁵, showed no effects on vanadate sensitivity of the mutant transporter (Fig. 5B). These results indicate that handling of ATP and ADP by mutant F368W is similar to that of wild type MRP4.

Because neither a change in substrate nor in ATP or ADP binding of F368W appeared to explain its opposite effects on rate of transport of E₂17βG and MTX, we made homology models of MRP4 to visualize the localization of this amino acid (Fig. 6). In the inward-facing, substrate binding, state of the homology model, Phe³⁶⁸ is positioned outside the binding cavity, whereas it moves into the binding cavity in the outward-facing state (Fig. 6). Therefore, this residue does not seem to be involved in the formation of the initial binding site, but it might be important for the conformational changes after initial binding of a substrate. For P-glycoprotein, it has been shown that the protein conformation adapts to the substrate that is transported, implicating translocation of multiple substrates, but also a substrate-dependent movement of the helices.²⁶ This could provide an explanation for the finding that the MRP4 substitution F368W increased the catalytic turnover rate of E₂17βG transport, whereas it decreased that of MTX, implicating that Phe³⁶⁸ plays a crucial role in the substrate-dependent conformational changes that are involved in the transport of MTX and E₂17βG to the extracellular side. Another explanation for these opposite effects of the F368W mutant could be that Phe³⁶⁸ plays a role in the dissociation of these substrates in the outward-facing conformation. Future studies should provide further evidence for one of these theories.

Docking of substrates to the MRP4 homology models illustrates the role of the two positively charged Arg residues and the aromatic Phe and Trp residues at the entrance of the binding pocket (Fig. 6). In the inward-facing situation substrates can bind to several sites within the pocket, possibly followed by an induced fit. Next, ATP- and substrate-dependent rearrangement of the TM helices and repositioning of Phe³⁶⁸, Trp⁹⁹⁵, Arg³⁷⁵ and Arg⁹⁹⁸ facilitates translocation of substrate across the membrane. These amino acids most likely funnel the substrates to their binding site at the opposite side of the membrane. Eventually, Arg³⁷⁵ is positioned at the bottom of the binding pocket, whereas Arg⁹⁹⁸ is now located somewhat more to the side of the pocket. Moreover, Phe³⁶⁸ and Trp⁹⁹⁵ are forming an aromatic wedge inside the outward-facing binding pocket, which could decrease binding



and facilitate the release of substrates.

In summary, Arg⁹⁹⁸ seems to be essential for transport of all substrates tested, whereas the effect of a Phe³⁶⁸ or Trp⁹⁹⁵ replacement was dependent on the amino acid introduced and the substrate studied. F368W increased E₂17βG transport and reduced MTX transport, which was not due to an altered substrate affinity. In conclusion, Phe³⁶⁸ and Trp⁹⁹⁵ do not play an important role in the initial binding of substrates, but might funnel the substrates to the exit site in the outward-facing conformation. Revealing the importance of different amino acid for substrate binding by MRP4 in combination with other technologies such as pharmacophore and homology modeling will ultimately lead to a better understanding of the substrate binding pocket of MRP4. This knowledge could be used for the development of specific inhibitors of MRP4, which could be helpful for further investigation of MRP4 function *in vitro* and *in vivo* and might be of therapeutic potential.

References

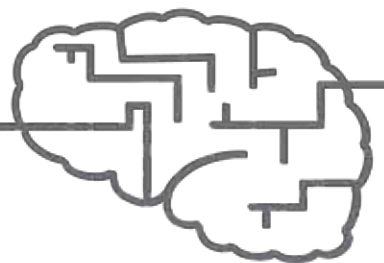
1. Russel, F. G.; Koenderink, J. B.; Masereeuw, R. Multidrug resistance protein 4 (MRP4/ABCC4): a versatile efflux transporter for drugs and signalling molecules. *Trends Pharmacol. Sci.* **2008**, *29*, 200-207.
2. Ritter, C. A.; Jedlitschky, G.; Meyer zu Schwabedissen H.; Grube, M.; Köck, K.; Kroemer, H. K. Cellular export of drugs and signaling molecules by the ATP-binding cassette transporters MRP4 (ABCC4) and MRP5 (ABCC5). *Drug Metab Rev.* **2005**, *37*, 253-278.
3. Borst, P.; de Wolf, C.; Van de Wetering, K. Multidrug resistance-associated proteins 3, 4, and 5. *Pflugers Arch.* **2007**, *453*, 661-673.
4. Zimmermann, C.; Gutmann, H.; Hruz, P.; Gutzwiller, J. P.; Beglinger, C.; Drewe, J. Mapping of multidrug resistance gene 1 and multidrug resistance-associated protein isoform 1 to 5 mRNA expression along the human intestinal tract. *Drug Metab Dispos.* **2005**, *33*, 219-224.
5. Janke, D.; Mehrlivand, S.; Strand, D.; Gödtel-Armbrust, U.; Habermeier, A.; Gradhand, U. *et al.* 6-mercaptopurine and 9-(2-phosphonyl-methoxyethyl) adenine (PMEA) transport altered by two missense mutations in the drug transporter gene ABCC4. *Hum. Mutat.* **2008**, *29*, 659-669.
6. Abula, N.; Chinn, L. W.; Nakamura, T.; Liu, L.; Huang, C. C.; Johns, S. J. *et al.* The human multidrug resistance protein 4 (MRP4, ABCC4): functional analysis of a highly polymorphic gene. *J. Pharmacol. Exp. Ther.* **2008**, *325*, 859-868.
7. Krishnamurthy, P.; Schwab, M.; Takenaka, K.; Nachagari, D.; Morgan, J.; Leslie, M. *et al.* Transporter-mediated protection against thiopurine-induced hematopoietic toxicity. *Cancer Res.* **2008**, *68*, 4983-4989.
8. El-Sheikh, A. A.; van den Heuvel, J. J.; Krieger, E.; Russel, F. G.; Koenderink, J. B. Functional role of arginine 375 in transmembrane helix 6 of multidrug resistance protein 4 (MRP4/ABCC4). *Mol. Pharmacol.* **2008**, *74*, 964-971.
9. Wittgen, H. G.; van den Heuvel, J. J.; van den Broek, P. H.; Dinter-Heidorn, H.; Koenderink, J. B.; Russel, F. G. Cannabinoid CB1 receptor antagonists modulate transport activity of multidrug resistance-associated proteins MRP1, MRP2, MRP3, and MRP4. *Drug Metab Dispos.* **2011**, *39*, 1294-1302.
10. van Aubel, R. A.; Smeets, P. H.; Peters, J. G.; Bindels, R. J.; Russel, F. G. The MRP4/ABCC4 gene encodes a novel apical organic anion transporter in human kidney proximal tubules: putative efflux pump for urinary cAMP and cGMP. *J. Am. Soc. Nephrol.* **2002**, *13*, 595-603.
11. Krieger, E.; Joo, K.; Lee, J.; Lee, J.; Raman, S.; Thompson, J. *et al.* Improving physical realism, stereochemistry, and side-chain accuracy in homology modeling: Four approaches that performed well in CASP8. *Proteins* **2009**, *77 Suppl 9*, 114-122.
12. Aller, S. G.; Yu, J.; Ward, A.; Weng, Y.; Chittaboina, S.; Zhuo, R. *et al.* Structure of P-glycoprotein reveals a molecular basis for poly-specific drug binding. *Science* **2009**, *323*, 1718-1722.
13. Notredame, C.; Higgins, D. G.; Heringa, J. T-Coffee: A novel method for fast and accurate multiple sequence alignment. *J. Mol. Biol.* **2000**, *302*, 205-217.
14. Canutescu, A. A.; Shelenkov, A. A.; Dunbrack, R. L. Jr. A graph-theory algorithm for rapid protein side-chain prediction. *Protein Sci.* **2003**, *12*, 2001-2014.

15. Hooft, R. W.; Vriend, G.; Sander, C.; Abola, E. E. Errors in protein structures. *Nature* **1996**, *381*, 272.
16. Morris, G. M.; Goodsell, D. S.; Halliday, R. S.; Huey, R.; Hart, W. E.; Belew, R. K. *et al.* Automated docking using a Lamarckian genetic algorithm and an empirical binding free energy function. *Journal of Computational Chemistry* **1998**, *19*, 1639-1662.
17. Duan, Y.; Wu, C.; Chowdhury, S.; Lee, M. C.; Xiong, G.; Zhang, W. *et al.* A point-charge force field for molecular mechanics simulations of proteins based on condensed-phase quantum mechanical calculations. *J. Comput. Chem.* **2003**, *24*, 1999-2012.
18. Dawson, R. J.; Locher, K. P. Structure of a bacterial multidrug ABC transporter. *Nature* **2006**, *443*, 180-185.
19. Situ, D.; Haimeur, A.; Conseil, G.; Sparks, K. E.; Zhang, D.; Deeley, R. G. *et al.* Mutational analysis of ionizable residues proximal to the cytoplasmic interface of membrane spanning domain 3 of the multidrug resistance protein, MRP1 (ABCC1): glutamate 1204 is important for both the expression and catalytic activity of the transporter. *J. Biol. Chem.* **2004**, *279*, 38871-38880.
20. Ren, X. Q.; Furukawa, T.; Aoki, S.; Sumizawa, T.; Haraguchi, M.; Nakajima, Y. *et al.* A positively charged amino acid proximal to the C-terminus of TM17 of MRP1 is indispensable for GSH-dependent binding of substrates and for transport of LTC₄. *Biochemistry* **2002**, *41*, 14132-14140.
21. Ito, K.; Olsen, S. L.; Qiu, W.; Deeley, R. G.; Cole, S. P. Mutation of a single conserved tryptophan in multidrug resistance protein 1 (MRP1/ABCC1) results in loss of drug resistance and selective loss of organic anion transport. *J. Biol. Chem.* **2001**, *276*, 15616-15624.
22. Ito, K.; Oleschuk, C. J.; Westlake, C.; Vasa, M. Z.; Deeley, R. G.; Cole, S. P. Mutation of Trp1254 in the multispecific organic anion transporter, multidrug resistance protein 2 (MRP2) (ABCC2), alters substrate specificity and results in loss of methotrexate transport activity. *J. Biol. Chem.* **2001**, *276*, 38108-38114.
23. Oleschuk, C. J.; Deeley, R. G.; Cole, S. P. Substitution of Trp1242 of TM17 alters substrate specificity of human multidrug resistance protein 3. *Am. J. Physiol Gastrointest. Liver Physiol* **2003**, *284*, G280-G289.
24. Campbell, J. D.; Koike, K.; Moreau, C.; Sansom, M. S.; Deeley, R. G.; Cole, S. P. Molecular modeling correctly predicts the functional importance of Phe594 in transmembrane helix 11 of the multidrug resistance protein, MRP1 (ABCC1). *J. Biol. Chem.* **2004**, *279*, 463-468.
25. Payen, L. F.; Gao, M.; Westlake, C. J.; Cole, S. P.; Deeley, R. G. Role of carboxylate residues adjacent to the conserved core Walker B motifs in the catalytic cycle of multidrug resistance protein 1 (ABCC1). *J. Biol. Chem.* **2003**, *278*, 38537-38547.
26. Loo, T. W.; Bartlett, M. C.; Clarke, D. M. Substrate-induced conformational changes in the transmembrane segments of human P-glycoprotein. Direct evidence for the substrate-induced fit mechanism for drug binding. *J. Biol. Chem.* **2003**, *278*, 13603-13606.



Chapter 7

General discussion



Introduction

The concentration of central nervous system (CNS) drugs in the brain is often limited by transport and metabolism of these drugs at the BBB or intestine via drug efflux transporters and metabolizing enzymes.¹ If compounds could be selected that have limited efflux or metabolism, CNS drugs with a better pharmacokinetic profile could be developed. In this thesis, different *in vitro* tools are described that were developed to investigate the transport of new compounds via efflux transporters. Besides using these tools to select compounds that are not transported via efflux transporters in CNS drug development, they can also be used to identify substrates for these proteins. Using P-gp transport affinity as a selection criterion is interesting for compounds that should not enter the brain to prevent unwanted CNS-mediated adverse effects. This was also thought to be an interesting strategy in the development of peripheral CB1 receptor antagonists, which would have less neuropsychiatric side effects than the brain-penetrating CB1 receptor antagonist rimonabant in treatment of obesity. In this thesis, the influence of drug efflux on the brain disposition of a class of 3,4-diarylpyrazoline CB1 receptor antagonists has been investigated (Chapter 2 and 3). In this chapter, the implications of using efflux transporter activity in the development of safe CB1 receptor antagonists in comparison to other strategies to improve the cost-benefit ratio of these antagonists are discussed. Furthermore, the advantages and disadvantages of our tools to identify substrates of efflux transporters and the use of these tools in CNS drug development are considered.

The progress made in improving the benefit-risk ratio of CB1 receptor antagonists

Inhibition of one of the key players of the endocannabinoid system, the cannabinoid type 1 (CB1) receptor, with the CB1 receptor antagonist/inverse agonist rimonabant has positive effects on weight, waist circumference, and cardiometabolic risk factors.^{2, 3} However, two years after its release on the European market, rimonabant was withdrawn due to psychiatric side effects of this compound in additional clinical studies.⁴⁻⁶ Although many companies subsequently stopped their CB1 receptor antagonist development programmes (*i.e.* for taranabant, surinabant, otenabant, and ibipinabant), some researchers thought it should be possible to increase their benefit-risk ratio.⁵ The possibilities to avoid adverse events comprised treatment of a subset of patients which might benefit the most from treatment, and the development of neutral or peripheral CB1 receptor antagonists.⁵

Based on the results from clinical studies with rimonabant, researchers hypothesized that patient selection could increase the benefit-risk ratio of already existing CB1 receptor antagonists.^{7, 8} Patients expected to benefit most from rimonabant treatment were people with abdominal obesity who have a cardiometabolic risk profile that is worse than



people with the same body mass index and global obesity. Rimonabant treatment had an increased benefit in these patients because it decreased the intra-abdominal fat and the associated cardiometabolic risk factors.⁸ In addition to selecting patients with a certain type of obesity, one should exclude patients with a history of depression to reduce the psychiatric side effects.^{8,9} Comparing clinical studies including or excluding these patients showed that patients with a history of depression or anxiety were more likely to have recurring psychiatric events upon rimonabant treatment.^{8,9} In addition, polymorphisms in genes encoding the CB1 receptor and the serotonin reuptake transporter (SERT) that lead to a lower expression of both proteins are correlated with a higher risk for anxiety and depression.⁹ These findings create opportunities for the development of pharmacogenomic tests and questionnaires to select patients with a lower risk for psychiatric adverse events for treatment with rimonabant. If the inclusion and exclusion criteria for most benefit of treatment and lowest risk for adverse events are applied, the benefit-risk ratio of CB1 receptor antagonist treatment should be much improved.⁸ Although progress has been made in understanding the involvement of CB1 receptor inhibition in anxiety or depression, and investigating possibilities to select patients with an increased benefit-risk ratio, this has not yet evolved in the re-approval of rimonabant for a subset of patients.

Another option was to develop neutral antagonists of the CB1 receptor instead of inverse agonists, such as rimonabant.⁵ In theory, inverse agonists decrease the basal activity of a receptor, whereas neutral antagonists only inhibit its ligand-mediated activity.¹⁰ Researchers hypothesized that the psychiatric side effects of rimonabant might be due to inhibition of the basal activity of the CB1 receptor and that neutral CB1 receptor antagonists might have a favourable pharmacodynamic profile.^{11,12} However, it is difficult to distinguish between neutral antagonists and inverse agonists with current assay technologies, because it depends on the sensitivity of the assay whether weak inverse agonistic activity may be revealed, possibly indicating false neutral antagonistic activity of a compound.¹⁰ In addition, endogenous endocannabinoid levels are thought to cause a basal endocannabinoid tone leading to additional ligand-mediated constitutive activity of the CB1 receptor that could be inhibited by a neutral antagonist, thereby displaying inverse agonistic properties.^{12,13} After withdrawal of rimonabant, an increasing number of putative neutral CB1 receptor antagonists has been developed (summarized by Ward *et al*).¹² One of these neutral antagonists, AM4113, retained beneficial effects on food intake and weight loss, but appeared to cause less nausea and a smaller contextual fear response and less anxiolytic effects than CB1 inverse agonists in rats.¹⁴⁻¹⁶ These results suggest that these compounds are as effective as rimonabant in reducing weight, with less side effects. However, there is still a chance that these compounds fail in clinical trials due to psychiatric side effects because the anxiolytic effects of these compounds have only been studied in a few animal studies. To further investigate their therapeutic potential, more animal studies with putative neutral antagonists should be performed.

Probably the most effective option for reduction of centrally mediated psychiatric side effects would be developing CB1 receptor antagonists that only act on peripheral CB1 receptors. However, these compounds might have less effect on food intake and weight, as these actions were shown to be largely mediated via the central CB1 receptor.^{17, 18} On the other hand, it was hypothesized that peripheral CB1 receptor antagonists preserve the effects of CB1 receptor antagonists on cardiometabolic risk factors that are thought to be, at least partly, affected by CB1 receptors in peripheral tissues.^{5, 19-21} Several putative peripheral CB1 receptor antagonists have been developed in the past years, of which two potent compounds, AM6545 and BPR697, convincingly show a role for peripheral CB1 receptors in energy balance and metabolism.^{12, 22-25} In animal studies, these compounds improved cardiometabolic risk factors, such as hepatic triglycerides, insulin, glucose, adiponectin, and leptin levels, and even caused weight loss or decreased weight gain, which is probably due to increased lipid oxidation.²²⁻²⁵ On the other hand, they did not interrupt with agonist-induced hypothermia, hypomotility, catalepsy, and analgesia mediated via the central CB1 receptor, indicating that they do not penetrate the brain.^{22, 23} Furthermore, AM6545 did not induce anxiolytic effects, while rimonabant did.²² In addition to being a peripheral antagonist, AM6545 is a neutral antagonist, and it was also shown to cause less nausea, most likely because of its lack of inverse agonistic action.^{24, 25} Parallel to the development of AM6545 and BPR697, the biotech company 7TM Pharma has made efforts to design a peripheral CB1 receptor antagonist, TM38837, and this compound has entered clinical studies.^{26, 27} They state that it is a potent compound in animal studies for obesity and type 2 diabetes and that a Phase I clinical study in 24 men showed that a therapeutic dose of TM38837 does not affect CNS-mediated effects of the CB1 receptor agonist Δ^9 -tetrahydrocannabinol, indicating that it does not enter the brain.²⁶ In conclusion, these compounds appear to have beneficial effects on cardiometabolic risk factors with reduced CNS-mediated side effects, and therefore might serve as good therapeutics for treatment of metabolic disease associated with obesity. To further support the exploration of the therapeutic potential of peripheral CB1 receptor antagonists, we investigated how transport of CB1 receptor antagonists via efflux transporters might limit the brain penetration of these compounds, to provide a strategy for selection of peripheral compounds early in drug development.

The role of efflux transporters in reducing brain penetration of CB1 receptor antagonists

7

The research described in Chapter 2 and 3 of this thesis was focused on the transport and interaction of a series of 3,4-diarylpyrazoline CB1 receptor antagonists with the efflux transporters MRP1, MRP2, MRP3, MRP4, and P-gp. We were the first to report interaction of CB1 receptor antagonists with MRP1-4. Vesicular interaction studies using membrane vesicles of HEK293 cells overexpressing these transporters showed that most of them



interacted with the transporters. The 3,4-diarylpyrazolines mainly inhibited MRP1- and MRP4-mediated E_2 17 β G transport and P-gp-mediated NMQ transport, whereas they stimulated transport of E_2 17 β G by MRP2 and MRP3 (Chapter 2 and 3). The inhibitory action of **13**, rimonabant, and most likely also of **15** on MRP1 and MRP4 was non-competitive, whereas for MRP2 and MRP3 the interaction appeared to be competitive (Chapter 2). Additional *in vivo* data of the effective dose (ED_{50}) of compounds **4**, **11**, **14**, and **15** in inhibiting CB1 agonist-induced hypotension suggested active transport of compound **4**, **11**, and **14** from the brain, for which MRP4 might be responsible (Chapter 2). On the other hand, the cellular accumulation assay using HEK293 cells overexpressing P-gp showed that, although all CB1 receptor antagonists inhibited P-gp-mediated NMQ transport, only one of them appeared to be a substrate of P-gp in this assay (Chapter 3). This suggests that the vesicular interaction assay is not predictive for transport of a compound via the transporter of interest. Therefore, transport studies with 3,4-diarylpyrazolines in cellular transport assays or knockout mice should be performed to determine the possible involvement of MRP1-4 in limiting the brain penetration of 3,4-diarylpyrazoline CB1 receptor antagonists.

By determining the accumulation of CB1 receptor antagonists in HEK293 cells overexpressing P-gp or a control protein, we showed that only 3,4-diarylpyrazoline **23** was transported via P-gp (Chapter 3). An *in vivo* study in rats revealed that the brain penetration of this compound was also reduced compared to rimonabant, which was not a P-gp substrate, and inhibition of P-gp with elacridar showed that P-gp was largely responsible for the limited brain penetration of **23** (Chapter 3). This implies that transport of CB1 receptor antagonists via P-gp could be used in the development of peripheral CB1 receptor antagonists.

In addition to P-gp, BCRP might also play a role in limiting the brain penetration of CB1 receptor antagonists. BCRP is present at the luminal membrane of the BBB and recent studies using LC-MS/MS quantification of proteins present at the human BBB revealed that BCRP abundance is even somewhat higher than P-gp (about 1.3-1.5 fold difference).^{28, 29} In rats and mice about 3- to 4-fold more P-gp than BCRP is present at the BBB. Therefore, the importance of BCRP transport in humans might be underestimated in studies with these animals.^{30, 31} In Chapter 3, we studied the transport of **23** and rimonabant via BCRP, and revealed that in addition to being a P-gp substrate, **23** is also a BCRP substrate. Although the influence of BCRP on **23** brain penetration in rats might be limited, together with P-gp it might form a very effective barrier at the human BBB against CB1 receptor antagonists (Fig. 1). Therefore, it would be interesting to further investigate the possibility to select for BCRP substrate activity in addition to P-gp activity to further reduce human brain penetration of peripheral CB1 receptor antagonists.

In our studies, we have focused on the possibility of using P-gp in the development of peripheral CB1 receptor antagonists and showed that transport via P-gp might serve as a selection criterion in this process. In fact, one other group showed that P-gp was the most important factor for limiting the brain penetration of their peripheral CB1 receptor

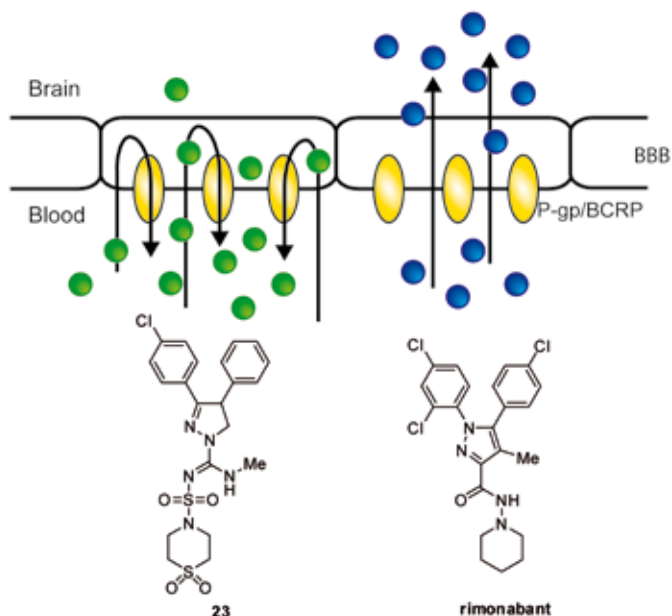


Figure 1 Transport by P-gp and, possibly, BCRP at the BBB limits the brain penetration of 3,4-diarylpyrazoline CB1 receptor antagonist **23** and not of rimonabant

antagonist AM6545.²² Another study speculates that some of the CB1 receptor antagonists developed are expected to have a lower brain/plasma ratio because they are substrates of P-glycoprotein and also have a high polar surface area (PSA).³² Unfortunately, brain and plasma concentrations have not been measured in that study to provide evidence for a low brain penetration of those compounds. However, the oral ED_{50} necessary for reversing CB1 agonist-induced hypotension was much higher for P-gp substrate than for non-P-gp substrate CB1 receptor antagonists, suggesting lower brain penetration or poor oral availability.³² Other ways to lower the brain penetration of compounds could be lowering the lipophilicity or increasing the PSA of a compound.²⁷ Changing these physicochemical characteristics will decrease their ability to penetrate membranes, and this method appears to be useful in lowering the brain penetration of CB1 receptor antagonists.²⁷ It would be interesting to investigate the tissue distribution of these type of compounds, because their low lipophilicity might also reduce their penetration into other tissues than the brain, where the target CB1 receptors are localized, thereby lowering the pharmacodynamic effect of these CB1 receptor antagonists. For P-gp substrate peripheral CB1 receptor antagonists, this problem is less likely to occur. However, for this type of compounds a decreased oral availability due to intestinal P-gp transport might be a problem in development.



P-gp transport can lower the oral availability of drugs, and this could be a general problem of using the P-gp transport strategy to develop peripheral CB1 receptor antagonists.³³ However, the impact of P-gp on intestinal absorption is thought to be lower than on BBB penetration because the higher concentrations of drug in the intestine appear to saturate intestinal P-gp.³⁴ Indeed, there are drugs for which P-gp transport activity has proven to be useful to limit the central side effects, in which P-gp has limited effects on determining the intestinal absorption after oral administration, such as domperidone, fexofenadine, and loperamide of which respectively about 100%, 30% and 65% of the oral dose is absorbed at the intestine.³⁵⁻⁴³ In addition, P-gp transport also did not appear to restrict the oral availability of the peripheral antagonist (and P-gp substrate) AM6545, because its plasma concentration was similar after oral and peritoneal dosing.²² Furthermore, in the CaCo-2 cell model for oral availability, AM6545 had an efflux ratio of 1.1, which indicates that its oral availability is not limited by active transport.²² Cellular assays to estimate the intestinal penetration have also been performed for the 3,4-diarylpyrazoline CB1 receptor antagonists in our study, and the efflux ratio for the P-gp substrate **23** in CaCo-2 cells was 1.5, and 28% of its dose passed the membrane of LLC-PK1-MDR1 cells (unpublished data). This indicates that oral availability of **23** is not expected to be limited by lower membrane passage and active efflux at the intestinal wall. Whether a compound will pass the intestinal barrier will not only depend on whether a compound is a P-gp substrate, but also on a combination of physicochemical characteristics, such as $\log P$, PSA, or size, in addition to active transport via influx and efflux transporters. If future CB1 receptor antagonist are selected on the basis of their P-gp transport affinity, additional cellular permeability studies predictive for oral availability could give an indication of what compounds to select for further development.

Importance of efflux transporters for the development of CNS drugs

The reduction of the brain concentration of CB1 receptor antagonist **23** by P-gp (Chapter 3), underlines that P-gp-mediated efflux at the BBB can lower the brain penetration of drugs. Previous studies evaluating the P-gp substrate activity of CNS drugs compared to non-CNS drugs revealed that only few marketed CNS drugs are transported via P-gp compared to non-CNS drugs, indicating that P-gp transport activity is not favourable for brain penetration.^{1,44} The knowledge that this transporter is an important gatekeeper of the brain has led to the use of multiple tools to predict or determine substrates of P-gp.

Identification of P-gp substrates using computational models could provide a cost-effective method to select lead compounds early in drug development.⁴⁵ Multiple computational models have been developed that describe the structure-activity-relationship (SAR) of compounds with P-gp and, over the past decades, the predictability of these models for P-gp substrates has increased.^{46, 47} However, because P-gp has multiple substrate binding sites, which explains its wide substrate specificity, it has been difficult to produce a conclusive

Table 1 Effects of homolog amino acid substitutions in MRP1-4 on E₂17βG and MTX transport activity

Mutation	Substitution	E ₂ 17βG (%) ^a	MTX (%) ^a
MRP1 – Trp ¹²⁴⁶	Ala	<10	<10
	Tyr	<10	10
MRP2 – Trp ¹²⁵⁴	Ala	<10	14
	Tyr	100	1
MRP3 – Trp ¹²⁴²	Ala	250	20
	Tyr	700	20
MRP4 – Trp ⁹⁹⁵	Ala	0	5
	Tyr	30	40

Data are from Ito *et al.* and Oleschuk *et al* and Chapter 6.⁵⁵⁻⁵⁷

^a Normalized transport activity of mutant compared to wild type (100%) transporter using 400 nM E₂17βG and 1000 nM MTX for determining MRP1-3 transport activity, and 120 nM E₂17βG and 500 nM MTX for MRP4.

SAR model for P-gp substrate activity of compounds.⁴⁸ Different pharmacophore models, which describe the chemical properties of a compound that determine interaction with a binding site, should be developed for the different bindings sites to predict the wide range of substrates. Not only P-gp, but also other efflux transporters, such as MRPs, possess a complex binding pocket with multiple drug binding sites (Chapter 6).⁴⁹⁻⁵⁴ This is further emphasized by the fact that mutation of amino acids that might be part of the substrate binding pocket of MRP4 showed different effects for varying substrates (Chapter 6). In addition, the discrepancy between the effects of mutation of W995 in MRP4 and its homologues in MRP1-3 on transport of estradiol 17β-D-glucuronide (E₂17βG) and methotrexate (MTX) suggests that the role of this amino acid homologue in the transport binding pocket is different between the transporters (Table 1).⁵⁵⁻⁵⁷ Therefore, binding of substrates will rely on interaction of substrates with several amino acids in the pocket that might differ for each substrate, leading to multiple binding sites. Combining SAR with substrate binding site modeling might improve the computational models to predict substrates for efflux transporters in CNS drug development.⁴⁸

Because the computational models cannot give a conclusive answer as to whether a compound is a substrate of P-gp, transport activity should be verified using experimental models. Different experimental tools are available to assess whether compounds are substrates or inhibitors of efflux transporters (summarized in Table 2).⁵⁸⁻⁶⁰ In this thesis, we mainly used HEK293 cells overexpressing different efflux transporters for a cellular



accumulation assay or a vesicular transport assay to assess interaction of compounds with efflux transporters (Fig. 2).

Vesicular transport assay

The vesicular transport assay is an experimentally convenient assay to investigate efflux transporters and it has been used for more than 20 years. In this thesis, we have used the vesicular transport assay for multiple purposes: I) Investigation of interaction of compounds with efflux transporters (Chapters 2, 3, and 5); II) Substrate identification via direct transport measurements (Chapter 4); III) Mutational analysis of transporter function (Chapter 6).

Interaction of compounds with the transport of a probe substrate into membrane vesicles has been used frequently to identify new modulators of transport.⁶¹⁻⁶⁴ Using this method, drug-drug interactions can also be detected.^{61, 65} Because modulators might have different effects on transport of different probe substrates, it would be best to use the combination of drugs that will be co-administered to investigate drug-drug interactions. Interaction of a compound with a transporter, inhibiting or stimulating transport of the probe substrate, might implicate that it is also transported via the transporter. However, comparison of the interaction of CB1 receptor antagonist with P-gp in membrane vesicles with their actual transport via this transporter in cells, revealed that interaction with this transporter did not necessarily predicted its substrate activity (Chapter 3). Therefore, one should be careful with the interpretation of transport interaction data in relation to possible substrate activity of a compound.

A better way to determine substrate specificity, is to measure the transport of the compound directly. Previously, this has been limited to radiolabeled or fluorescent compounds, but by using high-pressure liquid chromatography (HPLC), often combined with tandem mass spectrometry (LC-MS/MS), it is also possible to quantify vesicular transport of non-(radio)labeled compounds.⁶⁶⁻⁶⁸ Chapter 4 illustrates the use of measuring direct transport of the model compound 7-HC and 7-HC-G into membrane vesicles using HPLC. By investigation of transport of 7-HC and 7-HC-G via different efflux transporters, we were able to identify the efflux transporters influencing the human pharmacokinetics of coumarin and its metabolites 7-HC and 7-HC-G (Chapter 4). However, we also found that this method sometimes produces false negative results. In the case of CB1 receptor antagonist **23**, we identified it as a P-gp substrate using the cellular accumulation assay, whereas we could not detect uptake of this compound into P-gp vesicles (unpublished results). This might be due to the high lipophilicity of the CB1 receptor antagonists, having a greater propensity to diffuse over the vesicular membrane, leading to a higher background in the samples and a smaller difference between control and transporter-expressing vesicles. Substrates of P-gp are often more lipophilic than substrates of MRPs and BCRP.^{69, 70} The fact that the vesicular transport assay is less suitable for identification of lipophilic compounds is reflected by the fact that there are only few articles describing vesicular transport using P-gp vesicles, whereas there are many available describing transport into MRP- and BCRP-overexpressing vesicles.

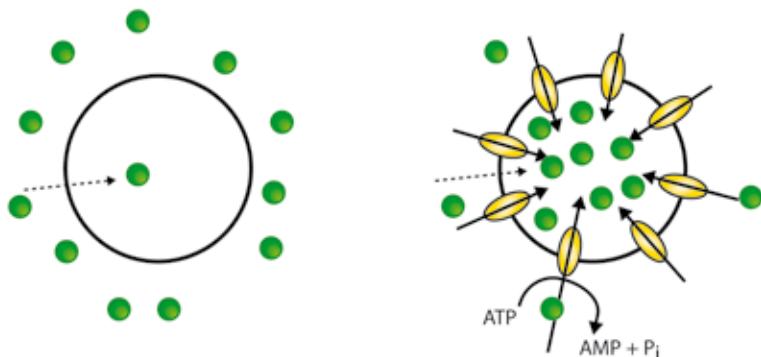
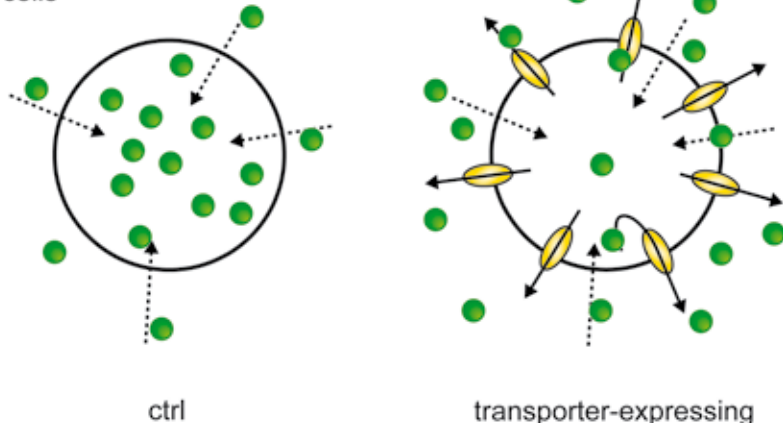
A vesicles**B** cells

Figure 2 Schematic overview of vesicular (A) and cellular (B) transport studies using control and transporter-expressing cells

Dashed lines represent passive transport of the compound of interest, whereas straight lines indicate active transport. Additional ATP should be added in substrate mix for vesicular transport studies to enable active transport via hydrolysis of ATP to AMP and phosphate (P_i).

In addition to finding new substrates or modulators of efflux transporters, membrane vesicles are often used to elucidate the mechanism of transport activity of these proteins. Introducing amino acid mutations might reveal which amino acids are important for substrate binding or for other steps in the transport cycle (Chapter 6).^{50, 56, 71-75} Because the vesicular transport assay is very suitable for the investigation of kinetic characteristics of transport activity of wild type and mutant proteins, *e.g.* determination of K_m and V_{max} , it provides a useful tool to characterize the mechanism of substrate transport via the transporter.



Table 2 Comparison of different *in vitro* models to identify substrates and inhibitors of efflux transporters

Model	Identifies	Advantages	Disadvantages
ATPase ^a	I	<ul style="list-style-type: none"> - no need for specific compound detection method 	<ul style="list-style-type: none"> - poor predictability of substrates and inhibitors - results depend on experimental conditions - difficult assay for transporters due to high background ATPase activity
Vesicular transport ^a	S, I	<ul style="list-style-type: none"> - measuring direct transport of compounds (substrate identification) - determination of kinetic transport characteristics (K_m or K_i) - high throughput 	<ul style="list-style-type: none"> - false negative results for substrates with high passive permeability or non-specific binding (often P-gp substrates)
Cytotoxicity assay ^b	S, I	<ul style="list-style-type: none"> - no need for specific compound detection method 	<ul style="list-style-type: none"> - only cytotoxic substrates can be identified as substrates - cytotoxicity varies between cell types
Cellular accumulation ^{b, c}	S, I	<ul style="list-style-type: none"> - measuring direct transport of compound (substrate identification) - relatively high throughput possible - determination of K_i of inhibitors 	<ul style="list-style-type: none"> - hydrophobic substrates may be not detected due to rapid passive diffusion - transport of low permeable compounds may be underestimated
Transwell transport ^c	S, I	<ul style="list-style-type: none"> - measuring direct transport of compounds (substrate identification) - determination of kinetic transport characteristics (K_m or K_i) - polarized cells with functional localization of transporters - assessment of permeability of compounds 	<ul style="list-style-type: none"> - labour intensive and more expensive - depends on passive permeability of compound - standard protocols should ensure tightness of cell monolayer

Cellular accumulation assay

The principle of efflux via transporters to protect the cell from accumulation of (toxic) compounds has been used in the development of cellular accumulation assays to identify substrates or inhibitors of efflux transporters. Previously, these assays were restricted to cytotoxic, radiolabeled or fluorescent compounds, but with new LC-MS/MS methods it is possible to investigate a wide variety of compounds in this assay.^{59, 60, 76} Because the assay is based on the accumulation of a compound due to its passive diffusion over the cell membrane, this assay is more suitable for lipophilic compounds than for hydrophilic compounds, which will not diffuse into the cell. However, too lipophilic compounds may escape efflux transport due to rapid diffusion into and out of the cell, which might also lead to false-negative results.^{46, 59} The advantage of HEK293 cells for this assay is that these cells are very suitable for transient expression of transporters using baculovirus. HEK293 cells transiently expressing a control protein serve as a good control for transporter-expressing HEK293 cells because these cells are treated equally and will diverge less in morphology and functionality than cell lines stably overexpressing control and transporter protein. A disadvantage of HEK293 cells is that they have a tendency to detach from the culture plates during washing. Furthermore, they express endogenous transporters that might reduce the effect induced by the overexpressed transporter, especially for high affinity substrates (Table 3).⁷⁷ However, endogenous transporters are present in most cell types, and might even differ between stable control and transporter expressing cell lines.⁷⁸ Other groups have also performed accumulation assays with different cell types overexpressing transporters, often in combination with transport inhibitors.^{79, 80} However, one should be careful with only using inhibitors to verify which transporter is involved, because they often lack transporter specificity (Chapter 5).⁶² Furthermore, we found that the P-gp inhibitor elacridar influenced the availability of some CB1 receptor antagonists in the medium. Because some of these lipophilic compounds had poor solubility or appeared to attach to the cells or the plate surface, less than the nominal concentration of CB1 receptor antagonists was available in the medium (Chapter 2). Adding the P-gp inhibitors similarly increased the medium concentration and thereby the cellular accumulation of some CB1 receptor antagonists, leading to false positive results if only the effect of P-gp inhibition in P-gp overexpressing cells

Table 2 continued

Content is based on experience with models used in this thesis and reviews describing other models.^{46, 58}

S, substrate; I, inhibitor

^{a, b, c} Preparations used for identification:

^a Membrane vesicles of cells overexpressing transporters or lipid membranes with reconstituted transporters.

^b Unpolarized cells overexpressing transporters, such as HEK293-P-gp.

^c Polarized cells overexpressing transporters, such as MDCKII-P-gp or LLC-PK1-P-gp.



Table 3 Determination of mRNA expression of efflux transporters in HEK293 cells using a whole genome expression array⁷⁷

Efflux transporter	Expressed
ABCC1 (MRP1)	yes
ABCC4 (MRP4)	yes
ABCC5 (MRP5)	yes
ABCB1 (P-gp)	yes
ABCC6 (MRP6)	yes
ABCC10 (MRP7)	yes
ABCG2 (BCRP)	yes
ABCC3 (MRP3)	no
ABCC2 (MRP2)	no
ABCC12 (MRP12)	no
ABCC11 (MRP8)	no

A GeneChip Human Genome U133 Plus 2.0 Array from Affymetrix was used to determine mRNA expression. Absent/present calls for individual gene expression values were obtained from a data set generated with the MAS5 (Affymetrix Microarray Suite version 5.0; Affymetrix) algorithm.⁷⁷

would have been tested (unpublished data). However, by comparing the accumulation in a HEK293 control to the accumulation in P-gp overexpressing cells, we circumvented this issue.

Comparison of transporter assays

Transwell transport studies that determine vectorial transport of a compound through a polarized cell line overexpressing P-gp are seen as the golden standard for the identification of P-gp substrates.^{46, 81} However, most of the limitations of the accumulation assay, *e.g.* high dependence on compound permeability, are also limitations to this type of transport studies (Table 2). The main advantage of using polarized instead of non-polarized cells is that it represent a more physiologically relevant model and that transport direction (apical to basolateral or basolateral to apical) and passive permeability can be determined.⁵⁹ Furthermore, there are papers describing how to determine kinetic characteristics of transport using these studies, which is more difficult in cellular assays.^{82, 83} On the other hand, the accumulation assay does serve as a more practical assay to identify lipophilic and membrane permeable substrates and it would allow for a higher throughput than transwell studies. For hydrophilic, less membrane permeable compounds the vesicular transport assay will provide a more suitable assay for substrate identification. These assays could therefore provide good alternatives for the polarized transport assays in the (CNS) drug

development process for finding MRP1-4 (vesicles), BCRP (vesicles/cell accumulation) or P-gp (cell accumulation) substrates.

Metabolism of CNS drugs

Metabolism of CNS drugs is also an important determinant of their plasma and eventually brain concentration.¹ Therefore, many companies use *in vitro* methods to study whether lead compounds in drug development are substrates or inhibitors of metabolism to estimate *in vivo* metabolism or drug-drug interactions.⁸⁴⁻⁸⁶ Because transporters and enzymes are thought to work in concert, an assay including both metabolizing enzymes and transporters might provide a more physiological assay to estimate metabolism and transport *in vivo*.^{86, 87} If the interaction between specific enzymes and transporters is studied, a cell model should be used in which endogenous transporters and metabolizing enzymes would not influence the metabolism and transport of the compound of interest. Previously, HEK293 cells co-expressing UGT2B7 and MRP1, MRP2 or MRP3 have been used to study the effect of transport on glucuronidation.^{88, 89} In our study, we also used HEK293 cells overexpressing UGT2B15 to study glucuronidation of the model compound 7-HC (Chapter 5). The absence of accumulation of the hydrophilic metabolite 7-HC-G, however, indicated the presence of endogenous transporters in these cells. Indeed, MRP4, one of the efflux transporters of 7-HC-G (Chapter 4), appears to be endogenously expressed in HEK293 cells (Chapter 5 and Table 3).⁷⁷ Therefore, a co-expression model of an enzyme and MRP4 in these HEK293 cells is less suitable to investigate enzyme-transporter interplay of parent compounds that have metabolites with a high substrate affinity for MRP4, because these metabolites are likely to be transported by endogenous MRP4.

Investigating intestinal metabolism of one of the 3,4-diarylpyrazoline CB1 receptor antagonists in Ussing Chamber experiments with human intestinal tissue showed that enzymes in the intestine could play a significant role in metabolism of this compound (personal communication, prof. dr. G. Groothuis, Groningen). Preliminary experiments studying metabolism of this compound in HEK-CYP3A4 and HEK-CYP3A5 cells suggested that CYP3A4 is involved (unpublished results). Because this metabolite was mainly effluxed to the apical side of the human intestinal tissue, it was hypothesized that P-gp might play a role in its transport. The HEK293 cell model would provide an interesting tool to investigate the interplay between CYP3A4 and P-gp in the metabolism of this CB1 receptor antagonist.

Conclusion and future perspectives

In this thesis, we used several *in vitro* models to study transport of compounds via drug efflux transporters and we argue that these tools could be implemented in CNS drug development. Especially the membrane vesicular transport assay could provide a useful tool



for pharmaceutical industry to screen transport of new compounds via MRPs, which are currently largely neglected in drug development.

In the development of peripheral CB1 receptor antagonists, the P-gp transport assay was used successfully to select CB1 receptor antagonists that do not enter the brain due to active P-gp efflux. The efficacy of peripheral antagonists, of which the development could be accelerated using the P-gp substrate strategy, as drugs against obesity and metabolic disease should be further established in (pre-)clinical studies.

References

1. Alavijeh, M. S.; Chishty, M.; Qaiser, M. Z.; Palmer, A. M. Drug metabolism and pharmacokinetics, the blood-brain barrier, and central nervous system drug discovery. *NeuroRx*. **2005**, *2*, 554-571.
2. Van Gaal, L. F.; Rissanen, A. M.; Scheen, A. J.; Ziegler, O.; Rossner, S. Effects of the cannabinoid-1 receptor blocker rimonabant on weight reduction and cardiovascular risk factors in overweight patients: 1-year experience from the RIO-Europe study. *Lancet* **2005**, *365*, 1389-1397.
3. Van Gaal, L. F.; Scheen, A. J.; Rissanen, A. M.; Rossner, S.; Hanotin, C.; Ziegler, O. Long-term effect of CB1 blockade with rimonabant on cardiometabolic risk factors: two year results from the RIO-Europe Study. *Eur. Heart J.* **2008**, *29*, 1761-1771.
4. Christensen, R.; Kristensen, P. K.; Bartels, E. M.; Bliddal, H.; Astrup, A. Efficacy and safety of the weight-loss drug rimonabant: a meta-analysis of randomised trials. *Lancet* **2007**, *370*, 1706-1713.
5. Jones, D. End of the line for cannabinoid receptor 1 as an anti-obesity target? *Nat. Rev. Drug Discov.* **2008**, *7*, 961-962.
6. US Food and Drug Administration Advisory committee. FDA briefing document NDA 21-888: Zimulti (rimonabant) Tablets 20 mg. Sanofi-Aventis Advisory committee. 13-6-2007. Ref Type: Internet Communication
7. Di Marzo, V. Play an ADAGIO with a STRADIVARIUS: the right patient for CB1 receptor antagonists? *Nat. Clin. Pract. Cardiovasc. Med.* **2008**, *5*, 610-612.
8. Di Marzo, V.; Després, J. P. CB1 antagonists for obesity - what lessons have we learned from rimonabant? *Nat. Rev. Endocrinol.* **2009**, *5*, 633-638.
9. Lazary, J.; Juhasz, G.; Hunyady, L.; Bagdy, G. Personalized medicine can pave the way for the safe use of CB receptor antagonists. *Trends Pharmacol. Sci.* **2011**, *32*, 270-280.
10. Giraldo, J. How inverse can a neutral antagonist be? Strategic questions after the rimonabant issue. *Drug Discov. Today* **2010**, *15*, 411-415.
11. Janero, D. R.; Makriyannis, A. Cannabinoid receptor antagonists: pharmacological opportunities, clinical experience, and translational prognosis. *Expert. Opin. Emerg. Drugs* **2009**, *14*, 43-65.
12. Ward, S. J.; Raffa, R. B. Rimonabant redux and strategies to improve the future outlook of CB1 receptor neutral-antagonist/inverse-agonist therapies. *Obesity* **2011**, *19*, 1325-1334.
13. Pertwee, R. G. Inverse agonism and neutral antagonism at cannabinoid CB1 receptors. *Life Sci.* **2005**, *76*, 1307-1324.
14. Sink, K. S.; Segovia, K. N.; Collins, L. E.; Markus, E. J.; Vemuri, V. K.; Makriyannis, A. *et al.* The CB1 inverse agonist AM251, but not the CB1 antagonist AM4113, enhances retention of contextual fear conditioning in rats. *Pharmacol. Biochem. Behav.* **2010**, *95*, 479-484.
15. Sink, K. S.; McLaughlin, P. J.; Wood, J. A.; Brown, C.; Fan, P.; Vemuri, V. K. *et al.* The novel cannabinoid CB1 receptor neutral antagonist AM4113 suppresses food intake and food-reinforced behavior but does not induce signs of nausea in rats. *Neuropsychopharmacology* **2008**, *33*, 946-955.
16. Sink, K. S.; Segovia, K. N.; Sink, J.; Randall, P. A.; Collins, L. E.; Correa, M. *et al.* Potential anxiogenic effects of cannabinoid CB1 receptor antagonists/inverse agonists in rats: comparisons between AM4113, AM251, and the benzodiazepine inverse agonist FG-7142. *Eur. Neuropsychopharmacol.* **2010**, *20*, 112-122.
17. Pang, Z.; Wu, N. N.; Zhao, W.; Chain, D. C.; Schaffer, E.; Zhang, X. *et al.* The central cannabinoid CB1 receptor is required for diet-induced obesity and rimonabant's antiobesity effects in mice. *Obesity (Silver Spring)* **2011**, *19*, 1923-1934.
18. Quarta, C.; Bellocchio, L.; Mancini, G.; Mazza, R.; Cervino, C.; Brulke, L. J. *et al.* CB1 signaling in forebrain and sympathetic neurons is a key determinant of endocannabinoid actions on energy balance. *Cell Metab*

- 2010**, *11*, 273-285.
19. Andre, A.; Gonthier, M. P. The endocannabinoid system: its roles in energy balance and potential as a target for obesity treatment. *Int. J. Biochem. Cell Biol.* **2010**, *42*, 1788-1801.
 20. Di Marzo, V. CB1 receptor antagonism: biological basis for metabolic effects. *Drug Discov. Today* **2008**, *13*, 1026-1041.
 21. Silvestri, C.; Ligresti, A.; Di Marzo, V. Peripheral effects of the endocannabinoid system in energy homeostasis: Adipose tissue, liver and skeletal muscle. *Rev. Endocr. Metab Disord.* **2011**, *12*, 153-162.
 22. Tam, J.; Vemuri, V. K.; Liu, J.; Bátkai, S.; Mukhopadhyay, B.; Godlewski, G. *et al.* Peripheral CB1 cannabinoid receptor blockade improves cardiometabolic risk in mouse models of obesity. *J. Clin. Invest* **2010**, *120*, 2953-2966.
 23. Vijayakumar, R. S.; Lin, Y.; Shia, K. S.; Yeh, Y. N.; Hsieh, W. P.; Hsiao, W. C. *et al.* Induction of fatty acid oxidation resists weight gain, ameliorates hepatic steatosis and reduces cardiometabolic risk factors. *Int. J. Obes.* **2011**, doi: 10.1038/ijo.2011.171.
 24. Cluny, N. L.; Vemuri, V. K.; Chambers, A. P.; Limebeer, C. L.; Bedard, H.; Wood, J. T. *et al.* A novel peripherally restricted cannabinoid receptor antagonist, AM6545, reduces food intake and body weight, but does not cause malaise, in rodents. *Br. J. Pharmacol.* **2010**, *161*, 629-642.
 25. Randall, P. A.; Vemuri, V. K.; Segovia, K. N.; Torres, E. F.; Hosmer, S.; Nunes, E. J. *et al.* The novel cannabinoid CB1 antagonist AM6545 suppresses food intake and food-reinforced behavior. *Pharmacol. Biochem. Behav.* **2010**, *97*, 179-184.
 26. 7TM Pharma. 7TM Pharma successfully conducts clinical Phase I trial of its first in class peripheral CB1 receptor antagonist TM38837 demonstrating restriction from the human CNS. 20-11-0010. Ref Type: Internet Communication
 27. Receveur, J. M.; Murray, A.; Linget, J. M.; Nørregaard, P. K.; Cooper, M.; Bjurling, E. *et al.* Conversion of 4-cyanomethyl-pyrazole-3-carboxamides into CB1 antagonists with lowered propensity to pass the blood-brain-barrier. *Bioorg. Med. Chem. Lett.* **2010**, *20*, 453-457.
 28. Shawahna, R.; Uchida, Y.; Declèves, X.; Ohtsuki, S.; Yousif, S.; Dauchy, S. *et al.* Transcriptomic and quantitative proteomic analysis of transporters and drug metabolizing enzymes in freshly isolated human brain microvessels. *Mol. Pharm.* **2011**, *8*, 1332-1341.
 29. Uchida, Y.; Ohtsuki, S.; Katsukura, Y.; Ikeda, C.; Suzuki, T.; Kamiie, J. *et al.* Quantitative targeted absolute proteomics of human blood-brain barrier transporters and receptors. *J. Neurochem.* **2011**, *117*, 333-345.
 30. Kamiie, J.; Ohtsuki, S.; Iwase, R.; Ohmine, K.; Katsukura, Y.; Yanai, K. *et al.* Quantitative atlas of membrane transporter proteins: development and application of a highly sensitive simultaneous LC/MS/MS method combined with novel in-silico peptide selection criteria. *Pharm. Res.* **2008**, *25*, 1469-1483.
 31. Warren, M. S.; Zerangue, N.; Woodford, K.; Roberts, L. M.; Tate, E. H.; Feng, B. *et al.* Comparative gene expression profiles of ABC transporters in brain microvessel endothelial cells and brain in five species including human. *Pharmacol. Res.* **2009**, *59*, 404-413.
 32. Lange, J. H.; van der Neut, M. A.; Borst, A. J.; Yildirim, M.; van Stuijvenberg, H. H.; van Vliet, B. J. *et al.* Probing the cannabinoid CB1/CB2 receptor subtype selectivity limits of 1,2-diarylimidazole-4-carboxamides by fine-tuning their 5-substitution pattern. *Bioorg. Med. Chem. Lett.* **2010**, *20*, 2770-2775.
 33. Oostendorp, R. L.; Beijnen, J. H.; Schellens, J. H. The biological and clinical role of drug transporters at the intestinal barrier. *Cancer Treat. Rev.* **2009**, *35*, 137-147.
 34. Lin, J. H.; Yamazaki, M. Clinical relevance of P-glycoprotein in drug therapy. *Drug Metab Rev.* **2003**, *35*, 417-454.
 35. Geneesmiddel Informatie Centrum van het Wetenschappelijk Instituut Nederlandse Apothekers *Informatorium Medicamentorum*; 2004.
 36. Schinkel, A. H.; Wagenaar, E.; Mol, C. A.; van Deemter, L. P-glycoprotein in the blood-brain barrier of mice influences the brain penetration and pharmacological activity of many drugs. *J. Clin. Invest* **1996**, *97*, 2517-2524.
 37. Kitamura, Y.; Koto, H.; Matsuura, S.; Kawabata, T.; Tsuchiya, H.; Kusuha, H. *et al.* Modest effect of impaired P-glycoprotein on the plasma concentrations of fexofenadine, quinidine, and loperamide following oral administration in collies. *Drug Metab Dispos.* **2008**, *36*, 807-810.
 38. Sadeque, A. J.; Wandel, C.; He, H.; Shah, S.; Wood, A. J. Increased drug delivery to the brain by P-glycoprotein inhibition. *Clin. Pharmacol. Ther.* **2000**, *68*, 231-237.
 39. Lappin, G.; Shishikura, Y.; Jochemsen, R.; Weaver, R. J.; Gesson, C.; Houston, B. *et al.* Pharmacokinetics of fexofenadine: evaluation of a microdose and assessment of absolute oral bioavailability. *Eur. J. Pharm. Sci.* **2010**, *40*, 125-131.
 40. Tahara, H.; Kusuha, H.; Fuse, E.; Sugiyama, Y. P-glycoprotein plays a major role in the efflux of fexofenadine in the small intestine and blood-brain barrier, but only a limited role in its biliary excretion. *Drug Metab Dispos.* **2005**, *33*, 963-968.



41. Heykants, J.; Hendriks, R.; Meuldermans, W.; Michiels, M.; Scheygrond, H.; Reyntjens, H. On the pharmacokinetics of domperidone in animals and man. IV. The pharmacokinetics of intravenous domperidone and its bioavailability in man following intramuscular, oral and rectal administration. *Eur. J. Drug Metab Pharmacokinet.* **1981**, *6*, 61-70.
42. Dan, Y.; Murakami, H.; Koyabu, N.; Ohtani, H.; Sawada, Y. Distribution of domperidone into the rat brain is increased by brain ischaemia or treatment with the P-glycoprotein inhibitor verapamil. *J. Pharm. Pharmacol.* **2002**, *54*, 729-733.
43. Miyazaki, H.; Nambu, K.; Matsunaga, Y.; Hashimoto, M. Disposition and metabolism of [¹⁴C]loperamide in rats. *Eur. J. Drug Metab Pharmacokinet.* **1979**, *4*, 199-206.
44. Doran, A.; Obach, R. S.; Smith, B. J.; Hosea, N. A.; Becker, S.; Callegari, E. *et al.* The impact of P-glycoprotein on the disposition of drugs targeted for indications of the central nervous system: evaluation using the MDR1A/1B knockout mouse model. *Drug Metab Dispos.* **2005**, *33*, 165-174.
45. Raub, T. J. P-glycoprotein recognition of substrates and circumvention through rational drug design. *Mol. Pharm.* **2006**, *3*, 3-25.
46. Demel, M. A.; Schwaha, R.; Krämer, O.; Ettmayer, P.; Haaksmä, E. E.; Ecker, G. F. In silico prediction of substrate properties for ABC-multidrug transporters. *Expert. Opin. Drug Metab Toxicol.* **2008**, *4*, 1167-1180.
47. Stouch, T. R.; Gudmundsson, O. Progress in understanding the structure-activity relationships of P-glycoprotein. *Adv. Drug Deliv. Rev.* **2002**, *54*, 315-328.
48. Srinivas, E.; Murthy, J. N.; Rao, A. R.; Sastry, G. N. Recent advances in molecular modeling and medicinal chemistry aspects of phospho-glycoprotein. *Curr. Drug Metab* **2006**, *7*, 205-217.
49. Bakos, E.; Homolya, L. Portrait of multifaceted transporter, the multidrug resistance-associated protein 1 (MRP1/ABCC1). *Pflugers Arch.* **2007**, *453*, 621-641.
50. El-Sheikh, A. A.; van den Heuvel, J. J.; Krieger, E.; Russel, F. G.; Koenderink, J. B. Functional role of arginine 375 in transmembrane helix 6 of multidrug resistance protein 4 (MRP4/ABCC4). *Mol. Pharmacol.* **2008**, *74*, 964-971.
51. Martin, C.; Berridge, G.; Higgins, C. F.; Mistry, P.; Charlton, P.; Callaghan, R. Communication between multiple drug binding sites on P-glycoprotein. *Mol. Pharmacol.* **2000**, *58*, 624-632.
52. Loo, T. W.; Clarke, D. M. Mutational analysis of ABC proteins. *Arch. Biochem. Biophys.* **2008**, *476*, 51-64.
53. van Aubel, R. A.; Smeets, P. H.; van den Heuvel, J. J.; Russel, F. G. Human organic anion transporter MRP4 (ABCC4) is an efflux pump for the purine end metabolite urate with multiple allosteric substrate binding sites. *Am. J. Physiol Renal Physiol* **2005**, *288*, F327-F333.
54. Zelcer, N.; Huisman, M. T.; Reid, G.; Wielinga, P.; Breedveld, P.; Kuil, A. *et al.* Evidence for two interacting ligand binding sites in human multidrug resistance protein 2 (ATP binding cassette C2). *J. Biol. Chem.* **2003**, *278*, 23538-23544.
55. Ito, K.; Olsen, S. L.; Qiu, W.; Deeley, R. G.; Cole, S. P. Mutation of a single conserved tryptophan in multidrug resistance protein 1 (MRP1/ABCC1) results in loss of drug resistance and selective loss of organic anion transport. *J. Biol. Chem.* **2001**, *276*, 15616-15624.
56. Ito, K.; Oleschuk, C. J.; Westlake, C.; Vasa, M. Z.; Deeley, R. G.; Cole, S. P. Mutation of Trp1254 in the multispecific organic anion transporter, multidrug resistance protein 2 (MRP2) (ABCC2), alters substrate specificity and results in loss of methotrexate transport activity. *J. Biol. Chem.* **2001**, *276*, 38108-38114.
57. Oleschuk, C. J.; Deeley, R. G.; Cole, S. P. Substitution of Trp1242 of TM17 alters substrate specificity of human multidrug resistance protein 3. *Am. J. Physiol Gastrointest. Liver Physiol* **2003**, *284*, G280-G289.
58. Xia, C. Q.; Milton, M. N.; Gan, L. S. Evaluation of drug-transporter interactions using in vitro and in vivo models. *Curr. Drug Metab* **2007**, *8*, 341-363.
59. Polli, J. W.; Wring, S. A.; Humphreys, J. E.; Huang, L.; Morgan, J. B.; Webster, L. O. *et al.* Rational use of in vitro P-glycoprotein assays in drug discovery. *J. Pharmacol. Exp. Ther.* **2001**, *299*, 620-628.
60. Rautio, J.; Humphreys, J. E.; Webster, L. O.; Balakrishnan, A.; Keogh, J. P.; Kunta, J. R. *et al.* In vitro P-glycoprotein inhibition assays for assessment of clinical drug interaction potential of new drug candidates: a recommendation for probe substrates. *Drug Metab Dispos.* **2006**, *34*, 786-792.
61. El-Sheikh, A. A.; van den Heuvel, J. J.; Koenderink, J. B.; Russel, F. G. Interaction of nonsteroidal anti-inflammatory drugs with multidrug resistance protein (MRP) 2/ABCC2- and MRP4/ABCC4-mediated methotrexate transport. *J. Pharmacol. Exp. Ther.* **2007**, *320*, 229-235.
62. Pedersen, J. M.; Matsson, P.; Bergström, C. A.; Norinder, U.; Hoogstraate, J.; Artursson, P. Prediction and identification of drug interactions with the human ATP-binding cassette transporter multidrug-resistance associated protein 2 (MRP2; ABCC2). *J. Med. Chem.* **2008**, *51*, 3275-3287.
63. Leslie, E. M.; Mao, Q.; Oleschuk, C. J.; Deeley, R. G.; Cole, S. P. Modulation of multidrug resistance protein 1 (MRP1/ABCC1) transport and atpase activities by interaction with dietary flavonoids. *Mol. Pharmacol.* **2001**, *59*, 1171-1180.

64. Matsson, P.; Pedersen, J. M.; Norinder, U.; Bergstrom, C. A.; Artursson, P. Identification of Novel Specific and General Inhibitors of the Three Major Human ATP-Binding Cassette Transporters P-gp, BCRP and MRP2 Among Registered Drugs. *Pharm. Res.* **2009**, *26*, 1816–1831.
65. Breedveld, P.; Zelcer, N.; Pluim, D.; Sönmezer, O.; Tibben, M. M.; Beijnen, J. H. *et al.* Mechanism of the pharmacokinetic interaction between methotrexate and benzimidazoles: potential role for breast cancer resistance protein in clinical drug-drug interactions. *Cancer Res.* **2004**, *64*, 5804–5811.
66. Staines, A. G.; Burchell, B.; Bánhegyi, G.; Mandl, J.; Csala, M. Application of high-performance liquid chromatography-electrospray ionization-mass spectrometry to measure microsomal membrane transport of glucuronides. *Anal. Biochem.* **2005**, *342*, 45–52.
67. Uchida, Y.; Kamiie, J.; Ohtsuki, S.; Terasaki, T. Multichannel liquid chromatography-tandem mass spectrometry cocktail method for comprehensive substrate characterization of multidrug resistance-associated protein 4 transporter. *Pharm. Res.* **2007**, *24*, 2281–2296.
68. Krumpochova, P.; Saphth, S.; Brouwers, J. F.; de Haas, M.; de Vos, R.; Borst, P. *et al.* Transportomics: screening for substrates of ABC transporters in body fluids using vesicular transport assays. *FASEB J.* **2011**.
69. Zhou, S. F.; Wang, L. L.; Di, Y. M.; Xue, C. C.; Duan, W.; Li, C. G. *et al.* Substrates and inhibitors of human multidrug resistance associated proteins and the implications in drug development. *Curr. Med. Chem.* **2008**, *15*, 1981–2039.
70. Schinkel, A. H.; Jonker, J. W. Mammalian drug efflux transporters of the ATP binding cassette (ABC) family: an overview. *Adv. Drug Deliv. Rev.* **2003**, *55*, 3–29.
71. Haimeur, A.; Deeley, R. G.; Cole, S. P. Charged amino acids in the sixth transmembrane helix of multidrug resistance protein 1 (MRP1/ABCC1) are critical determinants of transport activity. *J. Biol. Chem.* **2002**, *277*, 41326–41333.
72. Chen, Z. S.; Robey, R. W.; Belinsky, M. G.; Shchaveleva, I.; Ren, X. Q.; Sugimoto, Y. *et al.* Transport of methotrexate, methotrexate polyglutamates, and 17 β -estradiol 17-(β -D-glucuronide) by ABCG2: effects of acquired mutations at R482 on methotrexate transport. *Cancer Res.* **2003**, *63*, 4048–4054.
73. Grant, C. E.; Gao, M.; DeGorter, M. K.; Cole, S. P.; Deeley, R. G. Structural determinants of substrate specificity differences between human multidrug resistance protein (MRP) 1 (ABCC1) and MRP3 (ABCC3). *Drug Metab Dispos.* **2008**, *36*, 2571–2581.
74. Maeno, K.; Nakajima, A.; Conseil, G.; Rothnie, A.; Deeley, R. G.; Cole, S. P. Molecular basis for reduced estrone sulfate transport and altered modulator sensitivity of transmembrane helix (TM) 6 and TM17 mutants of multidrug resistance protein 1 (ABCC1). *Drug Metab Dispos.* **2009**, *37*, 1411–1420.
75. Qin, L.; Zheng, J.; Grant, C. E.; Jia, Z.; Cole, S. P.; Deeley, R. G. Residues responsible for the asymmetric function of the nucleotide binding domains of multidrug resistance protein 1. *Biochemistry* **2008**, *47*, 13952–13965.
76. Kannan, P.; Brimacombe, K. R.; Zoghbi, S. S.; Liow, J. S.; Morse, C.; Taku, A. K. *et al.* N-desmethyl-loperamide is selective for P-glycoprotein among three ATP-binding cassette transporters at the blood-brain barrier. *Drug Metab Dispos.* **2010**, *38*, 917–922.
77. Taub, M. E.; Mease, K.; Sane, R. S.; Watson, C. A.; Chen, L.; Ellens, H. *et al.* Digoxin is not a substrate for organic anion-transporting polypeptide transporters OATP1A2, OATP1B1, OATP1B3, and OATP2B1 but is a substrate for a sodium-dependent transporter expressed in HEK293 cells. *Drug Metab Dispos.* **2011**, *39*, 2093–2102.
78. Kuteykin-Teplyakov, K.; Luna-Tortós, C.; Ambroziak, K.; Löscher, W. Differences in the expression of endogenous efflux transporters in MDR1-transfected versus wildtype cell lines affect P-glycoprotein mediated drug transport. *Br. J. Pharmacol.* **2010**, *160*, 1453–1463.
79. Janneh, O.; Anwar, T.; Jungbauer, C.; Kopp, S.; Khoo, S. H.; Back, D. J. *et al.* P-glycoprotein, multidrug resistance-associated proteins and human organic anion transporting polypeptide influence the intracellular accumulation of atazanavir. *Antivir. Ther.* **2009**, *14*, 965–974.
80. Morrow, C. S.; Peklak-Scott, C.; Bishwokarma, B.; Kute, T. E.; Smitherman, P. K.; Townsend, A. J. Multidrug resistance protein 1 (MRP1, ABCC1) mediates resistance to mitoxantrone via glutathione-dependent drug efflux. *Mol. Pharmacol.* **2006**, *69*, 1499–1505.
81. Giacomini, K. M.; Huang, S. M.; Tweedie, D. J.; Benet, L. Z.; Brouwer, K. L.; Chu, X. *et al.* Membrane transporters in drug development. *Nat. Rev. Drug Discov.* **2010**, *9*, 215–236.
82. Bentz, J.; Tran, T. T.; Polli, J. W.; Ayrton, A.; Ellens, H. The steady-state Michaelis-Menten analysis of P-glycoprotein mediated transport through a confluent cell monolayer cannot predict the correct Michaelis constant K_m . *Pharm. Res.* **2005**, *22*, 1667–1677.
83. Troutman, M. D.; Thakker, D. R. Novel experimental parameters to quantify the modulation of absorptive and secretory transport of compounds by P-glycoprotein in cell culture models of intestinal epithelium. *Pharm. Res.* **2003**, *20*, 1210–1224.
84. Björnsson, T. D.; Callaghan, J. T.; Einolf, H. J.; Fischer, V.; Gan, L.; Grimm, S. *et al.* The conduct of in vitro and



- in vivo drug-drug interaction studies: a PhRMA perspective. *J. Clin. Pharmacol.* **2003**, *43*, 443-469.
85. Pelkonen, O.; Raunio, H. In vitro screening of drug metabolism during drug development: can we trust the predictions? *Expert. Opin. Drug Metab Toxicol.* **2005**, *1*, 49-59.
 86. Vermeir, M.; Annaert, P.; Mamidi, R. N.; Roymans, D.; Meuldermans, W.; Mannens, G. Cell-based models to study hepatic drug metabolism and enzyme induction in humans. *Expert. Opin. Drug Metab Toxicol.* **2005**, *1*, 75-90.
 87. Brimer, C.; Dalton, J. T.; Zhu, Z.; Schuetz, J.; Yasuda, K.; Vanin, E. *et al.* Creation of polarized cells coexpressing CYP3A4, NADPH cytochrome P450 reductase and MDR1/P-glycoprotein. *Pharm. Res.* **2000**, *17*, 803-810.
 88. van de Wetering K.; Zelcer, N.; Kuil, A.; Feddema, W.; Hillebrand, M.; Vlaming, M. L. *et al.* Multidrug resistance proteins 2 and 3 provide alternative routes for hepatic excretion of morphine-glucuronides. *Mol. Pharmacol.* **2007**, *72*, 387-394.
 89. Zelcer, N.; Van de Wetering, K.; Hillebrand, M.; Sarton, E.; Kuil, A.; Wielinga, P. R. *et al.* Mice lacking multidrug resistance protein 3 show altered morphine pharmacokinetics and morphine-6-glucuronide antinociception. *Proc. Natl. Acad. Sci. U. S. A* **2005**, *102*, 7274-7279.



Chapter 8

English summary

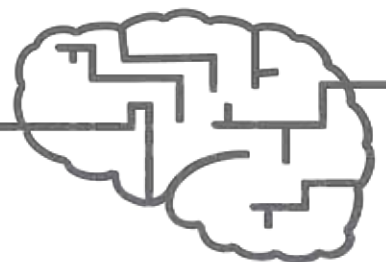
Nederlandse samenvatting

List of abbreviations and glossary

Curriculum vitae

List of publications

Dankwoord



English summary

Introduction

Absorption, distribution, metabolism, and excretion (ADME) are key determinants of drug efficacy and safety because these processes determine the availability of a drug at its target site. Before a drug reaches its site of action, it needs to cross several cellular barriers, such as the intestinal wall and the blood-brain barrier (BBB). Different transport proteins are located at these barriers that can influence the disposition of a drug in the body. One class of transporters expressed at the intestinal wall and the BBB are efflux transporters belonging to the ATP-binding cassette (ABC) transporter family. These proteins translocate substrates from inside the cell to outside the cell and need energy for their transport activity, which is provided by hydrolysis of ATP. P-glycoprotein (P-gp/ABCB1), multidrug resistance-associated proteins (MRP/ABCC), and breast cancer resistance protein (BCRP/ABCG2) are ABC transporters that have been shown to handle clinically relevant drugs. The intestinal wall plays an important role in determining the uptake of drugs into the blood after oral administration, and the oral availability of drugs can be influenced by their transport via efflux transporters in enterocytes. The BBB is formed by endothelial cells lining the small blood vessels in the brain together with a basal membrane covered with astrocytes. The main purpose of the BBB is to supply the brain with energy and to protect it from harmful compounds. Drug efflux transporters expressed at the BBB endothelial cells are involved in the latter task, and P-gp has been viewed as the most important gatekeeper of the brain. Therapeutic drugs that act on the central nervous system (CNS) have to cross both barriers before they enter the brain and can be effective. The clinical development of CNS drugs is lagging behind the development of other drugs, partly because intestinal and BBB efflux transporters limit their entrance into the brain.

In this thesis, we studied the role of efflux transporters in limiting the brain penetration of a class of anti-obesity drugs, cannabinoid type 1 (CB1) receptor antagonists. Furthermore, we investigated the interplay of these transporters with drug metabolizing enzymes and how efflux transporters can determine the rate of drug metabolism. In addition, we further explored how different amino acids contribute to the transport functionality of the efflux transporter MRP4.

Role of efflux transporters in the development of CB1 receptor antagonists as a treatment for obesity

Obesity is an illness defined by abnormal or excessive body fat accumulation that presents a risk to health. It is becoming an increasing burden to society and at least 2.8 million adults die each year as a result of overweight or obesity. Hyperactivity of the endocannabinoid system, of which the CB1 receptor is one of the key players, has been shown to play a role in the development of obesity. Therefore, inhibitors of the CB1 receptor were developed for treatment of obesity. One of these compounds, rimonabant, entered the market as an



effective anti-obesity drug in 2006. However, rimonabant was withdrawn in 2008 because it gave neuropsychiatric side effects, such as depression and anxiety. These adverse effects appeared to be caused by the action of rimonabant on CB1 receptors in the brain. Recently, it was found that the positive effects of the drug, such as a reduction of cardiometabolic risk factors, are also mediated via inhibition of CB1 receptors in the periphery of the body. Therefore, peripheral CB1 receptor antagonists, which act only on peripheral and not on brain CB1 receptors, were proposed to be effective drugs for treatment of metabolic disease and obesity without neuropsychiatric side effects. Because drug efflux transporters at the BBB can block the access of a compound to the brain, we hypothesized that affinity for these transporters could be used as a specific feature in the development of peripheral CB1 receptor antagonists. To test this hypothesis, we investigated whether a series of 3,4-diarylpyrazoline CB1 receptor antagonists were transported via these proteins, and whether transport could limit their brain penetration.

In **Chapter 2**, we showed that most of the 3,4-diarylpyrazoline CB1 receptor antagonists interact with MRP1, MRP2, MRP3, and MRP4 in a vesicular transport interaction assay. Rimonabant inhibited MRP1 transport activity more potently than MRP4, whereas the 3,4-diarylpyrazolines were stronger inhibitors of MRP4- than MRP1-mediated transport. A number of CB1 receptor antagonists, including rimonabant, stimulated MRP2 and MRP3 transport activity at low, but inhibited transport at high substrate concentrations. The interaction of 3,4-diarylpyrazolines and rimonabant with MRP1-4 indicate their potential for drug-drug interactions. Preliminary *in vivo* data of the effective dose (ED_{50}) of compounds **4**, **11**, **14**, and **15** in inhibiting CB1 agonist-induced hypotension suggest active transport of compound **4**, **11**, and **14** out of the brain, for which MRP4 might be responsible. However, follow-up studies with 3,4-diarylpyrazolines in cellular transport assays and knockout mice are required to determine whether MRP1-4 are actually involved in limiting the brain penetration of 3,4-diarylpyrazoline CB1 receptor antagonists.

In **Chapter 3**, we investigated for the same series of CB1 receptor antagonists if transport by the brain efflux transporter P-gp could be used as a selection criterion in the development of peripheral CB1 receptor antagonists. All 3,4-diarylpyrazolines and rimonabant inhibited P-gp transport activity in membrane vesicles isolated from HEK293 cells expressing the transporter, but only the 1,1-dioxo-thiomorpholino analogue **23** exhibited a reduced accumulation ($-38 \pm 2\%$) in these cells, which could be completely reversed by the P-gp/BCRP inhibitor elacridar. In addition, **23** appeared to be a BCRP substrate, whereas rimonabant was not. To further investigate the importance of P-gp and BCRP transport in limiting brain penetration of these compounds, we performed an *in vivo* experiment in rats in which we studied the effect of elacridar on the brain/plasma concentration ratio of **23** and rimonabant. The brain/plasma ratio and brain concentration of **23** was significantly lower than for rimonabant, indicating a lower penetration of **23** than of rimonabant into the brain. Co-administration of elacridar resulted in an 11-fold increase of the brain/plasma ratio for **23**, and only 1.4-fold for rimonabant, confirming the involvement of P-gp, and

possibly BCRP, in limiting the brain entrance of **23** *in vivo*. In conclusion, these data support the conception that transport via efflux transporters such as P-gp and BCRP can limit the brain penetration of CB1 receptor antagonists, and this property could be used in the development of peripheral antagonists for the treatment of obesity and metabolic disease.

The interplay between efflux transporters and metabolizing enzymes

Glucuronidation of drugs by uridine 5'-diphospho glucuronosyltransferases (UGTs) in enterocytes and hepatocytes plays an important role in first pass metabolism of drugs in intestine and liver. The hydrophilic glucuronide metabolites are excreted more effectively from the body via bile or urine than the unconjugated parent drug. Transport via efflux transporters such as MRPs is necessary for the extrusion of glucuronide conjugates from the cell. Because UGT metabolic activity can be decreased by product inhibition, it is hypothesized that UGTs and MRPs cooperate synergistically in the excretion of compounds from the body; MRPs remove the product and thereby prevent product inhibition of UGTs and increase the rate of UGT activity and total metabolism.

To test the hypothesis of a synergistic interplay between efflux transporters and glucuronidating enzymes, we used 7-hydroxycoumarin (7-HC) as a model substrate. 7-HC is a metabolite of coumarin (1, 2-benzopyrone), a natural compound that has been used as a fragrance in the food and perfume industry, and could have therapeutic usefulness in the treatment of lymphedema and different types of cancer. 7-HC and its glucuronide conjugate, 7-HC-G, are the main metabolites formed in humans, and active transport processes appear to be involved in the excretion of 7-HC-G into the urine. Because 7-HC is glucuronidated to 7-HC-G by multiple UGTs and active transport is required for efflux of 7-HC-G from cells, 7-HC would provide a good model substrate to study the transporter-enzyme interplay. The efflux transporters involved in 7-HC and 7-HC-G transport were unknown. Therefore, we first investigated whether the efflux transporters MRP1-4, BCRP, or P-gp play a role in 7-HC and 7-HC-G transport in **Chapter 4**. For this purpose, we measured uptake of the metabolites into membrane vesicles overexpressing these transporters. Our results showed that 7-HC is not transported by any of the efflux transporters tested, whereas 7-HC-G was a substrate of MRP3 and MRP4. These results are in line with the pharmacokinetic profile of coumarin, and suggest that MRP3 and MRP4 are the main transporters involved in the excretion of the coumarin metabolite 7-HC-G from liver and kidney. Furthermore, these results confirm that 7-HC is a good model substrate to study interplay between MRPs and UGTs.

In **Chapter 5**, we explored the possibility of synergistic interplay between the 7-HC-G transporters MRP3/4 and UGT2B15 in HEK293 cells using 7-HC. We identified sulindac as a potent inhibitor of MRP3 and MRP4 at concentrations that do not inhibit UGT2B15. Additionally, we showed that MRP4 is endogenously expressed in HEK293 cells, whereas there is very little expression of MRP3. Therefore, endogenous MRP4 is the most likely candidate to facilitate the excretion of 7-HC-G from HEK-UGT2B15 cells. Inhibition of efflux of 7-HC-G from these cells with the



MRP3/4 inhibitor sulindac increased the intracellular concentration of 7-HC-G and decreased its excretion. In addition, total metabolite formation was decreased, which suggests that efflux of 7-HC-G via MRP4 can influence the rate of metabolism of 7-HC by UGT2B15. This indicates that UGTs and MRPs can cooperate in synergy, thereby providing an efficient route of drug elimination via glucuronidation.

Molecular mechanism of substrate transport via MRP4

MRP4 is a membrane transporter that mediates the cellular efflux of a wide range of anionic drugs and endogenous molecules in different tissues, including the BBB. Because transport via MRP4 can influence the disposition of CNS drugs and their metabolites, it is relevant to gain more knowledge about the molecular determinants important for its transport function. In **Chapter 6**, we substituted amino acids Phe³⁶⁸, Trp⁹⁹⁵, and Arg⁹⁹⁸ with conservative or non-conservative residues, and determined the effect on transport of the model substrates estradiol 17- β -D-glucuronide (E₂17 β G), cyclic guanosine monophosphate (cGMP), methotrexate (MTX), and folic acid into membrane vesicles isolated from baculovirus-transduced HEK293 cells overexpressing the mutant MRP4 proteins. This revealed that all Arg⁹⁹⁸ mutations appeared to be deleterious, whereas the effect of a Phe³⁶⁸ or Trp⁹⁹⁵ replacement was dependent on the amino acid introduced and the substrate studied. Substitution of Phe³⁶⁸ with Trp (F368W) induced a gain-of-function of E₂17 β G transport and a loss-of-function of MTX transport, which could not be attributed to an altered substrate binding. Moreover, we did not observe any modification in ATP or ADP handling for F368W. These results, in combination with docking of substrates in a homology model of MRP4 in the inward- and outward-facing conformation, suggest that Phe³⁶⁸ and Trp⁹⁹⁵ do not play an important role in the initial binding of substrates. They, however, might interact with the substrates during rearrangement of helices for substrate translocation, funneling them to the exit site in the outward-facing conformation.

Conclusions and future perspectives

In this thesis, we used several *in vitro* models to study transport of compounds via drug efflux transporters and we argued in **Chapter 7** that these tools could be implemented in CNS drug development. Especially the membrane vesicular transport assay could provide a useful tool for pharmaceutical industry to screen transport of new compounds via MRPs, which are currently largely neglected in drug development.

In the development of peripheral CB1 receptor antagonists, the P-gp transport assay was used successfully to select CB1 receptor antagonists that do not enter the brain due to active P-gp efflux. The efficacy of peripheral antagonists, of which the development could be accelerated using the P-gp substrate strategy, as drugs against obesity and metabolic disease should be further established in (pre-)clinical studies.



Nederlandse samenvatting

Introductie

Nadat een geneesmiddel via de mond (oraal) is ingenomen, bepalen de processen van absorptie, distributie, metabolisme en uitscheiding (excretie) de lotgevallen van het middel in het lichaam. Omdat de werkzaamheid van een geneesmiddel afhangt van de beschikbaarheid van de stof op de plaats van werking, zijn deze processen medebepalend voor de effectiviteit en veiligheid van een geneesmiddel. Er zijn verschillende weefselbarrières in het lichaam die een geneesmiddel moet passeren voordat het de plaats van werking bereikt. Voorbeelden van deze barrières voor middelen die op de hersenen aangrijpen zijn de darmwand en de bloed-hersenbarrière. Hoewel sommige stoffen de cellen in de barrières vrijelijk kunnen passeren, zijn er voor andere stoffen membraangebonden eiwitten die het transport door deze weefsels bevorderen of juist verhinderen. Deze transporteiwitten zijn aanwezig op de plasmamembranen van de cellen en kunnen de passage door de barrière bepalen en daarmee de verspreiding (dispositie) van een geneesmiddel in het lichaam beïnvloeden. Een belangrijke klasse van dergelijke transporteiwitten behoort tot de ATP-binding-cassette (ABC)-familie. Deze eiwitten transporteren stoffen, zogenaamde substraten, van de binnenkant van de cel naar de buitenkant, een proces dat efflux wordt genoemd. Voor dit transport hebben ze energie nodig die vrijkomt door hydrolyse van ATP. Transport via deze eiwitten kan de cel beschermen tegen ophoping van schadelijke stoffen. P-glycoproteïne (P-gp/ABCB1), leden van de multidrug-resistance-associated-protein (MRP/ABCC)-subfamilie en breast-cancer-resistance-protein (BCRP/ABCG2) behoren tot deze klasse van transporteiwitten en het is bekend dat ze een rol spelen bij de efflux van geneesmiddelen. Na orale inname speelt de darmwand een belangrijke rol in het bepalen van de opname van geneesmiddelen in het bloed (orale beschikbaarheid). Transport door effluxtransporters in de darmwand kan de orale beschikbaarheid van een geneesmiddel beperken. De bloed-hersenbarrière wordt gevormd door endotheelcellen van de bloedvaten in de hersenen samen met de basaalmembraan die bedekt is met astrocyten, een soort zenuwcellen. De barrière tussen het bloed en de hersenen is extra sterk om ervoor te zorgen dat het centrale zenuwstelsel (CZS) wordt beschermd tegen schadelijke stoffen. Daarnaast zorgt de bloed-hersenbarrière voor de gecontroleerde aanvoer van voedingsstoffen en afvoer van afvalstoffen. Effluxtransporters zijn belangrijk voor het beschermen van de hersenen tegen schadelijke stoffen, omdat ze stoffen na binnenkomst in de cel weer terug naar het bloed transporteren. P-gp wordt gezien als de belangrijkste poortwachter van de hersenen. Als geneesmiddelen hun werking in het CZS hebben moeten ze zowel de darmwand als de bloed-hersenbarrière passeren voordat ze hun werk kunnen doen. De laatste jaren blijft de ontwikkeling van nieuwe CZS-geneesmiddelen achter in vergelijking tot perifere middelen, deels omdat transporteiwitten in de darmwand en in de bloed-hersenbarrière hun beschikbaarheid en daarmee hun werking in de hersenen kunnen beperken.

In dit proefschrift hebben we onderzocht of deze transporteiwitten ook een rol kunnen



spelen in het beperken van de orale en CZS-beschikbaarheid van een bepaalde klasse van geneesmiddelen tegen overgewicht, de cannabinoïd-type-1(CB1)-receptorantagonisten. Daarnaast hebben we onderzocht hoe effluxtransporters samenwerken met biotransformerende enzymen die de omzetting van geneesmiddelen in metabolieten katalyseren en zo de excretie bevorderen. We hebben hierbij het effect onderzocht van het remmen van metabolietefflux uit de cel op de snelheid van de vorming van deze metaboliet. Verder hebben we onderzocht hoe verschillende aminozuren bijdragen aan de structuurtransportfunctie van het effluxtransporteiwit MRP4.

Rol van effluxtransporters in de ontwikkeling van CB1-receptorantagonisten voor de behandeling van obesitas

Obesitas is een ziekte waarbij er sprake is van een abnormale of excessieve hoeveelheid lichaamsvet die een risico vormt voor de gezondheid door het ontstaan van diabetes en hart- en vaatziekten (metabool syndroom). Steeds meer mensen lijden aan obesitas en vanwege de gezondheidsproblemen vormt dit een toenemende last voor de maatschappij. Minstens 2,8 miljoen mensen overlijden wereldwijd elk jaar aan de gevolgen van overgewicht of obesitas. De afgelopen jaren is gebleken dat overactiviteit van het endocannabinoïdsysteem een belangrijke rol speelt bij de ontwikkeling van obesitas. Om die reden zijn er antagonist (remmers) van de CB1-receptor ontwikkeld voor de behandeling van obesitas. Eén van deze stoffen, rimonabant, is in 2006 geregistreerd als een effectief geneesmiddel tegen obesitas. In 2008 is rimonabant echter al weer van de markt gehaald omdat het ernstige bijwerkingen veroorzaakte zoals depressie en angst. Deze bijwerkingen bleken ook een gevolg te zijn van het remmende effect van rimonabant op CB1-receptoren in de hersenen. De laatste jaren is er steeds meer bewijs gevonden dat het enkel remmen van CB1-receptoren in andere gebieden in het lichaam dan de hersenen, ook wel de periferie genoemd, nog steeds positieve effecten heeft op het verbeteren van een aantal cardiometabole risicofactoren die geassocieerd zijn met obesitas. Voor deze gunstige effecten lijkt remming van de CB1-receptor in de hersenen niet nodig te zijn, terwijl hierdoor wel de ongewenste psychiatrische bijwerkingen ontstaan. Daarom heeft men bedacht dat perifere CB1-receptorantagonisten, die dus alleen de CB1-receptor in de perifere weefsels remmen en niet in de hersenen, een uitkomst zouden kunnen bieden voor een veiligere behandeling van obesitas. Omdat effluxtransporters in de bloed-hersenbarrière de toegang van een geneesmiddel tot de hersenen kunnen blokkeren heeft dit geleid tot de hypothese dat transport via deze eiwitten kan worden gebruikt in de ontwikkeling van perifere CB1-receptorantagonisten. Om deze hypothese te testen hebben we voor een serie van 3,4-diarylpyrazoline CB1-receptorantagonisten onderzocht of ze worden getransporteerd via deze eiwitten, en of dit transport hun beschikbaarheid in de hersenen kan beperken.

In **Hoofdstuk 2** hebben we laten zien dat de meeste 3,4-diarylpyrazoline CB1-receptorantagonisten en rimonabant een interactie aangaan met de effluxtransporters MRP1, MRP2, MRP3, en MRP4. Dit zou kunnen betekenen dat ze door deze eiwitten

worden getransporteerd. Om de interactie te bepalen hebben we membraanblaasjes (vesikels) gemaakt van cellen waarin deze transporteiwitten op de celmembraan aanwezig zijn. Deze vesikels hebben we gebruikt voor een transportexperiment waarin de opname van een radioactieve stof in de vesikels kan worden gemeten en het effect van de CB1-receptorantagonisten op de opname van dit substraat kan worden bepaald. Rimonabant remde het transport via MRP1 sterker dan het transport via MRP4, terwijl de 3,4-diarylpyrazolines juist betere remmers van MRP4- dan van MRP1-transport waren. Verschillende CB1-receptorantagonisten, inclusief rimonabant, stimuleerden het transport via MRP2 en MRP3 bij een lage substraatconcentratie en remden het transport bij een hoge substraatconcentratie. De interactie van de 3,4-diarylpyrazoline CB1-receptorantagonisten en rimonabant met MRP1-4 geeft aan dat deze stoffen een substraat kunnen zijn en mogelijk interacties kunnen geven als ze gecombineerd worden met andere geneesmiddelen die door deze eiwitten worden getransporteerd. Er zijn dierproeven gedaan met ratten waarin de effectieve dosis (ED_{50}) van de CB1-receptorantagonisten **4**, **11**, **14** en **15** is bepaald die nodig is om de helft van een stimulator(agonist)-gedieerd, bloeddrukverlagend effect te remmen. Deze resultaten suggereren dat actief transport van **4**, **11** en **14** de hersenconcentratie van deze stoffen heeft verlaagd, waarvoor MRP4 verantwoordelijk zou kunnen zijn. Om deze resultaten te bevestigen zouden er vervolgstudies moeten worden uitgevoerd waarin wordt getest of de 3,4-diarylpyrazolines daadwerkelijk substraat zijn voor MRP1-4 en of dit hun concentratie in de hersenen beïnvloedt. Hiervoor zouden cellulaire accumulatie-experimenten kunnen worden uitgevoerd of er kan worden onderzocht hoe deze stoffen de hersenen van normale (wild-type) muizen penetreren in vergelijking met de hersenen van knock-out-muizen waarin deze transporteiwitten niet aanwezig zijn.

In **Hoofdstuk 3** hebben we voor dezelfde serie CB1-receptorantagonisten onderzocht of transport via P-gp, de belangrijkste poortwachter van de hersenen, kan worden gebruikt als selectiecriterium in de ontwikkeling van perifere CB1-receptorantagonisten. Alle 3,4-diarylpyrazoline CB1-receptorantagonisten en rimonabant remden het transport van een bekend substraat via P-gp in de vesikels. Slechts één van hen, de 1,1-dioxythiomorfolino analoog **23**, bleek zelf een P-gp-substraat te zijn. Overexpressie van P-gp in cellen zorgde voor een 38% lagere ophoping (accumulatie) van **23**, die met behulp van de P-gp/BCRP-remmer elacridar kon worden verhoogd naar het niveau van **23** in cellen zonder P-gp. Naast dat **23** een P-gp-substraat was, bleek het ook een substraat voor BCRP te zijn, terwijl rimonabant door geen van beide werd getransporteerd. Om de rol van P-gp- en BCRP-transport in het belemmeren van de hersenpenetratie van CB1-receptorantagonisten verder te onderzoeken hebben we een dierexperiment (*in vivo*) met ratten uitgevoerd. In dit experiment hebben we **23** of rimonabant in het bloed gespoten met of zonder elacridar. Vervolgens hebben we op een vast tijdstip de bloed(plasma)- en hersenconcentraties bepaald van de stoffen en de hersen/plasma-concentratieratio berekend. Hieruit bleek dat de hersen/plasma-ratio en de hersenconcentratie van **23** lager was dan van rimonabant, wat duidt op een lagere penetratie van **23** in de hersenen dan van rimonabant. Wanneer de dieren tegelijkertijd



elacridar kregen bleek de hersen/plasma-ratio van **23** 11 keer hoger te zijn, terwijl dit voor rimonabant slecht 1,4 keer hoger was. De remming van transport van P-gp, en mogelijk BCRP, met elacridar zorgde dus voor een betere hersenpenetratie van **23** en niet van rimonabant. Dit bevestigt een rol voor P-gp, en mogelijk BCRP, in het beperken van de hersenconcentratie van CB1-receptorantagonist **23** *in vivo*. Deze resultaten ondersteunen dus de hypothese dat transport van CB1-receptorantagonisten via effluxtransporters aanwezig op de bloed-hersenbarrière, zoals P-gp en BCRP, de penetratie van deze stoffen in de hersenen kan beperken. Deze eigenschap zou kunnen worden gebruikt in de ontwikkeling van perifere CB1-receptorantagonisten voor de behandeling van obesitas en het metabool syndroom.

Het samenspel tussen effluxtransporteiwitten en biotransformerende enzymen

Geneesmiddelen die oraal worden ingenomen kunnen in de darmwand en in de lever worden omgezet (gebiotransformeerd) naar andere stoffen (metabolieten). Glucuronidering van geneesmiddelen is één van de omzettingen die kan plaatsvinden en deze wordt gefaciliteerd door enzymen in darm- en levercellen die behoren tot de familie van uridine 5'-difosfoglucuronosyltransferases (UGTs). Conjugatie (koppeling) met glucuronide zorgt ervoor dat het geneesmiddel beter oplosbaar wordt in water, waardoor het effectiever kan worden uitgescheiden via de gal of de urine. Omdat deze metabolieten goed wateroplosbaar zijn kunnen ze de lipofiele celmembraan niet goed meer passeren. Daarom zijn eiwitten zoals MRPs nodig om deze glucuronidemetabolieten uit de cel te transporteren. Biotransformatie via UGTs kan worden geremd door productinhibitie, wat inhoudt dat ophoping van het product, ofwel de glucuronidemetaboliet, in de cel de activiteit van het enzym vermindert. Omdat MRPs ervoor kunnen zorgen dat de glucuronidemetaboliet niet ophoopt in de cel, is het idee ontstaan dat MRPs en UGTs op een synergistische manier samenwerken; MRPs verwijderen het product uit de cel en voorkomen hiermee de productinhibitie van UGTs, wat resulteert in een optimale activiteit van UGT en dus meer biotransformatie.

Om de hypothese van een synergistisch samenspel tussen MRPs en UGTs te testen hebben we gebruik gemaakt van het modelsubstraat 7-hydroxycoumarine (7-HC). 7-HC is een metaboliet van coumarine (1,2-benzopyrone), een natuurlijke stof die eerder gebruikt is als geurstof in de voedsel- en parfumindustrie maar ook van therapeutische waarde zou kunnen zijn in de behandeling van lymfoedeem en verschillende soorten kanker. 7-HC en zijn glucuronideconjugaat, 7-HC-G, zijn de belangrijkste metabolieten in de mens. Actieve uitscheiding via transporteiwitten blijkt een belangrijke route te zijn voor de uitscheiding van 7-HC-G via de urine. Omdat 7-HC door meerdere UGTs wordt gebiotransformeerd tot 7-HC-G en actief transport door de cel nodig is om 7-HC-G uit te scheiden, leek 7-HC een goed modelsubstraat om de samenwerking tussen transporteiwitten en UGTs te bestuderen. Het was nog niet bekend welke transporteiwitten betrokken zijn bij de uitscheiding van 7-HC-G en 7-HC, en daarom hebben we in **Hoofdstuk 4** onderzocht of MRP1-4, P-gp en BCRP hierin een rol spelen. Daarom hebben we de opname van 7-HC en 7-HC-G bepaald in vesikels waarin deze transporteiwitten aanwezig waren. Hieruit bleek dat 7-HC door één van de

eiwitten werd getransporteerd, terwijl 7-HC-G een substraat bleek te zijn voor MRP3 en MRP4. Deze resultaten komen overeen met wat bekend is over de distributie en excretie van deze coumarinemetabolieten in de mens en suggereert dat MRP3 en MRP4 de belangrijkste transporteiwitten zijn voor uitscheiding van 7-HC-G door lever en nieren. Daarnaast bevestigden deze resultaten dat 7-HC een goede modelstof is om de samenwerking tussen MRPs en UGTs te onderzoeken.

In **Hoofdstuk 5** hebben we de mogelijkheid voor een synergistische samenwerking tussen MRP3/4 en UGT2B15 bestudeerd in HEK293-cellen waarin dit biotransformerende enzym tot overexpressie is gebracht. Eerst hebben we de glucuronidering van 7-HC door UGT2B15 bepaald. Als tweede hebben we sulindac geïdentificeerd als een krachtige remmer van MRP3 en MRP4, terwijl UGT2B15 bij eenzelfde concentratie van deze stof slechts zwak wordt geremd. Daarnaast hebben we met behulp van kwantitatieve PCR aangetoond dat MRP4 van nature voorkomt in HEK293-cellen, terwijl MRP3 nauwelijks tot expressie komt in deze cellen. Daarom lijkt MRP4 de meest voor de hand liggende kandidaat voor uitscheiding van 7-HC-G gevormd door UGT2B15 in HEK293-cellen. Remming van 7-HC-G-transport uit de cel met behulp van de MRP3/4-remmer sulindac verhoogde de concentratie van 7-HC-G in de cel en verlaagde de uitscheiding van 7-HC-G, wat duidt op verminderd transport van 7-HC-G uit de cel. Daarnaast reduceerde sulindac ook de totale glucuronidevorming, hetgeen suggereert dat transport van 7-HC-G via MRP4 de mate van glucuronidering van 7-HC via UGT2B15 beïnvloedt. Dit impliceert dat UGTs en MRPs inderdaad in synergie samen kunnen werken, waardoor ze op een efficiënte wijze geneesmiddelen uit het lichaam kunnen uitscheiden door middel van glucuronidering en transport.

Moleculaire mechanisme van substraattransport door MRP4

MRP4 is een membraaneiwit dat betrokken is bij het transport van zeer diverse, doorgaans negatief geladen, stoffen, zoals geneesmiddelen en lichaamseigen moleculen, in verschillende weefsels waaronder de bloed-hersenbarrière. Omdat transport via MRP4 de verdeling van CZS-geneesmiddelen en hun metabolieten in ons lichaam kan beïnvloeden, is het relevant om meer kennis te vergaren over de aminozuren die belangrijk zijn voor de transportfunctie van dit eiwit. Een eiwit bestaat uit een keten van bouwstenen, aminozuren genaamd, die op een bepaalde manier wordt gevouwen om een actief eiwit te krijgen. De aminozuurvolgorde bepaalt welke functionele onderdelen een eiwit heeft en het blijkt dat sommige aminozuren belangrijker zijn dan anderen. Om te onderzoeken welke aminozuren belangrijk zijn voor de transportfunctie van MRP4 hebben we in **Hoofdstuk 6** de aminozuren fenylalanine op positie 368 in de aminozuurketen (Phe³⁶⁸) en tryptofaan en arginine op positie 955 en 998 (Trp⁹⁹⁵ en Arg⁹⁹⁸) vervangen met conservatieve (vergelijkbare chemisch-fysische eigenschappen) en niet-conservatieve aminozuren. Hierna hebben we het effect van deze substituties op het transport van een aantal modelsubstraten bepaald met behulp van vesikels waarin deze mutante MRP4-eiwitten aanwezig waren. We hebben als substraten estradiol-17 β -D-glucuronide (E₂-17 β G), cyclisch guanosinemonofosfaat (cGMP),



methotrexaat (MTX) en foliumzuur gebruikt. De transportstudies lieten zien dat de Arg⁹⁹⁸-mutanten totaal geen transportactiviteit meer vertoonden, terwijl de activiteit van de Phe³⁶⁸- en Trp⁹⁹⁵-mutanten afhankelijk was van het aminozuur waarmee het was vervangen en het substraat waarvan het transport werd gemeten. Substitutie van Phe³⁶⁸ met het conservatieve aminozuur tryptofaan (F368W) induceerde een toename van transportactiviteit voor het substraat E₂17βG, terwijl het een afname van MTX-transport gaf. Deze veranderingen in transportactiviteit bleken niet veroorzaakt door een veranderde binding van het substraat aan het transporteiwit. Daarnaast zagen we tijdens E₂17βG-transport door F368W ook geen verandering in de binding van ATP of ADP, belangrijk voor de energie die nodig is voor conformatieveranderingen van de transporter. Deze resultaten, in combinatie met het bepalen van de locatie van de binding van de substraten in een homologiemodel van MRP4 in de in- en uitwaartsgerichte conformatie, suggereren dat Phe³⁶⁸ en Trp⁹⁹⁵ geen belangrijke rol spelen in de initiële binding van substraten aan MRP4. Ze zouden echter wel tijdens het herschikken van de transmembraanhelices een interactie met de substraten kunnen aangaan die van invloed is op de verplaatsing van het substraat van de binnenkant van de cel naar de uitgang van het transporteiwit aan de buitenkant van de cel in de uitwaartsgerichte conformatie.

Conclusie en toekomstperspectieven

In dit proefschrift hebben we verschillende celmodellen gebruikt om transport van stoffen via effluxtransporteiwitten te bestuderen. In **Hoofdstuk 7** beschrijven we hoe deze transportstudies zouden kunnen worden gebruikt in de ontwikkeling van CZS-geneesmiddelen. Vooral de transportexperimenten met vesikels zouden een geschikt gereedschap kunnen zijn voor de farmaceutische industrie om het transport van nieuwe stoffen via MRPs te testen; Deze transporteiwitten zijn op dit moment onderbelicht in het proces van geneesmiddelontwikkeling.

Voor de ontwikkeling van perifere CB1-receptorantagonisten hebben we de cellulaire transportstudies succesvol gebruikt om een stof te selecteren die *in vivo* door P-gp verhinderd werd om de hersenen te penetreren. Door middel van deze P-gp-transportstrategie zou de ontwikkeling van perifere CB1 receptor antagonisten kunnen worden versneld. De therapeutische effectiviteit van deze middelen bij obesitas en metabool syndroom moet nog verder worden bevestigd in (pre-)klinische studies.



List of abbreviations and glossary

7-HC	7-hydroxycoumarin
7-HC-G	7-hydroxycoumarin glucuronide
7-HC-S	7-hydroxycoumarin sulfate
$\Delta 9$ -THC	$\Delta 9$ -tetrahydrocannabinol, natural CB1 receptor agonist
A	alanine, small hydrophobic amino acid
ABC	ATP binding cassette
ABCB1	gene name for P-glycoprotein (P-gp) / multidrug resistance protein 1 (MDR1)
ABCC	gene name for multidrug resistance-associated proteins (MRPs)
ABCG2	gene name for breast cancer resistance protein (BCRP)
ACN	acetonitrile
ADP	adenosine 5'-diphosphate
agonist	a molecule that produces a physiological response through activation of a receptor by binding to the receptor in the active state
Ala	alanine, small hydrophobic amino acid
AM4113	brain-penetrating neutral CB1 receptor antagonist developed at the laboratory of Alexandros Makriyannes at the Centre for Drug Discovery, Northeastern University Boston, USA
AM6545	peripheral and neutral CB1 receptor antagonist and P-gp substrate developed at the laboratory of Alexandros Makriyannes at the Centre for Drug Discovery, Northeastern University Boston, USA
AMP	adenosine 5'-monophosphate
ANOVA	analysis of variance
Arg	arginine, positively charged amino acid
Asp	asparagine, polar uncharged amino acid
ATP	adenosine 5'-triphosphate
BBB	blood-brain barrier
BCRP	breast cancer resistance protein
BPR697	peripheral CB1 receptor antagonist developed by the group of M-S Hung at the Institute of Biotechnology and Pharmaceutical Research, Miaoli, Taiwan
BSA	bovine serum albumine
CaCo-2	colon carcinoma cell line that is often used as a representative for intestinal cells

CB1	cannabinoid type 1
cGMP	cyclic guanosine 3',5'-cyclic monophosphate
Ci	Curie
CI	confidence interval
cLogP	calculated octanol:water coefficient
CNS	central nervous system
CP55,940	CB1 receptor agonist
C _t	number of PCR cycles before threshold is reached
CYP	cytochrome P450 enzyme
DMEM	Dulbecco Eagle's modified medium
E ₁ S	estrone sulfate
E ₂ 17βG	estradiol-17β-D-glucuronide
EC ₅₀	concentration at which 50% of maximum response to that modulator is reached
ED ₅₀	effective dose at which 50% of maximum response to that modulator is reached
elacridar	mixed P-gp/BCRP inhibitor, also called GF120918 or G918
ER	endoplasmic reticulum
<i>ex vivo</i>	an experiment that is done with living tissue outside a living animal/human
eYFP	enhanced yellow fluorescent protein
F	phenylalanine, aromatic amino acid
FCS	fetal calf serum
GF120918	elacridar, mixed P-gp/BCRP inhibitor
GSH	reduced glutathione
HBSS	Hank's balanced salt solution
HEK293	human embryonic kidney cell line 293
HPLC	high pressure liquid chromatography
IC ₅₀	concentration at which 50% of maximum enzyme activity is inhibited
inverse agonist	molecule that reverses constitutive receptor activity by binding the receptor in the inactive state
<i>in vitro</i>	an experiment that is done in test tubes or plastic in the laboratory
<i>in vivo</i>	an experiment that is done in a living animal/human



K	lysine, positively charged amino acid
K_i	equilibrium constant for inhibitory affinity. Is equal to IC_{50} with non-competitive binding. Is lower than IC_{50} with competitive binding.
K_m	Michaelis constant: the substrate concentration at which an enzyme-catalyzed reaction proceeds at 50% of its maximum velocity
L	leucine, hydrophobic amino acid
LC-MS/MS	HPLC combined with tandem mass spectrometry, technique to quantify chemical compounds
Leu	leucine, hydrophobic amino acid
LLC-PK1	pig kidney epithelial cell line, often used for transwell experiments
LTC ₄	leukotriene C ₄
Lys	lysine, positively charged amino acid
MDCKII	Madine Darby canine kidney cell line II
MDR1	multidrug resistance protein 1 / P-glycoprotein
mQ	milli-Q, ultrapure water
MRP	multidrug resistance-associated protein
MS	mass spectrometry
MTX	methotrexate
NBD	nucleotide binding domain, binds and hydrolyzes ATP
neutral antagonist	molecule that competes with the agonist for the same binding domain of the receptor
NMQ	N-methyl quinidine
PAGE	polyacrylamide gel electrophoresis
PCA	perchloric acid
PCR	polymerase chain reaction
P_i	phosphate, is released during hydrolysis of ATP to ADP
Phe	phenylalanine, aromatic amino acid
P-gp	P-glycoprotein / multidrug resistance protein 1
PSA	polar surface area
R	arginine, positively charged amino acid
S	serine, polar uncharged amino acid
SAR	structure-activity-relationship
S.D.	standard deviation, represents variation in the experiment
SDS	sodium dodecyl sulfate

S.E.M.	standard error of the mean, represents variation in the population
Ser	serine, polar uncharged amino acid
substrate	compound that is subjected to a reaction catalyzed by an enzyme or transporter
synergy	a cooperation in which the total effect exceeds the effect expected from the sum of the individual effects
TFA	trifluoroacetic acid
TM	transmembrane helix
TMD	transmembrane domain, consist of 5 or 6 membrane helices for ABC transporters and can bind substrates
TM38837	peripheral CB1 receptor antagonist developed by 7TM Pharma
Trp	tryptophan, aromatic amino acid
TS buffer	Tris-sucrose buffer
Tyr	tyrosine, aromatic amino acid
UDP	uridine 5'-diphosphate
UDPGA	uridine 5'-diphospho glucuronic acid
UGT	uridine 5'-diphospho glucuronosyltransferase
u-HPLC	ultra high pressure liquid chromatography
vanadate	phosphate (P _i) analog that traps ADP to the nucleotide binding domain
vesicles	small bubbles of isolated membranes from cells expressing a transporter or control protein. Compounds can be transported into the cavity of inside-out oriented vesicles.
V_{\max}	the maximum velocity of an enzyme reaction when the binding site is saturated with substrate
VSV-G	vesicular stomatis virus
W	tryptophan, aromatic amino acid
Y	tyrosine, aromatic amino acid



Curriculum vitae

Hanneke Wittgen werd geboren op 23 mei 1984 te Venray. In 2002 behaalde zij haar VWO-diploma aan het Raayland College in Venray. Aansluitend begon zij met de studie Medische Biologie aan de Radboud Universiteit Nijmegen. Tijdens haar studie verrichtte ze in 2006 een masterstage bij de afdeling Pathologie van het UMC St Radboud in Nijmegen onder leiding van dr. L.C.L.T. van Kempen. In 2007 liep ze haar tweede masterstage bij de afdeling Fysiologie van het UMC St Radboud in het Nijmegen Centre for Molecular Life Sciences (NCMLS) onder leiding van dr. J.P.H. Schoeber, prof. dr. J.G.J. Hoenderop en prof. dr. R.J.M. Bindels. Met het verslag van haar tweede stage won ze de NCMLS-prijs voor het beste wetenschappelijke verslag van 2007. Naast haar studie was ze actief in verschillende activiteitencommissies en in het bestuur van de studievereniging voor (Medische) Biologie BeeVee en de faculteitsvereniging Olympus. Op 31 oktober 2007 behaalde ze haar doctoraal examen cum laude en in 2008 won ze de Unilever Research Prijs voor haar resultaten tijdens de masteropleiding. In januari 2008 startte ze haar promotieonderzoek op de afdeling Farmacologie en Toxicologie van het UMC St Radboud te Nijmegen, onder leiding van prof. dr. F.G.M. Russel en dr. J.B. Koenderink. Haar promotieonderzoek was onderdeel van het onderzoeksconsortium T5-105 van het Topinstituut Pharma en heeft uiteindelijk geresulteerd in meerdere artikelen en dit proefschrift. Tevens heeft zij tijdens haar promotietraject verschillende bachelor- and masterstudenten begeleid. Naast haar promotieonderzoek was ze lid van de AIO-commissie van het NCMLS en heeft ze, in samenwerking met andere leden van de commissie, in 2009 en 2010 het AIO-congres georganiseerd en de website voor promovendi van het NCMLS opgezet. Vanaf juni 2012 is ze werkzaam als adviseur voor KPMG Plexus, een organisatieadviesbureau gericht op de zorgsector.

List of publications

Hanneke G.M. Wittgen, Jeroen J.M.W. van den Heuvel, Elmar Krieger, Gijs Schaftenaar, Frans G.M. Russel, and Jan B. Koenderink. Phenylalanine 368 of multidrug resistance-associated protein 4 (MRP4/ABCC4) plays a crucial role in substrate-specific transport activity. *Biochem. Pharmacol.* **2012**, *84*, 366-373

Hanneke G.M. Wittgen, Jeroen J.M.W. van den Heuvel, Petra H.H. van den Broek, Sanna Siissalo, Geny M.M. Groothuis, Inge A.M. de Graaf, Jan B. Koenderink, Frans G.M. Russel. Transport of the coumarin metabolite 7-hydroxycoumarin glucuronide is mediated via multidrug resistance-associated proteins 3 and 4. *Drug Metab. Dispos.* **2012**, *40*, 1076-1079

Hanneke G.M. Wittgen, Rick Greupink, Jeroen J.M.W. van den Heuvel, Petra H.H. van den Broek, Heike Dinter-Heidorn, Jan B. Koenderink, Frans G.M. Russel. Exploiting transport activity of P-glycoprotein at the blood-brain barrier for the development of peripheral cannabinoid type 1 receptor antagonists. *Mol. Pharmaceut.* **2012**, *9*, 1351-1360

Hanneke G.M. Wittgen, Jeroen J.M.W. van den Heuvel, Petra H.H. van den Broek, Heike Dinter-Heidorn, Jan B. Koenderink, Frans G.M. Russel. Cannabinoid receptor type 1 (CB1) receptor antagonists modulate transport activity of multidrug resistance-associated proteins MRP1, MRP2, MRP3, and MRP4. *Drug Metab. Dispos.* **2011**, *39*, 1294-1302

Joost P.H. Schoeber, Stan F.J. van de Graaf, Kyu Pil Lee, **Hanneke G.M. Wittgen**, Joost G.J. Hoenderop, René J.M. Bindels. Conditional fast expression and function of multimeric TRPV5 channels using Shield-1. *Am. J. Physiol. Renal. Physiol.* **2009**, *296*, F204-211

Hanneke G.M. Wittgen and Léon C.L.T. van Kempen. Reactive oxygen species in melanoma and its therapeutic implications. *Melanoma Res.* **2007**, *17*, 400-409

